Mechanistic Studies on Synthetic Reactions Controlled by Multi-metallic Centers

Department of Chemistry
School of Science
The University of Tokyo

Naohiko Yoshikai

Preface

Nature has exploited cooperation of multi-metallic centers in chemical transformations. A number of active sites of enzymes contain two metal ions of close proximity, which operate cooperatively. A representative example is the dinuclear copper active sites of hemocyanin, which reversibly bind/activate a dioxygen molecule. Many artificial dinuclear copper, iron, cobalt and manganese complexes have been synthesized to mimic such metalloenzymes.

In recent years, organic and organometallic chemists have also been increasingly interested in design of a multi-metallic system as an entry to a synthetic transformation with unique/high reactivity and/or selectivity. However, it has not been well recognized that they have utilized many combinations of multiple metal reagents to achieve unique synthetic reactions for more than half century, in which multi-metallic cooperation plays a pivotal role. Thus, to uncover such a hidden role of multiple metals is not only interesting in a pure mechanistic view but also valuable for further design of new catalytic systems. In this thesis, the author describes theoretical and experimental studies on several synthetic reactions that utilize multi-metallic centers.

Chapter 1 describes a basic concept of multi-metallic cooperation and an overview of its current status in several organic transformations. Chapters 2-4 deal with the transition metal-catalyzed cross-coupling reaction between an aryl or a vinyl halide with a main group organometallic reagent as a typical transition metal/main group metal combination, with particular emphasis on the activation of a C(sp^2)-halogen bond (oxidative addition). The mechanistic studies were initiated from the classical organocuprate reaction with an alkenyl bromide (Chapter 2). In this study, the author revealed a bimetallic eliminative mode of C(sp^2)-Br bond cleavage, where the Cu and the Li atoms cooperatively act as a nucleophile and a Lewis acid, respectively. Generality of the bimetallic eliminative mechanism of C(sp^2)-halogen bond cleavage was explored by theoretical studies on oxidative addition of sp^2-halides to Ni^0/Pd^0

complexes with or without complexation with a magnesium salt (Chapter 3). These basic studies resulted in a new design of Ni-catalyzed cross-coupling reaction via activation of an unreactive C-F bond (Chapter 4).

Chapters 5-7 describe mechanistic studies on the reactions of transition metal clusters. Chapters 5 and 6 cover the C-H bond insertion reaction between a diazo compound and an alkane catalyzed by dirhodium tetracarboxylate: Chapter 5 focuses on the fundamental mechanism and the bimetallic cooperation, and Chapter 6 extends the studies to the exploration of stereoselectivity issues. In Chapter 7 is described a theoretical study on the propargylic substitution reaction catalyzed by a thiolate-bridged diruthenium complex. Throughout the above studies, the author established unique roles of metal-metal interaction in the dirhodium and the diruthenium catalyses. Finally, Chapter 8 describes the summary of the present studies and the future outlook.

Acknowledgment

I would like to express my deepest gratitude for the guidance received from my research mentor, Professor Eiichi Nakamura. All his professional guidance and insightful suggestions greatly contributed to the success of this project.

I am indebted to Dr. Masahiro Yamanaka for his guidance in computational and organometallic chemistry, and his contribution to the study of the dirhodium-catalyzed reaction (Chapter 5). I am also indebted to Dr. Salai Cheettu Ammal for her significant contribution to the study of the diruthenium-catalyzed reaction (Chapter 7). I wish to thank Dr. Yoshiaki Nishibayashi for valuable discussion about Chapter 7.

I am grateful to Dr. Masaharu Nakamura for valuable and encouraging discussions that I had with him throughout my undergraduate and graduate years.

I wish to thank my senior researchers including Prof. Masaya Sawamura, Dr. Hiroyuki Isobe and Dr. Yutaka Matsuo, and past and present members of the Nakamura group for their kind assistance in various aspects.

Finally, I would like to thank my parents, Shuichi and Tomoko for continuous encouragement, and the Japan Society for Promotion of Science for the predoctoral fellowship.

Naohiko Yoshikai

Hongo

March 2005

Table of Contents

CHAPTER 4

Design of Nickel/Magnesium Bimetallic System for Catalytic C-F Bond Activation/C-C Bond Formation

CHAPTER 5

Dirhodium-catalyzed C-H Insertion Reaction between Diazo Compound and Alkane. Mechanism and Dimetallic Effects in C-H Bond Activation

CHAPTER 6

Origin of Diastereo- and Enantioselectivity in Rhodium-catalyzed Cyclization of Diazo Compound via Intramolecular C-H Insertion

List of publications

(1) "Mechanism of C-H Bond Activation/C-C Bond Formation Reaction between Diazo Compound and Alkane Catalyzed by Dirhodium Tetracarboxylate", Nakamura, E.; Yoshikai, N.; Yamanaka, M. *J. Am. Chem. Soc.* **2002**, *124*, 7181-7192 (Chapter 5).

(2) "Theoretical Studies on Diastereo- and Enantioselective Rhodium-catalyzed Cyclization of Diazo Compound via Intramolecular C-H Insertion", Yoshikai, N.; Nakamura, E. *Adv. Synth. Catal.* **2003**, *345*, 1159-1171 (Chapter 6).

(3) "Mechanism of Substitution Reaction on sp^2-Carbon Center with Lithium Organocuprate", Yoshikai, N.; Nakamura, E. *J. Am. Chem. Soc.* **2004**, *126*, 12264-12265 (Chapter 2).

Publications not included in this thesis

(1) "Kinetic Reactivity of "Higher Order Cuprate" in S_N2 Alkylation Reaction", Nakamura, E.; Yamanaka, M.; Yoshikai, N.; Mori, S. *Angew. Chem., Int. Ed.* **2001**, *40*, 1935-1938.

(2) "[3 + 3] Cycloaddition Reaction of Dipolar Trimethylenemethane with Active Methylene Compound", Nakamura, M.; Yoshikai, N.; Toganoh, M.; Nakamura, E. *Synlett* **2001**, 1030-1033.

(3) "Carbozincation of Dipolar Trimethylenemethane. A New Route to Functionalized Organozinc Reagents", Nakamura, M.; Yoshikai, N.; Nakamura, E. *Chem. Lett.* **2002**, 146-147.

(4) "On the Reaction Mechanism of "Higher-Order Cuprate", Alias "Lipshutz Cuprate", Nakamura, E.; Yoshikai, N. *Bull. Chem. Soc. Jpn.* **2004**, *77*, 1-12.

(5) "L-shaped Three-center Two-electron $(C\text{-}C\text{-}C)^+$ Bonding Array", Yoshikai, N.; Ammal, S. C.; Nakamura, E. *J. Am. Chem. Soc.* **2004**, *126*, 12941-12948.

(6) "Enantioselective Allylic Substitution of Cinnamyl Esters Catalyzed by Iridium-Chiral Aryl Phosphine Complex: Conspicuous Change in the Mechanistic Spectrum by a Countercation and Solvent", Kinoshita, N.; Marx, K. H.; Tanaka, K.; Tsubaki, K.; Kawabata, T.; Yoshikai, N.; Nakamura, E.; Fuji, K. *J. Org. Chem.* **2004**, *69*, 7960-7964.

Abbreviations

Bu: Butyl

Cp: Cyclopentadienyl

Cp*: Pentamethylcyclopentadienyl

dppe: 1,2-Bis(diphenylphosphino)ethane

dppf: 1,1'-Bis(diphenylphosphino)ferrocene

dppp: 1,3-Bis(diphenylphosphino)propane

EIE: Equilibrium Isotope Effect

eq: equivalent

Et: Ethyl

GC: Gas Chromatography

GPC: Gel Permeation Chromatography

h: hour(s)

HOMO: Highest Occupied Molecular Orbital

Hz: Hertz

IRC: Intrinsic Reaction Coordinate

KIE: Kinetic Isotope Effect

LUMO: Lowest Unoccupied Molecular Orbital

Me: Methyl

MHz: MegaHertz

min: minute(s)

NBO: Natural Bond Orbital

NMR: Nuclear Magnetic Resonance

NPA: Natural Population Analysis

Ph: Phenyl

ppm: perts per million

rt: room temperature (ca. 25 °C)

SCRF: Self-Consistent Reaction Field

THF: Tetrahydrofuran

TS: Transition State

CHAPTER 1

General Introduction

Homogeneous metal catalysis is a rapidly evolving area of synthetic organic chemistry.[1] While single-site, well-defined monometallic complexes have played a pivotal role in this area, recent years have seen significant increase of the interest in exploitation of cooperative reactivity among multiple metal centers as an entry to challenging chemical transformations.[2,3] Advantages of multi-metallic cooperation are often categorized schematically as shown in Chart 1; (a) dual binding and activation of a single reactant, (b) simultaneous activation of different reactants, and (c) (when metals are bonded) providing a particular reactivity to the substrate through substrate-to-metal/metal-to-metal charge transfer. When designing multi-metallic catalysis, one expects these effects to be exerted to achieve unusual reactivity and selectivity that are inaccessible to monometallic systems.

Chart 1. Basic Concepts of Bimetallic Cooperation

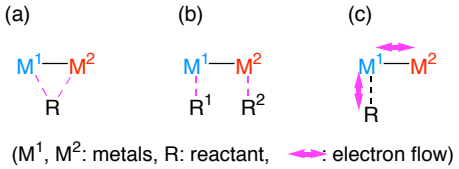

Multi-metallic catalysis can also be categorized in terms of the metal/metal combination. Main group metals and lanthanoids (denoted as MM) usually act as a Lewis acid to activate an electrophile, or as a counter cation of a nucleophile. While transition metals (denoted as TM) can also act as a Lewis acid, they show diverse reactivities toward organic molecules through their polarizable d-orbitals. Thus, there can be three metal/metal combinations – MM/MM, TM/MM and TM/TM.

While design of multi-metallic catalysis has attracted much interest in recent years,[2] it has

not been well recognized that synthetic chemists have utilized combination of various metals for a long time without expecting multi-metallic cooperation. For example, a lithium diorganocuprate (R_2CuLi), which was first synthesized in 1952,[4] is one of the most powerful polymetallic reagents for carbon-carbon bond formation.[5] However, mechanisms and Cu/Li cooperation in reactions such as carbocupration,[6] conjugate addition[7] and S_N2 alkylation[8] have been unknown before recent theoretical works by the Nakamura group (Scheme 1).[9,10] Thus, although conceptually simple as shown in Chart 1, there must exist many reactions that involve multi-metallic cooperation, the essence of which is unclear and awaits serious consideration. Investigation of such cooperative effects is valuable in terms of not only fundamental mechanistic interest, but also the provision of new guidelines for rational design of catalytic systems.

Scheme 1. Reaction Pathways of Lithium Organocuprate

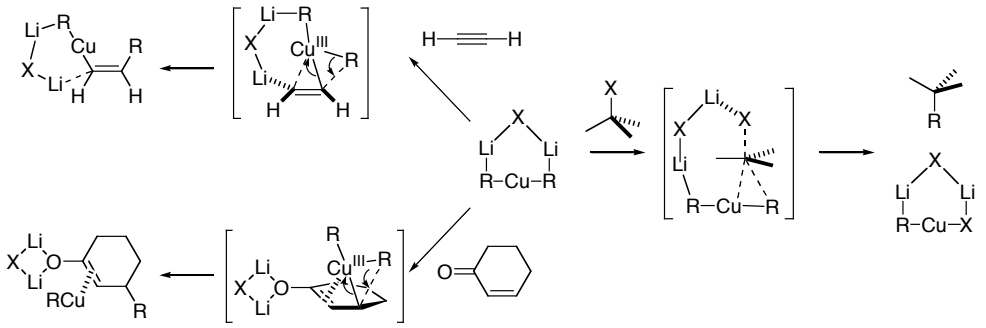

Above considerations in mind, the author has studied mechanisms of several synthetic reactions that utilize multi-metallic centers. This thesis covers two major topics: One is the transition metal (Cu, Ni, Pd)-catalyzed/mediated cross-coupling reaction between aryl and vinyl halides with main group organometallic (Li, Mg) reagents (TM/MM combination). The other is catalysis of transition metal clusters – C-H insertion reaction between a diazo compound and an alkane catalyzed by a dirhodium complex and nucleophilic substitution of a propargylic alcohol catalyzed by a diruthenium complex (TM/TM combination).

In the following sections, a brief survey of multimetallic cooperation in chemical

transformations and summary of present studies will be described. Theoretical contributions to this field will be also included. Note that this chapter does not cover sequential synthetic transformations using multiple metal catalysts, where they are likely to work independently in a single reaction system.[2b]

Main Group Metal/Main Group Metal Combination

Although the work presented in this thesis does not cover this type of metal/metal combination, it would be informative to describe a brief overview to show how multi-metallic cooperation plays important roles in modern synthetic chemistry.

Most of MM/MM reaction systems are directed to addition/substitution reactions of carbon- or heteroatom-centered nucleophiles with polar electrophiles. For a simplest example, methyllithium is in an equilibrium of several aggregate structures,[11] and a dimer has been proposed as a reactive species in addition reaction to a carbonyl compound (Scheme 2).[12] In the transition state, one lithium atom acts as a Lewis acid to activate the carbonyl group (electrophile) and the other transfers the methyl group (nucleophile).

Scheme 2. Equilibrium and Reaction Pathway of Methyllithium Aggregates

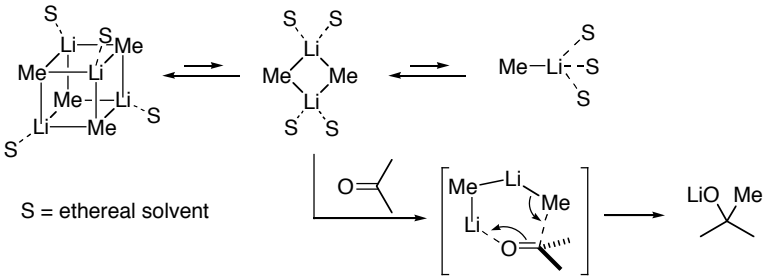

Many designed main-group multi-metallic reactions employ such a principle.[2c] Representative examples are borane-mediated, chiral oxazaborolidine-catalyzed enantioselective carbonyl reduction (CBS reduction, Scheme 3)[13] and chiral aminoalcohol-catalyzed asymmetric addition of dialkylzinc to carbonyl compounds (Scheme 4).[14] Extensive theoretical studies have

been carried out for the latter reaction to show the cooperation of two zinc centers in the transition state.[15]

Scheme 3. Oxazaborolidine-catalyzed, Borane-mediated Reduction of Ketones

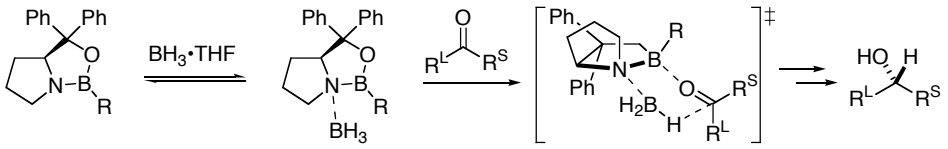

Scheme 4. Chiral Aminoalcohol-catalyzed Addition of Dialkylzinc to Aldehydes

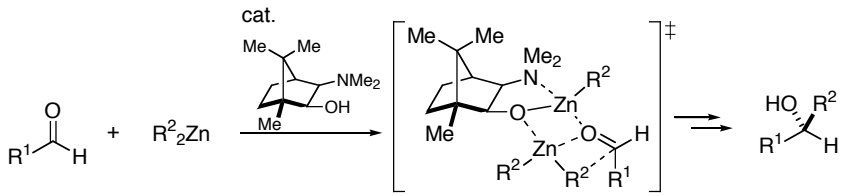

The development of catalytic enantioselective reactions with hetero-bimetallic complexes by Shibasaki and co-workers, in which each metal center plays a different role in the enantioselection, is a representative breakthrough in this area.[16] For example, chiral binaphthol-derived hetero-bimetallic complexes **1** and **2** show high catalytic activities in enantioselective conjugate addition of malonates to α,β-unsaturated carbonyl compounds. A highly ordered transition state such as **3**, where the central metal (M^1) and the alkali metal (M^2) alkoxide act as a Lewis acid and a Brønsted base, respectively, has been proposed to account for high level of enantioselection.

Scheme 5. Catalytic Asymmetric Michael Addition with Binaphthol-derived Heterobimetallic Complexes

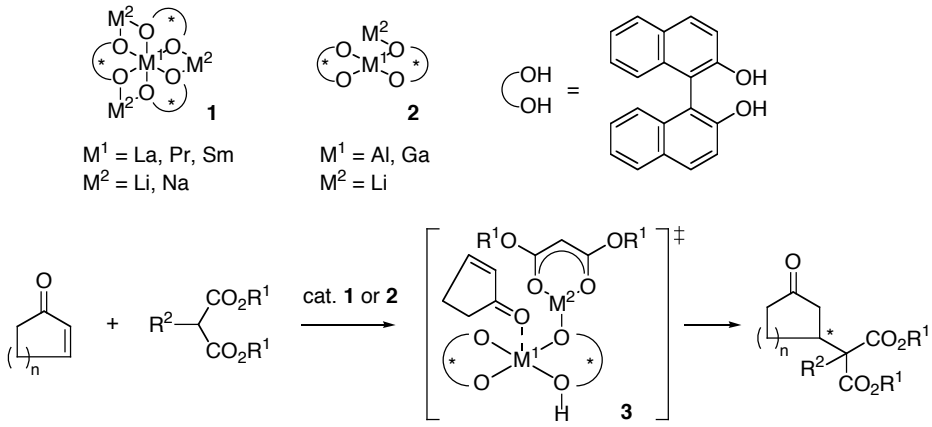

While above examples may be categorized as the type (b) reaction in Chart 1, Maruoka *et al.* reported an example of type (a) bimetallic effect: They have developed bidentate Lewis acids that activate a carbonyl group much better than monodentate derivatives.[17] For example, a bidentate aluminum Lewis acid **4** shows high reactivity in Mukaiyama aldol reaction, while a monodentate counterpart **5** affords no product under the same reaction conditions (Scheme 6).

Scheme 6. Mukaiyama Aldol Reaction with Bidentate Aluminum Lewis Acid

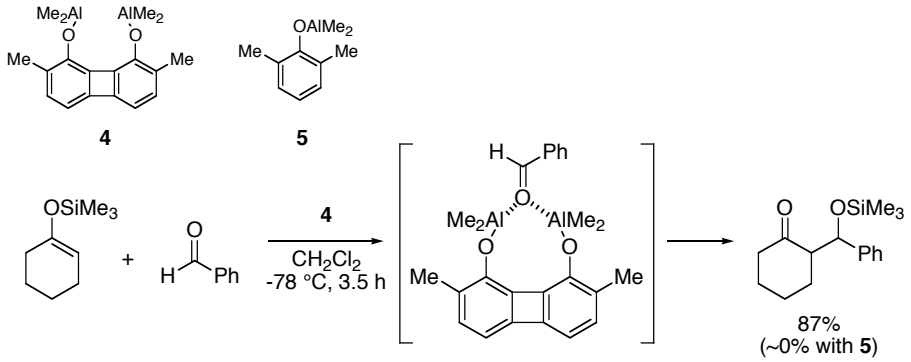

The Nakamura group has been interested in the essence of multi-metallic cooperation in main group organometallic reactions (especially Li, Mg and Zn) for decades. For example, they have revealed multi-metallic mechanisms of the Simmons-Smith reaction (cyclopropanation of an olefin with a zinc carbenoid)[18] and the Gaudemar-Normant reaction (addition of an allylzinc reagent to a vinyl magnesium reagent).[19]

Transition Metal/Main Group Metal Combination

Since Kharasch's seminal work on the effect of a transition metal salts on the reaction of a Grignard reagent,[20] combination of transition metal complexes (Cu, Pd, Ni, Rh, Fe, etc) and main group organometallic reagents (Li, Mg, Zn, Sn, B, etc) has provided a number of powerful carbon-carbon bond forming methods in synthetic organic chemistry. There are two important reaction types: one is a substitution reaction of an organic halide (Scheme 7a) or a pseudohalide, and the other is an addition reaction to an unsaturated carbon-carbon bond (Scheme 7b).

Scheme 7.

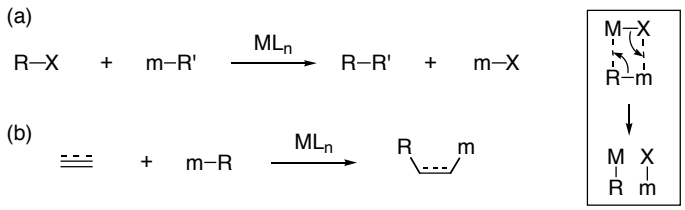

(m: main group metal, M: transition metal)

Mechanisms of those reactions are usually discussed on the basis of elementary reactions of mononuclear transition metal complexes. Thus, according to such mechanisms, the transition metal and the main group metal components interact with each other only in a transmetallation step (see inset of Scheme 7), in which the organic group on the main group metal is transferred to the transition metal center. Effects of the main group metal compounds on other catalytic steps have not been seriously considered.

The Nakamura group has a long-standing interest in such issues, and has studied the reaction mechanisms of organocopper reagents as typical TM/MM polymetallic reagents (vide infra). In this thesis, the author focuses his attention on the type (a) reaction in Scheme 7; cross-coupling reactions between aryl/vinyl halides and organometallic reagents (Li, Mg) mediated/catalyzed by transition metals including Cu, Ni and Pd (Figure 1). Since 1970's, various combinations of transition metals and main group organometallic reagents have been developed and established as powerful methods for construction of C-C bonds in natural products as well as π-conjugated materials (Figure 1).[21,22] Among various metal combinations, this thesis covers the most historical ones, that is, the stoichiometric reaction of lithium organocuprate (R_2CuLi)[23] and the Ni (Pd)-catalyzed reaction of a Grignard reagent (Kumada-Tamao-Corriu reaction).[24]

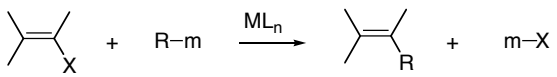

1967	R_2CuLi	Corey, Posner	stoichiometric
1971	$Fe(acac)_3/RMgX$	Kochi	catalytic
1972	$NiCl_2(PR_3)_2/RMgX$	Kumada, Tamao	
1972	$Ni(acac)_2/RMgX$	Corriu	
1975	$Pd/CuI/R_2NH/$ R'C≡CH	Sonogashira	
1976	Pd/R_3Al, R_2Zn, Cp_2ZrClR	Negishi	
1977	Pd/R_4Sn	Kosugi, Migita	
1979	Pd/R_4Sn	Stille	
1979	Pd/R_3B	Suzuki	
1988	$Pd/R_4Si/F^-$	Hiyama	

Figure 1. Chronological development of cross-coupling reaction

A textbook mechanism of the cross-coupling reaction is shown in Scheme 8. The catalytic cycle consists of three major elementary steps; oxidative addition, transmetallation and reductive elimination. The author particularly focused his attention on the mechanism and the main group metal effect on the oxidative addition step. It has been widely accepted, according to mechanistic studies on elementary reactions, that the oxidative addition proceeds through a three-centered transition state such as **X**.[25] However, the author found a new mechanism of oxidative addition, where both the transition metal and the main group metal participate in an eliminative transition state such as **Y**.

Scheme 8. A Textbook Mechanism of Cross-coupling Reaction

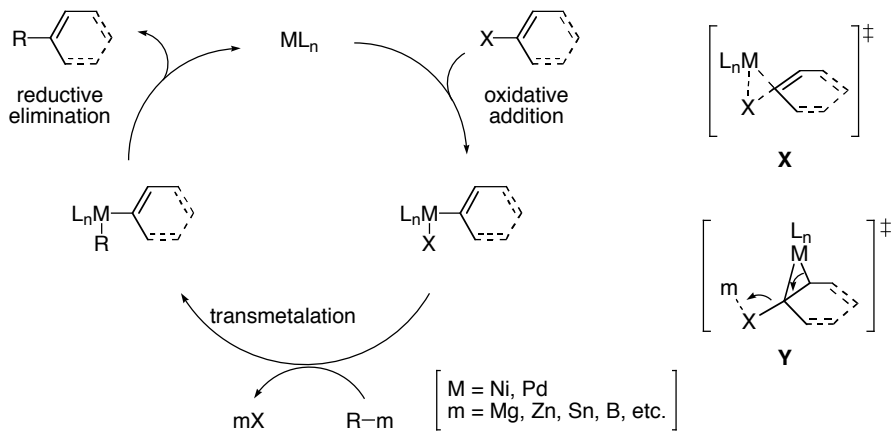

This new mechanism was initially discovered in a mechanistic study of the cuprate(I) reaction (Chapter 2). The mechanistic framework (i.e., three-centered vs. eliminative) was later found to be common in the chemistry of Ni(0) and Pd(0) complexes (Chapter 3), which possess d^{10} electron configuration as the cuprate(I). Furthermore, the author demonstrated that the new mechanism serves as a useful guideline for a rational design for catalytic activation of unreactive carbon-fluorine bonds (Chapter 4).

Another important TM/MM combination that has been known for a long time is olefin polymerization catalysis represented by the Ziegler-Natta system. Here the combination of the group 4 metals (Ti, Zr, Hf) and the Lewis acid cocatalyst (methylaluminoxane, $B(C_6F_5)_3$, etc) is critical for catalytic activity as well as stereoselectivity of the polymerization. Contrary to the cross-coupling reaction, a number of theoretical studies on the mechanism of monometallic/bimetallic olefin polymerization have been reported to date.[26,27]

Transition Metal/Transition Metal Combination

An important feature of transition metals is that they can form a cluster structure by formation of a metal-metal bond. Such cluster complexes sometimes show unusual reactivities toward unreactive bonds such as C-H, C-C, C=C etc.[28] A representative example is the chemistry of hydride-bridged trinuclear ruthenium clusters developed by Suzuki and co-workers.[29] For instance, a triruthenium cluster reacts with a cyclopentadiene to give a ruthenacyclopentadiene complex through sequential C-C/C-H bond activation processes.[30] Recently, theoretical studies on the cooperation of multiple ruthenium centers in this transformation was reported.[31]

Scheme 9. C-H Bond Activation with Trinuclear Ruthenium Complex

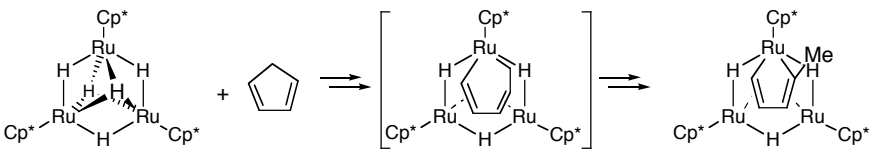

The Pauson-Khand reaction (PK reaction, $Co_2(CO)_8$-mediated/catalyzed cyclopentenone synthesis from an alkene, an alkyne and a carbon monoxide) is one the most useful synthetic method utilizing a transition metal cluster. Recently Nakamura and Yamanaka have reported density functional studies on the bimetallic pathway of the PK reaction.[32]

The intriguing reactivities notwithstanding, a problem in such metal cluster systems is that most of the reactions cannot be applied to catalysis (note that the original PK reaction was stoichiometric in the cobalt complex). This is probably because the product complex is so rigid and stable that metals cannot liberate the organic product and open the active sites again.

In above reactions, multiple transition metal centers directly interact with the target molecules. There is another type of reaction of multi-metallic clusters, where only one metal center directly interacts with the substrate, and the other seemingly behaves as an innocent spectator throughout the catalysis. In this thesis the author studied two reactions of such a type: One is a C-H insertion reaction between a diazo compound and an alkane catalyzed by dirhodium tetracarboxylate (Scheme 10),[33] and the other is nucleophilic substitution of a propargylic alcohol catalyzed by a thiolate-bridged diruthenium complex (Scheme 11).[34]

Scheme 10. C-H Insertion Reaction between Diazo Compound and Alkane Catalyzed by Dirhodium Tetracarboxylate

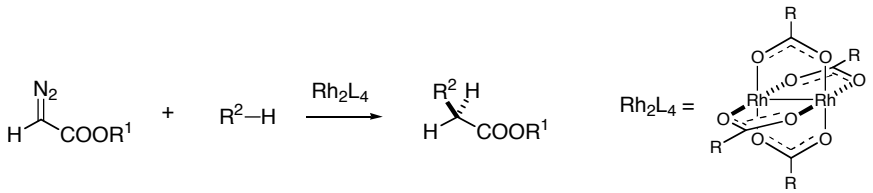

Scheme 11. Nucleophilic Substitution of Propargyl Alcohol Catalyzed by Thiolate-bridged Diruthenium Complex

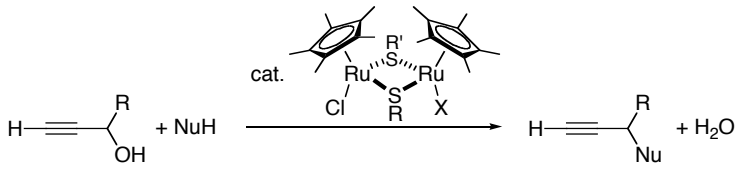

The former reaction involves a Rh-carbene complex as a reactive species, which is derived from nitrogen extrusion of the diazo compound. While a number of metal-carbene complexes are known to be formed in such a way and react with nucleophiles such as an olefin (cyclopropanation), only the dirhodium catalyst has been a practical catalyst for C-H insertion. In Chapter 5, the author describes the whole reaction pathway of the dirhodium catalysis as well as the origin of this unique reactivity. This study was further extended in Chapter 6, where the origin of stereoselectivity in intramolecular C-H insertion/cyclization reactions was explored.

The latter reaction involves a Ru-allenylildene complex as a reactive intermediate, which forms through dehydration of the propargyl alcohol. This reaction is also unique to the diruthenium complex. In Chapter 7 is described a theoretical study on this reaction.

Above studies have shown that the metal-metal bond plays a critical role in both reactions. In the former reaction, the spectator metal center act as a strong electron donor to the "reactive" metal center to facilitate the critical C-H bond insertion step. In the latter reaction, the second metal is an electron acceptor from the first: The catalyst turnover step, i.e., dissociative ligand exchange between the product and the substrate, proceeds smoothly owing to the stabilization of the coordinatively unsaturated complex by the strong Ru-Ru bond formation.

Another impressive example of transition metal-based bimetallic catalysis without apparent matal-metal bond may be the Rh-catalyzed hydroformylation reaction reported by Stanley and co-workers (Scheme 12).[35] A dinuclear rhodium-phosphine complex shows high reactivity and regioselectivity in hydroformylation of 1-alkenes. It is proposed that the key step in the catalytic cycle is an intramolecular hydride transfer from one Rh center to the other that contains the acyl chain. Later studies indicated the reaction mechanism is rather complicated and may involve Rh-Rh bond in some steps.[36]

Scheme 12. Hydroformylation of 1-Alkene Catalyzed by Dirhodium Complex

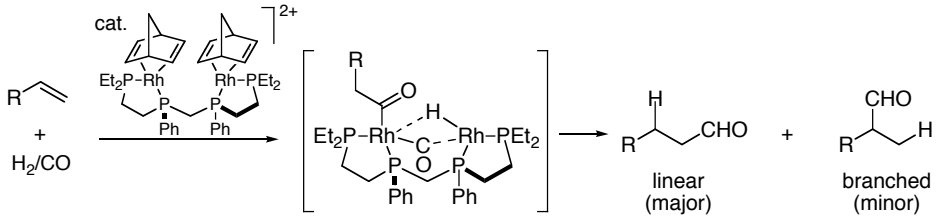

Another intriguing bimetallic catalysis is the Pd/Rh-catalyzed enantioselective allylic alkylation of α-cyano esters reported by Sawamura and Ito (Scheme 13)[37]. The palladium center reacts with an allylic carbonate to form a π-allylpalladium complex and the rhodium center generates an α-cyanoester enolate. Assembly of these two components in the transition state gives rise to high level of enantiodifferentiation.

Scheme 13. Enantioselective Allylic Alkylation Catalyzed by Two-component Pd/Rh Catalyst

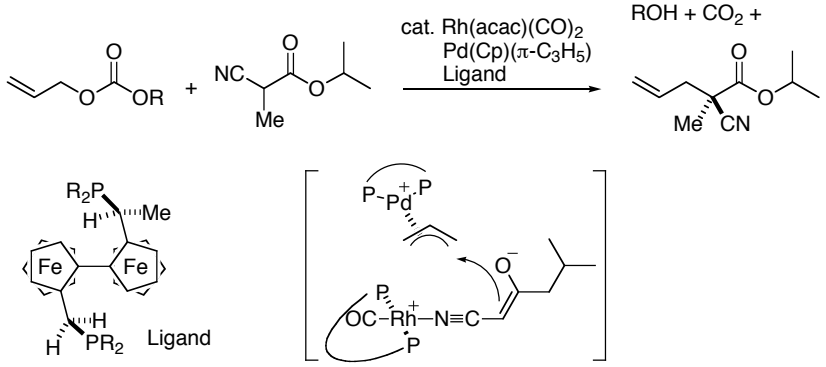

In summary, current status of multi-metallic systems in synthetic organic chemistry was described. The author believes that there must be a number of hidden or unexplored multi-metallic effects in known and unknown organic transformations. The following chapters will demonstrate the importance and the effectiveness of interplays between theory and experiments as well as between mechanistic and synthetic studies for understanding and exploiting the essence of multi-metallic cooperation.

References and Notes

1. Parshall, G. W.; Ittel, S. D. *Homogeneous Catalysis*, 2nd Ed., Wiley: New York, 1992.
2. *Multimetallic Catalysts in Organic Synthesis*, Shibasaki, M.; Yamamoto, Y. Eds., Wiley-VCH, Weinheim, 2004.
3. (a) van den Beuken, E. K. F., B. L. *Tetrahedron* **1998**, *54*, 12985-13011. (b) Lee, J. M. Na, Y.; Han, H.; Chang, S. *Chem. Soc. Rev.* **2004**, *33*, 302-312. (c) Ma, J-A.; Cahard, D. *Angew. Chem., Int. Ed.* **2004**, *43*, 4566-4583.
4. Gilman, H.; Jones, R. G.; Woods, L. A. *J. Org. Chem.* **1952**, *17*, 1630-1634.
5. (a) Lipshutz, B. H.; Sengupta, S. *Org. React.* **1992**, *41*, 135-631. (b) Lipshutz, B. H. in *Comprehensive Organometallic Chemistry II*, Vol. 12 (Eds. Abel, E. W.; Stone, F. G. A.; Wilkinson, G.), Pergamon, Oxford 1995, pp. 59-130. (c) *Organocopper Reagents*, Taylor, R. J. K. ed., Oxford University Press, Oxford, 1994. (d) Krause, N.; Gerold, A. *Angew. Chem Int. Ed.* **1997**, *36*, 186-204. (e) Ibuka, Y.; Yamamoto, Y. *Synlett* **1992**, 769-777.
6. Nakamura, E.; Mori, S.; Nakamura, M.; Morokuma, K. *J. Am. Chem. Soc.* **1997**, *119*, 4887-4899.
7. Nakamura, E.; Mori, S; Morokuma, K. *J. Am. Chem. Soc.* **1997**, *119*, 4900-4910; Mori, S.; Nakamura, E. *Chem. Eur. J.* **1999**, *5*, 1534.; Yamanaka, M.; Nakamura, E. *Organometallics* **2001**, *20*, 5675.
8. Nakamura, E.; Mori, S.; Morokuma, K. *J. Am. Chem. Soc.* **1998**, *120*, 8273-8274; Mori, S.; Nakamura, E.; Morokuma, K. *J. Am. Chem. Soc.* **2000**, *122*, 7294-7307.
9. Reviews: Nakamura, E.; Mori, S. *Angew. Chem., Int. Ed.* **2000**, *39*, 3750-3771; Nakamura, E.; Mori, S. In *Modern Organocopper Chemistry*, Krause, N. Ed., Wiley-VCH, Weinheim, 2002.
10. Experimental studies that have contributed mechanistic understanding of organocuprate reactions are also cited in ref. 8.
11. Beswick, M. A.; Wright, D. S. In *Comprehensive Organometallic Chemistry II*, Housecroft, C. E. Ed., Pergamon Press, New York, 1995; Vol. 1, Chapter 1.
12. Nakamura, M.; Nakamura, E.; Koga, N.; Morokuma, K. *J. Am. Chem. Soc.* **1993**, *115*, 11016-11017; Haeffner, F.; Sun, C. Z.; Williard, P. G. *J. Am. Chem. Soc.* **2000**, *122*, 12542-12546.
13. Corey, E. J.; Bakshi, R. K.; Shibata, S. *J. Am. Chem. Soc.* **1987**, *109*, 5551-5553; Corey, E. J.; Helal, C. J. *Angew. Chem., Int. Ed.* **1998**, *37*, 1986-2012.
14 For a review: Noyori, R.; Kitamura, M.; *Angew. Chem., Int. Ed.* **1991**, *30*, 49-69.
15. Yamakawa, M.; Noyori, R. *Organometallics* **1999**, *18*, 128-133; Goldfuss, B.; Steigelmann, M.; Khan, S. I.; Houk, K. N. *J. Org. Chem.* **2000**, *65*, 77-82; Vazquez, J.; Pericas, M. A.; Maseras, F.; Lledos, A. *J. Org. Chem.* **2000**, *65*, 7303-7309; Panda, M.; Phuan, P.-W.; Kozlowski, M. C. *J. Org. Chem.* **2003**, *68*, 564-571.
16. Reviews: Shibasaki, M.; Yoshikawa, N. *Chem. Rev.* **2002**, *102*, 2187-2209; Shibasaki, M.; Kanai, M.;

Funabashi, K. *Chem. Commun.* **2002**, 1989-1999.

17. Ooi, T.; Takahashi, M.; Maruoka, K. *J. Am. Chem. Soc.* **1996**, *118*, 11307-11308.

18 Nakamura, M.; Hirai, A.; Nakamura, E. *J. Am. Chem. Soc.* **2003**, *125*, 2341-2350.

19 Hirai, A.; Nakamura, M.; Nakamura, E. *J. Am. Chem. Soc.* **1999**, *121*, 8665-8666.

20. Kharasch, M. S.; Tawney, P. O. *J. Am. Chem. Soc.* **1941**, *63*, 2308-2315.

21. Tamao, K.; Negishi, E.-i.; Hiyama, T. *J. Organomet. Chem.* **2002**, *653*, 1.

22. *Metal-catalyzed Cross-coupling Reactions*, Diederich, F.; Stang, P. J., Eds.; Wiley-VCH: New York, 1998.

23. Corey, E. J.; Posner, G. H.; *J. Am. Chem. Soc.* **1967**, *89*, 3911-3912.

24. Tamao, K.; Sumitani, K.; Kumada, M. *J. Am. Chem. Soc.* **1972**, *94*, 4374; Corriu, R. J. P.; Masse, J. P. *Chem. Commun.* **1972**, 144.

25. (a) Amatore, C.; Pflüger, F. *Organometallics* **1990**, *9*, 2276-2282. (b) Portnoy, M.; Milstein, D. *Organometallics* **1993**, *12*, 1665-1673.

26 For examples: Vanka, K.; Xu, Z. T.; Ziegler, T. *Organometallics* **2004**, *23*, 52900-2910; Jensen, V. R.; Borve, K. J.; Ystenes, M. *J. Am. Chem. Soc.* **1995**, *117*, 4109-4117.

27 Recent experimental studies on a multinuclear polymerization catalyst that shows high activity and comonomer incorporation in ethylene/α-olefin copolymerization: Li, H.; Li, L.; Marks, T. J.; Liable-Sands, L.; Rheingold, A. L. *J. Am. Chem. Soc.* **2003**, *125*, 10788-10789.

28. *Catalysis by Di- and Polynuclear Metal Cluster Complexes*; Adams, R. A.; Cotton, F. A., Eds.; Wiley-VCH: New York, 1998.

29. Suzuki, H. *Eur. J. Inorg. Chem.* **2002**, 1009-1023. and references cited therein.

30. Suzuki, H.; Takaya, Y.; Takemori, T.; Tanaka, M. *J. Am. Chem. Soc.* **1994**, *116*, 10779-11780.

31 Khoroshun, D. V.; Inagaki, A.; Suzuki, H.; Vyboishchikov, S, F.; Musaev, D. G.; Morokuma, K. *J. Am. Chem. Soc.* **2003**, *125*, 9910-9911.

32 Yamanaka, M.; Nakamura, E. *J. Am. Chem. Soc.* **2001**, *123*, 1703-1708.

33. (a) Davies, H. M. L.; Antoulinakis, E. G. *J. Organomet. Chem.* **2001**, *617-618*, 47-55. (b) Doyle, M. P.; Forbes, D. C. *Chem. Rev.* **1998**, *98*, 911-935.

34. (a) Nishibayashi, Y.; Wakiji, I.; Hidai, M. *J. Am. Chem. Soc.* **2000**, *122*, 11019-11020; Nishibayashi, Y.; Wakiji, I.; Ishii, Y.; Uemura, S.; Hidai, M. *J. Am. Chem. Soc.* **2001**, *123*, 3393-3394; Nishibayashi, Y.; Imajima, H.; Onodera, G.; Hidai, M.; Uemura, S. *Organometallics* **2004**, *23*, 26-30.

35. Broussard, M. E.; Juma, B.; Train, S. G.; Peng, W.-J.; Laneman, S. A.; Stanley, G. G. *Science* **1993**, *260*, 1784-1788.

36 Matthews, R. C.; Howell, D. K.; Penk, W.-J.; Train, S. G.; Treleaven, W. D.; Stanley, G. G. *Angew. Chem., Int. Ed.* **1996**, *35*, 2253-2256.

37. Sawamura, M.; Sudoh, M.; Ito, Y. *J. Am. Chem. Soc.* **1996**, *118*, 3309-3310.

CHAPTER 2

Mechanism of Substitution Reaction on sp^2-Carbon Center with Lithium Organocuprate

2-1. Introduction

A report in 1967 that a lithium diorganocuprate (R_2CuLi) undergoes substitution reaction with an alkenyl bromide with retention of stereochemistry[1] changed the accepted wisdom that a nucleophilic substitution on an sp^2-hybridized carbon is synthetically impracticable.[2] The discovery opened up a way to solve synthetic problems that often had no other solution, one example of which is the first total synthesis of the cecropia juvenile hormone.[3] After more than three decades, the original cuprate reaction has become obsolete and of only historical importance in modern synthetic chemistry. However, the new paradigm–transition metal-mediated C-C bond formation through substitution on sp^2-carbon center–is now firmly established in chemistry through subsequent development of catalytic variants.[4,5]

A generally accepted mechanism of the cuprate reaction involves an oxidative addition/reductive elimination sequence (Scheme 1).[6,7,8] There underlie, however, a few questionable assumptions in such a scheme: The first is the neglect of the polymetallic structure of R_2CuLi that is essential for the reactivity of organocuprate.[9,10] In addition, the mechanism silently assumes direct insertion of the metal atom into the C-X bond to form the vinyl complex **II**, and hence underrate the role of the π-complex **I** (note that the σ*- and the π*-orbitals of the alkenyl bromide respsonsible for the σ- and the π-complexation are orthogonal to each other). On the basis of theoretical and experimental studies, we propose here a significant mechanistic modification, which is consistent with and adds a new dimension to the modern mechanistic pictures of organocuprate reactions.[9]

Scheme 1. Mechanistic Hypothesis for Substitution Reaction of Alkenyl Halide with Lithium Organocuprate

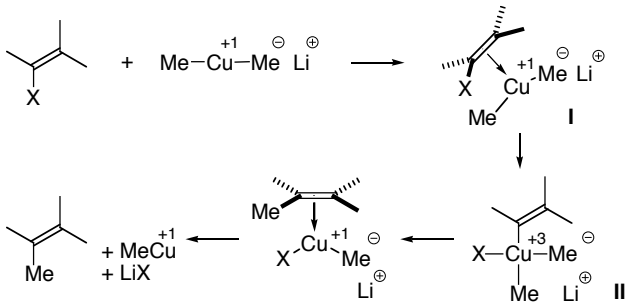

2-2. Computational Methods

All calculations were performed with a Gaussian 98 package.[11] The density functional theory (DFT) method was employed using the B3LYP hybrid functional.[12] Structures were optimized with a basis set consisting of the Stuttgart effective core potential for Cu,[13] the Ahlrichs SVP set for Br,[14] and 6-31G(d)[15] for the rest. The method and basis sets used here have been applied to other cuprate reactions and known to give reliable results.[16] Each stationary point was adequately characterized by normal coordinate analysis (no imaginary frequencies for an equilibrium structure and one imaginary frequency for a transition structure). The intrinsic reaction coordinate (IRC) analysis[17] was carried out to confirm that stationary points are smoothly connected to each other. Equilibrium and kinetic isotope effects (EIEs and KIEs) were calculated by Bigeleisen-Mayer's equation[18] with Wigner tunnel correction using frequencies scaled by 0.9614.[19] Solvent effect was evaluated in two ways: First, single-point energy calculation was performed on the gas-phase geometry with self-consistent reaction field (SCRF) method employing the polarized continuum model (PCM, ε = 4.335 for Et_2O).[20] Second, geometry optimization was performed for chemical models with coordination of one Me_2O (= S) molecule on each Li atom. The latter examination was limited to the C-Br bond cleavage steps. Natural population analysis was performed at the same level as the one used for geometry optimization.[21] For the reaction of 1-bromocyclooctene, the most stable conformer at the PM3 level was

employed as the starting geometry.

2-3. Reaction Pathways and Energetics

Experimental and theoretical studies in recent years have shown that the cyclic cuprate dimer **1** (in its solvated form, S = ethereal solvent) exists as a stable species in ethereal solution and reacts with electrophiles (Scheme 2).[9,10] Through Li-Br electrostatic interaction (**1•••2**) and $\mathbf{TS_{1\text{-}3}}$, the cuprate **1** undergoes a two-point interaction with vinyl bromide **2** to form a π-complex **3** as it does with cyclohexenone.[22] This π-complex, however, is less favorable here than in the case of more electrophilic cyclohexenone. This energetics was confirmed by ^{13}C NMR measurement on a mixture of Me_2CuLi•LiI and 1-bromocyclooctene in diethyl ether, which did not show any indication of a π−complex at -20 to -40 °C, and afforded directly the coupling product at > -10 °C (note that conjugate addition usually proceeds below -50 °C).

In the π-complex **3** that may be viewed as an ate complex of a cuprio(III)cyclopropane,[9] the two methyl groups and the vinyl carbon atoms serve as four anionic ligands in this d^8-square planar complex. Conversion of **3** to the conventional three-centered TS ($\mathbf{TS_{3\text{-}4}}$ then to **4**, path A) keeps the $Cu\text{-}C^1$ bond while breaking the $Cu\text{-}C^2$ bond. This process can therefore be viewed as rotation of the Me^1CuMe^2 moiety along $Cu\text{-}C^1$ bond as indicated as rotation A. This motion creates a vacant site on the metal and forms the Cu-Br bond. The vinylcopper(III) complex **4** undergoes quick reductive elimination via $\mathbf{TS_{4\text{-}5}}$ to give the mixed cuprate **5** and propene **6** with large exothermicity.[23]

Scheme 2. Two Pathways of the Reaction of Cuprate **1** with Vinyl Bromide to Give Propene[a]

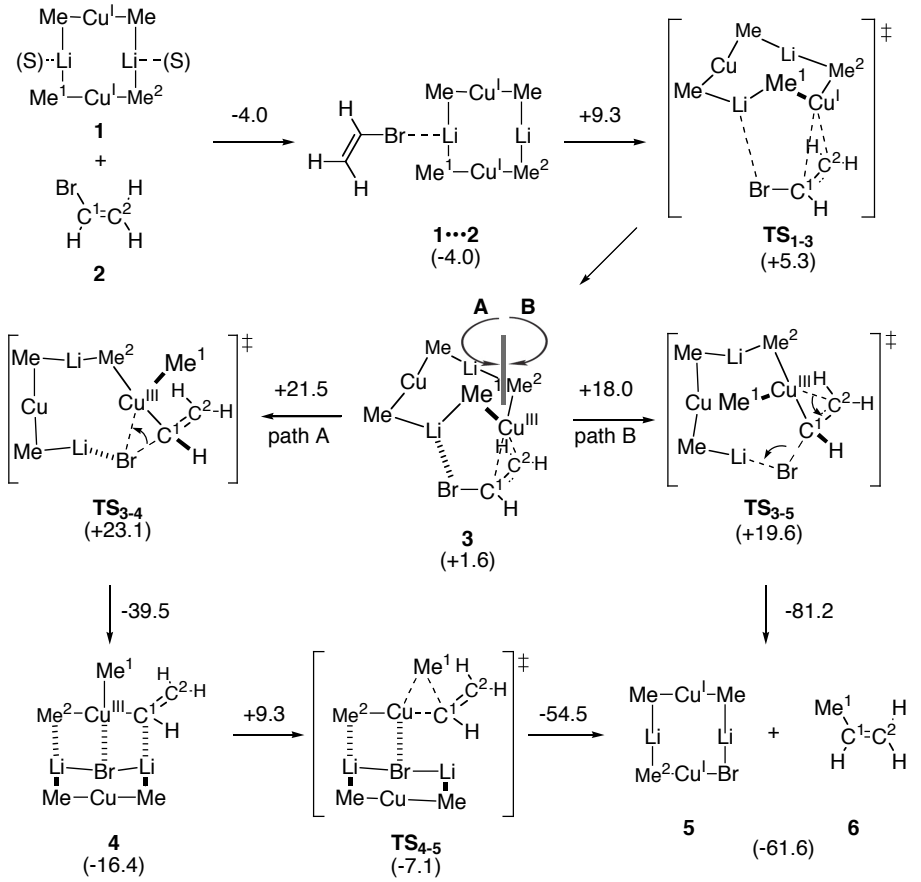

[a] A and B rotations indicate rotations along the Cu-C^1 axis. Energies (kcal/mol) are relative to [**1** + **2**]. Energy changes are shown above arrows.

While the above reaction pathway (A) is essentially the same as the textbook description (Scheme 1), there is another alternative mode (rotation B), wherein the Cu-C^2 bond is retained until the C-Br bond cleaving TS (**$TS_{3\text{-}5}$**). Here the Br atom eliminates by itself without interaction with the Cu atom, which may look rather surprising but is quite good since the leaving Br anion keeps strong interaction with the Li atom. The tetra-coordination that still exists in **$TS_{3\text{-}5}$** becomes disrupted as the Cu-C^1 bond becomes fully formed after the TS (vide infra), and the resulting tri-coordinated Cu^{III} complex undergoes spontaneous reductive elimination of the vinyl and the Me^1 groups without giving a discrete Cu^{III} intermediate.[24] The activation energies for paths A and B are ($\Delta E^{\ddagger}$) of 21.5 and 18.0 kcal/mol, respectively, and comparable to that for the S_N2 alkylation reaction of methyl bromide with **1**.[25] These values decrease by ca. 4 and 1 kcal/mol by inclusion

of solvent coordination (S = Me_2O) to Li atoms and by consideration of solvent polarity (PCM method, ε = 4.335 for Et_2O), respectively. With inclusion of solvent effects, path B is still favored by 3-4 kcal/mol over path A.

2-4. Molecular Orbital and IRC Analysis

Structure and orbital analysis shows the similarity and the difference between the two TSs of the C-Br bond cleavage (oxidative addition), **TS_{3-4}** and **TS_{3-5}** (Figure 1). In both TSs, the Me^1-Cu-Me^2 moiety is bent (117.0° and 104.0°), and the C^1 atom becomes nearly sp^3 hybridized (C^2 becomes closer to sp^2).

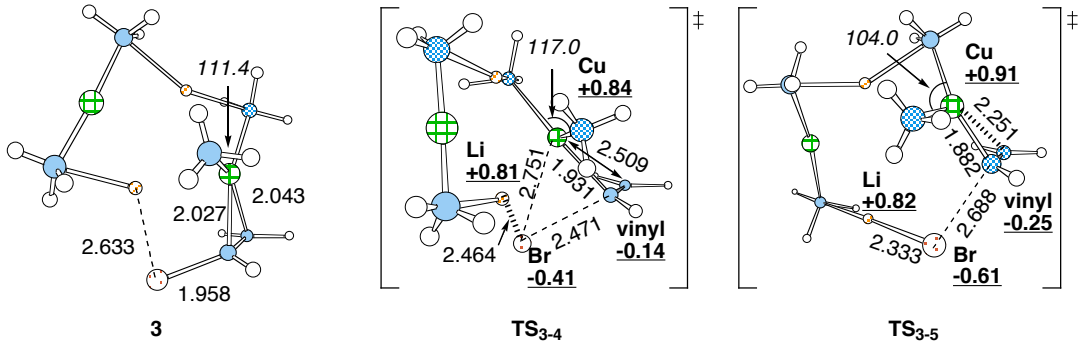

Figure 1. 3-D structures of π-complex and C-Br bond cleavage (oxidative addition) TSs. Numbers refer to bond length (Å, in roman), bond angles (degrees, in italic) and natural charges (underlined).

While the Me^1-Cu-Me^2 bending pushes up the energy level of the Cu $3d_{xz}$ orbital,[26] and the deformation of the C^1 center lowers the LUMO level of vinyl bromide through mixing of the C^1=C^2 π* and the C^1-Br σ* orbitals (Figure 2): For systematic study of the deformation of structures and molecular orbitals of vinyl bromide, geometry optimization of vinyl bromide was carried out by fixing the dihedral (Br-C^1-C^2-H^1) angle (θ, 0° to 40°) to simulate the structural changes of vinyl bromide during the π-complexation (Figure 2). Pictures and energy levels of LUMO and LUMO+1 are shown in Figure 2. One can see that, as the deformation proceeds (i.e., as θ increases), the C^1=C^2 π* and C^1-Br σ* orbitals (LUMO and LUMO+1 in a parent vinyl

bromide, respectively) mix with each other to lower the LUMO level and to push up the LUMO+1 level. With such structural change, the deformed vinyl bromide can have stronger interaction with incoming Me_2Cu^- (HOMO: Cu $3d_{xz}$) at C^1, which then leads to the C^1-Br bond cleavage. Vinyl bromide fragments cut out of the intermediary structures on the IRCs in paths A and B (C^1-Br: ca. 2.2 Å) gave similar π*/σ* mixed LUMO orbitals (see inset on the right). Thus, essentially the same frontier orbital interactions (HOMO: Cu $3d_{xz}$, LUMO: C=C π*/C-Br σ*) give the driving forces for both path A and B (Figure 3).

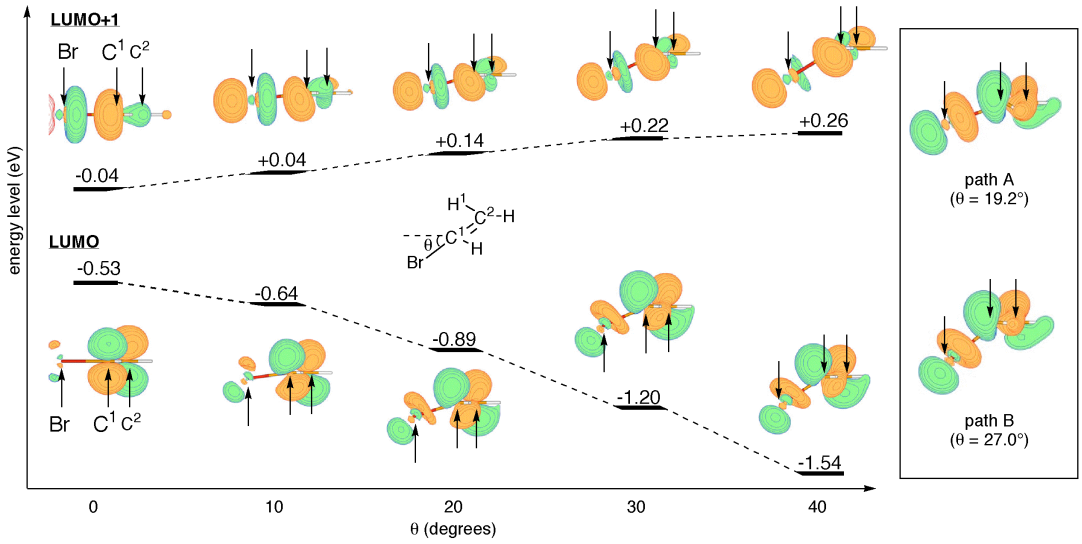

Figure 2. Pictures and energy levels (eV) of LUMO and LUMO+1 of vinyl bromide with respect to the Br-C^1-C^2-H^1 dihedral angle *θ*. Arrows show the positions of Br, C^1 and C^2 atoms. The LUMO pictures in the inset are for vinyl bromide fragments cut out of the intermediary structures on the IRCs of paths A and B.

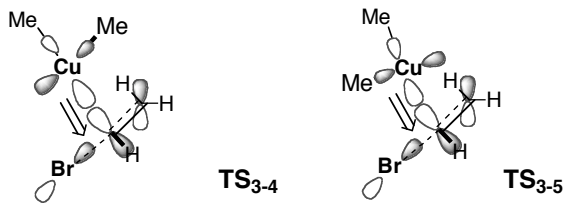

Figure 3. Schematic representation of orbital interaction between Me_2Cu- and vinyl bromide

The C-Br bond cleavage processes were probed in details by intrinsic reaction coordinate (IRC) analysis. In Figure 4 are plotted changes of several important bond lengths along the

reaction coordinates of path A (left) and B (right). It is clear that both the C^1-Br bond cleavage and the Cu-C^2 bond cleavage are taking place at the beginning. However, the order of these events is opposite for paths A and B: In path A, the Cu-C^2 cleavage takes place first and the C^1-Br cleavage follows. On the other hand, in path B, the C^1-Br bond cleavage takes place first.

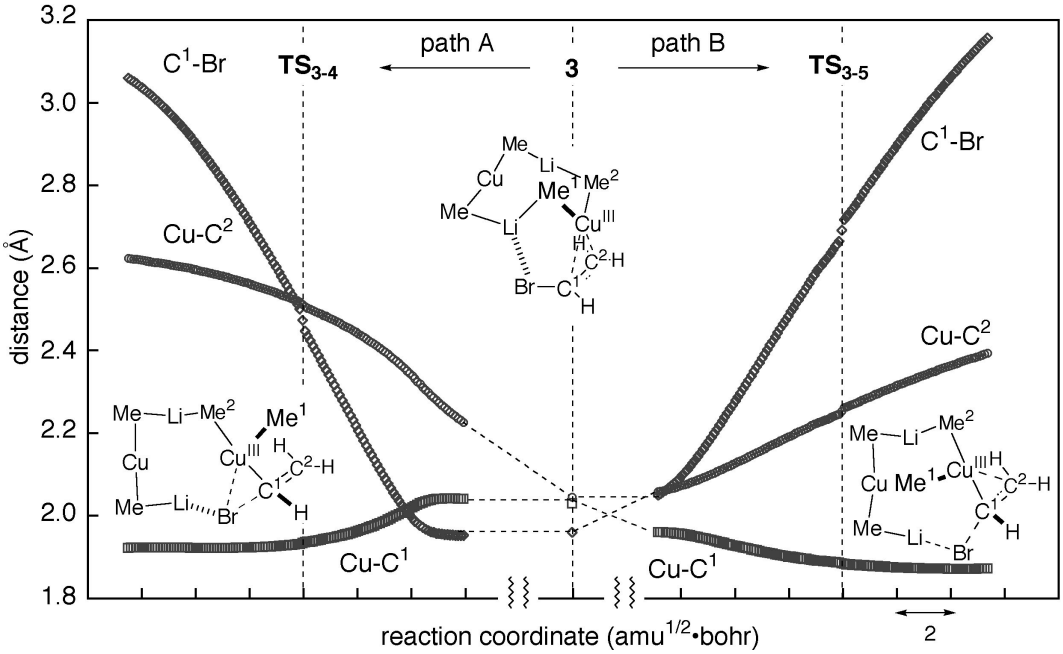

Figure 4. Changes of bond lengths C^1-Br, Cu-C^1 and Cu-C^2 along the reaction coordinates (π-complex: centered, path A: left direction, path B: rignt direction).

Above structural changes can be understood in terms of the coordination state of the Cu center (Scheme 3). Upon oxidative addition, the square-planar copper center deforms into a T-shaped coordination geometry that is indigenous to Cu^{III} oxidation state.[24] Depending on the reaction pathway, the T-geometry is oriented in an opposite way as to the vinyl bromide moiety, and so is the vacant orbital of the Cu^{III} center (Figure 1): In $\mathbf{TS_{3\text{-}4}}$, the vacant site can readily interact with the Br atom, while, in $\mathbf{TS_{3\text{-}5}}$, it can keep the interaction with the C^2 atom as long as it is possible. As one can immediately notice the similarity between $\mathbf{TS_{3\text{-}5}}$ and β-elimination reaction (Figure 1 inset; or also α-elimination) of the metallacyclopropane, we may call the $\mathbf{TS_{3\text{-}5}}$ as "eliminative TS" as opposed to the "three-centered" $\mathbf{TS_{3\text{-}4}}$.

Scheme 3. Schematic representation for changes of coordination state of Cu atom during the oxidative addition

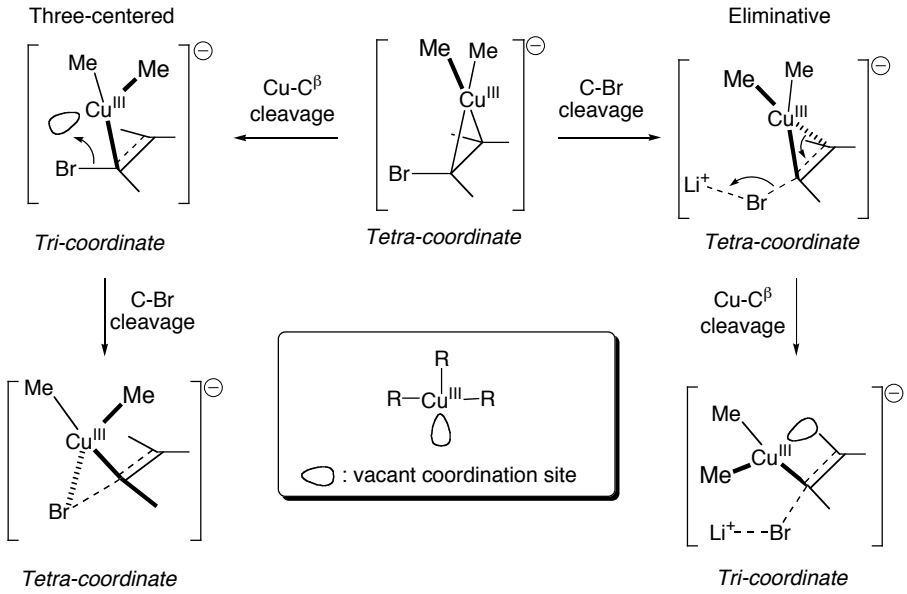

2-5. Kinetic Isotope Effects for Mechanism Elucidation

Taking place either via path A or B, the rate limiting step of the reaction is the C-Br bond cleavage and therefore we should be able to probe the reaction experimentally through kinetic isotope effect (KIE). On the basis of computational results, one can consider a simple kinetic model outlined below (Scheme 4). The reactant (R, cuprate) and the substrate (S, alkenyl bromide) are in a rapid equilibrium with the π-complex C (such as **3**) and the equilibrium overwhelmingly favors the R and S side (vide infra). The reaction proceeds from the π-complex via a rate-determining C-Br bond cleavage (either three-centered (A) or eliminative (B)) step.

Scheme 4.

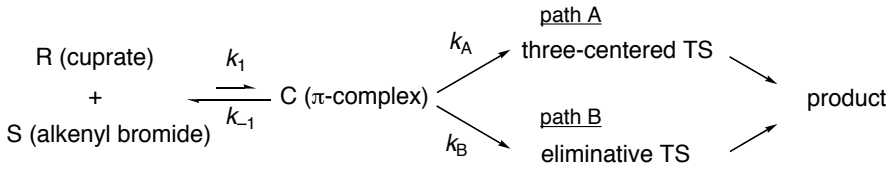

This model gives the following rate equations ($[S_{total}] = [S] + [C]$ = a total amount of alkenyl bromide in the reaction mixture):

$$-\frac{d[\mathrm{S_{total}}]}{dt} = \frac{K_1 k_\mathrm{A}[\mathrm{R}]}{1+K_1[\mathrm{R}]}[\mathrm{S_{total}}] \text{ (three-centered) or } \frac{K_1 k_\mathrm{B}[\mathrm{R}]}{1+K_1[\mathrm{R}]}[\mathrm{S_{total}}] \text{ (eliminative)}$$

Since the pre-equilibrium ($K_1 = k_1/k_{-1}$) overwhelmingly favors the starting materials (K_1[R] << 1; as indicated by the calculation and confirmed by the ^{13}C NMR analysis), these equations can be simplified as follows.

$$-\frac{d[\mathrm{S_{total}}]}{dt} = K_1 k_\mathrm{A}[\mathrm{R}][\mathrm{S_{total}}] \text{ (three-centered) or } K_1 k_\mathrm{B}[\mathrm{R}][\mathrm{S_{total}}] \text{ (eliminative)}$$

Thus, the experimental KIE will be the product of the equilibrium isotope effect (EIE) of the pre-equilibrium and the KIE of the C-Br bond cleavage step ($\mathrm{EIE_1 \bullet KIE_A}$ or $\mathrm{EIE_1 \bullet KIE_B}$). As shown in the first and the second columns of Table 1, the KIE values for C^1 (1.039 and 1.026 for paths A and B, respectively) are significantly different from each other reflecting the mechanistic difference, and indicate that the KIE serves as a measure to probe the mechanism.[27]

Table 1. Calculated and Experimental ^{12}C/^{13}C KIE Values for the Reaction between Me_2CuLi and Vinyl Bromide/1-Bromocyclooctene

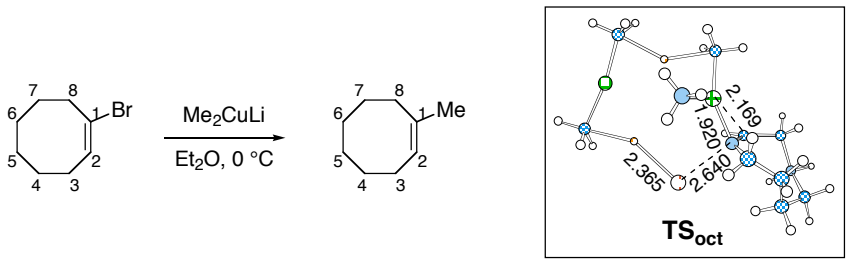

	calcd (A)[a]	calcd (B)[a]	calcd (B)[b]	run 1[c]	run 2[c]
C^1	1.039	1.026	1.024	1.023(3)	1.020(4)
C^2	1.015	1.018	1.016	1.015(2)	1.017(3)
C^3			1.003	0.999(1)	1.000(1)
C^4			1.000	1.003(2)	1.001(1)
C^5			1.000	1.000	1.000
C^6			1.000	0.997(2)	0.999(2)
C^7			1.001	0.997(2)	0.998(2)
C^8			1.007	1.004(1)	1.006(2)

[a] KIEs calculated for vinyl bromide. [b] KIEs calculated for 1-bromocyclooctene. [c] Experiments 1 and 2 are reactions carried out to 80.4% and 72.6% completion, respectively. The C^5 atom was taken as an "internal standard". Standard deviations in the last digit are shown in parentheses.

Therefore we compared experimental measurement (based on quantitative ^{13}C NMR measurement)[28] and theoretical prediction of KIE for the reaction between Me_2CuLi and 1-bromocyclooctene.[29] The calculated KIEs for path B (see $\mathbf{TS_{oct}}$ in the inset of Table 1) in column 3 show significant KIEs on C^1 (1.024) and C^2 (1.016), which agree very well with the experimental data in columns 4 and 5. For 1-bromocyclooctene, the conventional three-centered TS was higher in energy and could not be located as a stationary point. As one can surmise from $\mathbf{TS_{oct}}$, the counterclockwise rotation of the Me_2Cu moiety in path A suffers from steric repulsion between the ring structure and the Me^1 group.

2-6. Conclusion

In summary, we have proposed a new mechanism of "oxidative addition" between a cuprate and an alkenyl halide on the basis of theory and experiments. It is first necessary to note that the initially formed π-complex is not a simple Cu^I/alkenyl halide complex but behaves as a cuprio(III)cyclopropane; where charge transfer is taking place from the 3d orbital of the bent Me_2Cu moiety to the π*/σ*-mixed orbital of the deformed alkenyl halide. The subsequent C-Br bond cleavage in this complex may go through the "three-centered" or the "eliminative" way, of which the latter is preferred. The overall mechanistic framework and the cooperation of various components in the curprate cluster strongly suggest kinship between this and the conjugate addition reaction (and the carbocupration reaction, as well).[30] We expect that the present mechanistic framework applies not only to the stoichiometric cuprate(I) reaction but also to reactions involving d^{10}/d^8 transition metal catalytic cycles,[4] and that useful new designs of reactions will result.

Experimental Section

General. All the reactions dealing with air- or moisture-sensitive compounds were carried out in oven-dried reaction vessels under argon or nitrogen atmosphere. ^{1}H and ^{13}C nuclear magnetic resonance (NMR) spectra were measured on a JEOL EX-400 (400 MHz) or Bruker DRX500 (500 MHz) NMR spectrometer. Gas chromatographic (GC) analysis was performed on a Shimadzu GC-14B instrument equipped with an FID detector and a capillary column, HR-1 (25 m x 0.25 mm i.d., 0.25 μm film). Recycle preparative gel permeation chromatography (GPC) was performed on a Japan Analytical Industry LC-908 machine equipped with GPC columns (JAIGEL 1H and 2H) and an RI detector RI-5HC using chloroform as eluent (flow rate: 3.5 mL/min).

Materials. Unless otherwise noted, commercial reagents were purchased from Tokyo Kasei Co., Aldrich Inc., and other commercial suppliers and were used after distillation just before use. Anhydrous diethyl ether was purchased from KANTO Chemical Co. and stored over molecular sieves under nitrogen. The water content was determined with a Karl-Fischer moisture titrator (MKC-210, Kyoto Electronics Company) to be less than 20 ppm. Copper iodide (WAKO Chemical Co.) was purified according to the literature.[31] Methyllithium (Et_2O solution) was purchased from KANTO Chemical Co. and titrated before use. 1-Bromocyclooctene was prepared by dibromination of *cis*-cyclooctene and subsequent dehydrobromination with morpholine/DMSO.[32]

Discrimination of direct substitution and Cu-Br exchange/S_N2 alkylation pathways (see fn. 7 of the main text).

In view of a previous discussion on an iodobenzene reaction,[33] we first considered whether a direct substitution mechanism (discussed in the main text) or a Cu-Br exchange/S_N2 alkylation

mechanism operates in the alkenyl bromide substitution with Me_2CuLi. The following experiment was performed (Scheme 5):

Me_2CuLi (1eq) was allowed to react with a mixture of *trans*-β-bromostyrene and methyl iodide-d_3 (1 eq each). If the Cu-Br exchange pathway dominates as in the case of the iodobenzene reaction, the CD_3 group should be incorporated in the final product because the added CD_3I is much more reactive than CH_3Br (Scheme 5). If the direct substitution pathway operates as we assumed in our study, only the CH_3 group will be introduced into the substitution product. We found that the CD_3 group was not incorporated in the product at all (<1%), and conclude that the direct alkylation mechanism operates.

Scheme 5.

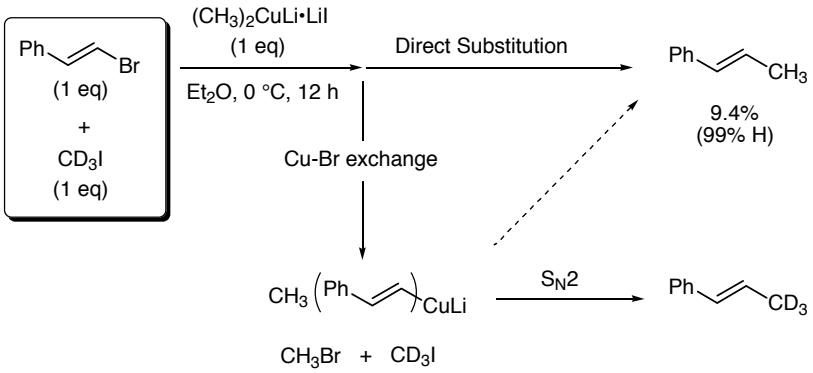

Experiment: To a suspension of CuI (193.3 mg, 1.02 mmol) in 18 mL of Et_2O was added MeLi (0.94 M in Et_2O, 2.17 mL, 2.04 mmol) over 5 min at -40 °C. The resulting solution was stirred at -40 °C for 35 min and then gradually warmed to 0 °C. To the cuprate solution was added a mixture of *trans*-β-bromostyrene (184.1 mg, 1.01 mmol), methyl iodide-d_3 (144.9 mg, 1.00 mmol) and decane (14.2 mg, 0.100 mmol, a GC internal standard) in 3 mL of Et_2O. After 12 h, the reaction was quenched by the addition of 1 mL of MeOH and subjected to GC analysis. The yield of *trans*-β-methylstyrene was determined to be 9.4% (the low yield is likely due to the reaction of Me_2CuLi with CD_3I to give ethane). The mixture was then treated with 2 mL of aq. NH_3/NH_4Cl (pH ~ 8), filtered through Florisil®, and washed with brine. The organic layer was

dried over $MgSO_4$ and concentrated under reduced pressure to give a crude product. ^{1}H NMR analysis showed that the crude product contains only the starting material and *trans*-β-methylstyrene. Comparison of the integrations of the vinylic and the methyl protons in the product confirmed virtually no incorporation of CD_3 group into the product (>99% ^{1}H for the methyl group).

^{13}C NMR measurement of the mixture of Me_2CuLi•LiI and 1-bromocyclooctene that indicated the very low cocentration of the π-complex such as 3 in the reaction mixture.

In an NMR tube that contains a glass capillary of acetone-d_6 (for NMR locking and shimming) were placed CuI (35.4 mg, 0.186 mmol) and 0.30 mL of Et_2O. To the mixture was added MeLi (1.15 M in Et_2O, 0.325 mL, 0.374 mmol) at -30 °C. The resulting mixture was shaken for 30 min at -30 °C, warmed to 0 °C for 5 min, and cooled again to -78 °C. 1-Bromocyclooctene (34.8 mg, 0.184 mmol) was added, and the NMR tube was sealed under vacuum. ^{13}C NMR spectra was then recorded between -40 and 0 °C at intervals of 10 °C (300-400 scans). The reaction started above -20 °C:

^{13}C NMR ($(C_2H_5)_2O$, 100 MHz, -20 °C) δ -10.07 ($(CH_3)_2Cu$), 25.30 (C5), 26.38 (C6), 27.34 (C7), 28.51 (C4), 29.97 (C3), 34.83 (C8), 124.56 (C1), 131.54 (C2). The S/N ratio for the peak of the C2 atom was ca. 16.

The spectra of the solution are essentially the same as the ^{13}C NMR spectrum of 1-bromocyclooctene in Et_2O, which indicates that the equilibrium concentration of the π-complex such as **3** is negligible: ^{13}C NMR ($(C_2H_5)_2O$, 100 MHz) δ 25.27 (C5), 26.21 (C6), 27.21 (C7), 28.27 (C4), 29.72 (C3), 34.81 (C8), 124.44 (C1), 131.12 (C2).

Experimental $^{12}C/^{13}C$ kinetic isotope effect (KIE) determination.[28]

Reaction of Me_2CuLi with 1-bromocyclooctene.

To a suspension of CuI (9.52 g, 50.0 mmol) in 42 mL of Et_2O was added MeLi (1.2 M in Et_2O, 84 mL, 100.8 mmol) over 30 min at -30 °C. The resulting solution was stirred for 30 min and gradually warmed to 0 °C. In another reaction vessel a solution of 1-bromocyclooctene (9.65 g, 51.0 mmol) and decane (0.704 g, 4.95 mmol) in 42 mL of Et_2O was prepared and cooled to 0 °C. Two reaction vessels were then connected with each other by a glass tube under vigorous N_2 flow. Subsequently, the cuprate solution was transferred to the substrate solution through the glass tube within 10 s. After complete addition, aliquots were taken periodically and analyzed by GC. The temperature of the reaction mixture was monitored and confirmed to be kept within 0.0 ± 1.0 °C during the reaction. After 8 h, the reaction was quenched by addition of 50 mL of ice-cold aq. NH_3/NH_4Cl (pH ~ 8). After quenching, the crude mixture was analyzed by GC to determine percent conversion (80.4 ± 0.7%). The mixture was allowed to room temperature and passed through a pad of Florisil® and Celite®. The organic layer was washed with aq. NH_3/NH_4Cl (pH~8) and brine, dried over $MgSO_4$ and concentrated under reduced pressure. The crude product was fractionally distilled to remove 1-methylcyclooctene and decane, and finally purified by GPC to recover highly pure (>99.5% by GC) 1-bromocyclooctene.

NMR measurements.

The 1-bromocyclooctene sample used for all experiments came from the same synthetic/commercial lot, and the signal integration of the recovered material was compared with that of the starting material. The NMR samples were prepared as follows: a 5-mm O.D. NMR tube was charged with ca. 500 mg of 1-bromocyclooctene, and then C_6D_6 was added to a height of 4.0 cm. The solution was degassed by freeze-thaw cycles (> 5 times) and sealed under vacuum. T_1 determination by the inversion-recovery method was carried out for each NMR sample. The

longest T_1 of ~15 s was found on the C^1 atom.

The ^{13}C NMR spectra were recorded at 125 MHz on a Bruker DRX500 NMR spectrometer with inverse gate decoupling using 90 s (> $5T_1$) delay time between calibrated $2\pi/9$ pulses. 262144 points were collected, which was zero-filled to 512K points before Fourier transformation. Zeroth-order baseline correction was applied. Integrations were determined by using a constant range of ±2.5 Hz around each peak. The measurements were performed three times for each sample.

Results.

The C^5 atom of 1-bromocyclooctene, of which isotopic composition can be safely assumed not to change during the reaction, was employed as an "internal standard" for ^{13}C integrations. The average integrations are shown in Table 2 with their standard deviations.

Table 2. Average ^{13}C integrations for 1-bromocyclooctene. Conversion of each reaction is shown in parenthesis.

	C^1	C^2	C^3	C^4	C^5	C^6	C^7	C^8
starting material	1014.5	992.7	1001.3	995.9	1000.0	1001.8	1002.0	999.6
Std. Dev.	4.0	2.2	1.2	1.4	–	1.3	1.8	1.7
run 1 (80.4±0.7%)	1052.6	1016.4	1000.1	1001.7	1000.0	998.0	997.9	1005.4
Std. Dev.	1.9	1.9	1.4	2.5	–	2.1	2.3	0.1
run 2 (72.6±0.5%)	1041.1	1014.4	1001.7	997.0	1000.0	1000.3	999.8	1007.6
Std. Dev.	2.9	3.3	1.3	0.6	–	2.3	2.2	1.9

The ^{13}C KIE values were calculated according to the following equation (F is the fraction conversion and R_0 and R are integrations of starting and recovered materials, respectively).

$$KIE_{calcd} = \ln(1-F)/\ln[(1-F)R/R_0]$$

For the derivation of the standard deviation, see ref. 34.

Table 3. R/R_0 and $^{12}C/^{13}C$ KIE values calculated from Table 2. Standard deviations in the last digit are shown in parentheses.

conversion	C^1	C^2	C^3	C^4	C^5	C^6	C^7	C^8
run 1								
R/R_0	1.038 (5)	1.024 (3)	0.999 (2)	1.006 (3)	1.000	0.996 (3)	0.996 (3)	1.006 (2)
$^{12}C/^{13}C$ KIE	1.023 (3)	1.015 (2)	0.999 (1)	1.003 (2)	–	0.998 (2)	0.997 (2)	1.004 (1)
run 2								
R/R_0	1.026 (6)	1.022 (4)	1.000 (2)	1.001 (2)	1.000	0.999 (3)	0.998 (3)	1.008 (3)
$^{12}C/^{13}C$ KIE	1.020 (4)	1.017 (3)	1.000 (1)	1.001 (1)	–	0.999 (2)	0.998 (2)	1.006 (2)

Appendix: On the Accuracy of the KIE Calculation

According to the conventional transition state theory, KIE is expressed by the following equation:

$$\mathrm{KIE} = \mathrm{MMI} \bullet \mathrm{EXC} \bullet \mathrm{ZPE}$$

where MMI is the mass-moment of inertia term, EXC is the vibrational excitation term, and ZPE is the zero-point energy term. The Bigeleisen-Mayer treatment of isotope effects requires only vibrational frequencies, because the MMI term can be expressed alternatively by the product of vibrational frequencies (VP).

$$\mathrm{MMI} = \mathrm{VP} = \frac{\nu_{\mathrm{L}}^{*}}{\nu_{\mathrm{H}}^{*}} \prod_i \frac{\nu_{\mathrm{L}_i}^{\mathrm{T}}}{\nu_{\mathrm{H}_i}^{\mathrm{T}}} \Bigg/ \prod_j \frac{\nu_{\mathrm{L}_j}^{\mathrm{R}}}{\nu_{\mathrm{H}_j}^{\mathrm{R}}}$$

$$\mathrm{EXC} = \prod_i \frac{1-\exp(-u_{\mathrm{H}_i}^{\mathrm{T}})}{1-\exp(-u_{\mathrm{L}_i}^{\mathrm{T}})} \Bigg/ \prod_j \frac{1-\exp(-u_{\mathrm{H}_j}^{\mathrm{R}})}{1-\exp(-u_{\mathrm{L}_j}^{\mathrm{R}})}$$

$$\mathrm{ZPE} = \prod_i \exp\{-(u_{\mathrm{L}_i}^{\mathrm{T}} - u_{\mathrm{H}_i}^{\mathrm{T}})/2\} \Bigg/ \prod_j \exp\{-(u_{\mathrm{L}_j}^{\mathrm{R}} - u_{\mathrm{H}_j}^{\mathrm{R}})/2\}$$

(R : reactant, T : transition state, L : light isotopomer, H : heavy isotopomer,
ν^{*} : imaginary frequency, $u = h\nu / k_{\mathrm{B}}T$)

For heavy isotopes such as $^{12}\mathrm{C}/^{13}\mathrm{C}$, differences of vibrational frequencies never exceed several percent (most of them are less than 1%). Thus, when ν_{L} (u_{L}) is set to $\nu_{\mathrm{H}} + \Delta\nu$ ($u_{\mathrm{H}} + \Delta u$), above terms can be roughly approximated as follows:

$$\mathrm{MMI} \approx 1 + \frac{\Delta\nu^{*}}{\nu_{\mathrm{H}}^{*}} + \sum_i \frac{\Delta\nu_i^{\mathrm{T}}}{\nu_{\mathrm{H}_i}^{\mathrm{T}}} - \sum_j \frac{\Delta\nu_j^{\mathrm{R}}}{\nu_{\mathrm{H}_j}^{\mathrm{R}}} \equiv 1 + \Delta_{\mathrm{MMI}}$$

$$\mathrm{EXC} \approx 1 - \sum_i \frac{\exp(-u_{\mathrm{H}_i}^{\mathrm{T}}) \bullet \Delta u_i^{\mathrm{T}}}{1-\exp(-u_{\mathrm{H}_i}^{\mathrm{T}})} + \sum_j \frac{\exp(-u_{\mathrm{H}_j}^{\mathrm{R}}) \bullet \Delta u_j^{\mathrm{R}}}{1-\exp(-u_{\mathrm{H}_j}^{\mathrm{R}})} \equiv 1 + \Delta_{\mathrm{EXC}}$$

$$\mathrm{ZPE} \approx 1 - \sum_i \frac{\Delta u_i^{\mathrm{T}}}{2} + \sum_j \frac{\Delta u_j^{\mathrm{R}}}{2} \equiv 1 + \Delta_{\mathrm{ZPE}}$$

Thus, the KIE is expressed as

$$\mathrm{KIE} \approx 1 + \Delta_{\mathrm{MMI}} + \Delta_{\mathrm{EXC}} + \Delta_{\mathrm{ZPE}}$$

This equation indicates that the difference of the calculated KIEs should be discussed with respect to the increase of the reaction rate ($\Delta_{\mathrm{MMI}} + \Delta_{\mathrm{EXC}} + \Delta_{\mathrm{ZPE}}$), not to the KIE itself (i.e., the ratio of the reaction rates). In the present case, the KIEs of 1.039 and 1.026 should be compared as "0.039 vs. 0.026" (not as "1.039 vs. 1.026"), where the former value is much larger than the latter, and one can conclude that these values are significantly large (or larger than the experimental error).

References and Notes

1. Corey, E. J.; Posner, G. H.; *J. Am. Chem. Soc.* **1967**, *89*, 3911-3912.
2. Recently Narasaka and co-workers have shown synthetic utility of in-plane S_N2 substitution of vinyl halides: Ando, K.; Kitamura, M.; Miura, K.; Narasaka, K. *Org. Lett.* **2004**, *6*, 2461-2463.
3. Corey, E. J.; Katzenellenbogen, J. A.; Gilman, N. W.; Roman, S. A.; Erikson, B. W. *J. Am. Chem. Soc.* **1968**, *90*, 5618.
4. (a) Tamura, M.; Kochi, J. K. *J. Am. Chem. Soc.* **1971**, *93*, 1487. (b) Tamao, K.; Sumitani, K.; Kumada, M. *J. Am. Chem. Soc.* **1972**, *94*, 4374. (c) Corriu, R. J. P.; Masse, J. P. *Chem. Commun.* **1972**, 144. (d) Yamamura, M.; Moritani, I.; Murahashi, S. *J. Organomet. Chem.* **1975**, *91*, C39. (e) Commercon, A.; Normant, J. F.; Villieras, J. *J. Organomet. Chem.* **1977**, *128*, 1-11.
5. *Metal-catalyzed Cross-coupling Reactions*, Diederich, F.; Stang, P. J., Eds.; Wiley-VCH: New York, 1998.
6. Bruckner, R. *Advanced Organic Chemistry: Reaction Mechanisms*; Academic Press: New York, 2002; Chapter 13.
7. A Cu-Br exchange/S_N2 alkylation sequence can be an alternative mechanism (ref. 8). This possibility was discarded by the following experiment: the reaction between Me_2CuLi and *trans*-β-bromostyrene in the presence of methyl iodide-d_3 resulted in no CD_3 group incorporation into the product (see Experimental Section).
8. Whitesides, G. M.; Fischer, W. F., Jr.; San Fillipo, J., Jr.; Bashe, R. W.; House, H. O. *J. Am. Chem. Soc.* **1969**, *91*, 4871.
9. Nakamura, E.; Mori, S. *Angew. Chem. Int. Ed.* **2000**, *39*, 3750-3771; Nakamura, E.; Mori, S. In *Modern Organocopper Chemistry*, Krause, N. Ed.; Wiley-VCH: Weinheim, 2002.

10. For a recent experimental study, see: Xie, X. L.; Auel, C.; Henze, W.; Gschwind, R. M. *J. Am. Chem. Soc.* **2003**, *125*, 1595-1601.
11. Gaussian 98, revision A.9, Frisch, M. J.; Trucks, G. W.; Schlegel, H. B.; Scuseria, G. E.; Robb, M. A.; Cheeseman, J. R.; Zakrzewski, V. G.; Montogomery, J. A., Jr.; Stratmann, R. E.; Burant, J. C.; Dapprich, S.; Millam, J. M.; Daniels, A. D.; Kudin, K. N.; Strain, M. C.; Farkas, O.; Tomasi, J.; Barone, V.; Cossi, M.; Cammi, R.; Mennucci, B.; Pomelli, C.; Adamo, C.; Clifford, S.; Ochterski, J.; Petersson, G. A.; Ayala, P. Y.; Cui, Q.; Morokuma, K.; Malick, D. K.; Rabuck, A. D.; Raghavachari, K.; Foresman, J. B.; Cioslowski, J.; Ortiz, J. V.; Baboul, A. G.; Stefanov, B. B.; Liu, G.; Liashenko, A.; Piskorz, P.; Komaromi, I.; Gomperts, R.; Martin, R. L.; Fox, D. J.; Keith, T.; Al-Laham, M. A.; Peng, C. Y.; Nanayakkara, A.; Challacombe, M.; Gill, P. M. W.; Johnson, B.; Chen, W.; Wong, M. W.; Andres, J. L.; Gonzalez, C.; Head-Gordon, M.; Pople, J. A. Gaussian. Inc.: Pittsburg, PA, 1998.
12. (a) Becke, A. D. *J. Chem. Phys.* **1993**, *98*, 5648-5652. (b) Lee, C.; Yang, W.; Parr, R. G.; *Phys. Rev. B* **1988**, *37*, 785-789.
13. Dolg, M.; Wedig, U.; Stoll, H.; Preuss, H. *J. Chem. Phys.* **1987**, *86*, 866-872.
14. Schafer, A.; Horn, H.; Ahlrichs, R. *J. Chem. Phys.* **1992**, *97*, 2571-2577.
15. Hehre, W. J.; Radom, L.; Schleyer, P. v R.; Pople, J. A. *Ab Initio Molecular Orbital Theory*; John Wiley & Sons, Inc.: New York, 1986. References cited therein.
16. Yamanaka, M.; Inagaki, A.; Nakamura, E. *J. Comput. Chem.* **2003**, *24*, 1401-1409.
17. (a) Fukui, K. *Acc. Chem. Res.* **1981**, *14*, 363-368. (b) Gonzalez, C.; Schlegel, H. B. *J. Chem. Phys.* **1989**, *90*, 2154-2161. Gonzalez, C.; Schlegel, H. B. *J. Phys. Chem.* **1990**, *94*, 5523-5527.
18. Bigeleisen, J.; Mayer, M. G. *J. Chem. Phys.* **1947**, *15*, 261-267. Bigeleisen, J.; Wolfsberg, M. *Adv. Chem. Phys.* **1958**, *1*, 15-76.
19. Scott, A. P.; Radom, L. *J. Phys. Chem.* **1996**, *100*, 16502-16513.
20. Miertus, S.; Scrocco, E.; Tomasi, J. *J. Chem. Phys.* **1981**, *55*, 117-129. Miertus, E.; Tomasi, J. *J. Chem. Phys.* **1982**, *65*, 239-245. Barone, V.; Cossi, M.; Tomasi, J. *J. Comput. Chem.* **1998**, *19*, 404-417.
21. Reed, A. E.; Weinstock, R. B.; Weinhold, F. *J. Chem. Phys.* **1985**, *83*, 735-746. NBO Version 3.1 in the Gaussian 98 package implemented by Glendening, E. D.; Reed, A. E.; Carpenter, J. E.; Weinhold, F.; University of Wisconsin: Madison, WI, 1990.
22. For examples: Nakamura, E.; Mori, S.; Morokuma, K. *J. Am. Chem. Soc.* **1997**, *119,* 4900-4910; Vellekoop, A. S.; Smith, R. A. J. *J. Am. Chem. Soc.* **1994**, *116,* 2902-2913.
23. The product **5** may undergo reorganization to give polymeric MeCu and Me_2CuLi•LiBr.
24. Dorigo, A. E.; Wanner, J.; Schleyer, P. v. R. *Angew. Chem. Int. Ed.* **1995**, *34*, 476-478; Snyder, J. P. *J. Am. Chem. Soc.* **1995**, *117*, 11025-11026; Nakamura, E.; Yamanaka, M.; Mori, S. *J. Am. Chem. Soc.*

2000, *122*, 1826-1827.

25. Mori, S.; Nakamura, E.; Morokuma, K. *J. Am. Chem. Soc.* **2000**, *122*, 7294-7307.
26. Mori, S.; Nakamura, E. *Tetrahedron Lett.* **1999**, *40*, 5319-5322.
27. Note that computational models with coordination of one Me_2O molecule to each Li atom gave almost the same KIE values (1.039 and 1.027).
28. Singleton, D. A.; Thomas, A. A. *J. Am. Chem. Soc.* **1995**, *117*, 9357-9358; Frantz, D. E.; Singleton, D. A.; Snyder, J. P. *J. Am. Chem. Soc.* **1997**, *119*, 3383-3384.
29. 1-Bromocyclooctene was chosen as a substrate because of its low volatility and the lack of stereochemical issues.
30. Mori, S.; Nakamura, E.; Morokuma, K. *Organometallics* **2004**, *23*, 1081-1088.
31. Lipshutz, B. In *Organometallics in Synthesis: A Manual, 2nd Ed.*, Schlosser, M. Ed.; John Wiley & Sons: Chichester, U.K., 2002.
32. Bandodakar, D. S.; Nagendrappa, G. *Synthesis* **1990**, 843-844.
33. In the reactions with aryl *iodides*, the copper-iodine exchange mechanism is indicated, and utilized further for the preparation of arylcuprate reagents: Whitesides, G. M.; Fischer, W. F., Jr.; San Fillipo, J., Jr.; Bashe, R. W.; House, H. O. *J. Am. Chem. Soc.* **1969**, *91*, 4871-4882; Piazza, C.; Knochel, P. *Angew. Chem. Int. Ed.* **2002**, *43*, 3263.

CHAPTER 3

Lewis Acid Effect on Oxidative Addition of Vinyl/Aryl Halides to Nickel(0) and Palladium(0) Complexes

3-1. Introduction

The oxidative addition of an alkenyl- or an aryl halide to a nickel(0) or a palladium(0) complex is a fundamental organometallic reaction that constitutes the first step in catalytic transformations of C(sp^2)-X bond to C(sp^2)-C or C(sp^2)-heteroatom bond, e.g., a cross-coupling reaction between an sp^2-halide with a main group organometallic reagent (Scheme 1).[1,2] A number of researchers have studied the mechanism of this process not only as a pure elementary reaction[3] but also in the context of catalysis.[4,5,6] While various suggestions have been made on the nature of the reactive metal species in catalytic reactions (e.g., halide-,[4] base-,[5] and amine[6]-ligated Pd^0 species etc), most of them silently assumes that the oxidative addition takes place through a three-centered transition state (**X** in Figure 1), as proposed for the elementary reaction of isolated Pd^0 complex.[3ab,7]

Scheme 1. Conventional Mechanism of Cross-coupling Reaction

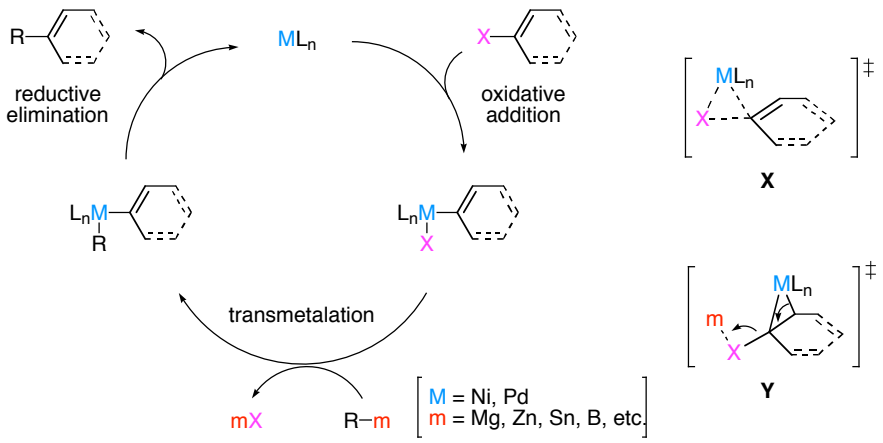

In the mechanistic studies on the nucleophilic substitution reaction between an alkenyl halide and a lithium organocuprate (Chapter 2), we found a new, eliminative mode of C(sp^2)-X

bond oxidative addition, in which the copper and the lithium atoms cooperatively act as a nucleophile and a Lewis acid, respectively. Since Ni^0 and Pd^0 complexes have the same d^{10} electron configuration as the cuprate(I), a similar mechanism (**Y**) might operate in Ni- and Pd-catalyzed cross-coupling reactions if a main group metallic component (Rm and/or mX in Scheme 1) has sufficient Lewis acidity. Here we carried out theoretical studies on the mechanism of oxidative addition of vinyl/aryl halides and related compounds to Ni^0 and Pd^0-bisphosphine complexes with or without coordination of a magnesium chloride, in view of the reaction conditions of Kumada-Tamao-Corriu coupling reaction (cross-coupling reaction between an sp^2-halide with a Grignard reagent).

3-2. Computational Models and Methods

3-2-1. Models

A general framework of the present theoretical study is shown in Scheme 2. Thus, we examined oxidative addition of vinyl- and phenyl halides, ether and sulfide to ML_2-type complexes of Ni^0 and Pd^0 (L: PH_3, PMe_3, $H_2PCH_2CH_2PH_2$ (denoted as dpe)) in the presence of $MgCl_2$•$(S)_n$ (S = OMe_2, n = 1-3). Previous studies have indicated such 14-electron dicoordinated complexes are reactive species in oxidative addition,[3abd] except for some complexes with bulky monodentatae phosphine or *N*-heterocyclic carbene ligands.[3c,8] Reactions of the bidentate complexes Ni(dpe) (**1a**) and Pd(dpe) (**1b**) were most thoroughly studied, and thus described here.[9] Two reaction pathways were examined: Path A represents a typical elementary reaction where only the transition metal participates in the C-X bond cleavage. In path B, $MgCl_2$•$(S)_n$ coordinates to the halogen or the heteroatom of the substrate through dissociation of one solvent molecule to give a bimetallic π-complex, which subsequently undergoes C-X bond cleavage. Stationary points will be referred to as $\mathbf{2a_{vb}}$ (structure number: **2**, central metal: nickel (**a**), substrate: **v**inyl **b**romide), $\mathbf{3b_{pc}}$ (**3**, palladium (**b**), **p**henyl **c**hloride), and so on (for details, see

footnote).[10]

Scheme 2. Oxidative Addition of Vinyl/Aryl Halide or Pseudohalide to ML_2-type Complex in the Presence of $MgCl_2$•$(OMe_2)_n$ (n = 1-3)

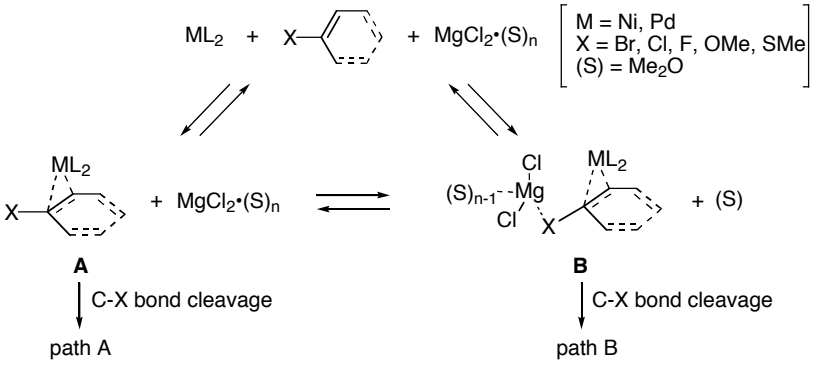

The choice of an appropriate model for a magnesium compound is the most difficult issue in the present study. There have been a number of studies on the structures of Grignard reagents and magnesium salts in ethereal solvents.[11] Most of solid-state structures involve a tetrahedral (four-coordinated) or an octahedral (six-coordinated) Mg center. Solution studies also indicate structures of the coordination number of four to six. The dimer-monomer equilibrium and the Schlenk equilibrium are also common features of organomagnesium chemistry. In spite of such a complicated situation, we employed $MgCl_2$•$(OMe_2)_n$ (n = 1-3) as models of magnesium compounds to study basic reaction pathways with reasonable computational time. It must be noted that models with less Me_2O coordination (n = 1) undoubtedly overestimate the Lewis acidity of the Mg^{II} center in solution, and the artifact works favorably on the bimetallic mechanism (vide infra).

3-2-2. Methods

All calculations were performed with Gaussian 98 and Gaussian 03 packages.[12] The density functional theory (DFT) method was employed using the B3LYP hybrid functional.[13] Geometry optimization was performed with a basis set (denoted as 631LAN) consisting of the LANL2DZ basis set including a double-zeta valence basis set with the Hay and Wadt effective core potential

(ECP) for Ni and Pd[14] and 6-31G(d) basis set for other elements.[15] Each stationary point was adequately characterized by normal coordinate analysis. The intrinsic reaction coordinate (IRC) analysis[16] was carried out to confirm that stationary points are smoothly connected to each other. Equilibrium and kinetic isotope effects (EIEs and KIEs) were calculated by Bigeleisen-Mayer's equation[17] with Wigner tunnel correction using frequencies scaled by 0.9614.[18]

Throughout this chapter, energetics will be discussed on the basis of the Gibbs free energy. However, it must be noted that one should not discuss about competition of two reaction pathways (with and without $MgCl_2$ complexation) simply by comparison of free energies ($\Delta G^{\ddagger}_{\mathrm{mono}}$ and $\Delta G^{\ddagger}_{\mathrm{di}}$ in Figure 1). Consider a kinetic situation as shown in Figure 1. Rates of monometallic and bimetallic oxidative addition will be:

$$r_{\mathrm{mono}} = k_{\mathrm{mono}}[\mathrm{A}], \quad r_{\mathrm{di}} = k_{\mathrm{di}}[\mathrm{B}] = \frac{Kk_{\mathrm{di}}[\mathrm{MgCl_2} \bullet (\mathrm{S})_{\mathrm{n}}][\mathrm{A}]}{[\mathrm{S}]}$$

Thus, the ratio of these reaction rates is

$$\frac{r_{\mathrm{mono}}}{r_{\mathrm{di}}} = \frac{k_{\mathrm{mono}}}{Kk_{\mathrm{di}}} \bullet \frac{[\mathrm{S}]}{[\mathrm{MgCl_2} \bullet (\mathrm{S})_{\mathrm{n}}]}$$

Under usual reaction conditions, the Mg concentration is much lower than the solvent concentration. Therefore, for the bimetallic pathway to be feasible, Kk_{di} ($\Delta G^{\ddagger}_{\mathrm{di}}$) must be *much* larger (smaller) than k_{mono} ($\Delta G^{\ddagger}_{\mathrm{mono}}$). For example, when [S] = 12.3 M (the value for THF) and $[MgCl_2 \bullet (S)_n]$ = 0.1 M are assumed, Kk_{di} must be 123 times larger than k_{mono} for the bimetallic pathway to compete with the monometallic pathway at an equal rate. This corresponds to ca. 2.8-kcal/mol Gibbs free energy difference at 298 K.

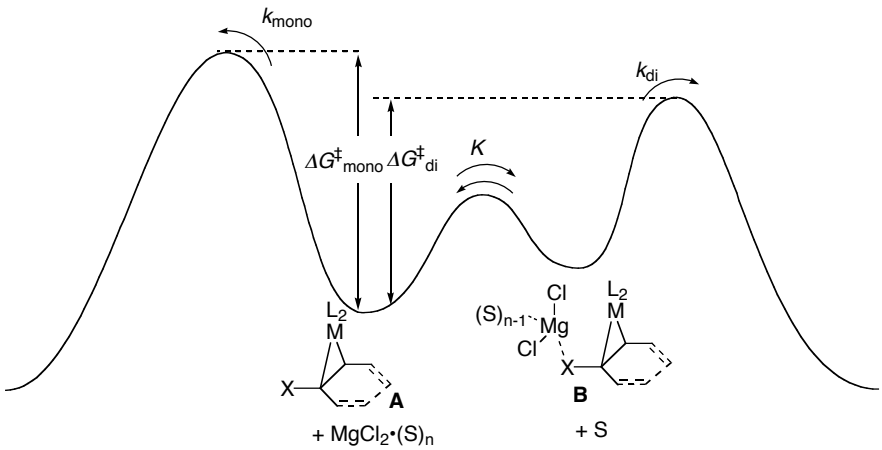

Figure 1. Schematic illustration of competition between monometallic and bimetallic pathways

3-3. Oxidative Addition of Vinyl/Aryl Halide to Ni^0 Complex

First, we examined oxidative addition of vinyl halides (X = Br, Cl and F), ether (X = OMe) and sulfide (X = SMe) to Ni(dpe) **1a** (Scheme 3, Figure 2). The complex **1a** and the substrate form a π-complex **2** with significant stabilization (20-25 kcal/mol). A three-centered transition state (TS) **3** was expectedly located as the only TS for C-X bond cleavage (oxidative addition) from **2**. The activation barriers are lowest for vinyl bromide (14.2 kcal/mol), moderate for vinyl chloride and sulfide (ca. 20 kcal/mol) and very high for vinyl fluoride and ether (> 35 kcal/mol). The TS **3** affords a square-planar Ni^{II} complex **4** as a product. Noteworthy is the stability of the oxidative addition product **4** relative to the π-complex **2**. While **4** is more stable than **2** for vinyl bromide and chloride (Figure 2ab), other substrates (X = F, OMe, SMe) showed endothermic energy profiles (Figure 2c-e). Such energy balance should depend on the strength of the C-X bond and the affinity of the leaving group X to the Ni center.

Scheme 3. Oxidative Addition of Vinyl/Aryl Halide or Pseudohalide and Pseudohalides to M(dpe) (M = Ni, Pd) with or without Coordination of $MgCl_2$ to the Leaving Group.

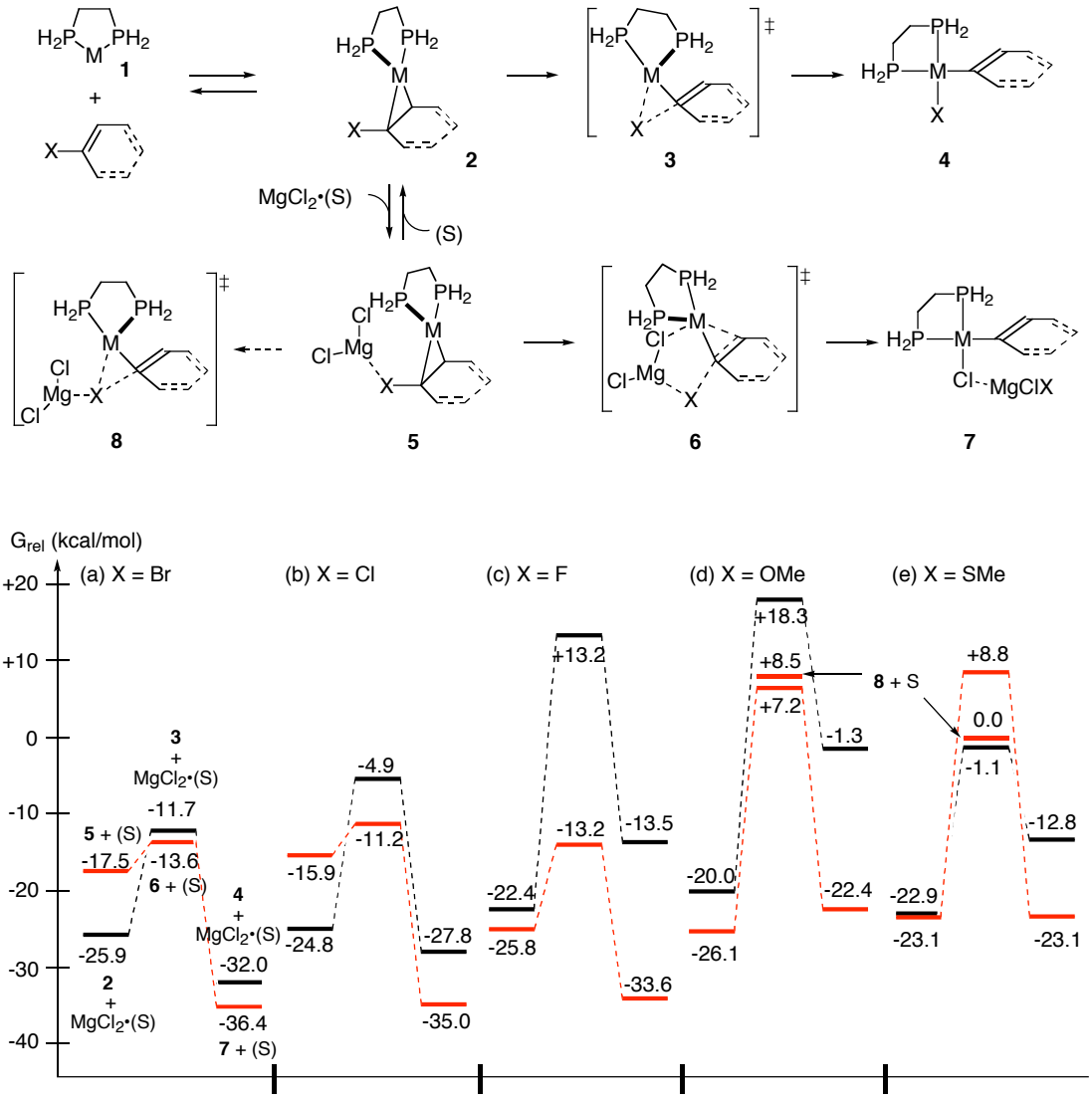

Figure 2. Free energy profiles for oxidative addition of vinyl halides and pseudohalides to Ni(dpe) with (red) or without (black) coordination of $MgCl_2$. Energies (kcal/mol) are relative to [Ni(dpe) + substrate + $MgCl_2$•(S)].

By dissociation of a Me_2O molecule, $MgCl_2$ coordinates to the halogen or the heteroatom X of **2** to give a Ni/Mg bimetallic complex **5**. This process is unfavorable for vinyl bromide and chloride and slightly favorable for vinyl fluoride and ether, reflecting Lewis basicity of the atom X relative to the solvent (Me_2O).[19] As with the cuprate reaction (Chapter 2), the coordination of $MgCl_2$ opens up an eliminative mode of C-X bond cleavage (TS **6**). While the Mg atom captures the leaving group X, the chloride anion that is originally bonded to the Mg atom is transferred to

the Ni center to afford an oxidative addition product **7**.[20] When the leaving group is a halide ion (Br, Cl, F), only the eliminative TS is located as a C-X cleavage TS. On the other hand, when X = OMe or SMe, a three-centered TS **8** is also located (Scheme 3).

One can immediately notice that the activation barriers for the eliminative C-X (X = halogen) bond cleavage (**5** -> **6**) are much lower than those of the three-centered oxidative addition (**2** -> **3**, Figure 2a-c). The most dramatic effect appeared in the case of vinyl fluoride, reflecting the strong Mg-F bond energy:[21] The activation energy decreased from 35.6 to 12.6 kcal/mol. The energy profiles for vinyl ether and sulfide are different. The activation energy for vinyl ether did not decrease very much (Figure 2d). For vinyl sulfide, the activation barrier (for the eliminative path) even increased from that of the three-centered path (Figure 2e). It is also noted that the thermodynamics of oxidative addition becomes to favor the product side upon complexation with $MgCl_2$.

The origin of the different energy profiles between vinyl halides and vinyl ether/sulfide can be explained as follows: Because a halide anion is isotopic by nature, the Mg atom can coordinate to the leaving halide anion from any direction. On the contrary, an alkoxide or a sulfide ion forms an anisotropic field of negative charge, which limits suitable approach of the Mg atom.

Selected structures of stationary points are shown in Figure 3. Comparison of π-complexes **2** indicates that the back-donation from the Ni center to the olefinic moiety is stronger for vinyl bromide and chloride, and weaker for vinyl ether and sulfide. The geometries of oxidative addition TSs **3** are much different with respect to the Ni-C^2 distance and the dihedral angle of the P-Ni-P and the Ni-C^1-X planes. The shorter Ni-C^2 distances and smaller dihedral angles of $\mathbf{3a_{vb}}$ and $\mathbf{3a_{vc}}$ (<2.5 Å, ~110°) than that of the rest (≥2.7 Å, ≥140°) indicate that the former TSs are much earlier than the latter: Thus, the "clockwise" rotation of the P-Ni-P moiety is less advanced in $\mathbf{3a_{vb}}$ and $\mathbf{3a_{vc}}$ (see Chapter 2). In the eliminative TSs (**6**), the interaction between the Ni center

and the C^2 atom is kept as demonstrated in the cuprate reaction: The phosphorous atoms and the olefinic carbon atoms are almost in the same plane in the TSs (dihedral angles between the P-Ni-P and the C^1-Ni-C^2 plane are 13-17°).

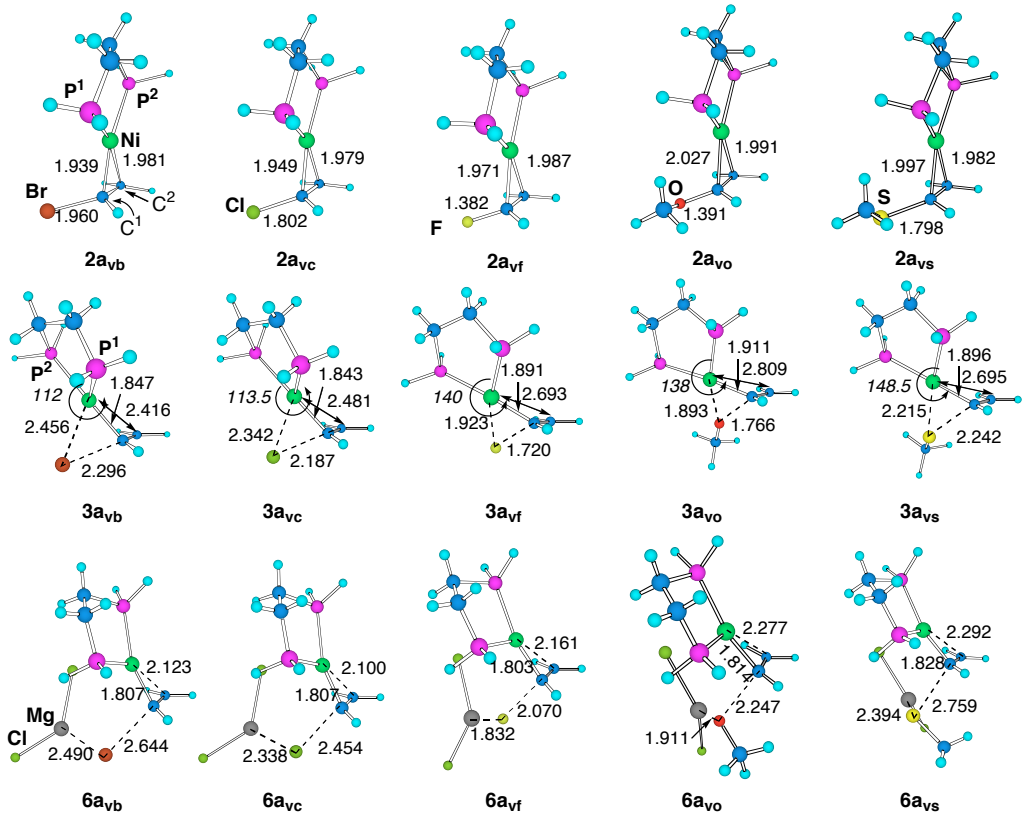

Figure 3. Selected stationary points for oxidative addition of vinyl halides to Ni(dpe). Strutures are shown in the Ni-C^1-X plane. Numbers refer to bond length (Å) and dihedral angles between the P-Ni-P and Ni-C^1-X planes (italic, degrees).

Next, oxidative addition of phenyl halide, ether, and sulfide was examined (Scheme 3, Figure 4, 5). The reaction pathways were essentially the same as that of vinyl halides and related compounds: Without the coordination of $MgCl_2$, a three-centered TS **3** was again located as the only TS for oxidative addition. When X is Br or Cl, the π-complex **2** spontaneously collapsed to the oxidative addition product **7** upon complexation with $MgCl_2$. For other substrates, effects of $MgCl_2$ coordination were similar to that for their vinyl counterparts (Figures 3 and 4). The major difference of the reactions of the phenyl substrates from that of the vinyl substrates is smaller π-complexation energy, which reflects the weaker acceptor ability of an aromatic C-C bond than an

olefinic C-C bond.

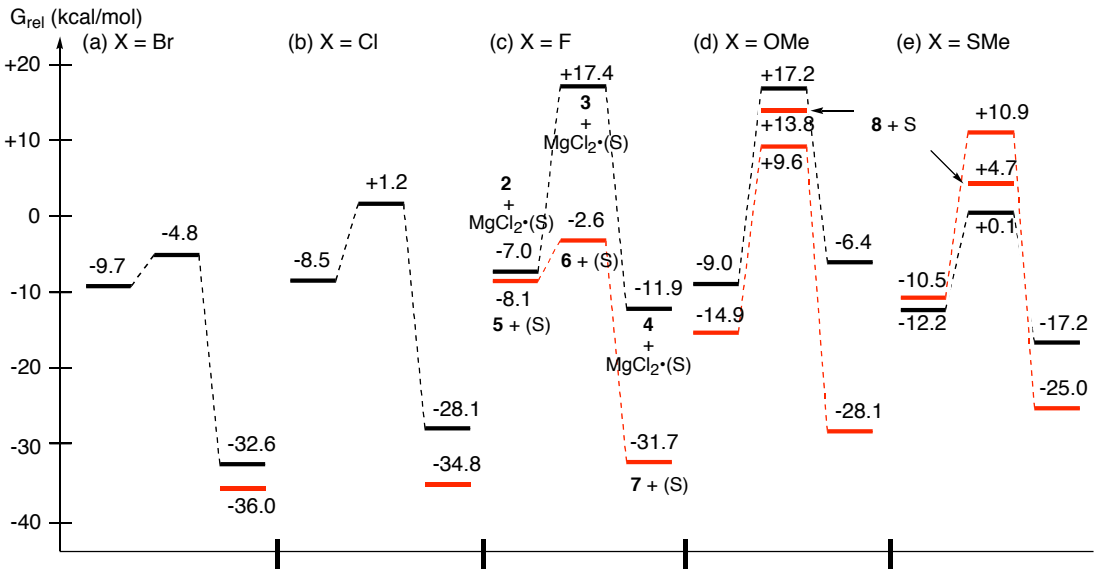

Figure 4. Free energy profiles for oxidative addition of vinyl halides to Ni(dpe) with (red) or without (black) coordination of $MgCl_2$. Energies (kcal/mol) are relative to [Ni(dpe) + substrate + $MgCl_2$•(S)].

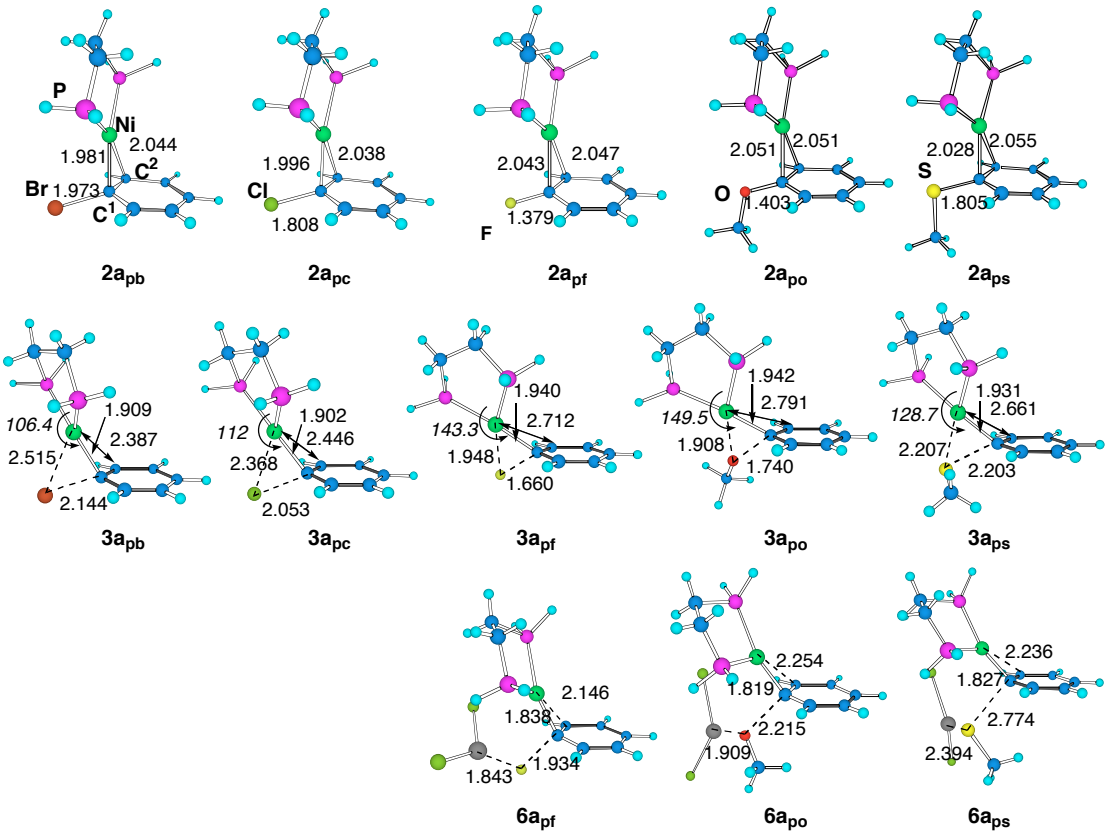

Figure 5. Selected stationary points for oxidative addition of aryl halides to Ni(dpe). Structures are in the Ni-C^1-X plane. Numbers refer to bond lengths (Å) and dihedral angles between the P-Ni-P and Ni-C^1-X planes (italic, degrees).

As shown in Figure 5, the structures of stationary points of the aryl halide reactions are very similar to that of the vinyl halide reactions (Figure 3), except for slightly longer Ni-C bond lengths.

Next, we added one more Me_2O molecule to the computational model, and examined the reactions of vinyl bromide, chloride and fluoride (Scheme 4, Figure 6). The π-complex **2** and $MgCl_2$•$2Me_2O$ form a complex **9** with dissociation of one Me_2O molecule. The complex **9** undergoes eliminative C-X bond cleavage via an eliminative TS **10** (three-centered TS not located). The magnesium atom is tetra-coordinated throughout the reaction pathway. The energy profiles in Figure 6 are not different very much from that of previous systems (Figure 1): The relative energies of Ni/Mg bimetallic eliminative TSs are close to (X = Br) or lower than (X = Cl, F) that of three-centered TSs.

Scheme 4.

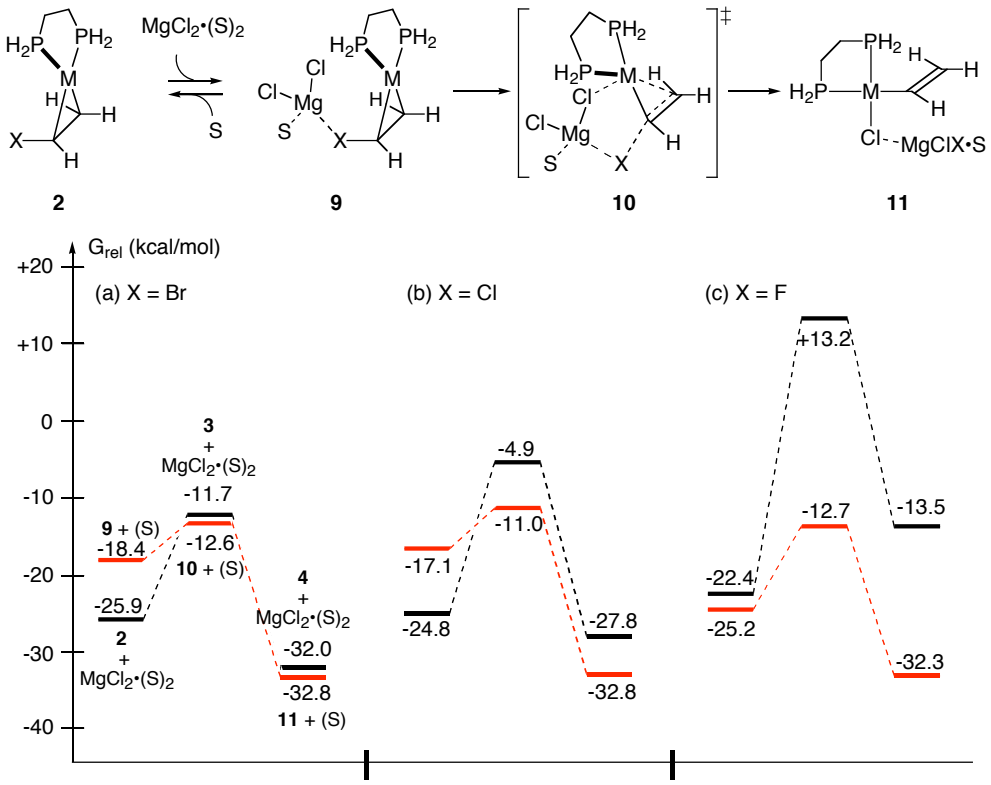

Figure 6. Free energy profiles for oxidative addition of vinyl bromide (a), chloride (b) and fluoride (c) to Ni(dpe) with (red) or without (black) coordination of $MgCl_2$•(S). Energies are relative to [Ni(dpe) + substrate + $MgCl_2$•$(S)_2$].

Further addition of a Me_2O molecule to the computational model that gives a penta-coordinated Mg center (n = 3 in Scheme 2), significantly affected relative energies of oxidative addition TSs of vinyl halides (only TSs were optimized). Free energy of a bimetallic eliminative TS relative to the three-centered TS has become positive (+4.7 kcal/mol) for X = Br, very small (-1.3 kcal/mol) for X = Cl and still largely negative (-23.0 kcal/mol) for X = F. Thus, in the actual Kumada coupling reaction, the bimetallic pathway is likely to dominantly operate for vinyl/aryl fluorides, and compete with the monometallic pathway for vinyl/aryl chlorides.

3-4. Oxidative Addition of Vinyl/Aryl Halide to Pd^0 Complex

Next, we studied oxidative addition of vinyl/aryl halides and pseudohalides to Pd(dpe) (Scheme 3, Figures 7, 8). The reaction pathways are essentially the same as that of Ni(dpe): Without coordination of $MgCl_2$, only a three-centered TS **3** was located. Upon complexation with $MgCl_2$, the reaction pathway switched to the eliminative one when the leaving group X is a halide, and both an eliminative and a three-centered TS were obtained when X is an alkoxide or a sulfide. As compared with the Ni reactions, the Pd reactions are characterized by lower π-complexation energies (10-20 kcal/mol difference) and higher activation energies (5-15 kcal/mol difference), which agree with known reactivity profiles.

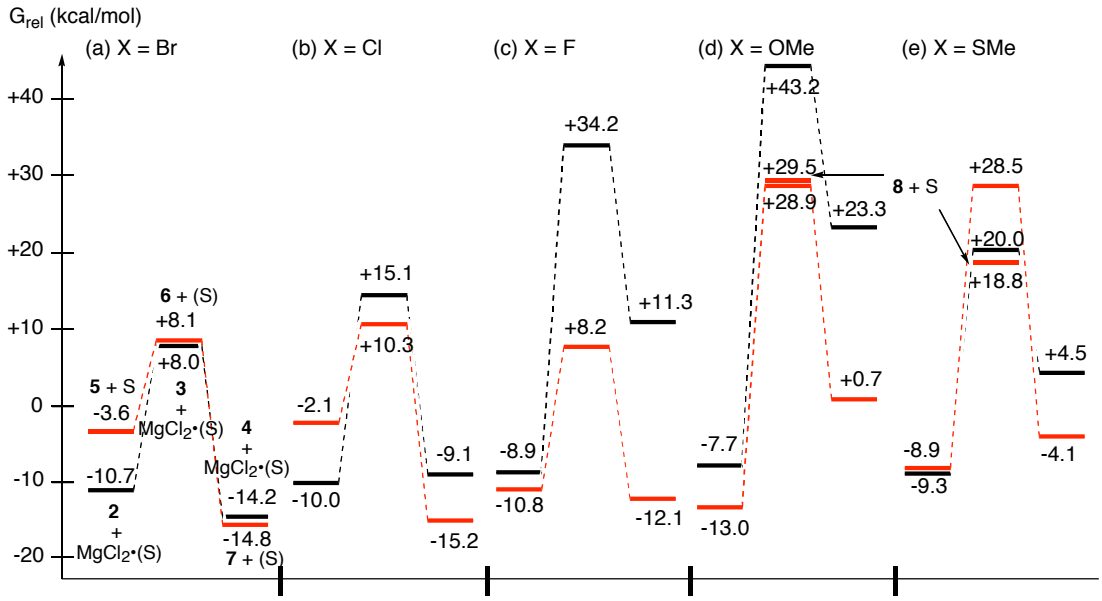

Figure 7. Free energy profile for oxidative addition of vinyl halides to Pd(dpe) with (red) or without (black) coordination of $MgCl_2$. Energies (kcal/mol) are relative to [Pd(dpe) + substrate + $MgCl_2$•(S)].

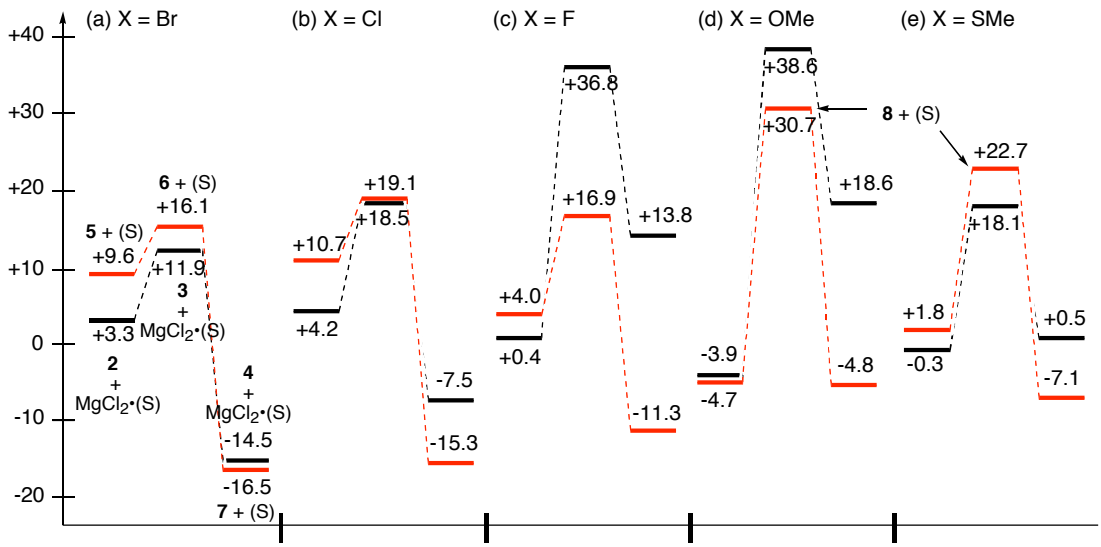

Figure 8. Free energy profile for oxidative addition of aryl halides to Pd(dpe) with (red) or without (black) coordination of $MgCl_2$. Energies (kcal/mol) are relative to [Pd(dpe) + substrate + $MgCl_2$•(S)]. Energy levels of TSs **7** and **8** are same for X = OMe. An eliminative TS **7** could not be located for X = SMe.

Figure 9 shows selected TS structures of oxidative addition. These TSs have much later character than that of the Ni reactions (Figures 3 and 5), as judged from the following structural features: For the three-centered TSs, the dihedral angles between the P-M-P and the M-C-X plane

are much larger in the Pd case (e.g., 128.8°, 165.5° and 174.5° for **2b**$_{vb}$, **2b**$_{vf}$ and **2b**$_{vo}$, respectively) than in the Ni case (112°, 140° and 138° for **2a**$_{vb}$, **2a**$_{vf}$ and **2a**$_{vo}$, respectively). For the eliminative TSs, the C^2-C^1-M angles are larger in the Pd case (89.5°, 92.2° and 97.8° for **6b**$_{vb}$, **6b**$_{vf}$ and **6b**$_{vo}$, respectively) than in the Ni case (82.8°, 85.0° and 90.6° for **6a**$_{vb}$, **6a**$_{vf}$ and **6a**$_{vo}$, respectively).

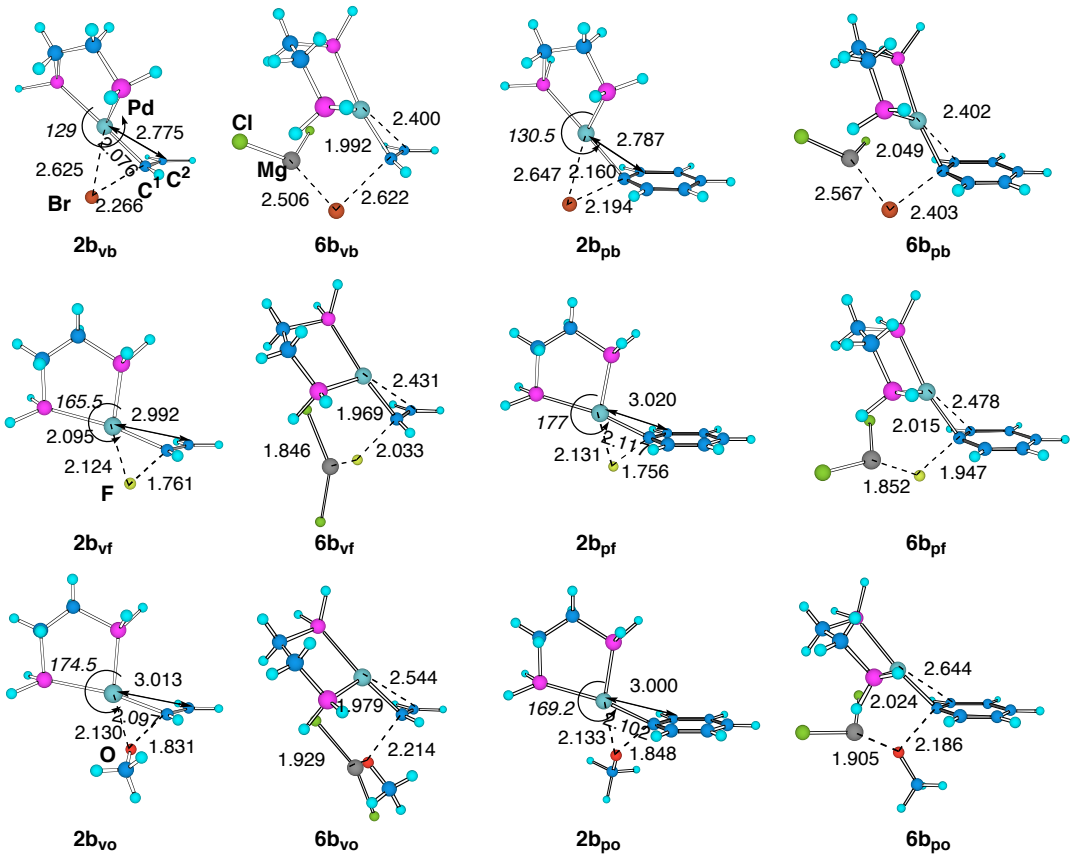

Figure 9. Selected stationary points in oxidative addition of vinyl/aryl halides to Pd(dpe). Structures are shown in the Pd-C^1-X plane. Numbers refer to bond lengths (Å) and dihedral angles between the P-Pd-P and the Pd-C^1-X planes (italic, degrees).

The effect of additional solvent coordination was also examined (Scheme 4, Figure 9). Being similar to those in the Ni reactions (Figure 6), relative energies of Ni/Mg bimetallic eliminative TSs **10** are comparable with (X = Br) or lower than (X = Cl, F) that of the three-centered TSs **3**. Upon further addition of a Me_2O molecule, the bimetallic pathway became less favorable (n = 3 in Scheme 2): The free energies of eliminative oxidative addition TSs relative to three-centered

TSs are +6.9, +1.3 and –23.5 kcal/mol for X = Br, Cl and F, respectively. Thus, only vinyl fluoride definitely favors the bimetallic pathway.

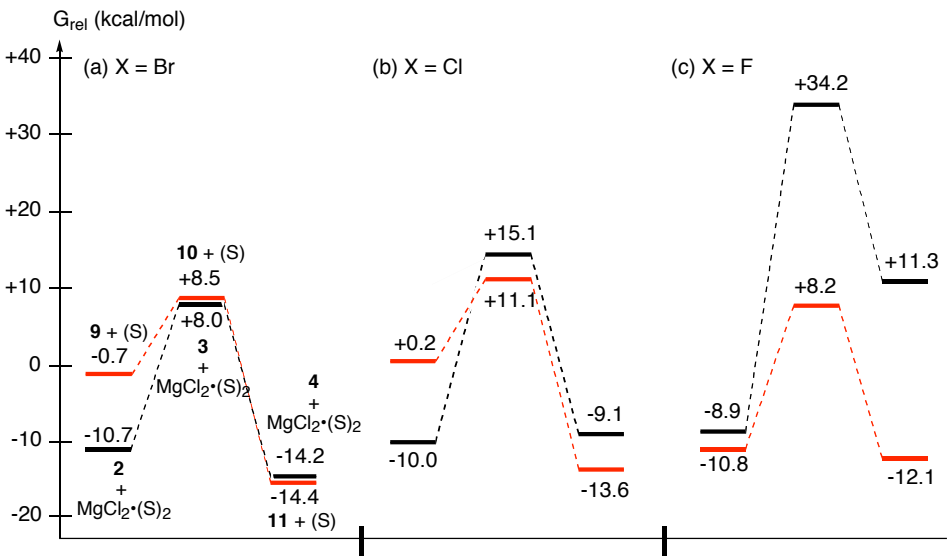

Figure 10. Free energy profiles for oxidative addition of vinyl bromide (a), chloride (b) and fluoride (c) to Pd(dpe) with (red) or without (black) coordination of $MgCl_2$•(S). Energies are relative to [Pd(dpe) + substrate + $MgCl_2$•$(S)_2$].

3-5. Kinetic Isotope Effects

Measurement of $^{12}C/^{13}C$ kinetic isotope effects (KIEs) using a reactant of natural abundance provides invaluable information on the mechanism of organic and organometallic reactions.[22,23] For a catalytic reaction, KIEs measured for a certain substrate reflects a catalytic step where the substrate is irreversibly converted into a catalytic intermediate (note that it is not necessarily the rate-limiting step of the whole catalytic cycle). Here we carried out $^{12}C/^{13}C$ KIE measurements for Ni- and Pd-catalyzed cross-coupling reactions between sp^2-halides and Grignard reagents. The change in ^{13}C isotopic composition in an sp^2-halide before and after the reaction of 80-90% conversion was analyzed by quantitative ^{13}C NMR measurments (Figure 11).

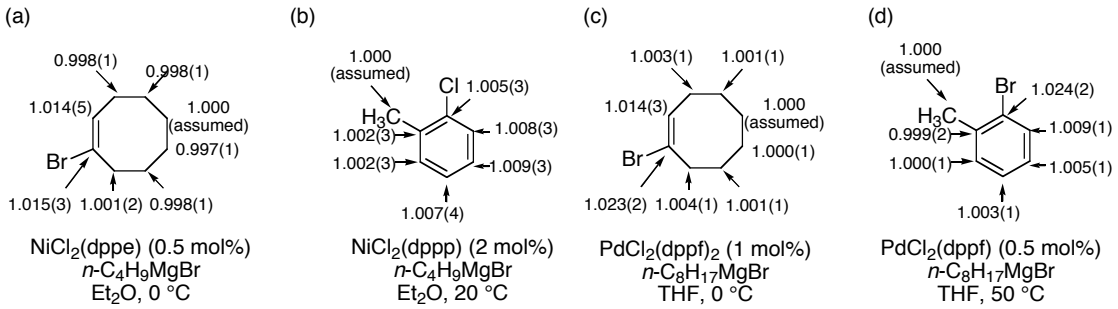

Figure 11. $^{12}C/^{13}C$ Kinetic isotope effects for Ni- and Pd-catalyzed cross-coupling reactions between sp^2-halides with Grignard reagents. Experimental errors in the last digit were shown in parentheses. Reaction conditions are described under substrate formulae (for details, see Experimental Section).

The Ni-catalyzed reaction of 1-bromocyclooctene giving 1-butylcyclooctene showed equal magnitudes of KIEs on the two olefinic carbon atoms (C^1: 1.015; C^2: 1.014) (Figure 11a). This suggests that the KIEs reflect the π-complexation, not the C-Br bond cleavage step. Because the complexation energy between a Ni^0-bidentate phosphine complex and an alkenyl halide is very large (vide infra),[24] once a π-complex is formed, it undergoes C-Br bond cleavage before dissociation and exchange of the alkenyl halide (Scheme 5a). Isotope effects for an equilibrium between [Ni(dpe) + 1-bromocyclooctene] and Ni(dpe)/1-bromocyclooctene π-complex was calculated to be 1.011 at both C^1 and C^2 atoms, the magnitude of which supports the above interpretation of the experimental KIE values. Note that "NiL_2" in Scheme 5 would not be a naked NiL_2, but be coordinated by a solvent, a product, and so on.

Scheme 5. Schematic Illustration of Kinetics of Vinyl/aryl Halide Transforming Step in Ni-catalyzed Kumada Coupling Reaction.

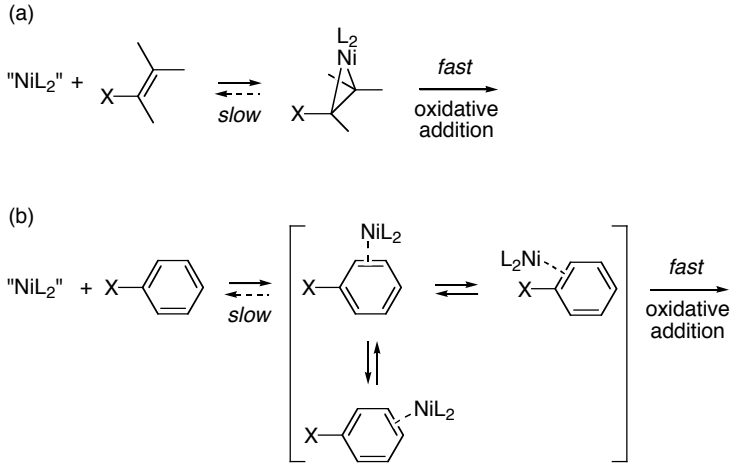

The Ni-catalyzed cross coupling reaction of 1-chloro-2-methylbenzene showed rather small but positive KIE values (1.005-1.009) on C^1, C^4, C^5 and C^6 (Figure 11b). The smaller KIE value on C^1 and the large difference between C^2/C^3 and C^5/C^6 again indicate that the KIE does not reflect the C^1-Cl bond cleavage process but reflects π-complexation of an Ni^0 intermediate to the aromatic π-system (Scheme 5b). Intramolecular migration of the Ni atom on the aromatic ring and subsequent C-Cl bond cleavage should be faster than the dissociation of the substrate. The larger KIE values at C^4-C^6 atoms indicate preferential complexation at sterically less hindered moieties. While the presence of a Ni^0 (Pd^0)-haloarene η^2-complex in cross-coupling reactions is often ignored in mechanistic considerations,[25] the above result clearly shows that such a complex is in fact on the reaction coordinate of aryl C-X bond cleavage. The KIE data also exclude a single-electron transfer mechanism in the present reaction.[26]

The intramolecular equilibrium process suggested above was computationally studied (Scheme 6). In fact, the migration of Ni atom on the aromatic ring requires very small activation energies, which indicates complete equilibration of isomeric η^2-complexes. For all η^2-isomers, EIEs on the coordinated carbon atoms were calculated to be ca. 1.01, which is comparable to experimental KIE values on the less hindered side of the aromatic ring.

Scheme 6. Intramolecular Equilibrium among Ni(dpe)/Chlorobenzene η^2-Complexes[a]

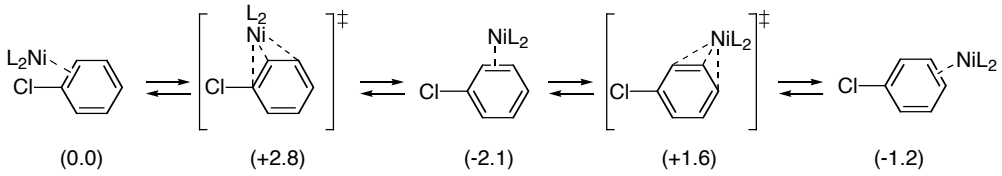

[a] The numbers in parentheses refer to relative energies in kcal/mol.

The Pd-catalyzed reactions showed different KIE profiles (Figure 11cd). The reaction of 1-bromocyclooctene exhibited a sizable KIE at C^1 (1.023) as well as at C^2 (1.014) (Figure 11c). Since Pd^0 is much less d-electron-donating than Ni^0 (vide infra),[24] we consider that the C-Br cleavage is now a slow process and the initial π-complexation is reversible in the Pd catalysis. The reaction of 1-bromo-2-methylbenzene showed a much larger KIE (1.024) at C^1 than on the other carbon atoms (e.g., 1.009 on C^6), indicating that the C-Br cleavage is the first irreversible step in the catalytic cycle (Figure 11d). Notably, however, the KIEs are unsymmetrical with respect to the benzene ring as in the Ni case, which may reflect that π-complexation takes place favorably at the less hindered side of the aromatic ring.

Transition states for oxidative addition of 1-bromocyclooctene to Pd(dpe), with or without coordination of $MgCl_2$•OMe_2, were located, and KIEs for both TSs were calculated (Figure 12). The KIE values for both TSs are not very different from each other, and almost equally deviated from the experimental values (Figure 11c). Thus, at the present stage, it is difficult to experimentally conclude which mechanism is operating in the reaction while the theoretical studies in the foregoing section indicated that the monometallic pathway operates.

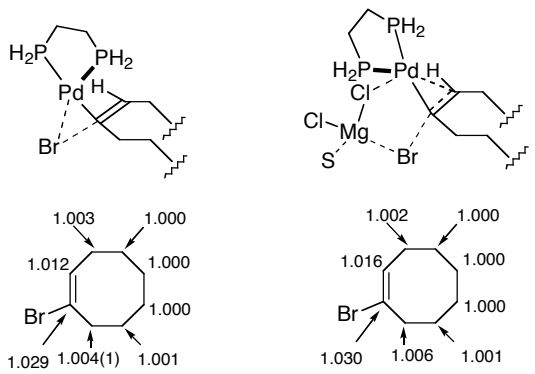

Figure 12. Calculated $^{12}C/^{13}C$ KIEs for oxidative addition of 1-bromocyclooctene to Pd(dpe) with (right) or without (left) coordination of $MgCl_2$•OMe_2.

3-6. Summary

In summary, we have established the "eliminative" carbon-halogen bond cleavage as a generally possible mechanism for oxidative addition of an sp^2-halide to nickel(0) and palladium(0) complexes in the presence of a magnesium salt. While the three-centered pathway is the only possible mechanism for a single metal elementary reaction (except for a radical mechanism), coordination of a Lewis acidic Mg atom switches the mechanism to the eliminative one. The extent of the Mg effect largely depends on the affinity of the Mg^{II} center to the leaving group: Thus, the most dramatic effect was observed for the reaction of vinyl/aryl fluorides. In contrast to the reactions of halide substrates, upon complexation with $MgCl_2$, $C(sp^2)$-heteroatom (O, S) bonds do not favor the eliminative mechanism very much since the anisotropic nature of the alkoxide and sulfide anions prevents the Mg center to effectively trap the negative charge in the eliminative TS. While the KIE experiments did not attain the initial purpose (i.e., discrimination of monometallic and bimetallic mechanisms), they have shown the different behavior of Ni^0 and Pd^0 complexes in oxidative addition. Further theoretical/experimental studies will demonstrate generality and viability of the present mechanistic framework in various cross-coupling reactions.

Experimental Section

General.

All reactions dealing with air- or moisture-sensitive compounds were carried out in oven-dried reaction vessels under argon or nitrogen atmosphere. ^{1}H and ^{13}C nuclear magnetic resonance (NMR) spectra were measured on JEOL EX-400 or Bruker DRX500 instruments. Gas chromatographic (GLC) analysis was performed on a Shimadzu 14A, machine equipped with a glass capillary column (0.25-mm i.d.x 25 m) coated with HR-1. Recycle preparative gel permeation chromatography (GPC) was performed on a Japan Analytical Industry LC-908 machine equipped with GPC columns (JAIGEL 1H and 2H) and an RI detector RI-5HC using chloroform as eluent (flow rate 3.5 mL/min). Anhydrous diethyl ether and THF were purchased from KANTO Inc. and stored over MS4A under nitrogen. $NiCl_2$(dppe) (dppe = 1,2-bis(diphenylphosphino)ethane) and $NiCl_2$(dppp) (dppp = 1,3-bis(diphenylphosphino)propane) were prepared according to the literature.[27] $PdCl_2$(dppf)•CH_2Cl_2 (dppf = 1,1'-bis(diphenylphosphino)ferrocene) was purchased from ACROS Chemical and used as received. 1-Chloro-2-methylbenzene and 1-bromo-2-methylbenzene were purchased from KANTO Inc. and distilled before use. 1-Bromocyclooctene was prepared by dibromination of cyclooctene and subsequent dehydrobromination with morpholine/DMSO.[28] Grignard reagents (*n*-C_4H_9MgBr/Et_2O and *n*-$C_8H_{17}MgBr$/THF) were prepared from corresponding halides and magnesium turnings, and titrated before use.

Nickel-catalyzed cross-coupling reaction of 1-chloro-2-methylbenzene and *n*-butylmagnesium bromide.

To a suspension of $NiCl_2$(dppp) (1.084 g, 2.00 mmol), 1-chloro-2-methylbenzene (12.67 g, 100.1 mmol), decane (1.404 g, 9.87 mmol) in Et_2O (124 mL) was added *n*-butylmagnesium bromide in Et_2O (1.57 M, 76.4 mL, 120.0 mmol). After complete addition, aliquots were taken

periodically and checked by GLC. The temperature was 20-22 °C during the reaction. The reaction was quenched after 25 h by the addition of 10 mL of saturated NH_4Cl/H_2O solution. After quenching, the crude mixture was analyzed by GLC to determine percent completion (87.7 ± 0.4%). The mixture was passed through a pad of Florisil. The organic layer was washed with 50 mL of aq. NH_4Cl, and 50 mL of brine, then dried over $MgSO_4$ and concentrated under reduced pressure. The crude product was distilled under vacuum to collect a fraction of low boiling point (including mainly 1-chloro-2-methylbenzene and decane), which was further purified by GPC to recover 1- chloro-2-methylbenzene (>98% pure by GLC).

Nickel-catalyzed cross-coupling reaction of 1-bromocyclooctene and *n*-butylmagnesium bromide.

A suspension of $NiCl_2$(dppe) (132.6 mg, 0.25 mmol), 1-bromocyclooctene (9.53 g, 50.4 mmol), decane (720.6 mg, 5.06 mmol) in Et_2O (133 mL) was cooled at 0 °C in an ice bath. To this was added *n*-butylmagnesium bromide in Et_2O (1.57 M, 33.4 mL, 52.4 mmol, also cooled). Aliquots were taken periodically and checked by GLC. The reaction was quenched after 100 min by the addition of 7.5 mL of saturated NH_4Cl/H_2O solution. After quenching, the crude mixture was analyzed by GLC to determine percent completion (84.9 ± 1.2%). Similar workup and purification procedures as above were applied to recover 1-bromocyclooctene (> 99% pure by GLC).

Palladium-catalyzed reaction of 1-bromo-2-methylbenzene and *n*-octylmagnesium bromide.

To a suspension of $PdCl_2$(dppf)•CH_2Cl_2 (328.5 mg, 0.40 mmol), 1-bromo-2-methylbenzene (13.66 g, 79.8 mmol), decane (1.15 g, 8.08 mmol) and hexadecane (1.77 g, 7.81 mmol) in THF (57 mL) was added *n*-octylmagnesium bromide in THF (0.93 M, 103 mL, 95.8 mmol. After complete addition, the resulting solution was warmed at 50 °C and aliquots were taken

periodically and checked by GLC. The reaction was quenched after 2 h by the addition of 10 mL of saturated NH_4Cl/H_2O solution. After quenching, the crude mixture was analyzed by GLC to determine percent completion (92.6 ± 0.2%). Similar workup and purification procedures as above were applied to recover 1-bromo-2-methylbenzene (> 99% pure by GLC).

Palladium-catalyzed reaction of 1-bromocyclooctene and *n*-octylmagnesium bromide.

A suspension of $PdCl_2(dppf)\bullet CH_2Cl_2$ (410.0 mg, 0.502 mmol), 1-bromocyclooctene (9.61 g, 50.8 mmol), decane (729 mg, 5.12 mmol) and hexadecane (1.09 g, 4.81 mmol) in THF (108 mL) was warmed to 50 °C. To this was added *n*-octylmagnesium bromide in THF (0.93 M, 59.1 mL, 55.0 mmol). Aliquots were taken periodically and checked by GLC. The reaction was quenched after 4 h by the addition of 7.5 mL of saturated NH_4Cl/H_2O solution. After quenching, the crude mixture was analyzed by GLC to determine percent completion (90.5±0.4%). Similar workup and purification procedures as above were applied to recover 1-bromo-2-methylbenzene (> 98% pure by GLC).

NMR measurements

The NMR samples were prepared as follows: A 5 mm NMR tube was charged with ca. 500 mg of substrate, and then deuterated solvent (acetone-d_6 for 1-chloro-2-methylbenzene and 1-bromo-2-methylbenzene, C_6D_6 for 1-bromocyclooctene) was added to a constant height of 4 cm. The solution was evacuated by freeze-thaw cycle (> 5 times) and sealed under vacuum. A T_1 determination by the inversion-recovery method was carried out on each NMR sample.

The ^{13}C NMR spectra were recorded at 125 Hz on a Bruker DRX500 NMR spectrometer with inverse gate decoupling, calibrated $2\pi/9$ pulses and pulse delays of > $5T_1$ (360, 170, 90 s for 1-chloro-2-methylbenzene, 1-bromo-2-methylbenzene, 1-bromocyclooctene, respectively). 256K points were collected, which was zero-filled to 512K points before Fourier transformation. A

zeroth-order baseline correction was applied. Integrations were determined by using a constant range of ±2.5 Hz around each peak. The measurements were performed for three times for each sample.

Results

The carbon atoms, of which isotopic compositions were assumed not to change during reaction, were employed as "internal standard" for ^{13}C integrations (methyl carbon for 1-chloro-2-methylbenzene and 1-bromo-2-methylbenzene, C^5 atom for 1-bromocyclooctene). The average integrations are shown below with their standard deviations. The ^{13}C KIE values were calculated according to the following equation (F is the fraction conversion and R_0 and R are integrations of starting and recovered materials, respectively).[22]

$$KIE_{calcd} = \ln(1-F)/\ln[(1-F)R/R_0]$$

For the derivation of the standard deviation, see ref. 22.

Table S1. ^{13}C Integrations and $^{12}C/^{13}C$ KIEs for Ni-catalyzed reaction of 1-chloro-2-methylbenzene with *n*-C_4H_9MgBr.

	C^1	C^2	C^3	C^4	C^5	C^6	C(Me)
standard	993.0 (4.7)	1007.6 (5.3)	1007.8 (4.4)	995.6 (5.7)	1005.1 (5.3)	990.0 (3.6)	1000
recovered (87.7%)	1002.5 (4.6)	1011.9 (4.4)	1011.8 (5.1)	1010.8 (5.4)	1023.3 (4.6)	1005.7 (5.1)	1000
R/R_0	1.010 (0.007)	1.004 (0.007)	1.004 (0.007)	1.015 (0.008)	1.018 (0.007)	1.016 (0.006)	1.000
$^{12}C/^{13}C$ KIE	1.005 (0.003)	1.002 (0.003)	1.002 (0.003)	1.007 (0.004)	1.009 (0.003)	1.008 (0.003)	1.000

Table S2. ^{13}C Integrations and $^{12}C/^{13}C$ KIEs for Pd-catalyzed reaction of 1-bromo-2-methylbenzene with *n*-$C_8H_{17}MgBr$.

	C^1	C^2	C^3	C^4	C^5	C^6	C(Me)
standard	1003.4 (2.8)	1011.5 (4.5)	1012.9 (1.0)	1024.4 (1.3)	1003.4 (2.4)	985.9 (1.7)	1000
recovered (92.6%)	1067.3 (4.0)	1007.6 (2.7)	1013.6 (3.4)	1032.5 (2.5)	1015.2 (0.9)	1010.3 (3.2)	1000
R/R_0	1.064 (0.005)	0.996 (0.005)	1.001 (0.004)	1.008 (0.003)	1.012 (0.003)	1.025 (0.004)	1.000
$^{12}C/^{13}C$ KIE	1.024 (0.002)	0.998 (0.002)	1.000 (0.001)	1.003 (0.001)	1.005 (0.001)	1.009 (0.001)	1.000

Table S3. ^{13}C Integrations and $^{12}C/^{13}C$ KIEs for Ni- or Pd-catalyzed reaction of 1-bromocyclooctene.

	C^1	C^2	C^3	C^4	C^5	C^6	C^7	C^8
standard	1014.5	992.7	1001.3	995.9	1000.0	1001.8	1002.0	999.6
	(4.6)	(2.2)	(1.2)	(1.4)		(1.3)	(1.8)	(1.7)
Ni-catalyzed reaction with n-C_4H_9MgBr								
recovered	1044.2	1018.5	998.0	991.4	1000.0	995.2	997.7	1000.9
(84.9%)	(3.9)	(9.0)	(0.6)	(1.3)		(1.9)	(1.8)	(2.3)
R/R_0	1.029	1.026	0.997	0.996	1.000	0.993	0.996	1.001
	(0.006)	(0.009)	(001)	(0.002)		(0.002)	(0.003)	(0.003)
$^{12}C/^{13}C$ KIE	1.015	1.014	0.998	0.998	1.000	0.997	0.998	1.001
	(0.003)	(0.005)	(0.001)	(0.001)		(0.001)	(0.001)	(0.002)
Pd-catalyzed reaction with n-$C_8H_{17}MgBr$								
recovered	1068.7	1024.8	1008.1	999.1	1000.0	1002.2	1005.4	1010.1
(90.5%)	(2.1)	(5.4)	(1.4)	(2.1)		(0.2)	(0.6)	(2.0)
R/R_0	1.053	1.032	1.007	1.003	1.000	1.000	1.003	1.010
	(0.005)	(0.006)	(0.002)	(0.003)		(0.001)	(0.002)	(0.003)
$^{12}C/^{13}C$ KIE	1.023	1.014	1.003	1.001	1.000	1.000	1.001	1.004
	(0.002)	(0.003)	(0.001)	(0.001)		(0.001)	(0.001)	(0.001)

Reference and Notes

1. Collman, J. P.; Hegedus, L. S.; Norton, J. R.; Finke, R. G. *Principles and Applications of Organotransition Metal Chemistry*, 2nd ed.; Wiley-Interscience: New York, 1987; pp 306-319.
2. Stille, J. K.; Lau, K. S. Y. *Acc. Chem. Res.* **1977**, *10*, 434-442.
3. (a) Amatore, C.; Pflüger, F. *Organometallics* **1990**, *9*, 2276-2282. (b) Portnoy, M.; Milstein, D. *Organometallics* **1993**, *12*, 1665-1673. (c) Hartwig, J. F.; Paul, F. *J. Am. Chem. Soc.* **1995**, *117*, 5373-5374. (d) Alcazar-Roman, L. M.; Hartwig, J. F. *Organometallics* **2002**, *21*, 491-502. and references therein.
4. Amatore, C.; Jutand, A. *Acc. Chem. Res.* **2000**, *33*, 314-321. and references therein.
5. Alcazar-Roman, L. M.; Hartwig, J. F. *J. Am. Chem. Soc.* **2001**, *123*, 12905-12906.
6. Singh, U. K.; Strieter, E. R.; Blackmond, D. G.; Buchwald, S. L. *J. Am. Chem. Soc.* **2002**, *124*, 14104-14114.
7. For a theoretical study: Sundermann, A.; Uzan, O.; Martin, J. M. L. *Chem. Eur. J.* **2001**, *7*, 1703-1711.
8. Stambuli, J. P.; Buhl, M.; Hartwig, J. F. *J. Am. Chem. Soc.* **2002**, *124*, 9346-9347; Lewis, A. K. D.; Caddick, S.; Cloke, F. G. N.; Billingham, N. C.; Hitchcock, P. B.; Leonard, J. *J. Am. Chem. Soc.* **2003**, *125*, 10066-10073.
9. The reaction pathways for complexes with monodentate ligands are essentially the same as the bidentate case. The major difference is the lower π-complexation energy in the monodentate case,

which originates from significant linear-to-bent deformation of the ML_2 fragment upon π-complexation.

10. The number refers to structure number described in Schemes. The alphabets **a** and **b** refer to nickel and palladium, respectively. The subscripts indicate the substrate type (**v** (vinyl) or **p** (phenyl)) and the leaving group (**b**: bromide, **c**: chloride, **f**: fluoride, **o**: methoxy, **s**: methylthio).
11. Lindsell, W. E. In *Comprehensive Organometallic Chemistry II*, Vol. 1; Abel, E. W.; Stone, F. G. A.; Wilkinson, G. Eds.; Pergamon Press: New York, 1995.
12. Gaussian 98, revision A.9, Frisch, M. J.; Trucks, G. W.; Schlegel, H. B.; Scuseria, G. E.; Robb, M. A.; Cheeseman, J. R.; Zakrzewski, V. G.; Montogomery, J. A., Jr.; Stratmann, R. E.; Burant, J. C.; Dapprich, S.; Millam, J. M.; Daniels, A. D.; Kudin, K. N.; Strain, M. C.; Farkas, O.; Tomasi, J.; Barone, V.; Cossi, M.; Cammi, R.; Mennucci, B.; Pomelli, C.; Adamo, C.; Clifford, S.; Ochterski, J.; Petersson, G. A.; Ayala, P. Y.; Cui, Q.; Morokuma, K.; Malick, D. K.; Rabuck, A. D.; Raghavachari, K.; Foresman, J. B.; Cioslowski, J.; Ortiz, J. V.; Baboul, A. G.; Stefanov, B. B.; Liu, G.; Liashenko, A.; Piskorz, P.; Komaromi, I.; Gomperts, R.; Martin, R. L.; Fox, D. J.; Keith, T.; Al-Laham, M. A.; Peng, C. Y.; Nanayakkara, A.; Challacombe, M.; Gill, P. M. W.; Johnson, B.; Chen, W.; Wong, M. W.; Andres, J. L.; Gonzalez, C.; Head-Gordon, M.; Pople, J. A. Gaussian. Inc.: Pittsburg, PA, 1998; Gaussian 03, Revision C.02, Frisch, M. J.; Trucks, G. W.; Schlegel, H. B.; Scuseria, G. E.; Robb, M. A.; Cheeseman, J. R.; Montgomery, Jr., J. A.; Vreven, T.; Kudin, K. N.; Burant, J. C.; Millam, J. M.; Iyengar, S. S.; Tomasi, J.; Barone, V.; Mennucci, B.; Cossi, M.; Scalmani, G.; Rega, N.; Petersson, G. A.; Nakatsuji, H.; Hada, M.; Ehara, M.; Toyota, K.; Fukuda, R.; Hasegawa, J.; Ishida, M.; Nakajima, T.; Honda, Y.; Kitao, O.; Nakai, H.; Klene, M.; Li, X.; Knox, J. E.; Hratchian, H. P.; Cross, J. B.; Adamo, C.; Jaramillo, J.; Gomperts, R.; Stratmann, R. E.; Yazyev, O.; Austin, A. J.; Cammi, R.; Pomelli, C.; Ochterski, J. W.; Ayala, P. Y.; Morokuma, K.; Voth, G. A.; Salvador, P.; Dannenberg, J. J.; Zakrzewski, V. G.; Dapprich, S.; Daniels, A. D.; Strain, M. C.; Farkas, O.; Malick, D. K.; Rabuck, A. D.; Raghavachari, K.; Foresman, J. B.; Ortiz, J. V.; Cui, Q.; Baboul, A. G.; Clifford, S.; Cioslowski, J.; Stefanov, B. B.; Liu, G.; Liashenko, A.; Piskorz, P.; Komaromi, I.; Martin, R. L.; Fox, D. J.; Keith, T.; Al-Laham, M. A.; Peng, C. Y.; Nanayakkara, A.; Challacombe, M.; Gill, P. M. W.; Johnson, B.; Chen, W.; Wong, M. W.; Gonzalez, C.; Pople, J. A. Gaussian, Inc.: Wallingford CT, 2004.
13. (a) Becke, A. D. *J. Chem. Phys.* **1993**, *98*, 5648-5652. (b) Lee, C.; Yang, W.; Parr, R. G.; *Phys. Rev. B* **1988**, *37*, 785-789.
14. Wadt, W. R.; Hay, P. J. *J. Chem. Phys.* **1985**, *82*, 299-310.
15. Hehre, W. J.; Radom, L.; Schleyer, P. v R.; Pople, J. A. *Ab Initio Molecular Orbital Theory*; John Wiley & Sons, Inc.: New York, 1986. References cited therein.
16. (a) Fukui, K. *Acc. Chem. Res.* **1981**, *14*, 363-368. (b) Gonzalez, C.; Schlegel, H. B. *J. Chem. Phys.*

1989, *90*, 2154-2161. Gonzalez, C.; Schlegel, H. B. *J. Phys. Chem.* **1990**, *94*, 5523-5527.

17. Bigeleisen, J.; Mayer, M. G. *J. Chem. Phys.* **1947**, *15*, 261-267. Bigeleisen, J.; Wolfsberg, M. *Adv. Chem. Phys.* **1958**, *1*, 15-76.
18. Scott, A. P.; Radom, L. *J. Phys. Chem.* **1996**, *100*, 16502-16513.
19. The Lewis basicity of the atom X in the π-complex **2** is stronger than that in the parent substrate due to the back-donation from the Ni center.
20. For X = OMe and SMe, the product finally located was not **7** but **7'**; spontaneous exchange of the Cl anion and the leaving group occurred on the Ni center during the geometry optimization. This is also the case for other reactions involving OMe or SMe as a leaving group.

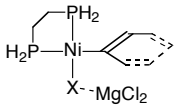

7'

21. Bond strengths in diatomic molecules are ≤327.2, 327.6±2.1, and 461.9±5.0 kJ/mol for Br-Mg, Cl-Mg and F-Mg, respectively: *CRC Handbook of Chemistry and Physics*, 84th Ed.; CRC Press: New York, 2003.
22. Method: Singleton, D. A.; Thomas, A. A. *J. Am. Chem. Soc.* **1995**, *117*, 9357-9358.
23. Recent examples: Nowlan III, D. T.; Gregg, T. M.; Davies, H. M. L.; Singleton, D. A. *J. Am. Chem. Soc.* **2003**, *125*, 15902-15911; Landis, C. R.; Rosaaen, K. A.; Uddin, J. *J. Am. Chem. Soc.* **2002**, *124*, 12062-12063; Kakiuchi, F.; Ohtaki, H.; Sonoda, M.; Chatani, N.; Murai, S. *Chem. Lett.* **2001**, 918-919.
24. Massera, C.; Frenking, G. *Organometallics* **2003**, *22*, 2758-2765.
25. Synthesis and isolation of a Ni-fluoroarene η^2-complex: Bach, I.; Pörschke, K.-R.; Goddard, R.; Kopiske, C.; Krüger, C.; Rufínska, A.; Seevogel, K. *Organometallics* **1996**, *15*, 4959-4966.
26. Tsou, T. T.; Kochi, J. K. *J. Am. Chem. Soc.* **1979**, *101*, 7547-7560.
27. Van Hecke, G. R.; Horrocks, D. W. Jr. *Inorg. Chem.* **1966**, *5*, 1968.
28. Bandodakar, B. S.; Nagendrappa, G. *Synthesis* **1990**, 843-844.

CHAPTER 4

Design of Nickel/Magnesium Bimetallic System for Catalytic C-F Bond Activation/C-C Bond Formation

4-1. Introduction

Ni- and Pd-catalyzed cross-coupling reactions of aryl and vinyl halides/triflates with a variety of organometallic compounds (Mg, Zn, Sn, B, Si etc.) have served as straightforward and powerful methods for formation of carbon-carbon bond.[1] Three decades after its discovery,[2] this chemistry has met significant innovation: While there has been no general method for cross-coupling of unactivated aryl chlorides until 1998, mild and versatile catalysts have been discovered and developed since then.[3] The key to the innovation was the use of "bulky and electron-rich" phosphorus and *N*-heterocyclic carbene ligands. These ligands provide coordinative unsaturation and high electron density at the metal center, which is suited for C-X bond oxidative addition. While a ML_2-type 14-electron complex is proposed as a reactive species in a conventional cross-coupling reaction,[4] a bulky ligand undergoes dissociation of one more ligand to give a highly reactive metal center of a ML-type 12-electron complex (Scheme 1).[5]

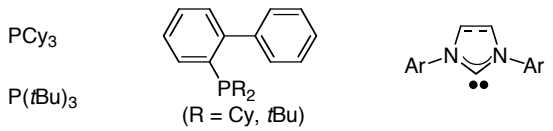

Scheme 1. Oxidative Addition of Aryl Halide to ML-type Complex of Bulky Ligand

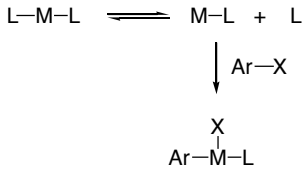

While development of ligands based on the above concept seems to come to maturity,[6] our studies on the Lewis acid effect on the oxidative addition of sp^2-halides to d^{10} transition metals

(Chapters 2, 3) provide a new guideline for activation of unreactive carbon-halogen bonds (Scheme 2): If there is given an appropriate ligand that contains donor atoms (L and D) to a transition metal (M) and a (main group) Lewis acid (m), respectively, it will form a bimetallic complex such as **A**. The complex **A** is expected to undergo facile C-X bond activation of an sp^2-halide through the eliminative mechanism.[7]

Scheme 2. Ligand Design for Bimetallic C(sp^2)-X Bond Activation

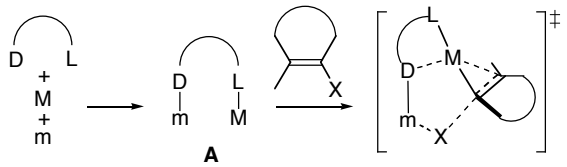

M: transition metal; m: Lewis acid
L: donor to transition metal; D: donor to Lewis acid

On the basis of this idea, here we carried out design and development of Ni-catalyzed cross-coupling reaction between an aryl fluoride and a Grignard reagent. The key to the activation of carbon-fluorine bond, one of the strongest bonds that carbon can form,[8] is a phosphine/hydroxy hybrid ligand (L = PR_3, D = RO^-) that is likely to generate Ni-phosphine, Mg-alkoxide bimetallic species. The bimetallic species would exert strong Mg-F interaction in the transition state.[9] The new system is not only as efficient as the one previously reported by Herrmann *et al.*, which employs an *N*-heterocyclic carbene as a ligand,[10] but also gives much higher selectivity toward a C-F bond rather than a C-heteroatom (such as O) bond.

4-2. Ligand Screening

On the basis of bimetallic mechanism of C(sp^2)-X bond activation, several phosphine ligands containing nitrogen/oxygen atoms in the neighborhood of the phosphorus atom were examined for Ni-catalyzed cross-coupling of 4-fluorotoluene and phenylmagnesium bromide (eq 1, Chart 1). As the result, 2-diphenylphosphinophenol (**L1**) showed remarkable activity in the catalytic C-F bond activation. When the hydroxy group was replaced by a methoxy group (**L2**), the catalytic

activity significantly dropped. Ligands containing pyridyl or pyrimidyl groups (**L3**-**L5**) as well as PPh_3 (**L6**) showed very little or no catalytic activity, too.

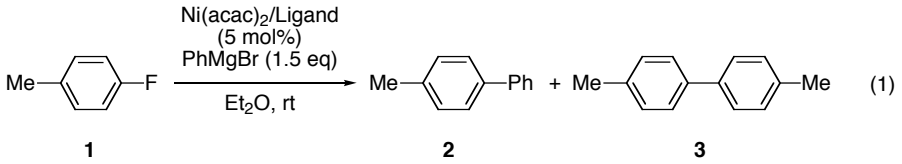

Chart 1. Catalytic Activity of Phosphorus Ligands in Eq 1[a]

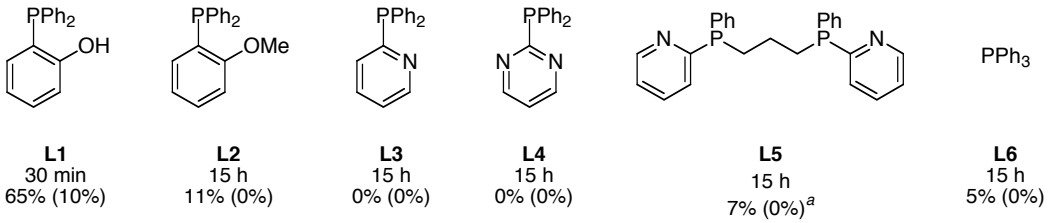

[a] Yields of **2** and **3** (in parentheses) were determined by GC using tridecane as an internal standard. [b] The reaction was carried out in THF. The ligand is ~1:1 mixture of *dl* and *meso*-form.

We examined other phosphine-phenol derivatives to further examine the role of the hydroxy group in the phosphine ligand **L1** (Chart 2). When a hydroxy group is in the *meta*- (**L7**) or *para*-position (**L8**) of the phosphorus center, the reaction proceeds very little. These results indicate that the *proximity* of the hydroxy group and the phosphorus center is important. In addition, the lower catalytic activity with **L9**, which contains two hydroxy groups in the neighborhood of the phosphorus center, suggest that the presence of only *one* hydroxy group in the phosphorus atom is essential for high catalytic activity of **L1**.[11] Replacement of the hydroxy group in **L1** with a carboxylic acid (**L10**) also resulted in low catalytic activity.

Chart 2. Catalytic Activity of Phosphine-phenol Ligands in Eq 1.[a]

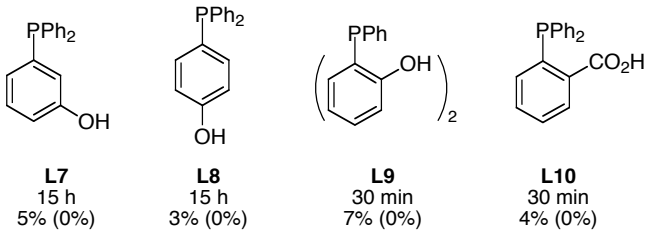

[a] Yields of **2** and **3** (in parentheses) were determined by GC using tridecane as an internal standard.

On the basis of the results described above, we consider a plausible mechanism for Ni/**L1**-catalyzed Kumada coupling as shown in Scheme 3. Fisrt, Ni^0-phosphine/Mg-alkoxide bimetallic species **A**, which forms by in-situ reduction of $Ni(acac)_2$ and deprotonation of **L1** by a Grignard reagent, undergoes oxidative addition of aryl fluoride (Ar^1F) to afford an arylnickel(II) intermediate **B**. Transmetalation of **B** with the Grignard reagent (Ar^2MgX) gives a diarylnickel(II) intermediate **C**. Reductive elimination of **C** gives the cross-coupling product and regenerates the Ni^0 species **A**. The intermediate **C** may also undergo aryl-aryl exchange reaction with Ar^2MgX to give another diarylnickel(II) intermediate **D** and Ar^1MgX. The intermediate **D** affords a Grignard reagent-derived homo-coupling product (Ar^2-Ar^2). The newly formed Grignard reagent (Ar^1MgX) further reacts with **B** to give **E**, followed by reductive elimination to afford the substrate-derived homo-coupling product (Ar^1-Ar^1).

Scheme 3. Proposed Catalytic Cycle for Ni/**L1**-catalyzed Cross-coupling between Aryl Fluoride and Grignard Reagent

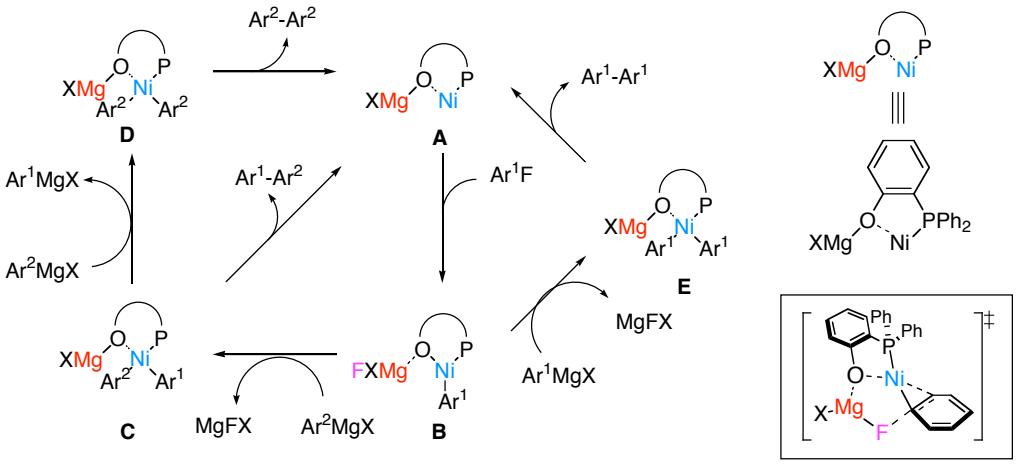

One problem associated with **L1** is the formation of a considerable amount of homo-coupling product **3** (see eq 1 and Chart 1). According to Scheme 3, this problem would be solved if one could accelerate the reductive elimination of **C** (**C** -> **A**) or slow down the Ar^1/Ar^2 exchange and formation of Ar^1MgX (**C** -> **D**). Thus, we first attempted the latter approach and slowly added the Grignard reagent into the reaction mixture via a syringe pump (eq 2). However,

this method was unsuccessful: While the starting aryl fluoride was almost quantitatively consumed, substantial amount (18%) homo-coupling product **3** was obtained.

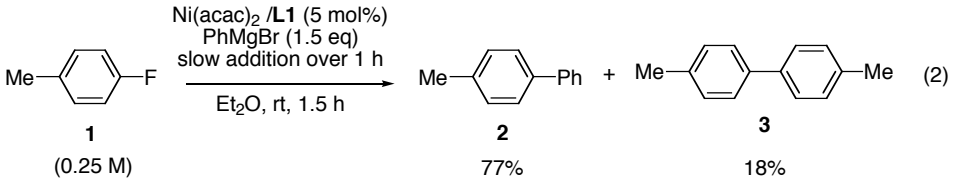

Next, we examined other phosphine/alcohol hybrid ligands. As the result, we found that slight modification of the ligand core structure is effective for suppression of the homo-coupling product (Chart 3). Replacement of the phenol moiety in **L1** with a benzyl alcohol (**L11**) or a cyclohexanol (**L12**) moiety resulted in much less homo-coupling product **3** without loss of high catalytic reactivity toward the C-F bond. We consider that increase of the bite angle from **L1** to **L11** and **L12** was essential. The larger bite angle in **L11** and **L12** than in **L1** would resulted in faster reductive elimination of a diarylnickel(II) intermediate such as **C**. It is also noted that the reaction is faster in Et_2O than in THF, which may reflect higher Lewis acidity of the Mg^{II} center in a less-coordinating solvent.

Chart 3. Catalytic Activity of Phosphine/Alcohol Ligand in Eq 1.

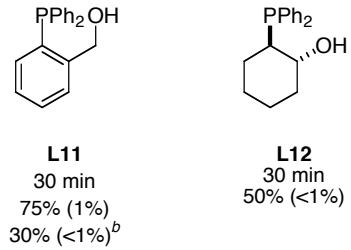

[a] Yields of **2** and **3** (in parentheses) were determined by GC using tridecane as an internal standard. [b] The reaction was carried out in THF.

4-3. Substrate Scope

After ligand screening, we applied the present Kumada coupling reaction to several aryl fluorides (Table 1). Electron-rich substrates such as 4-fluorotoluene and 4-fluoroanisole gave cross-coupling products in excellent yield (entries 1, 2). More electron-rich, dimethylamino substituent slowed down the reaction rate, but still gave a satisfactory result (entry 3). In the presence of an aryl C-S bond, substantial amount of *p*-terphenyl was obtained through cleavage of both C-S and C-F bonds (entry 4). Electron-deficient 2-fluoropyridine and 1,4-difluorobenzene reacted fast and efficiently (entry 5, 6). While a vinyl group is slightly electron-withdrawing, the reaction of 4-fluorostyrene was sluggish probably because strong interaction between the vinyl group and the Ni^0 center prevented oxidative addition (entry 7).[12] While an *o*-monosubstituted substrate could be tolerated, *o*-disubstituted substrate gave only trace amount of coupling product (entry 8, 9).

Table 1. Ni/**L11**-catalyzed Kumada Coupling of Aryl Fluorides

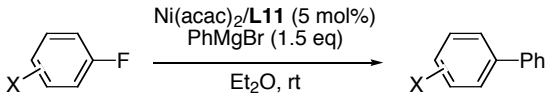

entry	substrate	product	time (h)	%yield[a]
1	Me—F	Me—Ph	2	94[b]
2	MeO—F	MeO—Ph	4	97
3	Me_2N—F	Me_2N—Ph	65	77
4	MeS—F	MeS—Ph	4	32[c]
5	F, N	Ph, N	0.5	100
6[d]	F—F	Ph—Ph	2	92[b]
7[e]	F	Ar	65	48
8	Me, F	Me, Ph	48	95
9	Me, F, Me	Me, Ph, Me	40	<1%[b]

[a] Isolated yields except for entries 1, 6 and 9. [b] Determined by GC using tridecane as an internal standard. [c] *p*-Terphenyl was obtained in 51% yield. [d] The amount of PhMgBr was 2.5 equiv. [e] 4-Methoxyphenylmagnesium bromide (Ar = $-C_6H_4$(4-OMe)) was used instead of PhMgBr.

Most notable in above results is the reaction of 4-fluoroanisole (entry 2). While the reaction with an *N*-heterocyclic carbene ligand gives the cross-coupling product in moderate yield accompanied by concomitant formation of *p*-terphenyl via C-F and C-O bond activation (eq 3), the present system shows perfect selectivity toward the C-F bond. This would be due to the carbon-halogen bond-selective stabilization of a bimetallic, eliminative TS of oxidative addition (see Chapter 2). The reaction of 4-thioanisole is also notable. While an aryl C-S bond is much

more reactive toward monometallic Ni (and Pd) complexes than a C-F bond,[13] the present system showed moderate selectivity toward the C-F bond.

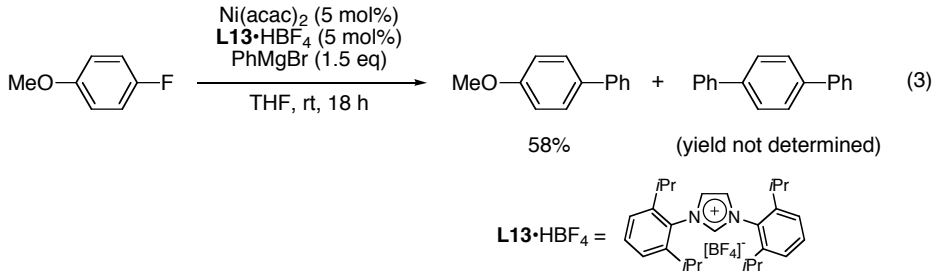

Next, several Grignard reagents were examined (Table 2). We found that the present system is very susceptible to the structural and electronic character of the Grignard reagent used. While sterically less hindered Grignard reagents gave moderate to good yields (entries 1, 2), increase of steric hindrance resulted in substantial decrease of catalytic efficiency (entries 3, 6). Such a phenomenon has not been observed in previous Kumada coupling reaction.[10,14] The reaction of 2-thienylmagnesium bromide was also sluggish (entry 4). Electron-deficient, 4-trifluoromethyl-phenylmagnesium bromide gave no cross-coupling product, but large amount of Grignard-derived homo-coupling product (entry 5). This indicates that transmetalation and further aryl/aryl exchange is very fast for this Grignard reagent (Scheme 3). While vinyl and ethynyl Grignard reagents have been known to be much less reactive in Kumada coupling reaction (entries 8, 9),[14,15] most surprising is that *n*-butylmagnesium bromide gave no cross-coupling product under present conditions (entry 7).

Table 2. Ni/**L11**-catalyzed Cross-coupling between Aryl Fluoride and Grignard Reagent

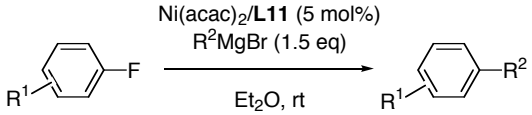

entry	R^1	R^2	time (h)	yield (%)[a]
1	4-Me	4-$MeOC_6H_4$	2	83 (83)
2	4-OMe	2-naphthyl	22	63 (72)
3	4-OMe	1-naphthyl	100	14 (21)
4	4-OMe	2-thienyl	76	5 (7)
5	4-OMe	4-$CF_3C_6H_4$	3	nd[b]
6	4-OMe	2,6-$Me_2C_6H_3$	4	trace[c]
7	H	n-C_4H_9	4	0[c]
8	H	CH_2=CH	22	0[c]
9	H	C_2H_2	22	0[c]

[a] Isolated yields. In parentheses are shown yields determined by ^{1}H NMR using tetrachloroethane as an internal standard. [b] Not detected. 4,4-bis(trifluoromethyl)biphenyl (0.6 mmol, determined by ^{1}H NMR) was obtained (1 mmol scale reaction). [c] Determined by GC.

Above results suggest that an organic group (R) rather than a halide (Chart 1) is likely to be bound to the Mg center of the Ni/Mg bimetallic species **A** (Scheme 2). Thus, the C-F bond activation step is much affected by the steric and electronic nature of the carbanion: An electron-rich R group would reduce the Lewis acidity of the Mg center and therefore the C-F bond cleavage ability, and a bulky R group would prevent the Ni/Mg bimetallic species to effectively interact with the substrate in a bidentate fashion (i.e., the Ni and the Mg centers to the aromatic π-system and the fluorine atom, respectively).

Chart 1.

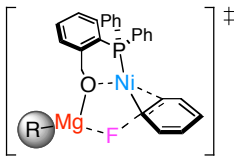

4-4. Summary

In summary, we described a new system for Ni-catalyzed cross-coupling between an aryl fluoride and a Grignard reagent. Throughout this study, we have demonstrated the effectiveness of the bimetallic, eliminative mechanism of C(sp^2)-X bond activation as a guideline for rational reaction design. Thus, highly efficient, catalytic C-F bond activation/C-C bond formation was achieved by the use of a phosphine/alcohol hybrid ligand that would form a Ni/Mg bimetallic reactive species. Although the present catalyst is not universally applicable to a wide variety of substrates and reagents, there should be plenty of room for further ligand modification. The present study further suggests that elaborate control of a transition metal and a main group metal in their spatial alignment will provide unprecedented reactivity and selectivity in chemical transformations.

Experimental Section

General. All the reactions dealing with air- or moisture-sensitive compounds were carried out in oven-dried reaction vessels under argon or nitrogen atmosphere. ^{1}H, ^{13}C and ^{31}P nuclear magnetic resonance (NMR) spectra were recorded with a JEOL ECA-500 (500 MHz) or ECX-400 (400 MHz) NMR spectrometer. Chemical shift values are reported in parts per million (ppm) from tetramethylsilane (δ 0.00), $CDCl_3$ (δ 77.0) and 85% H_3PO_4 (δ 0.0) for ^{1}H, ^{13}C and ^{31}P NMR, respectively. Gas chromatographic (GC) analysis was performed on a Shimadzu GC-14B instrument equipped with an FID detector and a capillary column, HR-1 (25 m x 0.25 mm i.d., 0.25 μm film). IR spectra were recorded on a React IR 1000 Reaction Analysis System equipped with DuraSample IR (ASI Applied System) and reported in cm^{-1}.

Materials. Unless otherwise noted, commercial reagents were purchased from Tokyo Kasei Co., Aldrich Inc., and other commercial suppliers and were used after distillation or recrystallization

just before use. Anhydrous diethyl ether and tetrahydrofuran were purchased from KANTO Chemical Co. and distilled over Na/benzophenone under argon atmosphere. The water content was determined with a Karl-Fischer moisture titrator (MKC-210, Kyoto Electronics Company) to be less than 20 ppm. Nickel acetylacetonate was purchased from Aldrich Inc. and used as received. Phosphine ligands including 2-diphenylphosphino-phenol (**L1**),[16] 2-methoxyphenyl(diphenyl)phosphine (**L2**),[17] 2-diphenylphosphinopyridine (**L3**),[18] 2-diphenylphosphinopyrimidine (**L4**),[19] 1,3-bis(phenyl(2-pyridyl)phosphino)propane (**L5**, ~1:1 mixture of *dl*- and *meso*-diastereomers),[20] 3-diphenylphosphinophenol (**L7**),[21] 4-diphenylphosphinophenol (**L8**),[22] bis(2-hydroxyphenyl)phenylphosphine (**L9**),[23] 2-diphenylphosphinobenzyl alcohol (**L11**)[24] and (±)-*trans*-(2-diphenylphosphino)cyclohexanol (**L12**)[25] were synthesized according to literature procedures. 2-Diphenylphosphinobenzoic acid (**L10**) was purchased from Aldrich Inc. Methylmagnesium bromide (Et_2O solution) was purchased from Tokyo Kasei Co. and titrated before use. Vinylmagnesium bromide and ethynylmagnesium bromide (THF solution) were purchased from Aldrich Inc. and used as received. Aryl Grignard reagents were prepared from corresponding aryl bromides and magnesium turnings in anhydrous diethyl ether and titrated prior to use.

Procedure for ligand screening in eq 1: An oven-dried glass tube containing a magnetic stirring bar was charged with $Ni(acac)_2$ (12.8 mg, 0.05 mmol), ligand (0.05 mmol), 4-fluorotoluene (110.1 mg, 1.00 mmol) and Et_2O (3.09 mL) under argon atmosphere. To this was added a 1.65-M Et_2O solution of phenylmagnesium bromide (0.91 mL, 1.50 mmol) at ambient temperature. After a fixed period of time (30 min or 15 h), the reaction was quenched by the addition of 1 mL of MeOH and subjected to GC analysis using an internal standard (*n*-tridecane, 184.4 mg, 1.00 mmol).

A typical procedure for the cross-coupling reaction in Table 1: An oven-dried Schlenk tube containing a magnetic stirring bar was charged with $Ni(acac)_2$ (12.8 mg, 0.05 mmol), 2-diphenylphosphinobenzylalcohol (14.6 mg, 0.05 mg), 4-fluoroanisole (126.1 mg, 1.00 mmol) and Et_2O (3.09 mL) under argon atmosphere. To this was added a 1.65-M Et_2O solution of phenylmagnesium bromide (0.91 mL, 1.50 mmol) at ambient temperature. The resulting mixture was stirred for 4 h, and quenched by the addition of 1 mL of MeOH. After standard aqueous workup, the reaction mixture was passed through a pad of Florisil, and concentrated *in vacuo*. The crude product was purified by silica gel chromatography (eluent: hexane) to afford 4-methoxybiphenyl as a colorless solid (179.0 mg, 97% yield).

Following compounds obtained by using this procedure were previously reported and were characterized either by comparison with authentic samples or by comparison of the spectral data:

4-Methylbiphenyl (CAS # 644-08-6)[26]
4-Methoxybiphenyl (CAS # 613-37-6)[27]
4-(*N*,*N*-Dimethylamino)biphenyl (CAS # 1137-79-7)[28]
2-Phenylpyridine (CAS # 1008-89-5)[29]
p-Terphenyl (CAS # 92-94-4)
4-(Methylthio)biphenyl (CAS # 19813-76-4)[30]
2-Methylbiphenyl (CAS # 643-58-3)[31]
4-Methoxy-4'-methylbiphenyl (CAS # 53040-92-9)[32]
2-(4-Methoxyphenyl)naphthalene (CAS # 59115-45-6)[33]
1-(4-Methoxyphenyl)naphthalene (CAS # 27331-33-5)[34]
4,4'-Bis(trifluoromethyl)biphenyl (CAS # 581-80-6)[35]
2-(4-Methoxyphenyl)thiophene (CAS # 42545-43-7)[36]

4-Methoxy-4'-vinylbiphenyl: IR (powder) 3004 (w), 2958 (w), 2919 (w), 2838 (w), 1629 (w), 1602 (m), 1578 (w), 1520 (w), 1497 (m), 1438 (w), 1399 (w), 1287 (m), 1248 (m), 1218 (m), 1183 (m), 1038 (m), 1011 (w), 992 (m), 905 (m), 824 (s), 814 (s), 750 (m), 654 (m); ^{1}H NMR

(400 MHz, $CDCl_3$): δ 3.83 (s, 3H), 5.26 (dd, *J* = 0.9, 11.0 Hz, 1H), 5.77 (dd, *J* = 0.9, 17.6 Hz, 1H), 6.74 (dd, *J* = 11.0, 17.6 Hz, 1H), 6.95-6.98 (m, 2H), 7.44-7.46 (m, 2 H), 7.50-7.54 (m, 4H); ^{13}C NMR (100 MHz, $CDCl_3$): δ 55.3, 113.5, 114.2, 126.6, 126.7, 127.9, 133.2, 136.0, 136.4, 140.2, 159.2; Anal. Calcd for $C_{15}H_{14}O$: C, 85.68; H, 6.71. Found: C, 85.47; H, 6.92.

References and Notes

1. (a) *Metal-catalyzed Cross-coupling Reactions*, Diederich, F.; Stang, P. J., Eds.; Wiley-VCH: New York, 1998. (b) *Cross-Coupling Reactions. A Practical Guide*, Miyaura, N. Ed.; Topics in Current Chemistry, Vol. 219; Springer: Berlin, 2002.
2. Tamao, K.; Sumitani, K.; Kumada, M. *J. Am. Chem. Soc.* **1972**, *94*, 4374-4375; Corriu, R. J. P.; Masse, J. P. *Chem. Commun.* **1972**, 144.
3. Littke, A. F.; Fu, G. C. *Angew. Chem., Int. Ed.* **2002**, *41*, 4176-4211.
4. (a) Amatore, C.; Pflüger, F. *Organometallics* **1990**, *9*, 2276-2282. (b) Portnoy, M.; Milstein, D. *Organometallics* **1993**, *12*, 1665-1673. (c) Alcazar-Roman, L. M.; Hartwig, J. F. *Organometallics* **2002**, *21*, 491-502. and references therein.
5. Hartwig, J. F.; Paul, F. *J. Am. Chem. Soc.* **1995**, *117*, 5373-5374; Stambuli, J. P.; Buhl, M.; Hartwig, J. F. *J. Am. Chem. Soc.* **2002**, *124*, 9346-9347; Lewis, A. K. D.; Caddick, S.; Cloke, F. G. N.; Billingham, N. C.; Hitchcock, P. B.; Leonard, J. *J. Am. Chem. Soc.* **2003**, *125*, 10066-10073.
6. Miura, M. *Angew. Chem., Int. Ed.* **2004**, *43*, 2201-2203; Walker, S. D.; Barder, T. E.; Martinelli, J. R.; Buchwald, S. L. *Angew. Chem., Int. Ed.* **2004**, *43*, 1871-1876; Altenhoff, G.; Goddard, R.; Lehmann, C. W.; Glorius, F. *J. Am. Chem. Soc.* **2004**, *126*, 15195-15201.
7. Recently Tamao and co-workers reported a BF_3-promoted cross-coupling reaction between an aryl triazene and an arylboronic acid, and proposed an eliminative mechanism where C-N bond cleavage and aryl group transfer take place in a single step: Saeki, T.; Son, E. C.; Tamao, K. *Org. Lett.* **2004**, *6*, 617-619.
8. Jones Jr., M. *Organic Chemistry*, 2nd Ed.; W. W. Norton & Company, Inc.: New York, 2000.
9. Mg-F bond energy: 461.9 kJ/mol. *CRC Handbook of Chemistry and Physics*, 84th Ed.; CRC Press: New York, 2003.
10. Böhm, V. P. W.; Gstöttmayr, C. W. K.; Weskamp, T.; Herrmann, W. A. *Angew. Chem., Int. Ed.* **2001**, *40*, 3387.
11. In the ligand screening for Ni-catalyzed cross-coupling between an aryl chloride and a Grignard reagent (>350 metal/ligand combinations), Herrmann *et al.* examined tris(2-hydroxyphenyl)phosphine as the only one phosphorus ligand that contain a hydroxy group. However,

the catalytic activity of the ligand was only moderate: Böhm, V. P. W.; Weskamp, T.; Gstöttmayr, C. W. K.; Herrmann, W. A. *Angew. Chem., Int. Ed.* **2000**, *39*, 1602-1604.

12. Cronin, L.; Higgitt, C. L.; Karch, R.; Perutz, R. N. *Organometallics* **1997**, *16*, 4920-4928.
13. Oxidative addition of C(sp^2)-S bond to Ni^0 and Pd^0 complexes: Osakada, K.; Maeda, M.; Nakamura, Y.; Yamamoto, T.; Yamamoto, A. *Chem. Commun.* **1986**, 442-443; Kuniyasu, H.; Ohtaka, A.; Nakazono, T.; Kinomoto, M.; Kurosawa, A. *J. Am. Chem. Soc.* **2000**, *122*, 2375-2376.
14. Tamao, K.; Sumitani, K.; Kiso, Y.; Zembayashi, M.; Fujioka, A.; Kodama, S.; Nakajima, I.; Minato, A.; Kumada, M. *Bull. Chem. Soc. Jpn.* **1976**, *49*, 1958-1969.
15. We could not find a Ni-catalyzed cross-coupling reaction between a halobenzene with ethynyl Grignard reagent in SciFinder database. For Pd-catalyzed cross-coupling of alkynyl metals, see: Negishi, E.-i. *Acc. Chem. Res.* **1982**, *340*, 340-348.
16. Rauchfuss, T. B. *Inorg. Chem.* **1977**, *16*, 2966-2967.
17. Gelman, D.; Jiang, L.; Buchwald, S. L. *Org. Lett.* **2003**, *5*, 2315-2318.
18. Maisonnet, A.; Farr, J. P.; Olmstead, M. M.; Hunt, C. T.; Balch, A. L. *Inorg. Chem.* **1982**, *21*, 3961-3967.
19. Reetz, M. T.; Demuth, R.; Goddard, R. *Tetrahedron Lett.* **1998**, *39*, 7089-7092.
20. Butler, I. R.; Licence, P.; Coles, S. J.; Hursthouse, M. B. *J. Organomet. Chem.* **2000**, *598*, 103-107.
21. Buhling, A.; Kamer, P. C. J.; van Leeuwen, P. W. N. M.; *J. Mol. Catal. A: Chem.* **1995**, *98*, 69-80.
22. Herd, O.; Hebler, A.; Hingst, M.; Tepper, M.; Stelzer, O. *J. Organomet. Chem.* **1996**, *522*, 69.
23. Tzschach, A.; Nietzschmann, E. *Zeitschrift fuer Chemie* **1980**, *20*, 341-342.
24. Brauer, D. J.; Hingst, M.; Kottsieper, K. W.; Like, C.; Nickel, T.; Tepper, M.; Stelzer, O.; Sheldrick, W. S. *J. Organomet. Chem.* **2002**, *645*, 14-26.
25. Thurner, C. L.; Barz, M.; Spiegler, M.; Thiel, W. R. *J. Organomet. Chem.* **1997**, *541*, 39-49.
26. Negishi, E.-i.; Takahashi, T.; Akiyoshi, K. *J. Organomet. Chem.* **1987**, *334*, 181-194.
27. Old, D. W.; Wolfe, J. P.; Buchwald, S. L. *J. Am. Chem. Soc.* **1998**, *120*, 9722-9723.
28. Brune, H. A.; Erte, J. *Liebigs Ann. Chem.* **1980**, 928-937.
29. Malmberg, H.; Nilsson, M. *Tetrahedron* **1986**, *42*, 3981-3986.
30. Li, G. Y. *J. Org. Chem.* **2002**, 67, 3643-3650.
31. Arai, N.; Narasaka, K. *Bull. Chem. Soc. Jpn.* **1995**, *68*, 1707-1714.
32. Farina, V.; Krishnan, B.; Marshall, D. R.; Roth, G. P. *J. Org. Chem.* **1993**, 58, 5434-5444.
33. Duan, J.-P.; Cheng, C.-H. *Organometallics* **1995**, *14*, 1608-1618.
34. Shen, H.-C.; Pal, S.; Lian, J.-J.; Liu, R.-S. *J. Am. Chem. Soc.* **2003**, *125*, 15762-15763.
35. Jutand, A.; Mosleh, A. *J. Org. Chem.* **1997**, *62*, 261-274.
36. Hebel, A.; Haag, R. *J. Org. Chem.* **2002**, *67*, 9452-9455.

CHAPTER 5

Dirhodium-catalyzed C-H Insertion Reaction between Diazo Compound and Alkane. Mechanism and Dimetallic Effects in C-H Bond Activation

5-1. Introduction

Carbon-carbon bond forming reactions that rely on catalytic activation of the C-H bond in a saturated hydrocarbon have become standard synthetic protocols.[1,2] Among them, the reaction of an α-diazoester catalyzed by a dirhodium tetracarboxylate or a related catalyst is the reaction widely utilized as a practical synthetic method (Scheme 1).[3] In an ideal case, a new C-C bond between two sp^3 carbon centers is created through activation of the C-H bond of a saturated hydrocarbon in a diastereo- and enantioselective manner.[4]

Scheme 1. Schematic representation of the catalytic cycle of the rhodium tetracarboxylate-catalyzed C-H bond activation/C-C bond forming reaction of an α-diazoacetate with an alkane.

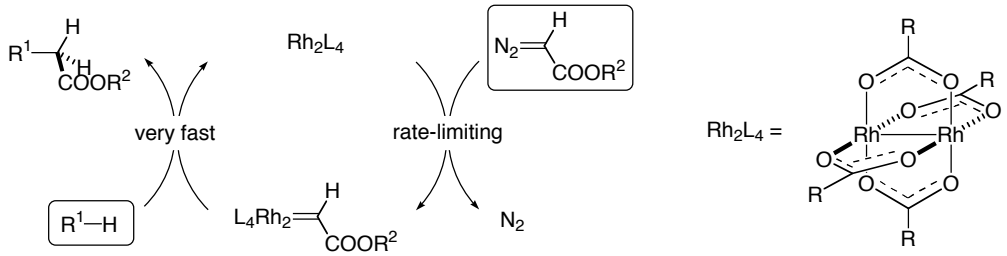

It has been generally assumed that the reaction involves a rhodium-carbene complex, and that the catalytic cycle consists of three steps–Rh-catalyzed nitrogen extrusion from the diazo compound, C-H activation, and C-C bond formation. The latter two steps are assumed to take place more or less as a single reaction (Scheme 1).[3] The first step is rate limiting for secondary C-H insertion,[5] and hence the mechanistic information on the subsequent steps is scarce, generating various speculations. In addition, there has been scarcity of discussions about such fundamental issues as the roles of the dinuclear structure of the catalyst that appears to be responsible for the

unique success of the dirhodium catalyst, and the function of the bridging carboxylates (except their known ability to harness chiral centers).

Although the majority of previous reports on the rhodium-catalyzed C-H activation/C-C formation reaction focused on synthetic applications, there exist several data that provide information on the reaction mechanism: (1) The activation enthalpy of the $Rh_2(OAc)_4$-catalyzed nitrogen extrusion reaction of ethyl diazoacetate ($\Delta H^{\ddagger}$ = 16.4 ± 1.4 kcal/mol) that is the rate-limiting step of the catalytic cycle for secondary C-H insertion,[5a] (2) $^1H/^2H$ kinetic isotope effects (KIEs) of the C-H bond activation,[6] which have been shown to depend on the nature of the carboxylate ligands in the rhodium catalyst, (3) qualitative structure/reactivity correlation indicating a reactivity order of primary << secondary < tertiary C-H bond[7] and the enhanced reactivity of a C-H bond adjacent to a heteroatom,[8] (4) carboxylate ligand effects on the regio- and stereoselectivity of the C-H insertion reaction,[9] and (5) retention of the configuration of the carbon at which the C-H activation occurs.[10]

Based on the facts listed above and the stereochemical outcomes of intra- and intermolecular C-H insertion reactions, various working models of the transition state (TS) of the C-H bond activation process have been proposed.[7b,11] Representative examples are illustrated in Figure 1. Figure 1a illustrates a three-centered concerted transition state of the C-H activation, which was described by Doyle and now is widely accepted.[7b] Figure 1b illustrates a four-centered hypothesis by Taber, where an interaction between the hydrogen atom and the rhodium atom is assumed.[11a] A three-centered mechanism involving a stepwise character was also suggested.[9b]

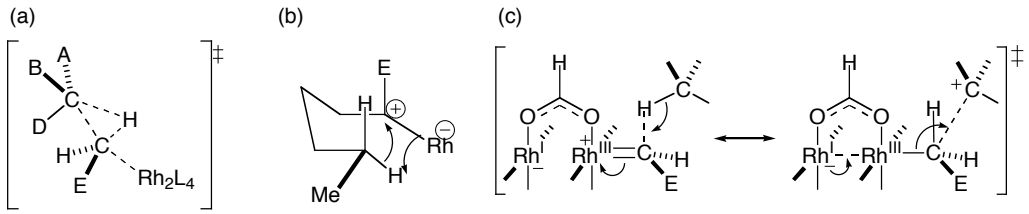

Figure 1. Transition state models of C-H bond activation with dirhodium-carbene complex described by Doyle (a), Taber (b), and this work (c).

For further development of the C-H activation chemistry, it was felt that deeper understanding of the reaction mechanism was indispensable. We report herein the pathways of the rhodium-catalyzed reactions of diazomethane and methyl diazoacetate as revealed by density functional calculations. The reaction pathways that we propose here provide the first qualitative to semi-quantitative account of the experimental data, as well as the structures of important intermediates and TSs involved in the catalytic cycle. With respect to the crucial C-H insertion step, we have found that two important events are involved in the transition state (Figure 1c). One is hydride transfer from the alkane to the carbene carbon and the other is regeneration of the Rh-Rh bond and formation of a new C-C bond, as depicted as two resonance structures in Figure 1c. While the reaction is concerted, not stepwise, it is markedly non-synchronous, with hydride transferpreceding C-C bond formation. The theoretical analyses of the properties of intermediates and TSs revealed unique roles of the rhodium catalyst that originate from its dimetallic structure.

5-2. Chemical Models and Computational Methods

5-2-1. Chemical Models

In the present studies, dirhodium tetraformate (**1**) was employed as a model of a common catalyst, dirhodium tetraacetate, in the interest of computational facility. With this model catalyst, two model catalytic reactions were studied. One was the reaction of diazomethane with methane or propane (CH_2 insertion, eq 1). This reaction has not been reported in the literature. Nonetheless this simple model was investigated to understand the fundamental characters of the

dirhodium-carbene complex and the mechanism of its C-H insertion reaction. The central mechanistic principle established with this model was found to hold also in a more realistic reaction model. The reaction of methyl diazoacetate with methane or propane (CH_3- and CH_2-insertion) was also studied (eq 2). This system is much more relevant to the actual synthetic reactions. Unlike the relatively unreactive substrates such as methane and propane, SiH_4 and dimethyl ether reacted with the rhodium carbene complex without any activation energy.[12] A 1:1 stoichiometry of the rhodium catalyst and the diazo compound was assumed on the basis of the kinetic study by Pirrung et al.[5b]

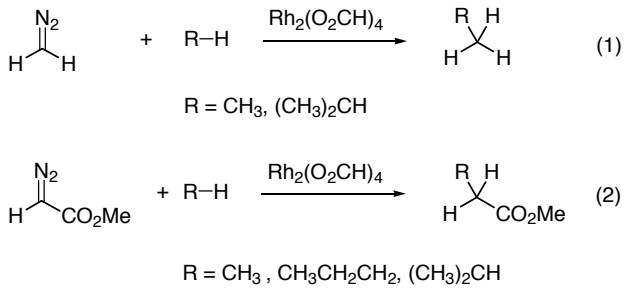

5-2-2. Computational Methods

All calculations were performed with Gaussian 94[13] and Gaussian 98[14] packages. The density functional theory (DFT) method was employed using the B3LYP hybrid functional.[15] Structures were optimized with a basis set (denoted as 631LAN) consisting of the LANL2DZ basis set including a double-ζ valence basis set with the Hay and Wadt effective core potential (ECP)[16] for Rh and the 6-31G(d) basis set[17] for C, H, N and O. The method and the basis sets used here are known to give reliable results for transition metal reactions including rhodium (carbene) complexes.[18,19] Some stationary points were optimized with symmetry assumption (*vide infra*). The structures of **1** and **5** (methylene carbene complex of **1**) optimized at the B3LYP/631LAN level show good agreement with those optimized at the MP2(FC)/631LAN level.[20] The

B3LYP/631LAN level calculation of $Rh_2(OAc)_4 \bullet 2H_2O$ reasonably reproduced the X-ray crystallographic data of the same compound.[21]

Each stationary point was adequately characterized by normal coordinate analysis. The intrinsic reaction coordinate (IRC) analysis[22] was carried out throughout the reaction pathways to confirm that all stationary points are smoothly connected to each other. Enthalpies and Gibbs free energies were obtained based on the calculated frequencies scaled by 0.9614.[23] Electronic energies will be discussed first, and enthalpies and Gibbs free energies second. To evaluate the effect of the solvent polarity on the energetics of the diazomethane model, single-point energy calculation was performed with self-consistent reaction field (SCRF) method (based on the polarized continuum model (PCM),[24] $\varepsilon = 8.93$ for CH_2Cl_2) on the gas-phase geometry. The Boys localization procedure[25] was performed to obtain localized Kohn-Sham orbitals[26] (LOs). Natural population analysis and natural bond orbital (NBO) analysis were performed at the same level as the one used for geometry optimization.[27] All charge distribution analyses discussed throughout this article are made based on the natural population analysis.

It should be pointed out that the calculations give us only the stationary points on the potential surface of electronic energy. As will be discussed in detail, the entropy changes in this reaction are too large to be neglected. Thus, the structures reported here (especially C-H insertion transition states) might not necessarily be close to those of the stationary points on the potential surface of Gibbs free energy. However, reasonable agreement of calculated and experimental data such as the value of KIE suggests that the optimized transition structures of C-H insertion reflect the reality.

5-3. Reaction of Diazomethane with Methane and Propane

5-3-1. Reaction Pathways and Energetics

We first investigated the reactions of diazomethane with methane and propane as basic model reactions. In Scheme 2 (R = H) and Figure 2 are shown the reaction course and the energy profile of the C-H insertion reaction of diazomethane with methane and propane catalyzed by $Rh_2(O_2CH)_4$ (**1**). The catalytic cycle involves seven steps: First, **1** and diazomethane interact to form a Rh/diazomethane complex **2** with a 19.9-kcal/mol stabilization energy. Then nitrogen extrusion proceeds via **TS-3** with a 16.6-kcal/mol activation energy, which is followed by the formation of a rhodium-methylene carbene complex **5**. After **TS-3**, there exists a weak complex (**4**) between **5** and dinitrogen (2.1 kcal/mol more stable than **TS-3**). The next step toward the final product first involves a **5**/alkane complex **6a** (methane reaction is denoted as **a**, 0.2-kcal/mol stabilization) or **6b** (propane reaction (CH_2 insertion) is denoted as **b**, 2.3-kcal/mol stabilization). C-H activation/C-C formation then takes place thorough **TS-7a** or **TS-7b** with a small activation energy (5.9 kcal/mol for **TS-7a** and 0.2 kcal/mol for **TS-7b**) followed by a downhill path to the final product with large exothermicity (60-62 kcal/mol), and the catalyst is regenerated. In **TS-7**, the C-H bond activation and the C-C bond formation take place in a single step. No intermediates were located near **TS-7** along the intrinsic reaction coordinate.

Scheme 2. Pathway of the $Rh_2(O_2CH)_4$-catalyzed C-H bond activation/C-C bond formation reaction of a diazo compound and an alkane.

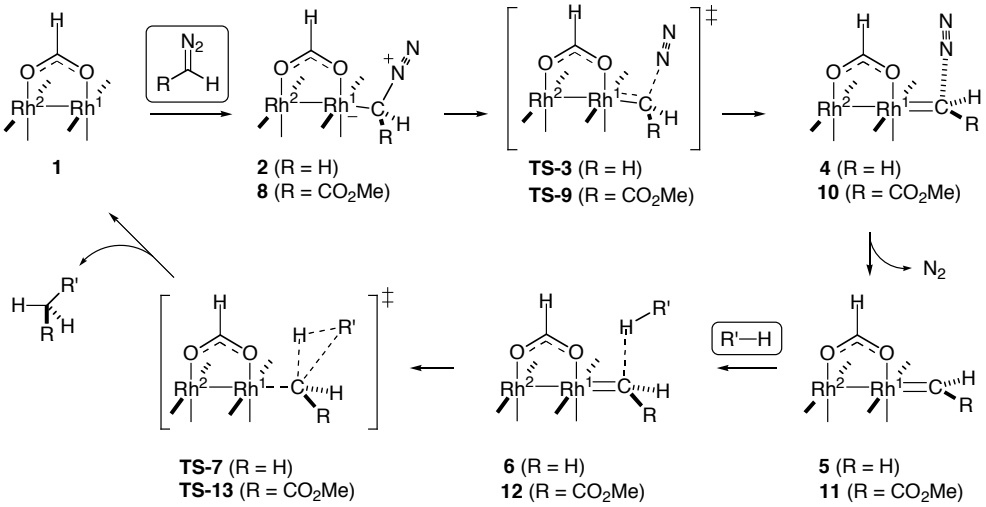

To probe the solvent effect on the reaction energetics, SCRF calculations (PCM) were performed on the gas-phase geometry (Figure 2, in parentheses). Dichloromethane (ε = 8.93) was investigated since it is frequently used for the C-H insertion reaction.[3] The energy profile did not change very much from the one in the gas-phase calculations. Thus, the reaction would not be affected by the solvent polarity as much as by coordination of basic solvent molecules to the rhodium atoms.[5b]

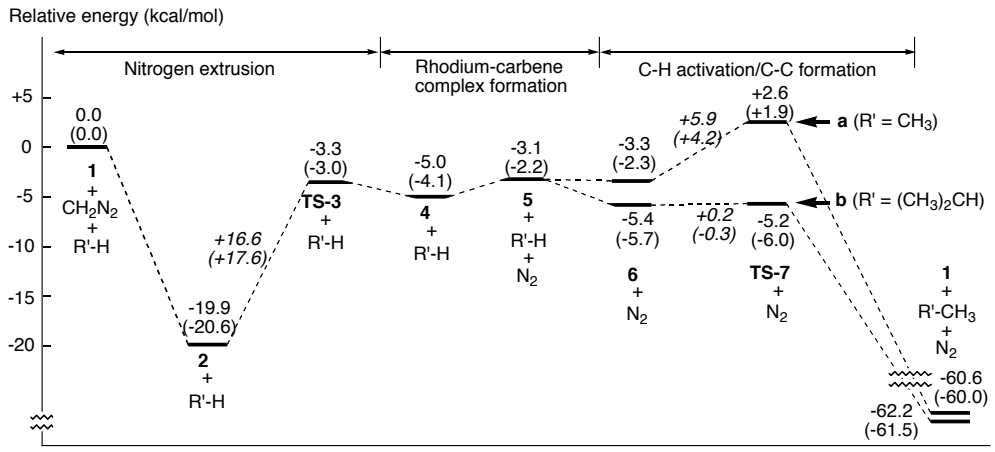

Figure 2. Energy profile of the $Rh_2(O_2CH)_4$-catalyzed reaction of diazomethane with methane (denoted as a) and propane (CH_2 insertion, denoted as b) at the B3LYP/631LAN level. In parentheses are shown the result of single-point energy calculations with the SCRF method based on the polarized continuum model (ε = 8.93 for CH_2Cl_2).

The 3D structures of representative stationary points are shown in Figure 3.[28] The Rh^1-Rh^2 bond of **1** gradually becomes elongated toward the formation of the carbene complex **5** (2.400 Å -> 2.482 Å, 3.4% increase). The Rh^1-C^1 bond of **2** (2.247 Å) significantly shortens in the nitrogen extrusion stage **TS-3** (1.981 Å, 11.8% decrease), which indicates that **TS-3** has the character of the carbene complex **5** (Rh^1-C: 1.906 Å).

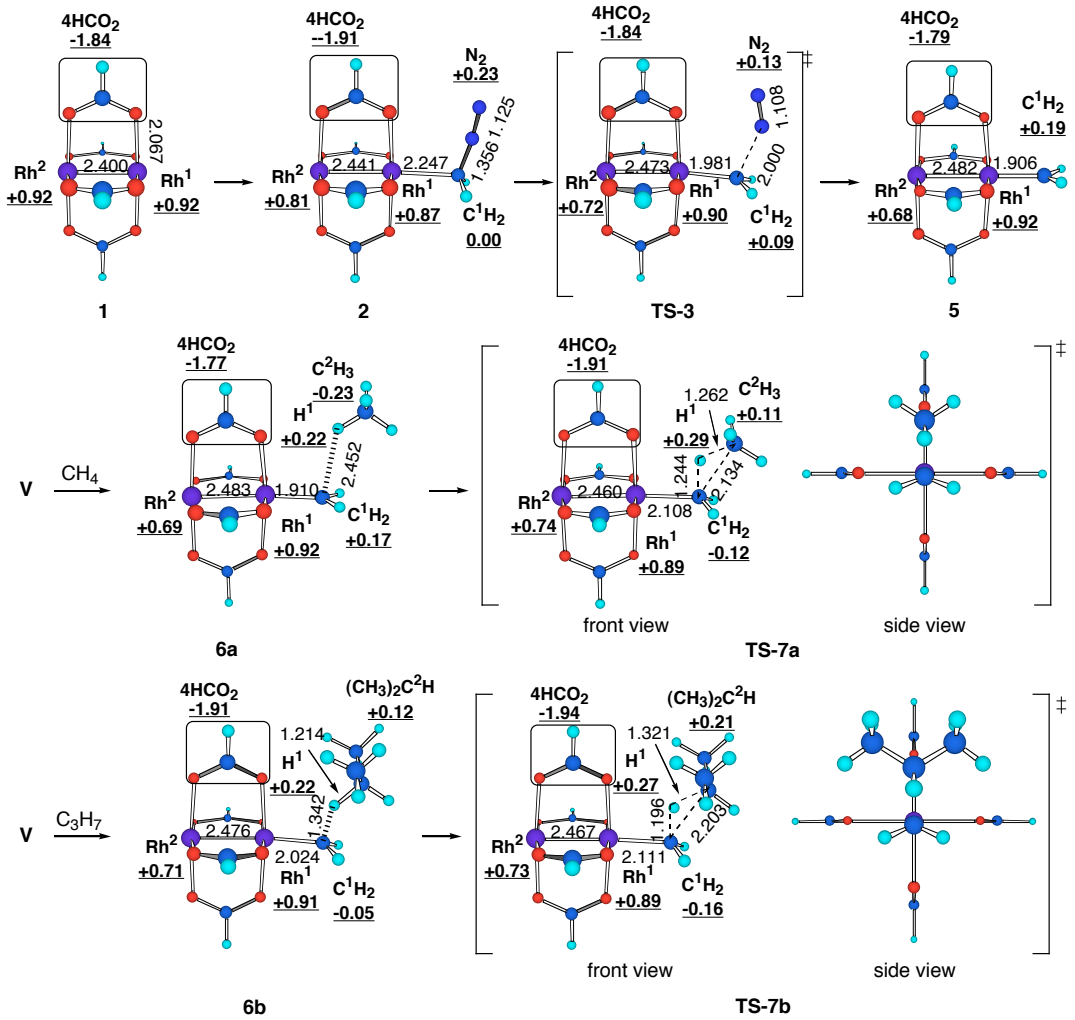

Figure 3. B3LYP/631LAN structures of stationary points in the C-H insertion reaction of diazomethane with methane and propane (at the CH_2 part). The numbers refer to bond length (Å) and natural charges (underlined).

Analysis of the charge distribution during the reaction course was found to be informative, and showed strong parallelism between this simple model (Figure 4a) and the more realistic diazoacetate model discussed later (Figure 4b). The dinitrogen moiety release negative charge

(+0.03 –> +0.23) upon formation of **2**, and the negative charge moves largely into the Rh^2 atom (+0.92 –> +0.81) and the carboxylate groups (-1.84 –> -1.91). In the nitrogen extrusion stage (**TS-3**), the nitrogen moiety becomes less positive (+0.23 –> +0.13) and the methylene group becomes cationic (0.00 –> +0.09). The carboxylate groups become less negatively charged (-1.91 –> -1.84) while the negative charge accumulates on the Rh^2 atom (+0.81 –> +0.72). These are consistent with Pirrung's results[5b] that (1) a diazo compound strongly binds to the rhodium catalyst as the electrophilicity of carboxylate ligands increases and (2) the nitrogen extrusion step is decelerated by highly electrophilic carboxylate ligands.

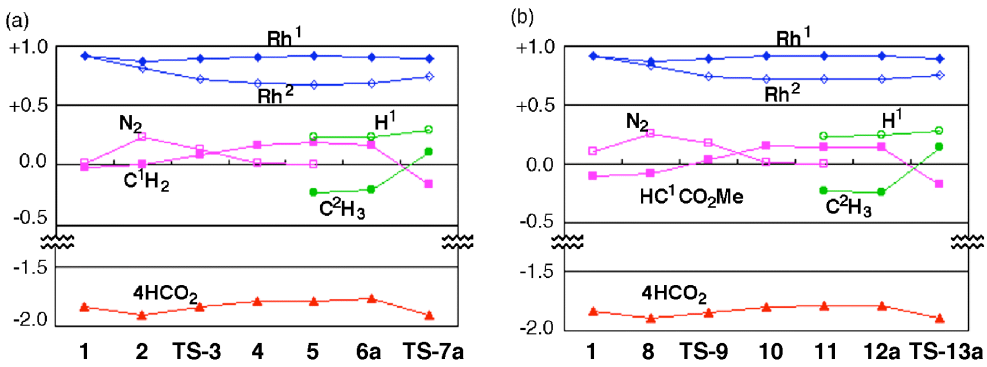

Figure 4. Charge distribution along the reaction coordinate for (a) the reaction between diazomethane and methane and (b) the reaction between methyl diazoacetate and methane.

In the carbene complex **5**, the methylene moiety is positively charged (+0.19), since the negative charge moves largely from the σ-type orbital of the methylene carbon into the Rh^2 atom (increased electron occupancy of the $4d_{z2}$ orbital during conversion from **2** to **5**). The charge of the Rh^1 atom changes little during the carbene complex formation (+0.87 ~ +0.92). The carboxylate groups of **5** are less negatively charged (-1.79) compared to those of the catalyst **1** (-1.84), which is considered to be induced by the back-donation from the Rh^1 atom to the methylene group.

In the reaction of **5** with methane, a weak complex **6a** is formed first with little stabilization energy (0.2 kcal/mol). In **6a**, the distance between the carbene carbon and the methane hydrogen

is very long (2.462 Å) and methane has little influences on the geometry and the charge distribution of the original carbene complex **5**.

In the C-H insertion TS (**TS-7a**), the Rh^1-Rh^2 bond shortens (2.482 Å -> 2.460 Å) and the Rh^2 atom loses negative charge (+0.68 -> +0.74). The methane moiety becomes positively charged (increase by +0.40) due to loss of the C-H σ-bonding electrons (hydride transfer to the carbene carbon). Some negative charge is also transferred to the four formate groups (-0.12 all together). In this TS, the hydride transfer from methane is half complete (the forming C^1-H bond being 1.244 Å; the carbene carbon being partially pyramidalized). The C-C bond formation (C^1-C^2 distance: 2.134 Å) lags behind the hydride transfer, and hence one can conclude that the C-H bond activation/C-C bond formation process is a non-synchronous concerted reaction. It should be noted that the Rh^1-C^1 bond is significantly elongated in the C-H insertion stage (1.906 Å (**5**) –> 2.108 Å (**TS-7a**), 10.6% increase).

In the CH_2 insertion reaction with propane, the carbene complex part of **6b** looks much different from **5**. The Rh^1-C^1 bond is elongated (1.906 Å –> 2.024 Å) and the carbene carbon is being pyramidalized (sum of the bond angles around C^1: 350.0°). A considerable negative charge is transferred from propane to the methylene moiety (the charge of the methylene moiety: +0.19 (**5**) –> -0.05 (**6b**)). **TS-7b** is again a three-centered hydride transfer TS, as shown by the negative charge of the methylene moiety (-0.16) and the positive charge of the propyl group (+0.21).

Charge distributions of **TS-7a** and **TS-7b** indicate that the charge transfer from an alkane to the carbene complex takes place to a larger extent in the propane reaction than in the methane reaction, which reflects the relative stability of methyl cation and secondary propyl cation. This is consistent with the more advanced hydride transfer in the propane reaction than in the methane reaction (length of the forming C^1-H^1 bond is 1.244 Å in **TS-7a** and 1.196 Å in **TS-7b**).

5-3-2. Orbital Analysis of Rh-Rh-C Bonding

To probe the function of the dinuclear structure of the dirhodium catalyst, the nature of the Rh-Rh-C π– and σ-bond systems in **5** (carbene complex) and **TS-7a** (methane C-H insertion TS) was analyzed in several ways. Important Kohn-Sham orbitals of **5** and localized Kohn-Sham orbital (LO) of **TS-7a** are shown in Figure 5. First, LUMO of the complex **5** was found to be exactly what is expected, and composed mainly of the carbene vacant 2p orbital, which accepts rather small back donation from the Rh^1 $4d_{xz}$ orbital (83.3% in $4d_{xz}$ orbital)[29] to form an extended π*-system that possesses a strongly electrophilic carbene carbon (Figure 5a). Bond alternation due to interaction of the LUMO with the C-H σ-bonding orbital of methane can be identified in the LO shown in Figure 5b. Thus, the hydride transfer and the C-C bond formation take place as a single event. The approach of the C-H bond to the carbene center is directed by the steric effect of the formate bridge and by the node between the 2p (carbene carbon) and the $4d_{xz}$ (Rh^1 atom) orbitals in the LUMO (see Figure 5a).

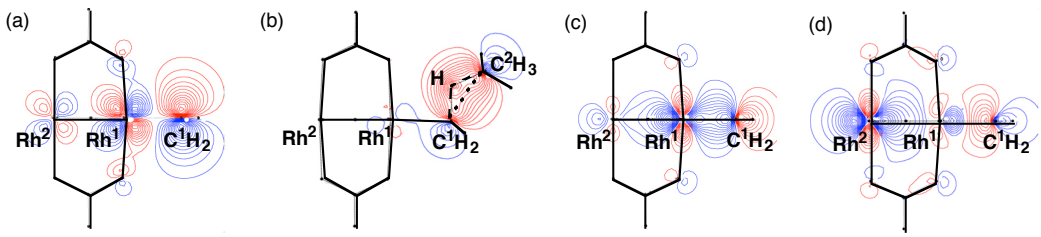

Figure 5. Kohn-Sham orbitals of **5** (a: LUMO, c: HOMO-19 and d: HOMO-3) and LO of **TS-7a** responsible for bond alternation (b). The contour intervals are 0.025 e•au^{-3}.

There are two ways to describe the Rh-Rh-C σ-system (Ψ_1, Ψ_2 and Ψ_3 in Chart 1). HOMO-19, HOMO-3 (Figure 5c, 5d), and LUMO+2 (not shown) correspond to Ψ_1, Ψ_2, and Ψ_3, respectively. In one analysis, the Rh^2 non-bonding $4d_{z2}$ orbital interacts with the Rh^1-C^1 σ/σ*-orbitals (Chart 1a), which weakens the Rh^1-C^1 σ-bond. This interaction is important in the reaction with an alkane, where Rh^2 moves toward Rh^1 and the Rh^1-C^1 bond is being cleaved as the C-H insertion proceeds. In this sense, the Rh^2 atom possessing high-lying $4d_{z2}$ electrons is

ideally positioned by the carboxylate bridges. In another analysis (Chart 1b), the non-bonding carbene 2sp orbital interacts with the Rh^1-Rh^2 σ/σ*-orbitals.[30] With this interaction, the Rh^1-Rh^2 bond weakens and negative charge moves from the carbene to the Rh^2 atom, which accounts for the changes of the structure and the charge distribution along the carbene complex formation as discussed above.

Chart 1. Rh-Rh-C σ-System (Ψ_1, Ψ_2 and Ψ_3) Constructed in Two Ways

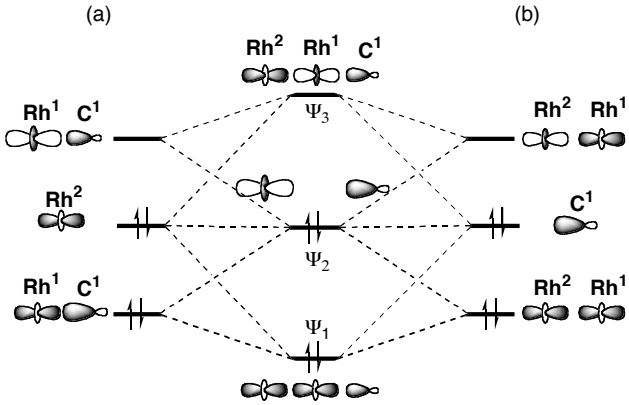

(a) From Rh^2 non-bonding $4d_{z2}$ orbital and Rh^1-C^1 σ/σ* orbitals, and (b) from Rh^1-Rh^2 σ/σ*-orbitals and non-bonding carbene 2sp orbital.

The above molecular orbital discussion is supported by the natural bond orbital analysis,[27,29] which indicates that **5** can be described with nearly equal contributions of two resonance structures **LSa** and **LSb**.[31] In the Lewis structure **LSa**, a cationic Rh^1 carbene complex is coordinated with the non-bonding electrons of the Rh^2 atom (indicated as a dative bond arrow). In **LSb**, non-bonding carbene electrons coordinate to the Rh^1-Rh^2 unit, while the vacant carbene 2p orbital forms a π bond with the Rh^1 $4d_{xz}$ orbital ("π-bonding without σ– covalent bond" is expressed as a pair of broken lines).

Chart 2.

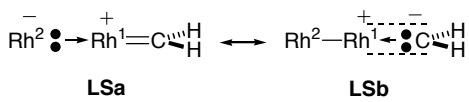

5-4. Reaction of Methyl Diazoacetate with Methane and Propane

α-Diazoesters are the most important compounds for the rhodium-catalyzed C-H insertion reaction. In Figure 6 is shown the energy profile of the $Rh_2(O_2CH)_4$-catalyzed C-H insertion reaction of methyl diazoacetate with methane (denoted as **a**) and propane (CH_3 insertion (denoted as **b**) and CH_2 insertion (denoted as **c**)). The reaction pathway and the energetics obtained for the diazoacetate model are essentially the same as those of the diazomethane model (Scheme 2). The Rh/diazoacetate complex **8** forms with 13.0-kcal/mol stabilization energy. The activation energy for the nitrogen extrusion (**TS-9**) is 16.7 kcal/mol, which is nearly identical with that of the diazomethane model (16.6 kcal/mol). Unlike in the diazomethane model, [**11** (carbene complex) + N_2] is more stable than **TS-9** by 3.7 kcal/mol. The C-H activation/C-C formation step proceeds with a moderate (9.8 kcal/mol for methane insertion) or a small (4.7 kcal/mol for propane CH_3 insertion and 0.2 kcal/mol for propane CH_2 insertion) activation energy with large exothermicity (52-54 kcal/mol). The activation energy for propane methylene insertion is much lower than the activation energy for methane insertion, with propane methyl insertion inbetween. Details of each reaction step and properties of equilibrium and transition structures will be discussed below.

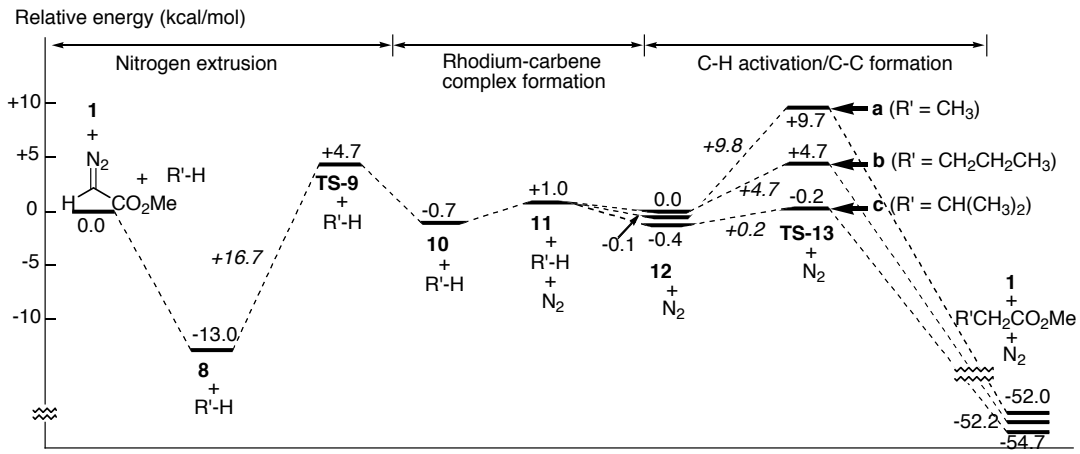

Figure 6. Energy profile of the $Rh_2(O_2CH)_4$-catalyzed reaction of methyl diazoacetate with methane (denoted as **a**) and propane (CH_3 insertion (denoted as **b**) and CH_2 insertion (denoted as **c**)) at the B3LYP/631LAN level.

The 3D structures of **8** and **TS-9** are shown in Figure 7. The nitrogen extrusion step starts with complex formation between the rhodium catalyst and diazoester (**8**).[32,33] HOMO-18 of **8** (Figure 7b) illustrates donation from the diazoacetate to the Rh^1-Rh^2 σ*-orbital. On the other hand, no back-donation from the Rh^1 occupied $4d_{xz}$ orbital to the diazoester was identified in **8**. Thus, **8** is a simple Lewis acid/Lewis base complex.

In the nitrogen extrusion transition state **TS-9**, the Rh^1-C^1 bond shortens (2.337 Å -> 2.041 Å, 13% decrease) and the C^1-N bond lengthens (1.335Å -> 1.933 Å, 45% increase). In addition, substantial change of hybridization (sp^3 –> sp^2) at the C^1 atom takes place from **8** to **TS-9** (sum of bond angles around C^1: 324.0° (**8**) –> 349.0° (**TS-9s**)). The charge distribution shows the same tendency as found for the diazomethane model (cf. Figure 4). This is also found in the events after the nitrogen extrusion. As seen in the energy profile of the reaction (Figure 6), **TS-9** is a very late transition state and shows some character of the rhodium-carbene complex, and back-donative interaction is identified in the LO of **TS-9** (Figure 7c, **LO2**). This back-donation from the Rh^1 occupied $4d_{xz}$ orbital to the C^1-N σ*-orbital is an important driving force of the nitrogen extrusion.[5b,9b] The activation enthalpy ($\Delta H^{\ddagger}$) of the nitrogen extrusion (15.2 kcal/mol) is in reasonable agreement with the experimental value (16.4 ± 1.4 kcal/mol, $Rh_2(OAc)_4$ and ethyl diazoacetate).[5a]

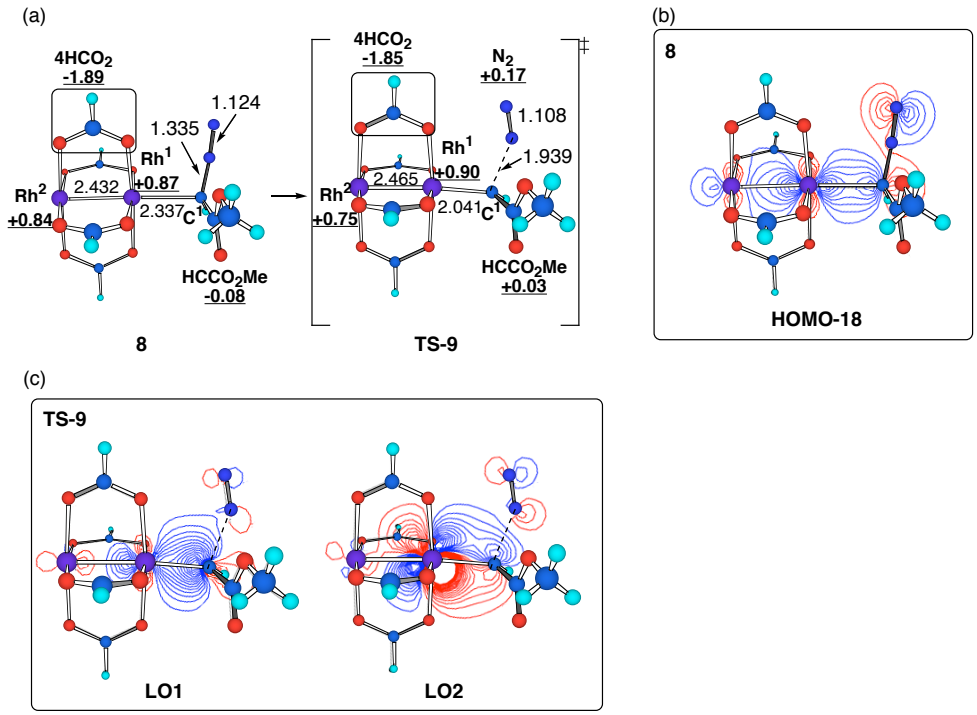

Figure 7. (a) 3D structures of the $Rh_2(O_2HC)_4$/methyl diazoacetate complex **8** and the nitrogen extrusion TS (**TS-9**) optimized at the B3LYP/631LAN level. The numbers refer to bond lengths (Å) and natural charges (underlined). (b) HOMO-18 orbital of **8** indicating donative interaction. (c) Localized orbitals of **TS-9** indicating donative (**LO1**) and back-donative (**LO2**) interaction. Orbitals are shown in the Rh^1-C^1-N plane and contour intervals are 0.025 e•au^{-3} for HOMO-18 and **LO1**, 0.010 e•au^{-3} for **LO2**.

The 3D structure of the dirhodium methoxycarbonyl carbene complex **11** is shown in Figure 8. The important issue to be addressed here is the influence of the methoxycarbonyl group on the character of the Rh^2-Rh^1-C^1 bond system. The carbene carbon center of **11** is electrophilic, as indicated from the positive charge of the carbene moiety (+0.14) and significant contribution of the 2p orbital of the carbene carbon in the LUMO of **11** (Figure 8b). One will expect that the carbene carbon of **11** is more electrophilic than that of the methylene carbene complex (**5**) since **11** has the electron-withdrawing ester group. To the contrary, the energy levels of LUMO is the same (-3.7 eV) for **5** and **11**, because the vacant 2p orbital of the carbene carbon of **11** is *not conjugated* with the ester carbonyl group. There is one notable structural feature in **11** that is described below.

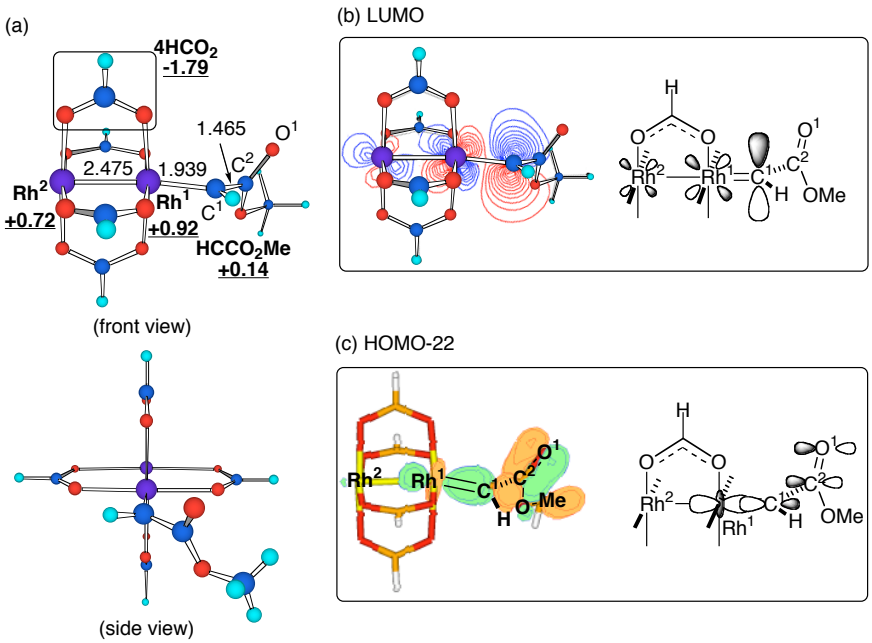

Figure 8. (a) 3D structure of the dirhodium methoxycarbonyl carbene complex **11** optimized at the B3LYP/631LAN level**.** The numbers refer to bond lengths (Å) and natural charges (underlined). (b) The contour map of LUMO and (c) the surface of HOMO-22 of **11** and their schematic representations. The orbitals are shown in the Rh^1-Rh^2-C^1 plane. The contour intervals for (b) is 0.025 e•au^{-3} and the contour value for (c) is 0.060 e•au^{-3}.

The Rh^1-C^1 π-bond and the ester carbonyl C^2-O^1 π-bond are orthogonal to each other and not conjugated with each other (the dihedral angle <Rh^1-C^1-C^2-O^1 = 112.0°).[34,35] This orientation of the ester group has thus far escaped attention of chemists working in this area. For instance, the Rh^1=C^1-C^2=O^1 π-array has often been depicted to be planar and conjugated.[9bc,11b,36] In this structure the C^2=O^1 π-bond and the Rh^1-C^1 σ–bond (not the Rh^1-C^1 π-bond) are considered to have some interaction like an α-metaloester. Indeed, one can identify HOMO-22 of **11** that comprises a four-electron out-of-phase interaction between Rh^1-C^1 σ- and C^2=O^1 π-orbitals (Figure 8c). Thus, the ester carbonyl group affects the character of the Rh-Rh-C σ-system of the carbene complex rather than that of the π-system. When the carbene complex was optimized with C_s symmetry restriction (keeping the Rh^1=C^1-C^2=O^1 moiety in a plane; this structure is denoted as **11-*C*$_s$**), **11-*C*$_s$** was less stable than **11** by 6.4 kcal/mol. The C^1-C^2 bond length of **11** (1.465 Å) is shorter than that of **11-*C*$_s$** (1.495 Å). Putting together this result and the orbital interaction shown

in Figure 8c, we conclude that the C^2-O^1 π-bond is conjugated with the Rh^1-C^1 σ-bond (instead of the Rh^1-C^1 π-bond).The orthogonal geometry of **11** described here creates a diastereomerism in the C-H activation stage–a stereochemical issue so far escaped attention (*vide infra*).

Structural changes around the methane C-H insertion transition state (**TS-13a**) is shown in Figure 9.[37] The potential energy surface is very flat before **TS-13a**, but it is very steep after **TS-13a**. As it goes from [**11 +** methane] to **TS-13a**, positive charge develops in the methane moiety (0.00 -> +0.42) and the carbene moiety becomes negatively charged (+0.14 -> -0.18). The C-H bond of the methane approaches **11** to have maximum interaction with the LUMO (Figure 8b) and the LO of **TS-13a** shows three-centered interaction between the C^3-H^1 σ–orbital of methane and the vacant 2p orbital of the carbene carbon C^1. The C-H activation is an electrophilic reaction, and the bond alternation including the C^1-H^1-C^3 moiety takes place as a single event in **TS-13a**. In spite of a previous suggestion that the Rh^1 atom may interact with the C-H bond,[11b] we could not locate such a TS. Such a TS is difficult to achieve due to electronic and steric reasons; that is, there is a node in the LUMO of **11** (Figure 8b) and the Rh^1 atom is sterically too congested to interact with any nucleophile.

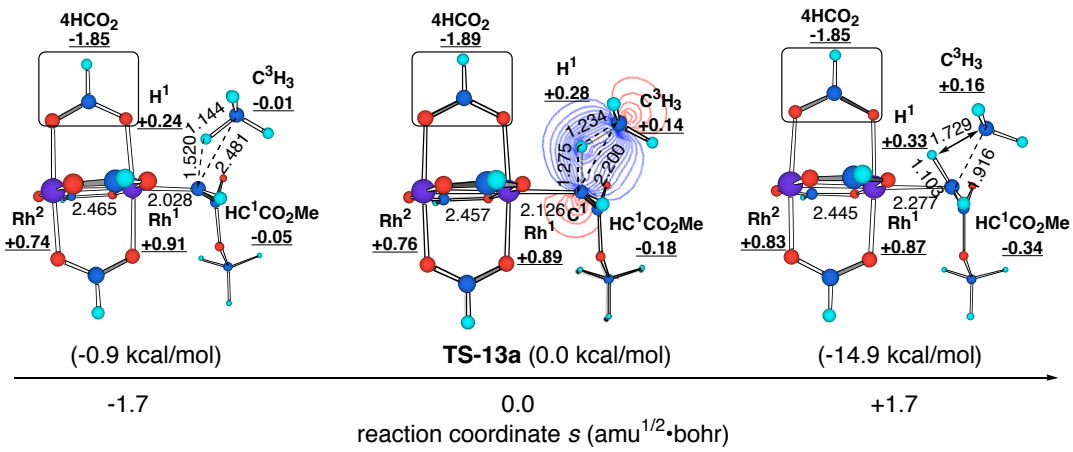

Figure 9. 3D structures of methane C-H insertion TS (**TS-13a**) and intermediary structures on the IRC of both forward (+1.7 $amu^{1/2}$•bohr) and reverse (-1.7 $amu^{1/2}$•bohr) direction at the B3LYP/631LAN level. The numbers refer to bond lengths (Å) and natural charges (underlined). The localized orbital of **TS-13a** is shown together with its 3D structure.

Changes of the lengths of breaking C-H bond, forming C-H bond, and forming C-C bond along the IRC (Figure 9) indicate non-synchronicity of the C-H bond activation/C-C bond formation stage. In the structure of s = +1.7 amu$^{1/2}$•bohr from **TS-13a**, the C^1-H^1 bond is completely formed (1.10 Å), but the C^1-C^2 bond is yet to be formed (1.92 Å). The Rh^1-C^1 bond becomes much elongated near **TS-13a** (2.028 Å –> 2.126 Å –> 2.277 Å), while the change of the Rh^1-Rh^2 bond length is small.

The activation energy of the C-H insertion is rather high with methane (9.8 kcal/mol), moderate (4.7 kcal/mol) with propane (CH_3 insertion), and extremely low (0.2 kcal/mol) with propane (CH_2 insertion). This parallels the experimental fact that the reactivity of a C-H bond increases in an order of primary, secondary, and tertiary.[7] Three TSs of C-H activation shown in Figure 10 are compared. The net positive charges of alkyl groups are +0.14, +0.20, and +0.25 in **TS-13a** (methane insertion), **TS-13b** (propane CH_3 insertion), **TS-13c** (propane CH_2 insertion), respectively. These values are consistent with the stability order of the incipient carbocation (methyl < primary < secondary).

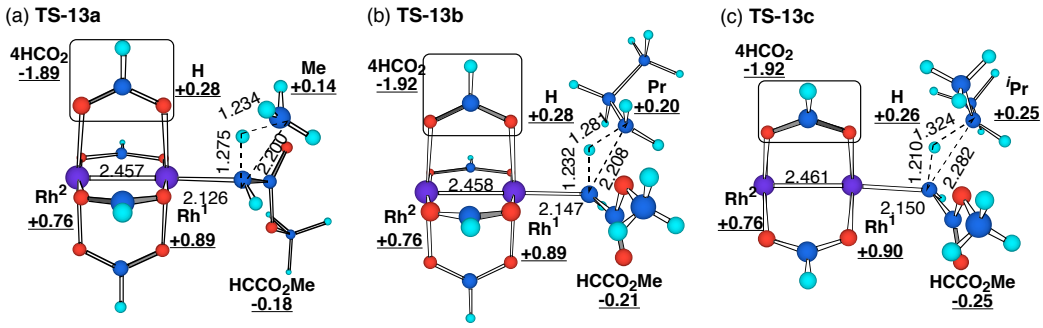

Figure 10. 3D structures of the C-H insertion TSs of (a) methane (**TS-13a**), (b) propane (CH_3, **TS-13b**), and (c) propane (CH_2, **TS-13c**) with the carbene complex **11** optimized at the B3LYP/631LAN level. The numbers refer to bond lengths (Å) and natural charges (underlined).

Bond lengths also give important information on the C-H activation/C-C formation reaction. Lengths of the breaking C-H bonds are 1.234 Å, 1.281 Å, and 1.324 Å and those of forming C-H bonds are 1.275 Å, 1.232 Å, and 1.210 Å for **TS-13a**, **TS-13b**, and **TS-13c**, respectively. Thus, hydrogen transfer is the most advanced in the propane CH_2 insertion. On the other hand, the C-C

bond formation is the most advanced in the methane reaction (C-C distance: 2.200 Å, 2.208 Å, and 2.282 Å for **TS-13a**, **TS-13b**, and **TS-13c**, respectively). Putting all these data together, one can conclude that the C-H activation/C-C bond formation process is a non-synchronous concerted reaction bearing a character of hydride abstraction. It should be pointed out that the Rh^1-C^1 bond of the carbene complex **11** (1.939 Å) is much elongated in the C-H insertion TSs (2.126-2.150 Å, about 10% increase).

Kinetic isotope effects (KIEs) data have proven to be useful to correlate the nature of the TSs inferred by experiments and by theory.[38] The KIE calculated for the insertion to secondary C-H/C-D bond of propane/propane-d_8 was found to be 2.03 (eq 3), which can be favorably compared with the experimental data: The KIE values of 2.45 and 1.55 were reported for the reaction of ethyl diazoacetate with a cyclohexane/cyclohexane-d_{12} pair under the catalysis of $Rh_2(OAc)_4$ and $Rh_2(OCOCF_3)_4$, respectively.[6a] The correlation looks reasonable since the electron-withdrawing ability of the formate ligand falls between that of acetate and trifluoroacetate ligands (i.e., inversely related to the acidity of the conjugate acid).[39]

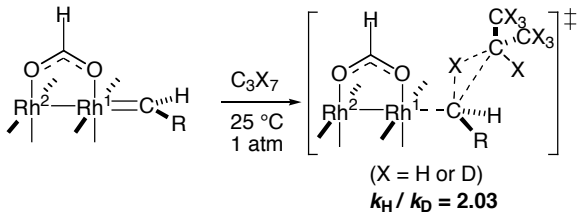

(3)

5-5. Enthalpy and Gibbs Free Energy Profiles of the Catalytic Cycles

The enthalpies and the Gibbs free energies of the present reactions were calculated for the structures optimized at the B3LYP/631LAN level. The enthalpy (a) and the Gibbs free energy profiles (b) of the diazomethane model are shown in Figure 11. When free energies are considered (Figure 11b), the complex between **5** (carbene complex) and N_2 (**4**) becomes no longer more stable than [**5** + N_2]. The complexes between **5** and an alkane (methane (**6a**) or

propane (**6b**)) also becomes less stable than [**5** + R'-H]. Therefore, these complexes may not exist as stable intermediates in actual reactions (therefore omitted from Figure 11).[40] While the thermal correction for enthalpy did not change the energy profile very much (Figure 2 and Figure 11a), consideration of the entropy term expectedly change the energy profile (Figure 11b). The stabilization energy of the complexation between **1** and diazomethane has become 9.9 kcal/mol, whereas the activation energy of the nitrogen extrusion (15.2 kcal/mol) is not much affected. The carbene complex [**5** + N_2] becomes much more stable than the nitrogen extrusion TS (**TS-3**). The activation energies of the C-H insertion (the energy difference between [**5** + R'-H] and **TS-7**) significantly increase.

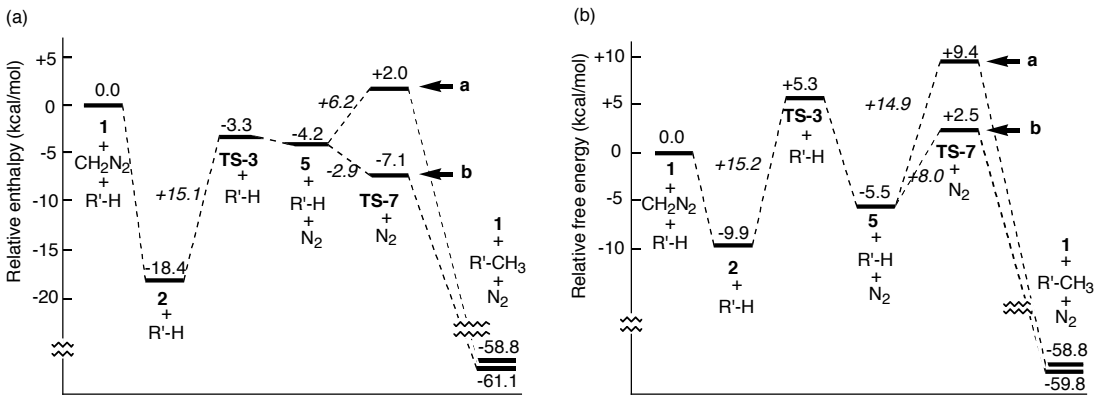

Figure 11. (a) Enthalpy and (b) Gibbs free energy profiles of the $Rh(O_2CH)_4$-catalyzed reaction of diazomethane with methane and propane, obtained with the structures optimized at the B3LYP/631LAN level.

The enthalpy (a) and the Gibbs free energy profiles (b) of the diazoester model are shown in Figure 12. Similarly to the diazomethane model, the entropy term exerts a considerable influence on the free energy changes, especially on the activation energy of the C-H insertion step. The activation energy of the nitrogen extrusion step was not affected very much again. In accordance with experiments, the nitrogen extrusion step was found to be the rate-limiting for secondary C-H insertion reaction (Figure 12b).[41]

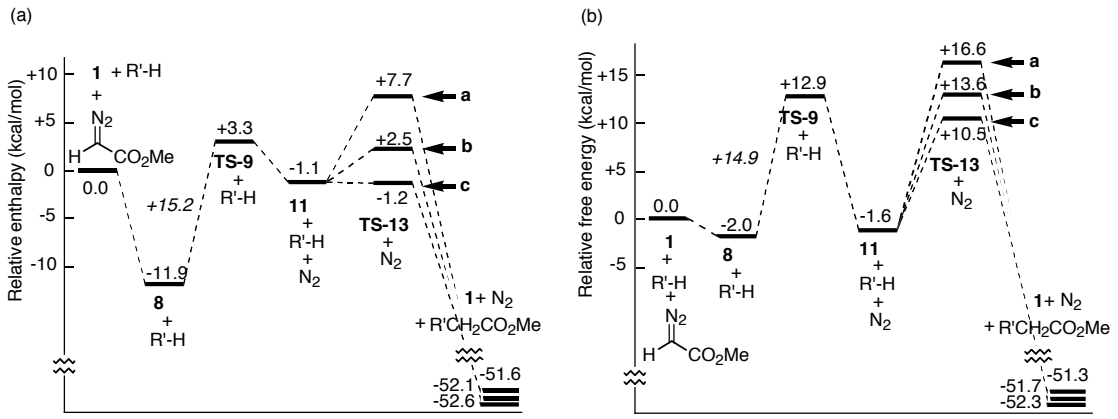

Figure 12. (a) Enthalpy and (b) Gibbs free energy profiles of $Rh_2(O_2CH)_4$-catalyzed reaction of methyl diazoacetate with methane and propane, obtained with the structures optimized at the B3LYP/631LAN level.

5-6. Uniqueness of Dirhodium Catalyst in C-H Insertion

The molecular orbital and NBO analyses combined with the known experimental data[5-9] indicate that the C-H insertion comprises an electrophilic attack of the carbene 2p orbital onto the C-H σ-bonding orbital of an alkane. The reaction proceeds through a relatively late TS, where the Rh^1-C^1 bond cleavage is therefore involved. This appears to be general for the C-H bond activation reaction of metal carbene complexes (*vide infra*) and metal carbenoids and represents the difference between the C-H insertion reaction and the cyclopropanation reaction. The TS of the latter reaction involves much earlier transition state (i.e., little metal-carbene bond cleavage was found by us and by Salvatella et al.).[35,42] For the reaction with such a nucleophilic substrate as an olefin, the electrophilicity of the carbene carbon atom controls the reaction. On the other hand, in the C-H activation, the lability of the metal-carbene σ-bond in the TS is as important as the high electrophilicity of the carbene carbon.

We consider that the structure of the dirhodium complex **1** is ideal for the C-H bond activation reaction, since the Rh^2 atom acts as a bifunctional electron pool. Thus, the Rh^2 atom is detached from the Rh^1-C^1 moiety to enhance the electrophilicity of the carbene center (net result

is charge transfer from the carbene to the Rh^2 atom and formation of a formal cationic Rh^1-carbene complex as shown in Chart 2) or attached to it to facilitate the cleavage of the Rh^1-C^1 bond in the transition state (loosening of the Rh^1-C^1 bond). The carboxylate groups serve as anchors of the Rh^2 atom and also as electron-withdrawing groups that enhance the electrophilicity of the carbene center. It also serves as the site to harness chirality. Much related synergistic effects of two equal transition metals have also been pointed out for the $Co_2(CO)_8$-catalyzed Pauson-Khand reaction.[43]

To further probe the role of the dinuclear structure, the rhodium reaction was compared with single metal model reactions. Methane C-H insertion reactions of copper-[44] (**14**) and ruthenium-methylene carbene complexes (**16**)[45] were briefly studied (eq 4 and 5).[46,47] The activation energy of the C-H insertion is 15.6 kcal/mol for **14**, and 27.6 kcal/mol for **16**, values much higher than that for the dirhodium carbene complex **5** (+5.7 kcal/mol).[48]

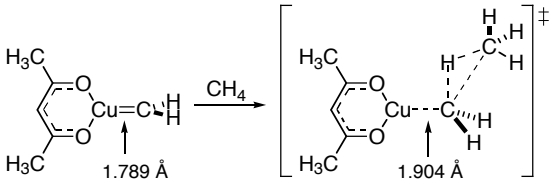

(4)

14 **TS-15**

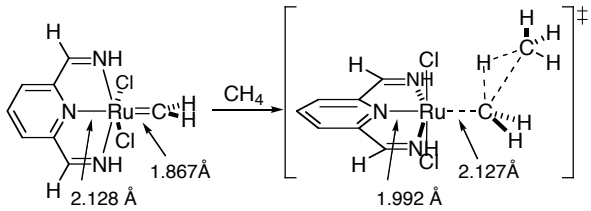

(5)

16 **TS-17**

Significant metal-carbon bond cleavage is found in the C-H insertion TSs (**TS-15** and **TS-17**) as found for the rhodium-carbene complex (eq 4 and 5, see also Figure 2). The N (pyridine)-Ru bond shortens by 6.4% (2.128 Å –> 1.992 Å) as the carbene group is transferred to methane.

One may consider that trans effect of the ligand in these complexes might play significant roles in the C-H insertion reaction. In the Cu complex **14**, there is no ligand *trans* to the carbene

group. In the Ru complex **16**, a pyridine ligand is positioned *trans* to the carbene ligand and facilitates the Ru-C bond cleavage. However, its effect must be rather weak since the lone pair of the nitrogen atom is a weak donor to the Ru-C σ*-orbital. The Rh^2 atom in **5** causes much stronger trans effect to the neighboring Rh^1-C^1 σ*-orbital, since the Rh^2 non-bonding $4d_{z2}$ orbital is energetically very close to the Rh^1-C^1 σ*-orbital (cf. Chart 1).

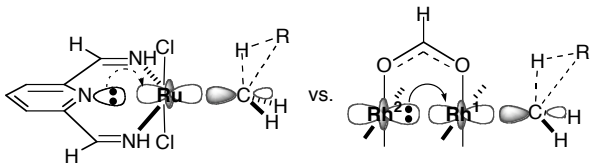

5-7. Conclusion

The present studies have revealed, for the first time, the energetics, the electronic nature and the 3D structures of the intermediates and the TSs in the catalytic cycle of the dirhodium tetracarboxylate-catalyzed C-H bond activation/C-C bond formation reaction (Scheme 3). The reaction is initiated by complexation between the rhodium catalyst and the diazo compound. Driven by the back-donation from the Rh $4d_{xz}$ orbital to the C-N σ*-orbital, nitrogen extrusion takes place to afford a rhodium-carbene complex. The carbene carbon of the complex is strongly electrophilic due to its vacant 2p orbital. The nature of the C-H activation/C-C formation step, which has so far been little known, was found to be concerted but non-synchronous. Two important events are taking place in the concerted, non-synchronous TS as illustrated with two resonance structures (bracket in Scheme 3). The first event is the hydride transfer from the alkane to the carbene carbon. The second is the C-C bond formation and the regeneration of the Rh-Rh bond.

Scheme 3.

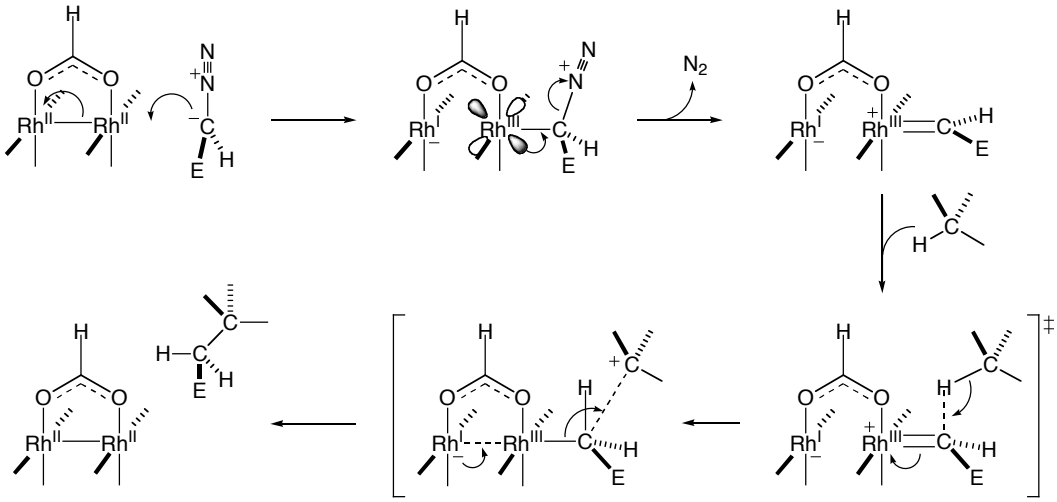

Only one of the two rhodium atoms works as a carbene binding site throughout the reaction, and the other rhodium atom assists the C-H insertion reaction. The second Rh atom acts as a mobile ligand for the first one to enhance the electrophilicity of the carbene moiety and to facilitate the cleavage of the rhodium-carbon bond. Some pertinent experimental data have been reasonably reproduced by the DFT calculations; that is, the activation enthalpy of the rate-limiting nitrogen extrusion, relative reactivity of C-H bonds, and the kinetic isotope effect for the C-H insertion step. The theoretical analysis delineated above will contribute to the rational designing of useful synthetic transformations.

References and Notes

1. (a) Shilov, A. E.; Shul'pin, G. B. *Chem. Rev.* **1997**, *97*, 2879-2932. (b) Dyker, G. *Angew. Chem., Int. Ed.* **1999**, *28*, 1698-1712.
2. (a) *Selective Hydrocarbon Activation*; Davies, J. A., Watson, P. L., Greenberg, A., Liebman, J. F., Eds.; VCH Publishers: New York, 1990. (b) *Activation and Functionalization of Alkanes*; Hill, C. L., Ed.; John Wiley & Sons, Inc.: New York, 1989. (c) Kakiuchi, F.; Murai, S. In *Activation of Unreactive Bonds and Organic Synthesis*; Murai, S., Ed.; Splinger: Berlin, 1999.
3. (a) Doyle, M. P. *Chem. Rev.* **1986**, *86*, 919-939. (b) Taber, D. F. In *Comprehensive Organic Synthesis*; Trost, B. M., Fleming, I., Eds.; Pergamon Press, New York, 1991; Vol. 3, Chapter 4.2. (c) Doyle, M. P. In *Comprehensive Organometallic Chemistry II*; Hegedus, L. S., Ed.; Pergamon Press, New York, 1995; Vol. 12, Chapters 5.1 and 5.2. (d) Ye, T.; McKervey, M. A. *Chem. Rev.* **1994**, *94*, 1091-1160. (e)

Doyle, M. P.; McKervey, M. A.; Ye, T. *Modern Catalytic Methods for Organic Synthesis with Diazo Compounds*; John Wiley & Sons, Inc.: New York, 1998. (f) Dörwald, F. Z.; *Metal Carbenes in Organic Synthesis*; Wiley-VCH: Weinheim, 1999.

4. (a) Davies, H. M. L.; Antoulinakis, E. G. *J. Organomet. Chem.* **2001**, *617-618*, 47-55. (b) Doyle, M. P.; Forbes, D. C. *Chem. Rev.* **1998**, *98*, 911-935.
5. (a) Alonso, M. E.; García, M. del C. *Tetrahedron* **1989**, *45*, 69-76. (b) Pirrung, M. C.; Morehead, A. T., Jr. *J. Am. Chem. Soc.* **1996**, *118*, 8162-8163. Pirrung, M. C.; Liu, H.; Morehead, A. T., Jr. *J. Am. Chem. Soc.* **2002**, *124*, 1014-1023.
6. (a) Demondeceau, A.; Noels, A. F.; Costa, J-L. *J. Mol. Catal.* **1990**, *58*, 21-26. (b) Wang, P.; Adams, J. *J. Am. Chem. Soc.* **1994**, *116*, 3296-3305.
7. (a) Taber, D. F.; Ruckle, R. E., Jr. *J. Am. Chem. Soc.* **1986**, *108*, 7686-7693. (b) Doyle, M. P.; Westrum, L. J.; Wolthuis, W. N. E.; See, M. M.; Boone, W. P.; Bagheri, V.; Pearson, M. M. *J. Am. Chem. Soc.* **1993**, *115*, 958-964.
8. Adams, J.; Spero, D. M. *Tetrahedron* **1991**, *47*, 1765-1808.
9. (a) Padwa, A.; Austin, D. J.; Price, A. T.; Semones, M. A.; Doyle, M. P.; Protopopova, M. N.; Winchester, W. R.; Tran, A. *J. Am. Chem. Soc.* **1993**, *115*, 8669-8680. (b) Pirrung, M. C.; Morehead, A. T., Jr. *J. Am. Chem. Soc.* **1994**, *116*, 8991-9000. (c) Wang, J.; Chen, B.; Bao, J. *J. Org. Chem.* **1998**, *63*, 1853-1862.
10. Taber, D. F.; Petty, E. H.; Raman, K. *J. Am. Chem. Soc.* **1985**, *107*, 196-199.
11. (a) Taber, D. F.; You, K. K.; Rheingold, A. L. *J. Am. Chem. Soc.* **1996**, *118*, 547-556. (b) Taber, D. F.; Malcolm, S. C. *J. Org. Chem.* **1998**, *63*, 3717-3721.
12. These results are consistent with the fact that a C-H bond adjacent to an oxygen atom and a Si-H bond are 103-104 times more reactive than a C-H bond of a normal hydrocarbon: Davies, H. M. L.; Hansen, T.; Churchill, M. R. *J. Am. Chem. Soc.* **2000**, *122*, 3063-3070.
13. Gaussian 94, revision D.3, Frisch, M. J.; Trucks, G. W.; Schlegel, H. B.; Gill, P. M. W.; Johnson, B. G.; Robb, M. A.; Cheeseman, J. R.; Keith, T.; Petersson, G. A.; Montogomery, J. A.; Raghavachari, K.; Al-Laham, M. A.; Zakrzewski, V. G.; Ortiz, J. V.; Foresman, J. B.; Cioslowski, J.; Stefanov, B. B.; Nanayakkara, A.; Challacombe, M.; Peng, C. Y.; Ayala, P. Y.; Chen, W.; Wong, M. W.; Andres, J. L.; Replogle, E. S.; Gomperts, R.; Martin, R. L.; Fox, D. J.; Binkley, J. S.; Defrees, D. J.; Baker, J.; Stewart, J. P.; Head-Gordon, M.; Gonzalez, C.; Pople, J. A. Gaussian. Inc.: Pittsburg, PA, 1995.
14. Gaussian 98, revision A.9, Frisch, M. J.; Trucks, G. W.; Schlegel, H. B.; Scuseria, G. E.; Robb, M. A.; Cheeseman, J. R.; Zakrzewski, V. G.; Montogomery, J. A., Jr.; Stratmann, R. E.; Burant, J. C.; Dapprich, S.; Millam, J. M.; Daniels, A. D.; Kudin, K. N.; Strain, M. C.; Farkas, O.; Tomasi, J.; Barone, V.; Cossi, M.; Cammi, R.; Mennucci, B.; Pomelli, C.; Adamo, C.; Clifford, S.; Ochterski, J.;

Petersson, G. A.; Ayala, P. Y.; Cui, Q.; Morokuma, K.; Malick, D. K.; Rabuck, A. D.; Raghavachari, K.; Foresman, J. B.; Cioslowski, J.; Ortiz, J. V.; Baboul, A. G.; Stefanov, B. B.; Liu, G.; Liashenko, A.; Piskorz, P.; Komaromi, I.; Gomperts, R.; Martin, R. L.; Fox, D. J.; Keith, T.; Al-Laham, M. A.; Peng, C. Y.; Nanayakkara, A.; Challacombe, M.; Gill, P. M. W.; Johnson, B.; Chen, W.; Wong, M. W.; Andres, J. L.; Gonzalez, C.; Head-Gordon, M.; Pople, J. A. Gaussian. Inc.: Pittsburg, PA, 1998.

15. (a) Becke, A. D. *J. Chem. Phys.* **1993**, *98*, 5648-5652. (b) Lee, C.; Yang, W.; Parr, R. G.; *Phys. Rev. B* **1988**, *37*, 785-789.
16. Wadt, W. R.; Hay, P. J. *J. Chem. Phys.* **1985**, *82*, 299-310.
17. Hehre, W. J.; Radom, L.; Schleyer, P. v R.; Pople, J. A. *Ab Initio Molecular Orbital Theory*; John Wiley & Sons, Inc.: New York, 1986. References cited therein.
18. Niu, S.; Hall, M. B. *Chem. Rev.* **2000**, *100*, 353-405.
19. (a) Padwa, A.; Snyder, J. P.; Curtis, E. A.; Sheehan, S. M.; Worsencroft, K. J.; Kappe, C. O. *J. Am. Chem. Soc.* **2000**, *122*, 8155-8167. Sheehan, S. M.; Padwa, A.; Snyder, J. P. *Tetrahedron Lett.* **1998**, *39*, 949-952. (b) Schmid, R.; Herrmann, W. A.; Frenking, G. *Organometallics* **1997**, *16*, 701-708.
20. MP2(FC) (FC = frozen core): Møller, C.; Plesset, M. S. *Phys. Rev.* **1934**, *46*, 618-622; Pople, J. A.; Krishman, R.; Schlegel, H. B.; Binkley, J. S. *Int. J. Quantum. Chem. Symp.* **1979**, *13*, 225-241.
21. Cotton, F. A.; Deboer, B. G.; Laprade, M. D.; Pipal, J. R.; Ucko, D. A. *Acta Cryst.* **1971**, *B27*, 1664-1671.
22. (a) Fukui, K. *Acc. Chem. Res.* **1981**, *14*, 363-368. (b) Gonzalez, C.; Schlegel, H. B. *J. Chem. Phys.* **1989**, *90*, 2154-2161. Gonzalez, C.; Schlegel, H. B. *J. Phys. Chem.* **1990**, *94*, 5523-5527.
23. Scott, A. P.; Radom, L. *J. Phys. Chem.* **1996**, *100*, 16502-16513.
24. Miertus, S.; Scrocco, E.; Tomasi, J. *J. Chem. Phys.* **1981**, *55*, 117-129. Miertus, E.; Tomasi, J. *J. Chem. Phys.* **1982**, *65*, 239-245. Barone, V.; Cossi, M.; Tomasi, J. *J. Comput. Chem.* **1998**, *19*, 404-417.
25. (a) Boys, S. F. *Quantum Theory of Atoms, Molecules, and the Solid State*; Lowdin, P. O., Ed.; Academic Press: New York, 1968; pp 253-262. (b) Haddon, R. C.; Williams, G. R. J. *Chem. Phys. Lett.* **1976**, *42*, 453-455.
26. Kohn, W.; Sham, L. J. *Phys. Rev.* **1965**, *140*, A1133-1138.
27. Reed, A. E.; Weinstock, R. B.; Weinhold, F. *J. Chem. Phys.* **1985**, *83*, 735-746. Reed, A. E.; Curtiss, L. A.; Weinhold, F. *Chem. Rev.* **1988**, *88*, 899-926. NBO Version 3.1 in the Gaussian 98 package implemented by Glendening, E. D.; Reed, A. E.; Carpenter, J. E.; Weinhold, F.; University of Wisconsin: Madison, WI, 1990.
28. Symmetry of stationary points are as follows: **1**: D_{4h}, **5**: C_{2v}, **2**, **TS-3**, **6**, **TS-7**: C_s.
29. For NBO analysis of metal-carbene complexes, see: (a) Vyboishchikov, S. F.; Frenking, G. *Chem. Eur.*

J. **1998**, *4*, 1428-1438. (b) Sheehan, S. M.; Padwa, A.; Snyder, J. P. *Tetrahedron Lett.* **1998**, *39*, 949-952.

30. The energy levels of the Rh^1-Rh^2 σ- and σ*-orbital of **1** and the σ-donor orbital of singlet methylene carbene (optimized at the B3LYP/6-31G(d) level) are -9.1 eV, -3.7 eV, and -6.6 eV, respectively, which forms the background of the orbital interaction diagram shown in Figure 5b.
31. The two Lewis structures **LSa** and **LSb** showed nearly the same percentage of the total electron density (**LSa**: 97.65%, **LSb**: 97.60%), and hence were considered to equally contribute to the nature of the complex.
32. Both the *s-trans* and *s-cis* conformers of methyl diazoacetate were examined for the catalyst/diazoacetate complex and the nitrogen extrusion TS from it. The energy differences are very small and only the result of *s-trans* isomer is shown in this chapter.
33. The existence of such a complex was experimentally demonstrated: Maxwell, J. L.; Brown, K. C.; Bartley, D. W.; Kodadek, T. *Science* **1992**, *256*, 1544-1547.
34. Similar structures were found in ruthenium alkoxycarbonyl carbene complexes: Nishiyama, H.; Aoki, K.; Itoh, H.; Iwamura, T.; Sakata, N.; Kurihara, O.; Motoyama, Y. *Chem. Lett.* **1996**, 1071-1072. Galardon, E.; Le Maux, P.; Toupet, L.; Simonneaux, G. *Organometallics* **1998**, *17*, 565-569.
35. Such orientation of ester carbonyl group was also noted in theoretical studies of copper-catalyzed cyclopropanation reaction with α-diazoester: Fraile, J. M.; García, J. I.; Martínez-Merino, V.; Mayoral, J. A.; Salvatella, L. *J. Am. Chem. Soc.* **2001**, *123*, 7616-7625.
36. Examples: Timmons, D. J.; Doyle, M. P. *J. Organomet. Chem.* **2001**, *617-618*, 98-104. Bulugahapitiya, P.; Landais, Y.; Parra-Rapado, L.; Planchenault, D.; Weber, V. *J. Org, Chem.* **1997**, *62*, 1630-1641.
37. For the methane reaction, two diastereomeric TSs were located. Only one of the two is shown in this chapter since the energy difference was very small (0.2 kcal/mol).
38. Examples: DelMonte, A. J.; Haller, J.; Houk, K. N.; Sharpless, K. B.; Singleton, D. A.; Strassner, T.; Thomas, A. A. *J. Am. Chem. Soc.* **1997**, *119*, 9907-9908. Frantz, D. E.; Singleton, D. A. *J. Am. Chem. Soc.* **2000**, *122*, 3288-3295.
39. Bordwell, F. G. *Acc. Chem. Res.* **1988**, *21*, 456-463.
40. Rapid and reversible complexation between a rhodium-carbene complex and a C-H bond is assumed in ref. 11a.
41. For the methane insertion, the C-H activation step was calculated to be rate-limiting as shown in Figure 12b. Experimental investigation of methane insertion has not been reported and it may be true that the C-H activation is the rate-limiting step in this reaction.
42. Nakamura, E.; Hirai, A.; Nakamura, M. *J. Am. Chem. Soc.* **1998**, *120*, 5844-5845.

43. Yamanaka, M.; Nakamura, E. *J. Am. Chem. Soc.* **2001**, *123*, 1703-1708.
44. Nozaki, H.; Moriuti, S.; Yamabe, M.; Noyori, R. *Tetrahedron Lett.* **1966**, 59-63. Wulfman, D. S.; McDaniel, R. S.; Peace, B. W. *Tetrahedron* **1976**, *32*, 1241-1249.
45. Nishiyama, H.; Itoh, Y.; Matsumoto, H.; Park, S.-B.; Itoh, K. *J. Am. Chem. Soc.* **1994**, *116*, 2223-2224.
46. The B3LYP method was employed for geometry optimization. The basis sets used are as follows: the Ahlrichs SVP set (ref. 48) for Cu, the LANL2DZ set for Ru, and the 6-31G(d) sets for the rest.
47. Schäfer, A.; Horn, H.; Ahlrichs, R. *J. Chem. Phys.* **1992**, *97*, 2571-2577.
48. Recently an efficient Cu(I)-catalyzed C-H insertion reaction has been reported: Díaz-Requejo, M. M.; Belderraín, T. R.; Nicasio, M. C.; Trofimenko, S.; Pérez, P. J. *J. Am. Chem. Soc.* **2002**, *124*, 896-897.

CHAPTER 6

Origin of Diastereo- and Enantioselectivity in Rhodium-catalyzed Cyclization of Diazo Compound via Intramolecular C-H Insertion

6-1. Introduction

Carbon-carbon bond forming reactions that rely on activation of a C-H bond have seen a remarkable progress in recent years.[1,2] Among them, a dirhodium tetarcarboxylate-catalyzed intramolecular C-H insertion reaction of an α-diazocarbonyl compound has proved to be one of the most reliable methods for carbo- and heterocycle construction that goes through activation of a sp^3 C-H bond.[3] A new C-C bond between two sp^3 carbon centers has been successfully created in a highly diastereo- and enantioselective manner (Scheme 1).[4]

Scheme 1. Stereoselective Cyclization via Intramolecular C-H Insertion of Rh-carbene Complex

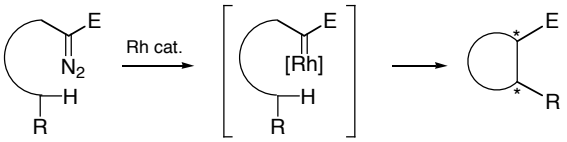

This class of reaction has already become a standard method for laboratory scale synthesis, and is being considered as a promising protocol for commercial processes.[5] Although a high level of stereoselectivity is often achieved in the reaction, the origin of the selectivity is not clearly understood owing to the lack of precise knowledge about the reaction mechanism and the transition state (TS) of the C-H bond activation/C-C bond formation process. For further improvement of the reaction, such information is obviously indispensable.

In the previous chapter, we described the first thorough analysis of the reaction pathways of intermolecular C-H insertion reaction between a Rh-carbene complex and an alkane as revealed by hybrid density functional calculations (Scheme 2).[6] It was found that the reaction proceeds via a three-centered transition state involving simultaneous cleavage of the alkane C-H bond and the

formation of the new C-C bond. We report herein the results of our theoretical studies to probe the TSs of the intramolecular C-H insertion reactions and the origin of the diastereo- and enantioselectivities in the cyclization process.

Scheme 2. The Reaction Pathway of the $Rh_2(O_2CR)_4$-Catalyzed C-H Insertion Reaction of a Diazo Compound and an Alkane

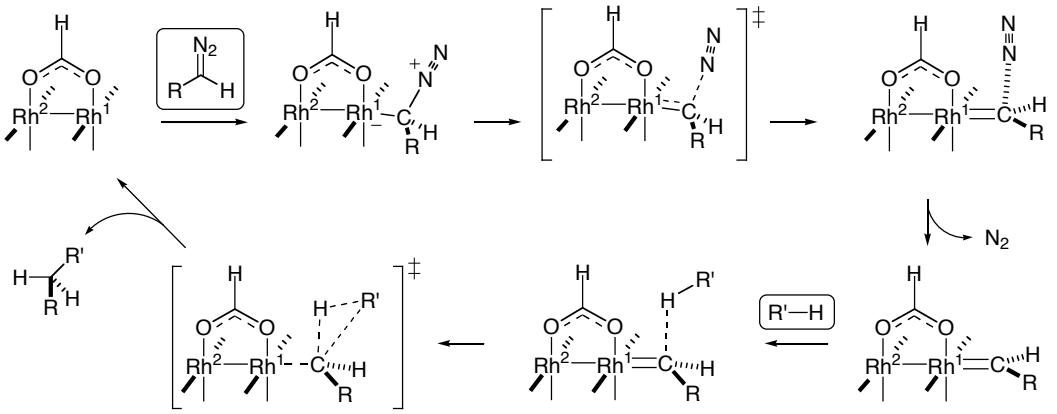

6-2. Reactions to Be Studied

Numerous examples of successful cyclization reactions have been reported. To define the scope of the present studies, some representative experimental results are listed and briefly discussed below. Whenever there are possibilities of four-, five- and six-membered formation, five-membered ring formation is generally preferred if the reactivities of the corresponding C-H bonds are not different very much. In the early stage of experimental studies, the $Rh_2(OAc)_4$-catalyzed reactions of disubstituted diazo compounds **1** were examined by Taber[7] and Doyle[8] (eq 1). They found that the C-C bond formation proceeds in a *trans* fashion to give cyclopentanone derivatives (X = CH_2, E = CO_2R) or γ-lactones (X = O, E = COR) **2**. The reactions were found to be diastereoselective for the newly formed C-C bond and for the remote stereogenic center. A representative example is shown in eq 2.[7b] The $Rh_2(OAc)_4$-catalyzed cyclization of **3** gives the all *trans* cyclopentanone **4**.

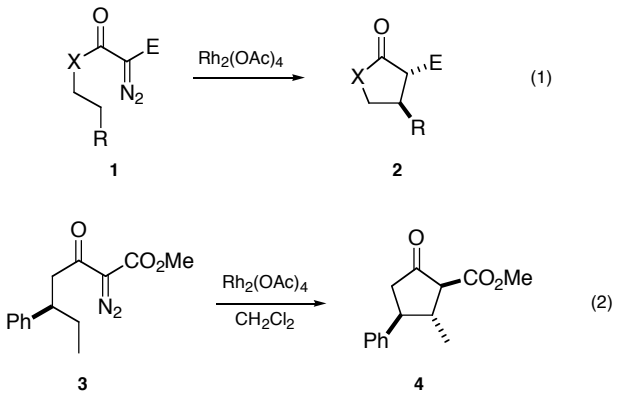

The reaction is effective also for four-membered ring construction. A β-lactam **6** is formed by the reaction of an *N*-alkyldiazoacetamide **5** with a catalytic amount of $Rh_2(OAc)_4$ (eq 3). This reaction takes place with exclusive *trans* selectivity ($R^1 = C_6H_5$, $R^2 = C_6H_5$ and $R^3 = C_2H_5$).[9] Interestingly, a thermodynamically unfavorable *cis* product was obtained exclusively in the asymmetric β-lactam formation with a Rh_2(*S*-PTPA)$_4$ (PTPA: *N*-phthaloyl-phenylalaninate) catalyst (eq 4).[10]

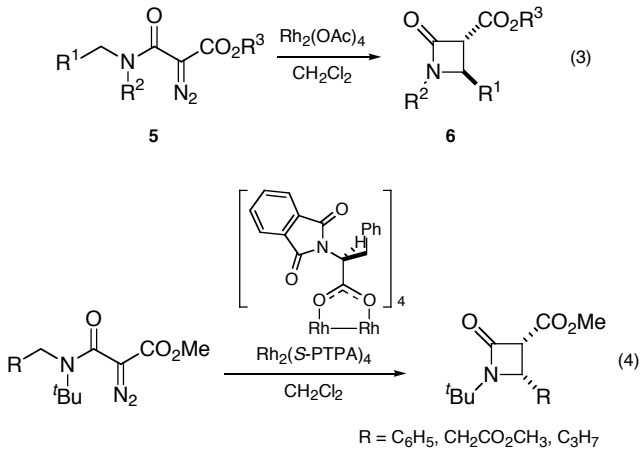

A Rh catalyst having chiral carboxylate or carboxamidate ligands has been used for asymmetric C-H insertion reaction. Highly enantioselective intramolecular C-H insertion reaction was reported by Doyle et al. in 1991 (eq 5).[11] The chiral Rh_2(5*S*-MEPY)$_4$ (MEPY: methyl 2-pyrrolidone-5-carboxylate) complex catalyzes the cyclization of an α-diazoester **7** to the *S*-enantiomer of a γ-lactone **8** with good enantioselectivity (~90% ee).

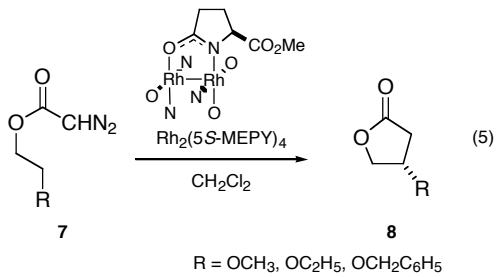

(5)

The best example to illustrate the power of the enantio- and diastereocontrol by a chiral Rh complex is the reaction of a cycloalkyl diazoacetate, which affords a fused bicyclic compound (eq 6). Doyle has achieved excellent diastereo- (*cis*) and enantiocontrol by using a $Rh_2(4S\text{-MACIM})_4$ (MACIM: methyl 1-acetylimidazolidin-2-one-4-carboxylate) catalyst. In contrast, $Rh_2(5S\text{-MEPY})_4$ gives poor diastereoselectivity.[12]

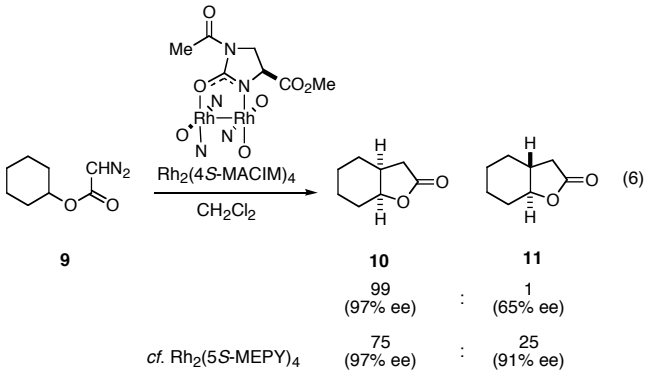

(6)

Stereoselectivity of these reactions has been discussed often by schematic molecular modeling[7bc,12b,13] and sometimes by molecular mechanics or semi-empirical calculations based on a hypothetical transition structure.[8,14] Although some of them were successful in explaining individual experimental observation, more realistic mechanistic models are undoubtedly desirable for further improvement of catalysts and substrates. We focused in the present studies on three topics: Diastereoselectivity in five-membered ring (cyclopentanone and γ-lactone derivatives) formation catalyzed by an achiral Rh catalyst (eq 1, 2), diastereoselctivity in four-membered ring (β-lactam) formation (eq 3, 4), and enantio- and diastereoselectivity in γ-lactone formation catalyzed by Doyle's catalysts $Rh_2(5S\text{-MEPY})_4$ and $Rh_2(4S\text{-MACIM})_4$ (eq 5, 6).

6-3. Computational Methods

The studies were carried out in two stages since the highly substituted realistic substrates and catalysts are too large for treatment with a high level of theory. Transition structures of cyclization of unsubstituted substrates were first calculated with the density functional theory (DFT) method using the B3LYP hybrid functional[15] as in our previous work.[6] Structures were optimized with the basis set (denoted as 631LAN) consisting of the LANL2DZ basis set including a double-ζ valence basis set with the Hay and Wadt effective core potential (ECP)[16] for Rh and the 6-31G(d) basis set[17] for C, H, N and O. As in the previous studies, dirhodium tetraformate was employed as a Rh catalyst in the interest of computational time. Transition structures were adequately characterized by normal coordinate analysis (one imaginary frequency for a transition structure). To estimate the activation barrier of the reaction, the starting Rh-carbene complex precursors were pertially optimized at the same level of theory (until the energy change becomes less than 0.01 kcal/mol).

In the second stage, appropriate substituents were attached to the optimized transition structure of the simple models to investigate the stereoselectivity of cyclization. These structures were optimized at the PM3(tm)[18] level: The rhodium carboxylate (carboxamidate) was fixed throughout the calculation because the PM3 method does not give correct geometry for $Rh_2(O_2CH)_4$. The interatomic distances among the carbene carbon and the carbon and the hydrogen atoms of the reacting C-H bond are also fixed, since the C-H insertion transition structure depends very much on the theory used.[19] The Rh-carbene bond was allowed to rotate, however. With these structural constraints (denoted as PM3/B3LYP model), the PM3-optimized structures showed reasonable agreement with the B3LYP-optimized structures (differences of bond lengths and bond angles are < 2% and < 4%, respectively). Structures of chiral complexes Rh_2(5*S*-MEPY)$_4$ and Rh_2(4*S*-MACIM)$_4$ were taken from Cambridge Crystallographic Database. For these systems, the Rh atoms and the pyrrolidone (or the imidazolidinone) moieties were fixed

throughout the calculations. DFT and semi-empirical calculations were performed with a Gaussian 98[20] package and MacSpartan Pro ver. 1.0.2 program,[21] respectively. Cartesian coordinates and pdb files of the B3LYP-optimized TSs and the step-by-step procedures for the semi-empirical calculations are described in the Supporting Information.

A comment on the accuracy of the calculated stereoselectivity is given before describing the results. The agreement between the theory and the experiment was good, while the theoretical selectivity was always much better than reality with a few exceptions. This seems to arise from two factors: One is the structural constraints imposed on the computational models, which would work against sterically disfavored transition state which may relax in the absence of the constraints. The other is the fact that the selectivity calculation is based on potential energy, not on free energy. The calculated activation energy is small (~10 kcal/mol) and hence entropy contribution must be quite large in reality.

6-4. Diastereoselectivity in Five-membered Ring Formation Catalyzed by Achiral Rh Complex

The cyclization of a model compound **1a** (E = CO_2Me, X = CH_2, R = H) into 2-methoxycarbonylcyclopentanone was first examined at the B3LYP/631LAN level, and two isomeric TSs (half-chair **TS1a-1** and boat **TS1a-2**) were located (Scheme 3). In both TSs, the reaction center takes a six-membered cyclic structure involving the transferred hydrogen atom. The activation energies of cyclization are small (8.7 and 9.9 kcal/mol for **TS1a-1** and **TS1a-2**, respectively). As suggested by the previous work, these values will significantly decrease when an alkyl substituent is attached on the C5 atom (ca. 5 kcal/mol decrease per one alkyl group).[6] Thus, the activation energy for the real system would be around (or less than) 5 kcal/mol, and entropy contribution the the Gibbs free energy must be very large.

Scheme 3. Reaction Pathways of the Cyclization of a Diazocarbonyl Compound **1a** into a Cyclopentanone **2a**.[a]

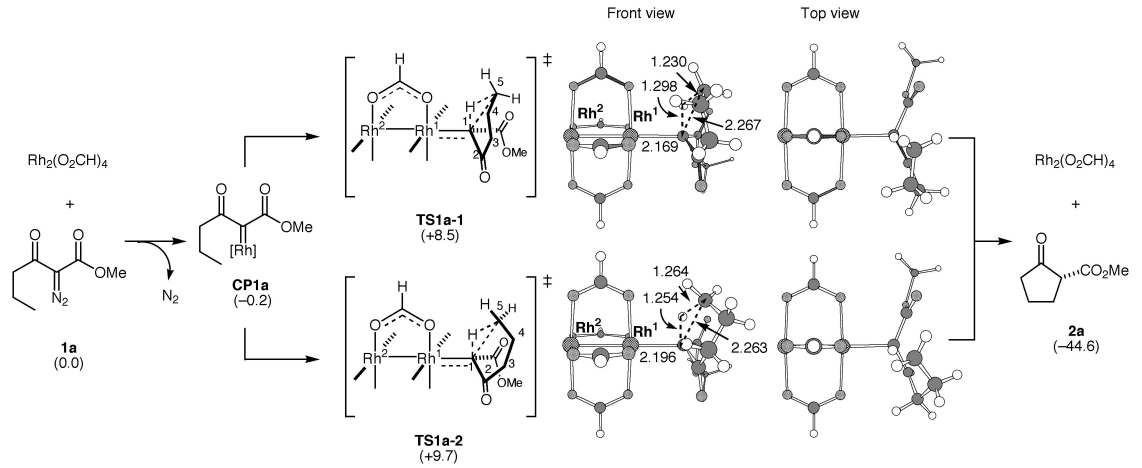

[a] The numbers in parentheses refer to the energies relative to [**1a** + $Rh_2(O_2CH)_4$ - N_2] (kcal/mol). The numbers in 3-D structures refer to bond lengths in Å.

Similarly, cyclization of **1b** (E = COMe, X = O, R = H) into a γ-lactone was examined also at the B3LYP/631LAN level, and two isomeric TSs (**TS1b-1** and **TS1b-2**) were obtained (Scheme 4). The activation barriers for the half-chair TS (**TS1b-1**) and the boat TS (**TS1b-2**) are 12.7 and 17.8 kcal/mol, respectively. The large difference of the activation energy would arise from the fact that the Rh^1-C^1-C^2=O dihedral angle changes more in the transformation of **CP1b** to **TS1b-2** (91.6° to 64.0°) than in that to **TS1b-1** (91.6° to 83.5°).[6]

Scheme 4. Reaction Pathways of the Cyclization of a Diazocarbonyl Compound **1b** into a γ-Lactone **2b**.[a]

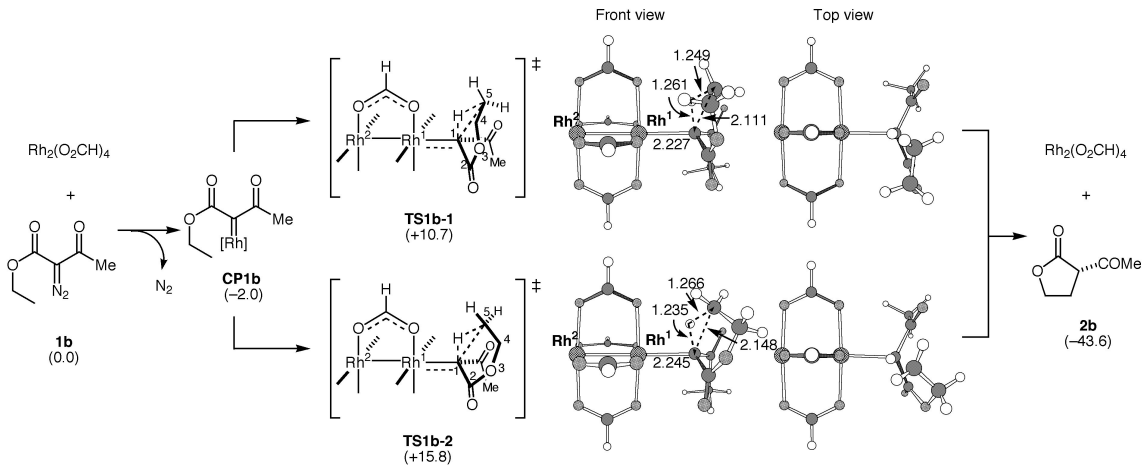

[a] The numbers in parentheses refer to the energies relative to [**1b** + $Rh_2(O_2CH)_4$ - N_2] (kcal/mol). The numbers in 3-D structures refer to bond lengths in Å.

With the above structures in hand, the experimentally observed diastereoselectivity was examined by the PM3/B3LYP method for a variety of substituents listed in Table 1. Four isomeric structures were examined for each substituent (Scheme 5). Structures were optimized at the PM3(tm) level with the rhodium carboxylate and the reaction center frozen at the B3LYP geometry (see Computational Details section).[22]

Scheme 5. Four Diastereomeric TSs of Five-membered Ring Formation.

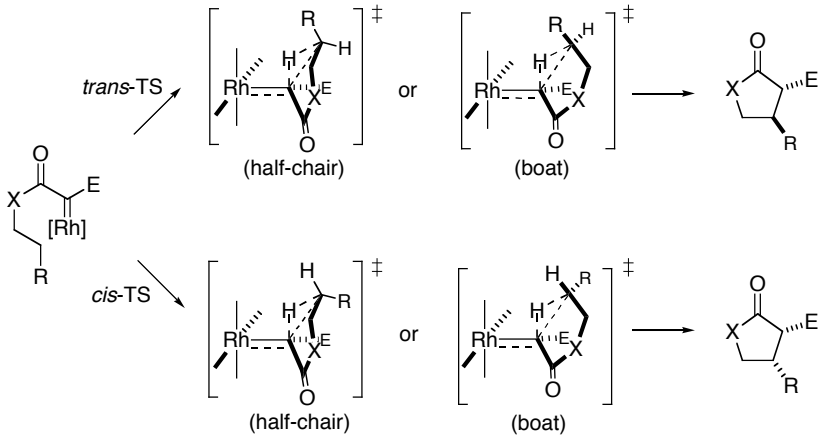

The results are shown in Table 1. In all cases, the most stable TS was the *trans*-TS with half-chair conformation. Product ratio was calculated with energy differences ($\Delta\Delta E^{\ddagger}$) and reaction temperatures described in the literature. In entry 1, 3, 4 and 5, the *trans*/*cis* ratio was calculated to be > 98:2, which agree with the experimental fact that only the *trans* products were observed in these reactions.

Table 1. PM3/B3LYP modeled relative energies (kcal/mol) of five-membered ring formation TSs (half-chair conformers; boat conformers in parentheses). Product ratios were calculated based on these energy differences.

entry	starting material	product	*trans*-TS[a]	*cis*-TS[a]	ref.
1[b]	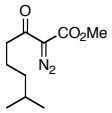	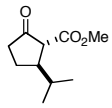	0.0 (+4.5) > 99.9 :	+4.9 (+4.9) 0.1	7a
2[b]	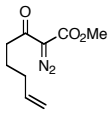	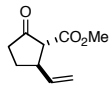	0.0 (+1.3) 90.9 :	+1.3 (+3.8) 9.1	7a
3[b, c]	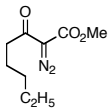	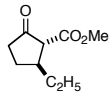	0.0 (+3.5) 98.5 :	+2.5 (+7.4) 1.5	7a
4[b]	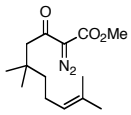	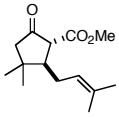	0.0 (+2.9) 99.2 :	+6.7 (+2.9) 0.8	7a
5[c, d]	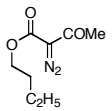	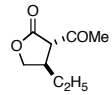	0.0 (+5.1) 98.6 :	+3.0 (+8.2) 1.4	8
6[d]	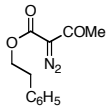	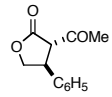	0.0 (+1.3) 91.0 :	+1.5 (+5.3) 9.0	8

[a] Relative energies of half-chair and boat TSs (kcal/mol) are shown in plain and in parentheses, respectively.
[b] The product ratio was calculated with T = 300 K (reaction conditions: CH_2Cl_2, rt).
[c] A *n*-octyl group was replaced by an ethyl group.
[d] The product ratio was calculated with T = 350 K (reaction conditions: C_6H_6, reflux).

The origin of the diastereoselectivity is illustrated by the analysis of the *trans*- and *cis*-TSs for the case in entry 1 (R = $CH(CH_3)_2$). Figure 1 shows 3-D structures of the half-chair *trans*-TS and *cis*-TS. In *trans*-TS, the isopropyl group occupies the sterically favored equatorial position of the six-membered ring. On the other hand, in the *cis*-TS, the isopropyl group is in the axial position and suffers from 1,3-diaxial repulsion. Therefore the *trans*-TS becomes favorable compared to the *cis*-TS.

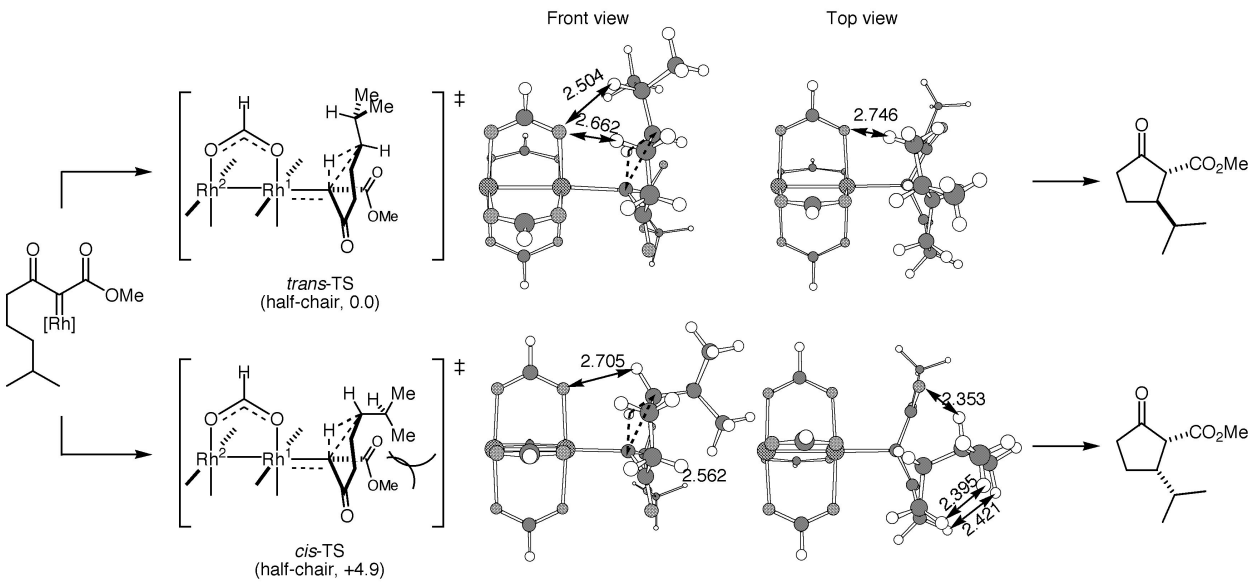

Figure 1. 3-D structures of *trans*-TS and *cis*-TS (half-chair conformers) in Table 1, entry 1. The numbers refer to atomic distances in Å.

When the substituent is a vinyl or a phenyl group (entry 2, 6), the *trans*-TS is more stable than the *cis*-TS by only 1.3 and 1.5 kcal/mol, respectively. The calculated *trans*/*cis* ratios are ~91:9, while only the *trans* product was observed experimentally. This discrepancy would arise from the fixed C-H bond in the present calculations. As suggested by previous studies,[6] the vinyl and the phenyl group should stabilize the cationic carbon of the reacting C-H bond, and hence the cleaving C-H bond would become longer in the TS. This effect would certainly reduce the steric repulsion in the *trans*-TS (but not taken into account in the PM3/B3LYP model).

Rh-catalyzed intramolecular C-H insertion can also set three contiguous stereogenic centers in a five-membered ring. A few cases in the literature were examined (Table 2). Since the C-C bond formation sets *trans* geometry as to the forming C-C bond as discussed in the previous paragraphs, only the *trans*/*cis* diastereoselectivity with respect to the existing stereogenic center was considered (Scheme 6).[23]

Table 2. PM3/B3LYP modeled relative energies (kcal/mol) of five-membered ring formation TSs (half-chair conformers; boat conformers in parentheses).

entry	starting material	product(s)	*trans-trans* TS[a]		*trans-cis* TS[a]	ref.
1[b]	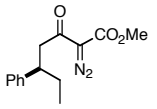	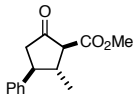	0.0 (+1.3)		+5.1 (+5.9)	7b
			> 99.9	:	0.1	
2[b]	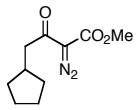	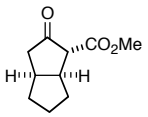	0.0 (–)		–6.0 (–4.9)	7c
			< 0.1	:	99.9	
3[b]	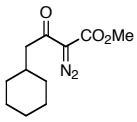	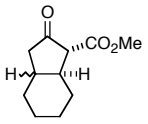	0.0 (–)		+2.0 (+2.8)	7c
		trans:cis = 3:1	95.7	:	4.3	

[a] Relative energies of half-chair and boat TSs (kcal/mol) are shown in plain and in parentheses, respectively.
[b] The product ratio was calculated with T = 300 K (reaction conditions: CH_2Cl_2, rt)

Scheme 6. Four Diastereomeric TSs of Five-membered Ring Formation with *trans* Configuration of the Forming C-C bond.

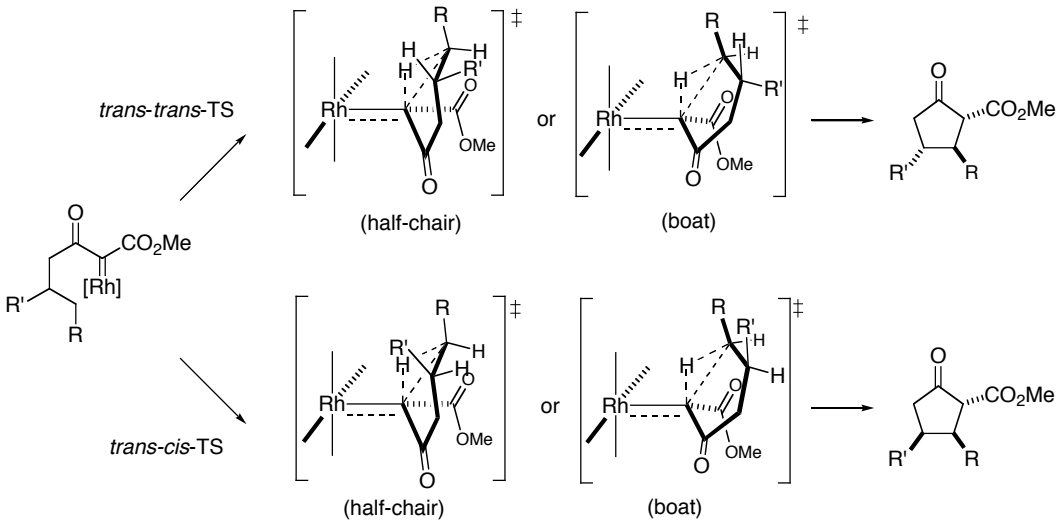

For the linear substrate in entry 1 of Table 2, the calculations showed good agreement with the experiment. *Trans-trans*-TSs are much more stable than *trans-cis*-TSs, which gives product ratio of > 99.9:0.1. As shown in Scheme 7, *trans-cis*-TSs are disfavored due to the steric repulsion between the phenyl group and the catalyst (half-chair conformer) or the methyl group (boat conformer).

Scheme 7. Schematic Representation of Diastereomeric TSs of Cyclization (Table 2, entry 1).

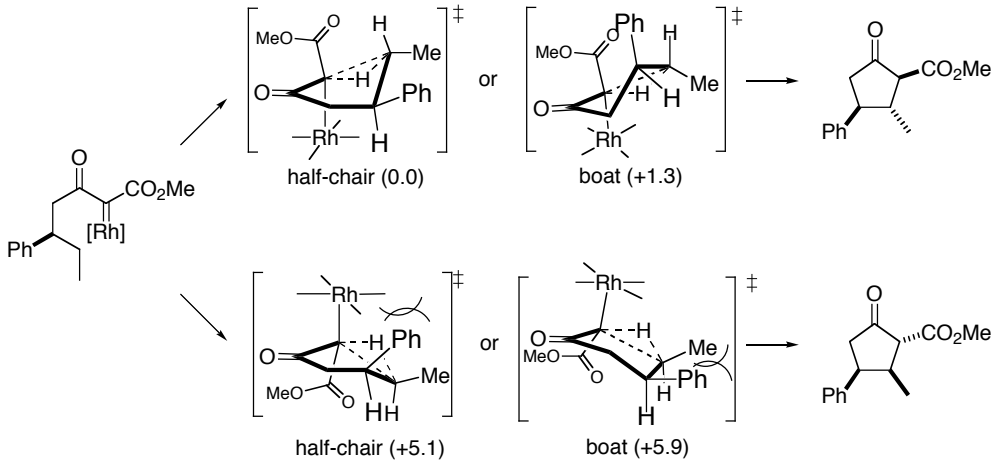

Entries 2 and 3 of Table 2 illustrate the applications to fused bicyclic ring formation reactions. Calculations and experiment showed good agreement in the formation of bicyclo[3.3.0] octane, which gives *cis*-fused product predominantly (entry 2). The selectivity reflects the product stability, which is so large that it manifests itself already in the TS of C-C bond formation (*cis*-fused product is calculated to be more stable than *trans*-fused one by ca. 13 kcal/mol). On the other hand, diastereoselectivity of the bicyclo[4.3.0] system is a subtle matter (entry 3). The theoretically predicted *trans*/*cis* ratio (95.7:4.3) is consistent with but overestimates trend of *trans*-rich product (*trans*:*cis* = 3:1).

Since the bicyclo[4.3.0] system is a very important ring structure in organic chemistry, it is discussed in more details. There are a priori three approaches of the Rh-carbene to the C-H bond (Figure 2), which are (i) equatorial Rh-carbene inserting to equatorial C-H bond, (ii) axial Rh-carbene to equatorial C-H bond and (iii) equatorial Rh-carbene to axial C-H bond. While the approach (i) gives the *trans*-fused product, the approaches (ii) and (iii) lead to the *cis*-fused product. For each approach, there takes place a facial selection of the Rh-carbene, where the conformation of the reaction center (half-chair or boat) and relative configuration of the newly formed C-C bond are determined. Thus, there are total six diastereomeric TSs of cyclization (Table 3). Among them, eq-eq TS with half-chair conformation (entry 1) is the most stable and

gives the *trans-trans* product. The origins of higher energies of other TSs would be unfavorable boat conformation of the reaction center (entry 2, 4, 6), 1,3-diaxial repulsion (entry 3, 4) and steric repulsion between the cyclohexane ring and the Rh carboxylate (entry 5) or the methoxycarbonyl group (entry 2, 6). Precise evaluation of the energetics of all pathways is evidently impossible at the present time because of the lack of theoretical method to accurately evaluate such energetics in terms of free energy.

Table 3. PM3/B3LYP modeled relative energies (kcal/mol) of all possible conformers of bicyclo[4.3.0] ring formation TS.

entry	TS	relative energy	product
1	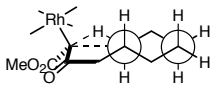 (eq-eq/half chair)	+0.0	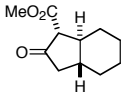
2	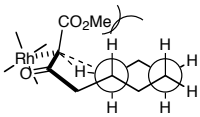 (eq-eq/boat)	+5.4	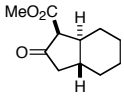
3	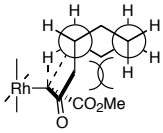 (ax-eq/half chair)	+1.8	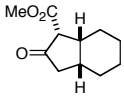
4	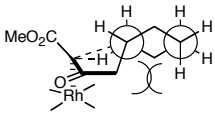 (ax-eq/boat)	+2.8	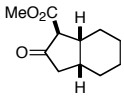
5	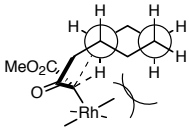 (eq-ax/half chair)	+2.0	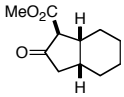
6	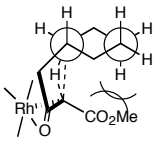 (eq-ax/boat)	+6.5	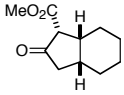

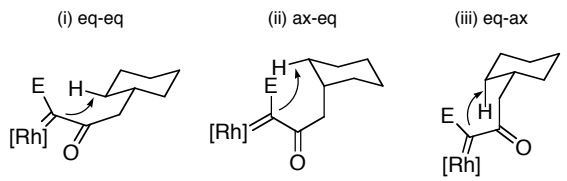

Figure 2. Three approaches of the Rh-carbene to the cyclohexane C-H bond.

6-5. Diastereoselectivity in Four-membered Ring Formation Catalyzed by Achiral Rh Complex

Diastereoselectivity in the β-lactam forming reaction such as the one shown in eq 3 was next studied. Cyclization of a model compound **5a** (R^1 = H, R^2 = H and R^3 = CH_3) was examined at the B3LYP/631LAN level (Scheme 8). A five-membered cyclic transition structure (**TS5a**) was obtained. Although the activation energy of this model is high (22.5 kcal/mol) compared with the five-membered ring formation (vide supra), it will decrease as (cation-stabilizing) substituents are attached.

Scheme 8. Reaction Pathway of the Cyclization of a Diazocarbonyl Compound **5a** into a β-Lactam **6a**.[a]

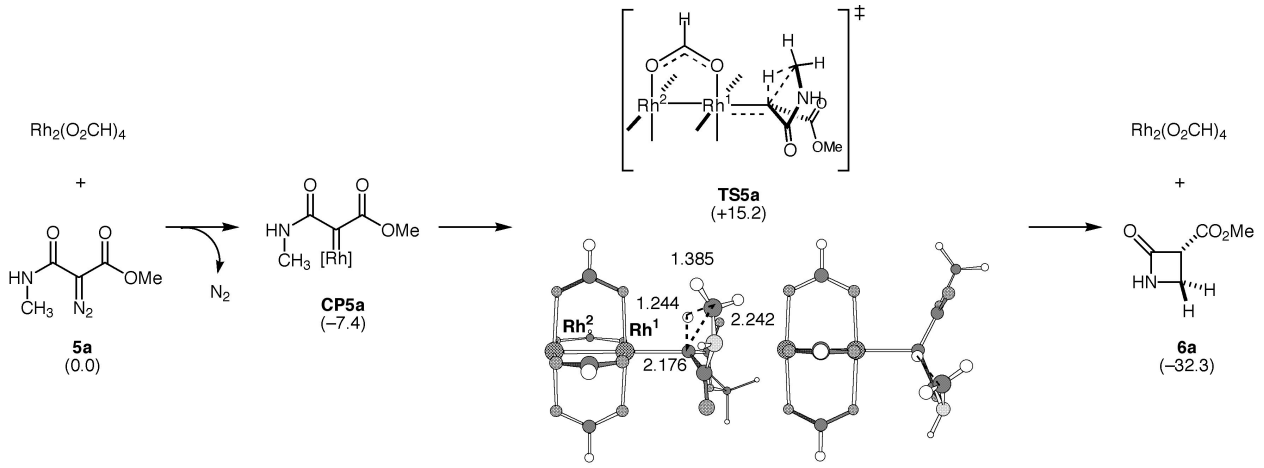

[a] The numbers in parentheses refer to the energies relative to [**5a** + $Rh_2(O_2CH)_4$ - N_2] (kcal/mol). The numbers in 3-D structures refer to bond lengths in Å.

Calculations of more realistic model (R^1 = C_6H_5, R^2 = C_6H_5 and R^3 = CH_3) **5b** were performed with the PM3/B3LYP modeling (Scheme 9). Although the TS into the *trans*-β-lactam

(**TS5b-1**) was more stable than the one into the *cis* isomer (**TS5b-2**), the energy difference (1.0 kcal/mol, corresponding to the *trans*/*cis* ratio of 84:16) was too small in the light of the experiment. The disagreement of the calculations and the experiment is similar to the cases of five-membered ring forming reactions involving a vinyl or a phenyl substituent (Table 1, vide supra). The steric repulsion in the **TS5b-1** may be overestimated because of the fixed C-H bond in the present calculations.

Scheme 9. Diastereomeric TSs of β-Lactam Formation from **5b**.

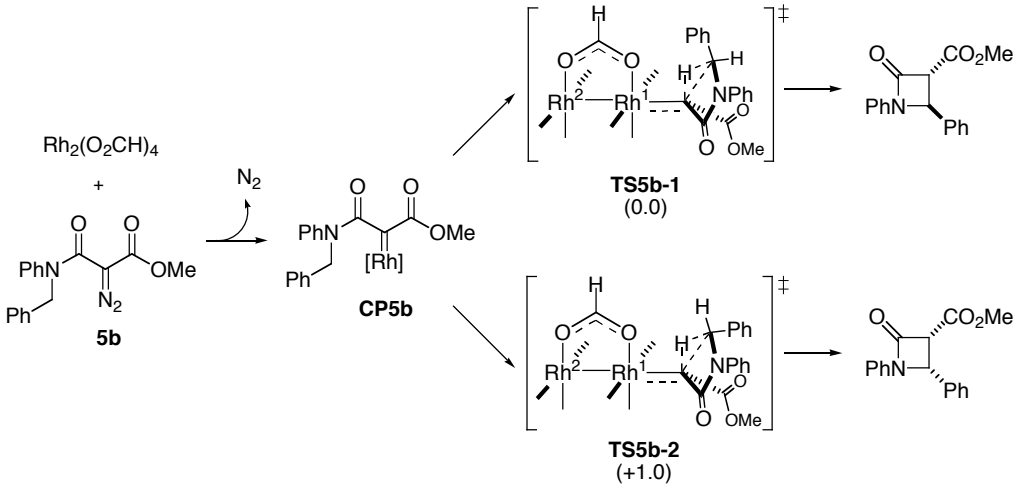

In the asymmetric β-lactam formation reported by Hashimoto et al, exclusive *cis*-selective cyclization was observed (eq 6, R = C_6H_5, $CH_2CO_2CH_3$, C_3H_7). This reversal of the stereoselectivity upon changing the achiral catalyst to the chiral one can be understood by the transition structures of cyclization illustrated below (Figure 3). Replacement of the formate ligand with a bulky *S*-PTPA ligand causes significant steric repulsion between the R group (phenyl in Figure 3b) and the benzyl group of the carboxylate ligand in the *trans*-TS. Such repulsion does not occur in the *cis*-TS (Figure 3a). Therefore the thermodynamically unfavorable *cis*-β-lactam is predominantly formed.[24]

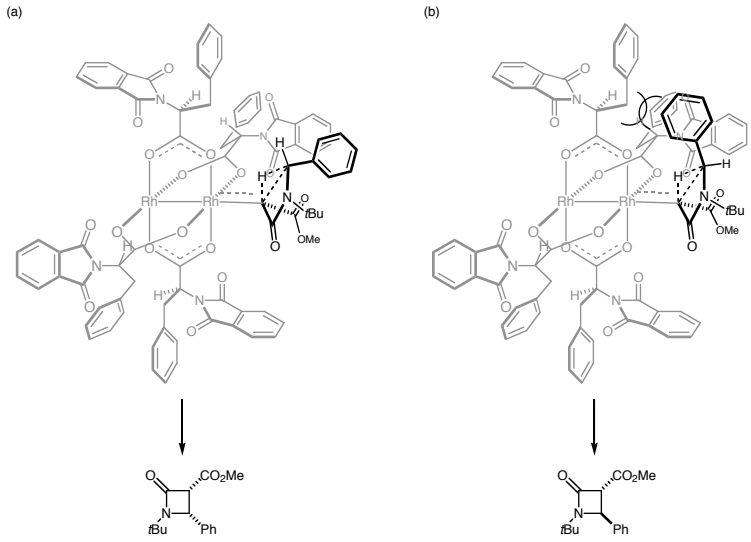

Figure 3. Schematic representation of β-lactam formation TSs with Rh_2(S-PTPA)$_4$ complex.

6-6. Enantio- and Diastereoselectivity in Five-membered Ring Formation Catalyzed by Chiral Rh Complex

Enantioselective cyclization is an important topic as illustrated in eq 5 and 6, where γ-lactone derivatives are obtained. To model these reactions, cyclization of an unsubstituted diazoacetate **7a** (R = H) with $Rh_2(O_2CH)_4$ was examined first at the B3LYP/631LAN level (Scheme 10). Both a half-chair TS (**TS7a-1**) and a boat TS (**TS7a-2**) were located, and the energy difference between them was 4.4 kcal/mol. On the basis of these structures, cyclization of **7b** (R = OCH_3) with the Rh_2(5*S*-MEPY)$_4$ complex was examined with the PM3/B3LYP modeling.

Scheme 10. Reaction Pathways of the Cyclization of a Diazocarbonyl Compound **7a** into a γ-Lactone **8a**.[a]

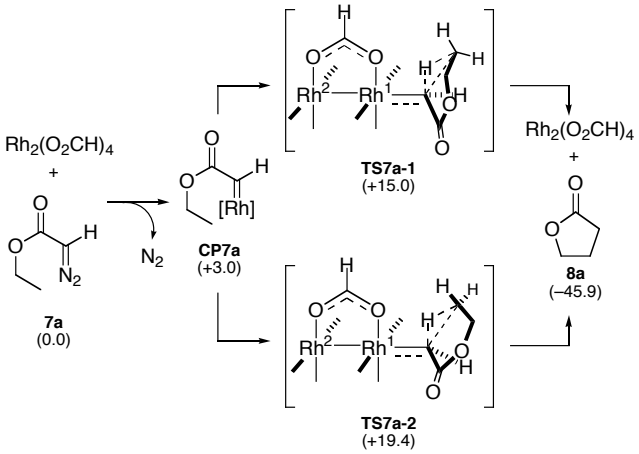

[a] The numbers in parentheses refer to the energies relative to [**7a** + $Rh_2(O_2CH)_4$ - N_2] (kcal/mol).

The carbene complex derived from Rh_2(5*S*-MEPY)$_4$ and **7b** is shown in Figure 4. The ester group of the carbene ligand is placed in a sterically less hindered position. Unlike an achiral Rh carbene complex, the two faces of the chiral carbene complex are no longer in equal environment. Thus, there are two approaches of the reacting C-H bond (**A** and **B**, Figure 4). For each approach, the methoxy group can be either *cis*- or *trans* with respect to the hydrogen atom bonded to the carbene carbon. In addition, both half-chair and boat conformers are possible. Thus, there exist eight transition structures of cyclization as illustrated in Scheme 11. Among them, the most stable transition structure takes the approach **A**, *cis* configuration and half-chair conformation, and gives *S*-enantiomer of the γ-lactone (Scheme 11, **TS7b-1**). The most stable *R*-enantiomer forming TS was 5.0 kcal/mol higher in energy (**TS7b-3**, the approach **B** and *cis* configuration). Thus, these calculations qualitatively agree with the experiments.

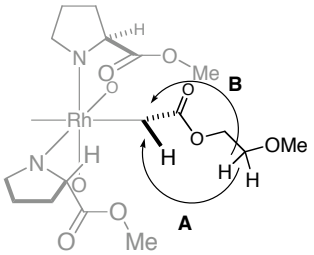

Figure 4. Schematic representation of a carbene complex derived from Rh_2(5S-MEPY)$_4$ and **7b**.

Scheme 11. Schematic Representation of the Carbene Complex and the Cyclization TSs of **7b** with $Rh_2(5S\text{-MEPY})_4$, Illustrated along with the C (carbene)-Rh-Rh Axis[a]

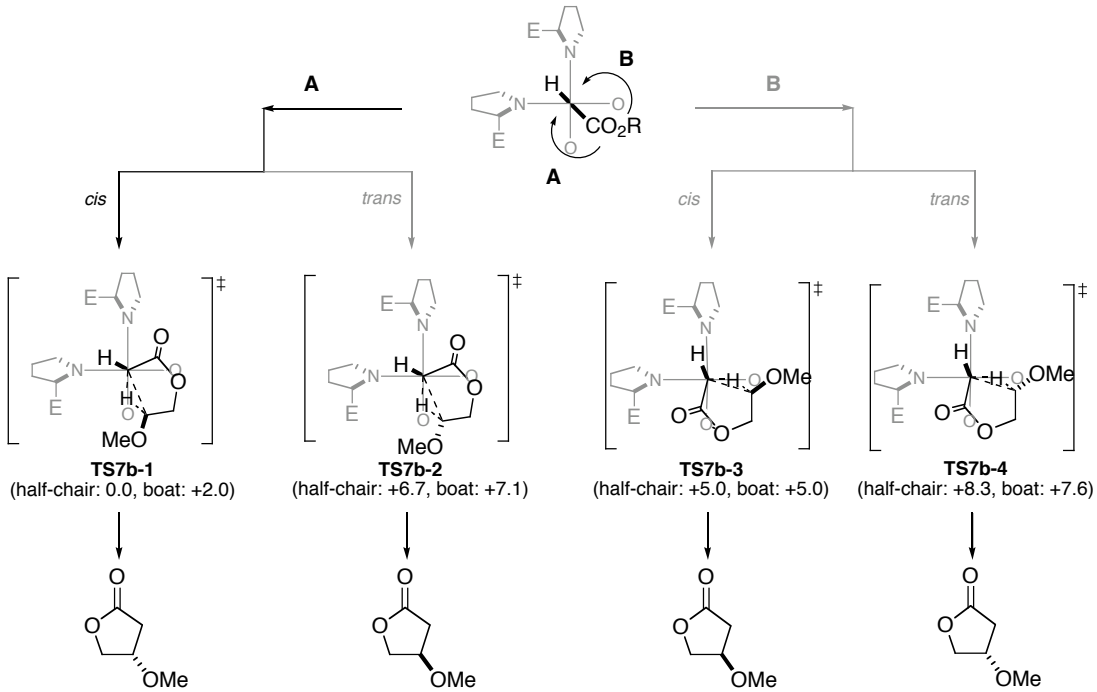

[a] E and R are CO_2Me and $CH_2CH_2OCH_3$, respectively. The Rh metals are therefore "hidden" behind the carbene moiety. Relative energies (kcal/mol) of TSs are shown in parentheses.

From Scheme 11, one can find that the face (**A**/**B**)- and *cis*/*trans* selectivities are equally critical factors of the enentioselecitvity. The conformation of the cyclic TS is less important because the change of the conformation does not cause much energy change while changes of other factors need more energy. The selectivity for the path **A** can be rationalized by the relative orientation of the carbonyl group of the substrate and the ester substituent of the MEPY ligand (Figure 5). In the path **B**, the carbonyl group of the substrate is projected toward the ester substituent of the ligand (Figure 5b), while they lie apart from each other in the path **A** (Figure 5a). Thus, the former TS suffers from steric and electrostatic repulsion between these polar functionalities.[25]

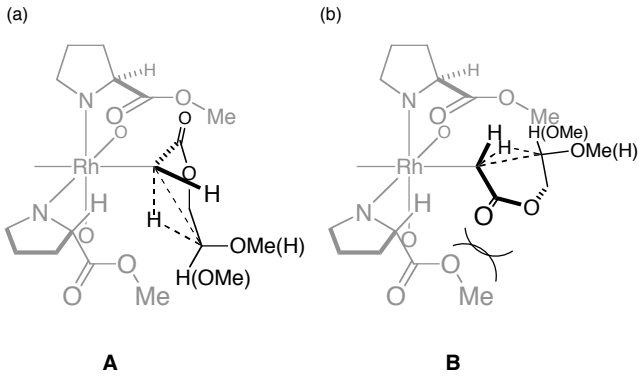

Figure 5. Schematic illustration of the face (A/B) selectivity in the Rh_2(5S-MEPY)$_4$-catalyzed cyclization of **7b**.

The *cis* selectivity of the present reaction stands in contrast to the *trans* selectivity in the reactions catalyzed by an achiral Rh catalyst (see section 1). This is due to the change of both the ligand and the substrate. The larger steric bulk of the MEPY ligand destabilizes the *trans*-TS (Figure 6b). In addition, the change of the substituent on the carbene carbon (from a methoxycarbonyl group to a hydrogen) reduces the 1,3-diaxial repulsion in the *cis*-TS and makes it less unstable (Figure 6a). The latter change should play an important role since so far enantioselective intramolecular C-H insertion of disubstituted diazo compounds is not as successful as that of monosubstituted diazo compounds.[26]

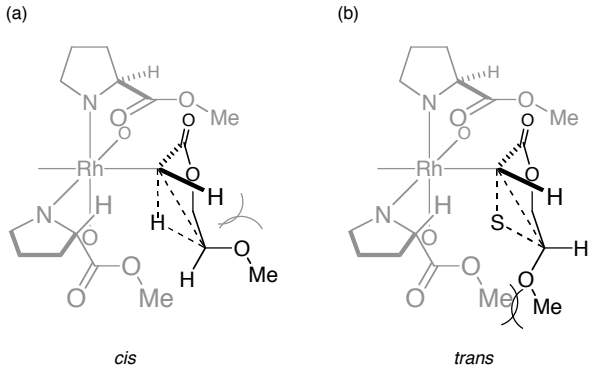

Figure 6. Schematic representation of *cis*- and *trans*-TSs (approach A) in Rh_2(5S-MEPY)$_4$-catalyzed cyclization of **7b**.

Next, bicyclo[4.3.0] ring formation reaction was studied for both the Rh_2(5*S*-MEPY)$_4$ and Rh_2(4*S*-MACIM)$_4$ complexes (eq 4). As already described in section 1, there are six

diastereomeric TSs of the bicyclo[4.3.0] ring formation with an achiral Rh complex. When a chiral Rh complex is used, two faces of the carbene carbon become diastereotopic (see Figure 4, path **A** and **B**) and there result twelve diastereometric TSs. Results are shown in Table 4. Similarly as the above results, the path **A** was favored compared with the path **B**. The most stable transition structure (**TS9-3**), where the axial-bound Rh carbenoid inserts into the equatorial C-H bond, gives experimentally dominant *cis*-fused (3a*S*, 7a*S*) product (entry 3). As for *trans* ring fusion, the most stable TS (**TS9-1**) is 2.8 and 7.0 kcal/mol higher in energy in the MEPY system and the MACIM system, respectively. This is in agreement with the experimental observation that $Rh_2(MACIM)_4$-catalyzed reaction is much more *cis*-selective (99:1) than $Rh_2(MEPY)_4$-catalyzed one (75:25).

Table 4. PM3/B3LYP modeled relative energies (kcal/mol) of bicyclo[4.3.0] ring formation TSs with Rh_2(5*S*-MEPY)$_4$ or Rh_2(4*S*-MACIM)$_4$ catalyst. The illustration shows TSs of the path **A** and their product. Energies of TSs of the path **B** are shown in parentheses.

entry	TS[a]	relative energy[b] 5*S*-MEPY	4*S*-MACIM	product[a]
1	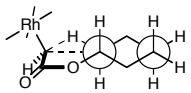 **TS9-1**	+2.8 (+6.5)	+7.0 (+11.3)	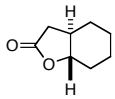
2	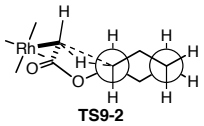 **TS9-2**	+7.1 (+12.0)	+9.7 (+20.6)	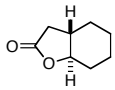
3	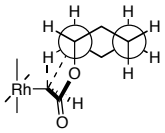 **TS9-3**	0.0 (+7.7)	0.0 (+10.1)	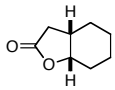
4	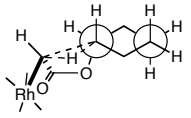 **TS9-4**	+4.0 (+11.0)	+8.3 (+15.8)	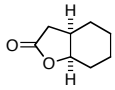
5	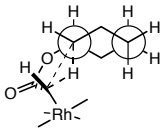 **TS9-5**	+4.0 (+10.7)	– (–)[c]	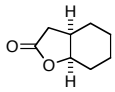
6	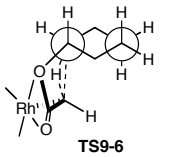 **TS9-6**	+6.2 (+11.1)	+7.8 (+15.3)	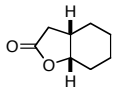

[a] TSs and products through the path **A** are illustrated.
[b] Energies relative to **TS9-3** (path **A**). Energies of TSs through the path **B** are shown in parentheses.
[c] Calculations were not performed because of inevitable overlap of the ligands and the cyclohexane ring.

The enhancement of *cis* selectivity in Rh_2(4*S*-MACIM)$_4$-catalyzed reaction can be rationalized by the analysis of structures of **TS9-1** and **TS9-3** (Figure 7). Being similar to the Rh_2(5*S*-MEPY)$_4$-catalyzed reaction of **7b** (Scheme 11), the chiral environment created by the 4*S*-MACIM ligands places the cyclohexane ring on the same side with the *N*-acetyl group of the ligand. Thus, significant steric repulsion between the cyclohexane ring and the acetyl group results in **TS9-1**. In fact, the acetyl group in **TS9-1** is significantly distorted to avoid the cyclohexane ring (Figure 7b). This should make *trans* ring fusion much less favorable.

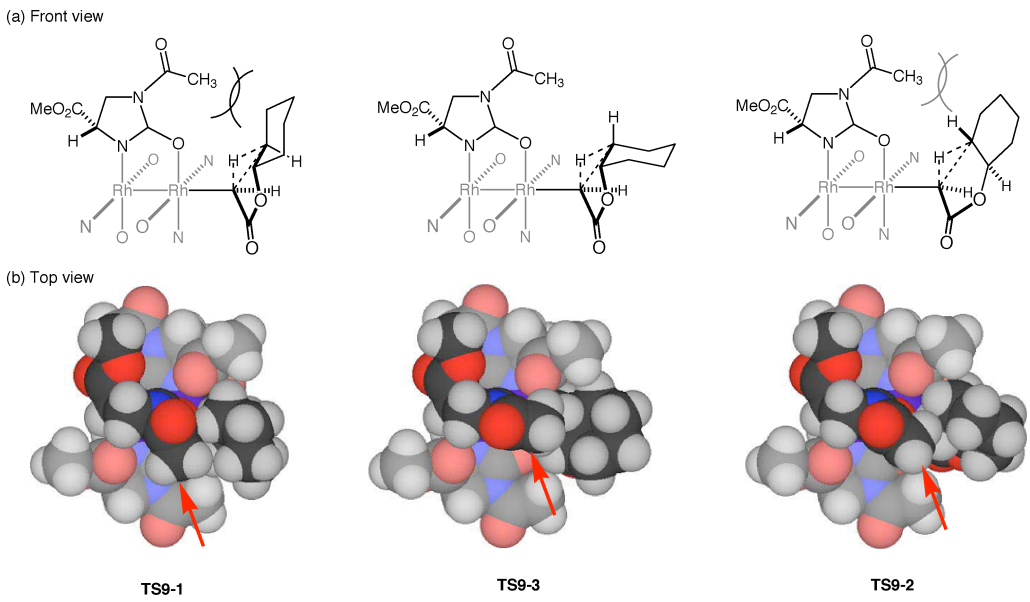

Figure 7. (a) Schematic representations and (b) space-filling models of the bicyclo[4.3.0] ring formation TSs with Rh_2(4*S*-MACIM)$_4$ complex. The deep-colored moieties of the space-filling models correspond to the parts of schematic representations drawn by black lines. Arrows indicate the acetyl group.

It is also noted that the enantiomeric excess in the *trans*-fused product is lower in the MACIM system (65% ee) than in the MEPY system (91% ee) (eq 6). In fact, the energy difference between **TS9-1** and **TS9-2** is larger in the MEPY system (4.3 kcal/mol) than in the MACIM system (2.7 kcal/mol). This fact can be rationalized as follows: As described above, in the MACIM system, **TS9-1** is much destabilized by the steric repulsion between the acetyl group and the cyclohexane ring. On the other hand, **TS9-2** is not as much destabilized as **TS9-1** because the distance between the cyclohexane ring and the acetyl group is longer. In fact, the distortion of the acetyl group is smaller in **TS9-2** than in **TS9-1** (Figure 7b). Therefore the energy difference between them becomes smaller than that of the MEPY system.

6-7. Summary

In summary, the present studies have addressed the origin of diastereo- and enantioselectivity in several cyclization reactions of diazo compounds that proceed via intramolecular C-H insertion of Rh-carbene complexes. A *n*-membered ring formation reaction proceeds via [n + 1]-membered cyclic transition state involving the transferred hydrogen atom. The stereoselectivities are controlled by the conformation of the [n + 1]-membered ring, the substitution pattern of the substrate and the steric environment created by the ligands, and these factors are closely engaged with each other. Although still unsatisfactory for precise prediction of experimental results, the calculations succeeded in reproducing the experimental selectivities in a semi-quantitative manner. The present work has provided a computational procedure and model structures that may be utilized by bench chemists who explore the Rh-catalyzed intramolecular C-H insertion reactions. While admittedly incomplete, the present theoretical procedure will be useful to make prediction of the enantioselectivity by a new chiral ligand.

References and Notes

1. (a) Shilov, A. E.; Shul'pin, G. B. *Chem. Rev.* **1997**, *97*, 2879-2932. (b) Dyker, G. *Angew. Chem., Int. Ed.* **1999**, *28*, 1698-1712.
2. (a) *Selective Hydrocarbon Activation* (Eds.: J. A. Davies, P. L. Watson, A. Greenberg, J. F. Liebman), VCH Publishers, New York, **1990**. (b) *Activation and Functionalization of Alkanes* (Ed.: C. L. Hill), John Wiley & Sons, Inc., New York, **1989**. (c) Kakiuchi, F.; Murai, S. in *Activation of Unreactive Bonds and Organic Synthesis* (Ed.: S. Murai), Splinger, Berlin, **1999**.
3. (a) Doyle, M. P. *Chem. Rev.* **1986**, *86*, 919-939. (b) Taber, D. F. in *Comprehensive Organic Synthesis*, Vol. 3 (Eds.: B. M. Trost, I. Fleming), Pergamon Press, New York, **1991**, Chapter 4.2. (c) Doyle, M. P. in *Comprehensive Organometallic Chemistry II*, Vol. 12 (Ed.: L. S. Hegedus), Pergamon Press, New York, **1995**, Chapters 5.1 and 5.2. (d) Ye, T.; McKervey, M. A. *Chem. Rev.* **1994**, *94*, 1091-1160. (e) Doyle, M. P.; McKervey, M. A.; Ye, T. *Modern Catalytic Methods for Organic Synthesis with Diazo Compounds*; John Wiley & Sons, Inc., New York, **1998**. (f) Dörwald, F. Z. *Metal Carbenes in Organic Synthesis*; Wiley-VCH, Weinheim, **1999**.
4. (a) Doyle, M. P.; Forbes, D. C. *Chem. Rev.* **1998**, *98*, 911-935. (b) Lydon, K. M.; McKervey, M. A. in

Comprehensive Asymmetric Catalysis, Vol. 2 (Eds.: E. N. Jacobsen, A. Pfaltz, H. Yamamoto), Splinger, Berlin, **1999**, Chapter 16.2. (c) Doyle M. P. in *Catalytic Asymmetric Synthesis* (Ed.: I. Ojima), Wiley-VCH, New York, **2000**, Chapter 5. (d) Davies, H. M. L.; Antoulinakis, E. G. *J. Organomet. Chem.* **2001**, *617-618*, 47-55.

5. Merck employs Rh-catalyzed N-H insertion reaction of diazo compound for the production of carbapenems.
6. Nakamura, E.; Yoshikai, N.; Yamanaka, M. *J. Am. Chem. Soc.* **2002**, *124*, 7181-7192.
7. (a) Taber, D. F.; Petty, E. H. *J. Org. Chem.* **1982**, *47*, 4808-4809. (b) Taber, D. F.; Ruckle, Jr, R. E. *Tetrahedron Lett.* **1985**, *26*, 3059-3062. (c) Taber, D. F.; Ruckle, Jr, R. E. *J. Am. Chem. Soc.* **1986**, *108*, 7686-7693.
8. Doyle, M. P.; Westrum, L. J.; Wolthuis, W. N. E.; See, M. M.; Boone, W. P.; Bagheri, V.; Pearson, M. M. *J. Am. Chem. Soc.* **1993**, *115*, 958-964.
9. (a) Brown, D. S.; Elliot, M. C.; Moody, C. J.; Mowlem, T. J.; Marino, J. P.; Padwa, A. *J. Org. Chem.* **1994**, *59*, 2447-2455; b) M. P. Doyle, R. J. Pieters, J. Taunton, H. Q. Pho, A. Padwa, D. L. Hertzog, L. Precedo, *J. Org. Chem.* **1991**, *56*, 820-829.
10. Watanabe, N.; Anada, M.; Hashimoto, S.; Ikegami, S. *Synlett* **1994**, 1031-1033.
11. Doyle, M. P.; van Oeveren, A.; Westrum, L. J.; Protopopova, M. N.; Clayton, T. W. Jr. *J. Am. Chem. Soc.* **1991**, *113*, 8982-8984.
12. (a) Doyle, M. P.; Dyatkin, A. B.; Roos, G. H. P.; Cañas, F.; Pierson, D. A.; van Basten, A. *J. Am. Chem. Soc.* **1994**, *116*, 4507-4508. (b) Doyle, M. P.; Kalinin, A. V.; Ene, D. G., *J. Am. Chem. Soc.* **1996**, *118*, 8837-8846.
13. (a) Doyle, M. P. *Recl. Trav. Chim. Pays-Bas.* **1991**, *110*, 305-316. (b) Timmons, D. J.; Doyle, M. P. *J. Organomet. Chem.* **2001**, *617-618*, 98-104.
14. Taber, D. F.; You, K. K.; Rheingold, A. L. *J. Am. Chem. Soc.* **1996**, *118*, 547-556.
15. (a) Becke, A. D.*J. Chem. Phys.* **1993**, *98*, 5648-5652. (b) Lee, C.; Yang, W.; Parr, R. G. *Phys. Rev. B* **1988**, *37*, 785-789.
16. Wadt, W. R.; Hay, P. J. *J. Chem. Phys.* **1985**, *82*, 299-310.
17. Hehre, W. J.; Radom, L.; Schleyer, P. v R.; Pople, J. A. *Ab Initio Molecular Orbital Theory*, John Wiley & Sons, Inc., New York, **1986**. References cited therein.
18. Stewart, J. J. P. *J. Comput. Chem.* **1989**, *10*, 209-220.
19. Gordon, M. S.; Gano, D. R. *J. Am. Chem. Soc.* **1984**, *106*, 5421-5425. Bach, R. D.; Su, M-D.; Aldabbagh, E.; Andrés, J. L.; Schlegel, H. B. *J. Am. Chem. Soc.* **1993**, *115*, 10237-10246.
20. Gaussian 98, revision A.9, M. J. Frisch, G. W. Trucks, H. B. Schlegel, G. E. Scuseria, M. A. Robb, J. R. Cheeseman, V. G. Zakrzewski, J. A. Montogomery, Jr., R. E. Stratmann, J. C. Burant, S. Dapprich,

J. M. Millam, A. D. Daniels, K. N. Kudin, M. C. Strain, O. Farkas, J. Tomasi, V. Barone, M. Cossi, R. Cammi, B. Mennucci, C. Pomelli, C. Adamo, S. Clifford, J. Ochterski, G. A. Petersson, P. Y. Ayala, Q. Cui, K. Morokuma, D. K. Malick, A. D. Rabuck, K. Raghavachari, J. B. Foresman, J. Cioslowski, J. V. Ortiz, A. G. Baboul, B. B. Stefanov, G. Liu, A. Liashenko, P. Piskorz, I. Komaromi, R. Gomperts, R. L. Martin, D. J. Fox, T. Keith, M. A. Al-Laham, C. Y. Peng, A. Nanayakkara, M. Challacombe, P. M. W. Gill, B. Johnson, W. Chen, M. W. Wong, J. L. Andres, C. Gonzalez, M. Head-Gordon, J. A. Pople, Gaussian. Inc., Pittsburg, PA, 1998.

21. MacSpartan Pro, ver. 1.0.2, Wavefunction, Inc., 1999-2000.
22. The PM3/B3LYP modeling was also applied to B3LYP-optimized structures themselves to find that the relative stability of the half-chair and boat isomers did not change: **TS1a-1** and **TS1b-1** were calculated to be more stable than their boat isomers by 3.2 and 5.1 kcal/mol, respectively (1.2 and 5.1 kcal/mol at the B3LYP level).
23. The *cis-trans* and *cis-cis* TSs were also examined, and *trans*/*cis* selectivities with respect to the forming C-C bond were calculated to be 98.8:1.2 (entry 1), 98.7:1.3 (entry 2) and 95.3:4.7 (entry 3), which qualitatively reproduced the experimental results.
24. Before Hashimoto's work (ref. 10), Doyle found the *cis* geometry in a similar system using achiral dirhodium perfluorobutyrate (M. P. Doyle, J. Taunton, H. Q. Pho, *Tetrahedron Lett.* **1989**, *30*, 5397-5400). In this case, an ethoxycarbonyl group was attached to the reacting carbon atom. Since it destabilizes a neighboring carbocation, the TS of C-H insertion is expected to become later. This would be unfavorable for the *trans*-TS due to significant steric repulsion between the ester group and the dirhodium carboxylate framework.
25. Steric repulsion may be more significant than electrostatic one since replacement of the methoxy group by phenyl, benzyl, and ethyl groups results in only modest decrease in enantioselectivity.
26. Examples of five-membered ring formation of a disubstituted diazo compound with > 90% ee: (a) Davies, H. M. L.; Grazini, M. V. A.; Aouad, E. *Org. Lett.* **2001**, *3*, 1475-1477. (b) Saito, H.; Oishi, H.; Kitagaki, S.; Nakamura, S.; Anada, M.; Hashimoto, S. *Org. Lett.* **2002**, *4*, 3887-3890.

CHAPTER 7

Synergistic Dimetallic Effect in Propargylic Substitution Reaction Catalyzed by Thiolate-bridged Diruthenium Complex

7-1. Introduction

Development of homogeneous catalysis of polynuclear transition metal complexes has attracted much interest since cooperation of multiple transition metals can be expected for the activation of substrates, and will produce new synthetic transformations that are not accessible with conventional monometallic complexes.[1] Multi-metallic centers are often expected to have multi-centered interaction with a single reactant or simultaneous interactions with multiple reactants.[2] On the other hand, a thiolate-bridged diruthenium complex-catalyzed reaction of a propargylic alcohol, developed by Nishibayashi et al, represents another type of multi-metallic catalysis, where only one metal center works as an "active site" that binds and transforms a substrate.[3] Diruthenium complexes such as $[Cp^*RuCl(\mu_2\text{-}SR)]_2$ ($Cp^* = \eta_5\text{-}C_5Me_5$; R = Me, *n*-Pr, *i*-Pr) and $[Cp^*RuCl(\mu_2\text{-}SMe)_2RuCp^*(OH_2)]OTf$ ($OTf = OSO_2CF_3$) have achieved catalytic transformations of a propargylic alcohol with a variety of heteroatom- and carbon-centered nucleophiles, none of which can be catalyzed by common monoruthenium complexes (eq 1).

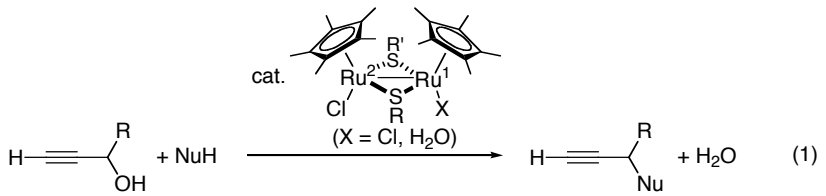

(1)

A proposed mechanism for the diruthenium-catalyzed transformations of propargylic alcohols is shown in Scheme 1.[3] It must be noted first that the catalytic cycle is essentially symmetric as to the broken line in the scheme. The first half concerns the loss of water from the propargylic alcohol to form a vinylidene complex **D**, and the second half the addition of NuH to

regenerate the catalyst. A cationic, coordinatively unsaturated (for Ru^1) diruthenium complex **A** first forms a π-complex **B** with the propargylic alcohol substrate. 1,2-Migration of the acetylenic proton then occurs to generate a γ-hydroxy vinylidene complex **C**. The complex **C** is spontaneously dehydrated to give the allenylidene complex **D** as a key reactive intermediate.[4] In the second half, addition of a nucleophile (alcohol, amine, thiol, etc.) to the allenylidene complex **D** now gives a vinylidene complex **C'**, followed by proton migration affording a product π-complex **B'**. Because the complex **B'** is 18-electron with respect to the Ru^1 center, exchange of the product with the substrate (**B'** -> **A** -> **B**) takes place in a dissociative fashion.[5] Among the proposed catalytic species, the allenylidene complex **D** has been identified as an intermediate on the basis of stoichiometric and catalytic reactions. In this proposal, only the Ru^1 atom takes part in the reaction,[6] yet the catalysis has so far never been achieved by any similar mono-metallic complexes. How can then the second metal Ru^2 activate Ru^1, and what is unique in the catalysis by such bi-metallic complexes possessing a metal-metal bond in their resting state?

Scheme 1.

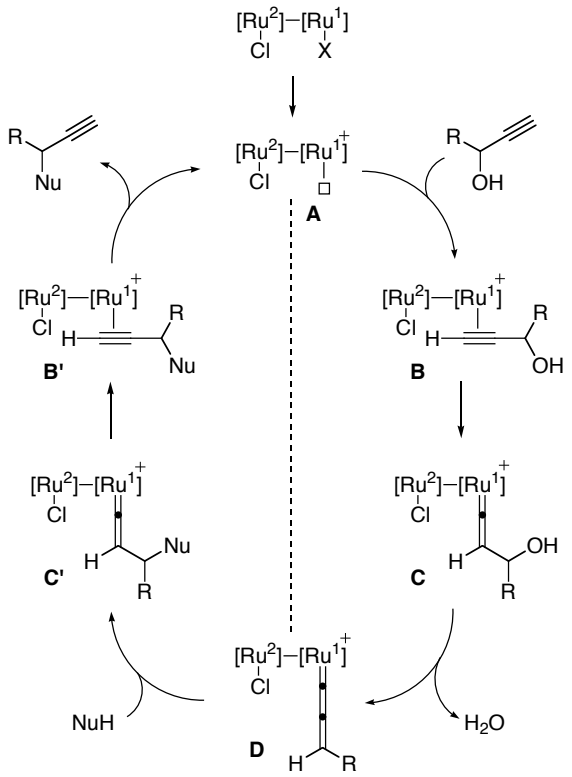

Pursuing our interest in polymetallic cooperation in transition metal catalysis,[7,8,9] we carried out a density functional study on the reaction pathways of diruthenium-catalyzed transformation of a propargyl alcohol in the absence or the presence of MeOH molecule(s). Comparison of diruthenium and monoruthenium complexes in their reactivity, structural and electronic properties revealed the origin of unique catalytic activity of the diruthenium complex. The key finding is that the metal-metal bond dissociates and reforms during the catalysis while the whole structure of the catalyst is rigidly maintained by the chalcogen bridges. Having essentially the same electron configuration as the first metal, the second metal acts as a powerful internal ligand that affects much the reactivity of the first metal even with very small change of geometry. The present study has also shown an important role of the alcohol to mediate smooth proton transfer during the transformation of the substrate on the Ru center.

Experimental Background

The reactivity of a cationic metal-allenylidene complex as a stabilized propargylic cation has been intensively studied.[10] In fact, reactions of monoruthenium allenylidene complexes with a variety of nucleophiles have been reported, where the nucleophile attacks either the C^{α} or C^{γ} carbon centers of the allenylidene ligand to give a Fischer-type carbene complex or an alkynyl complex, respectively. The regioselectivity of the nucleophilic addition is controlled by the electronic and steric properties of the metallic fragment: Electron-richness and/or bulkiness favor the addition to the C^{γ} center.[11]

In spite of the above intriguing reactivities, most reactions of monoruthenium allenylidene complexes are limited to stoichiometric ones. Thus, conventional monoruthenium complexes such as $[CpRuCl(PPh_3)_2]$ (Cp = η_5-C_5H_5), $[RuCl_2(dppe)_2]$ (dppe = 1,2-bis(diphenylphosphino)ethane), $[RuCl_2(PPh_3)_3]$, and $[RuCl_2(p\text{-cymene})]$, which are known to react with propargylic alcohols to produce the corresponding allenylidene complexes,[10] do not

work at all in the catalytic transformation of propargylic alcohols.[12] In fact, only a few examples of catalytic reactions via allenylidene intermediates have been reported until now.[13]

An experimental approach has been taken to obtain insight into the role of two Ru atoms in the catalytic cycle: A series of calcogenolate (S, Se and Te) bridged diruthenium complexes have been synthesized, and their structures, catalytic activities and electrochemical properties have been studied.[14] These studies suggested the importance of electronic communication between the two Ru atoms, which enhances the electrophilicity of the allenylidene ligand (**D** -> **C'** in Scheme 1) and/or facilitates the ligand exchange of the product with the substrate (**B'** -> **B**). The experimental observations notwithstanding, the origin of the cooperative effect of two Ru atoms has not been established yet at the molecular level.

7-2. Computational Models and Methods

7-2-1. Models

In the present studies, we employed $[Cp(Cl)Ru(\mu_2\text{-}SMe)_2RuCp]^+$ (**1a**) as a model of the diruthenium catalyst. While the real catalyst bears a bulky Cp* ligand that is likely to be the origin of γ-selective nucleophilic attack to the corresponding allenylidene complex,[3] it was replaced by a Cp ligand in the interest of computational time. For comparison with the diruthenium catalysis, we also examined the reaction of $[CpRu(PH_3)_2]^+$ (**1b**), a PPh_3-version of which has been known to react with a propargyl alcohol to give an allenylidene complex.[10]

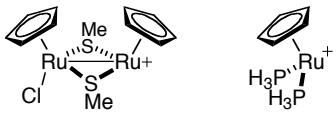

1a **1b**

The catalytic cycle being quasi-symmetric (Scheme 1), we mainly focus on the reaction between these model catalysts and propargyl alcohol leading to Ru-allenylidene complexes (eq 2). Since the second half is a "mirror image" of the former, the former reaction must consist of fast

equilibrium through smooth and low-energy potential surface. To mimic the reaction conditions for MeOH substition where MeOH is used as a solvent, we employed zero to two MeOH molecules that are hydrogen-bonded to each other as well as to the propargyl alcohol. The results will be described with an increasing number of the MeOH molecules.

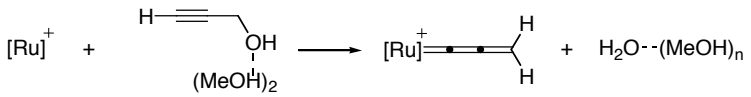

$[Ru]^+$ = **1a** or **1b**, n = 0-2

7-2-2. Methods

All calculations were performed with a Gaussian 98 and Gaussian 03 packages.[15] The density functional theory (DFT) method was employed using the B3LYP hybrid functional.[16] Geometry optimization was performed with a basis set (denoted as 631LAN) consisting of the LANL2DZ basis set including a double-zeta valence basis set with the Hay and Wadt effective core potential (ECP) for Ru[17] and 6-31G(d) basis set for C, H, O, P and S.[18] The B3LYP/631LAN-optimized structure of $[Cp^*RuCl(\mu_2\text{-SMe})]_2$ showed good agreement with the X-ray crystallographic data.[19] Each stationary point was adequately characterized by normal coordinate analysis. The intrinsic reaction coordinate (IRC) analysis[20] was carried out to confirm that stationary points are smoothly connected to each other. However, owing to flatness of the potential energy surface, some of the stationary points could not be fully connected computationally, whereas they are, by all means, chemically connected to each other. Natural population analysis was performed at the same level as the one used for geometry optimization.[21] Throughout this chapter, energetics of reaction pathways will be discussed on the basis of Gibbs free energy, while electronic energy data are given in the Appendix and discussed when necessary.

7-3. Reaction Pathways for Ru-Allenylidene Complex Formation

7-3-1. Without MeOH Molecule

We first examined the reaction pathway for the Ru-allenylidene complex formation without a methanol molecule (Scheme 2 and Figure 1). First, complexation of coordinatively unsaturated complex **1** with the C-C triple bond of propargyl alcohol gives a π-complex **2** with energy changes of +2.2 and -14.6 kcal/mol for di- and mono-Ru systems, respectively. Relocation of the metal atom in **2b** takes place via TS **3b** ($\Delta G^{\ddagger}$ = +10.7 kcal/mol) to afford an unstable C-H σ-complex **4b** (less stable than **2b** by +10.1 kcal/mol). In the case of the di-Ru complex **2a**, corresponding TS and σ-complex could not be located. Subsequent 1,2-migration of the acetylenic proton (TS **5**), which has been well documented for transition metal-mediated vinylidene formation,[22,23] gives a vinylidene complex **6**. Net activation barriers for this process are +12.3 (from **1a**) and +16.3 kcal/mol (from **2b**) for di-Ru and mono-Ru systems, respectively. The γ-hydroxy vinylidene complex **6** undergoes very difficult dehydration via a four-centered TS **7** ($\Delta G^{\ddagger}$ = +39.8 and +43.5 kcal/mol for di- and mono-Ru) to give the allenylidene complex **8**. While the reaction proceeds with moderate activation barriers from **1** to the vinylidene complex **6**, the dehydration process requires unreasonably high activation barriers. Thus, we considered that there should be solvent assistance in this step and examined the reaction pathways including MeOH molecules (vide infra).

Scheme 2. Reaction Pathway for Mono- and Di-ruthenium Allenylidene Complex Formation from **1** and Propargyl Alcohol[a]

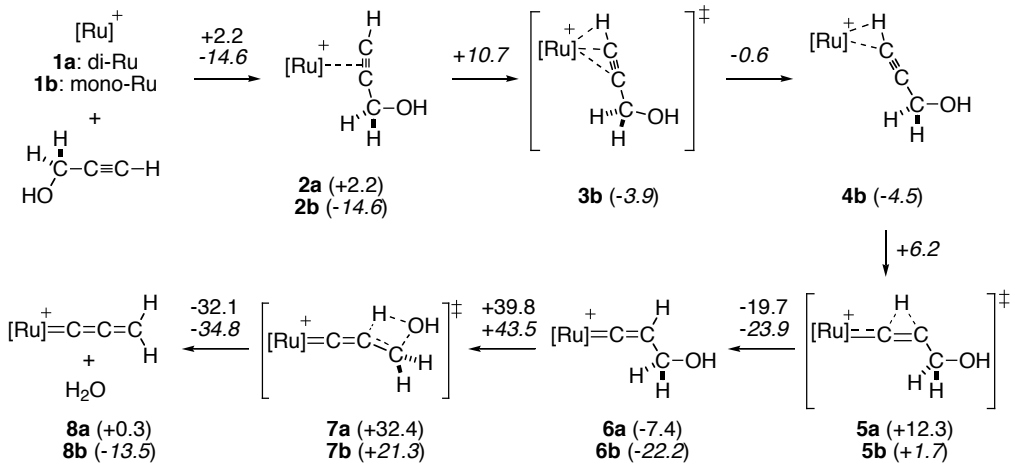

[a] [Ru] refers to **1a** ($[Cp(Cl)Ru(\mu_2\text{-}SMe)_2RuCp]^+$) and **1b** ($[CpRu(PH_3)_2]^+$). Free energies (kcal/mol) are relative to [**1** + $HCCCH_2OH$] (diruthenium in roman and monoruthenium in italic). Energy changes are shown above arrows.

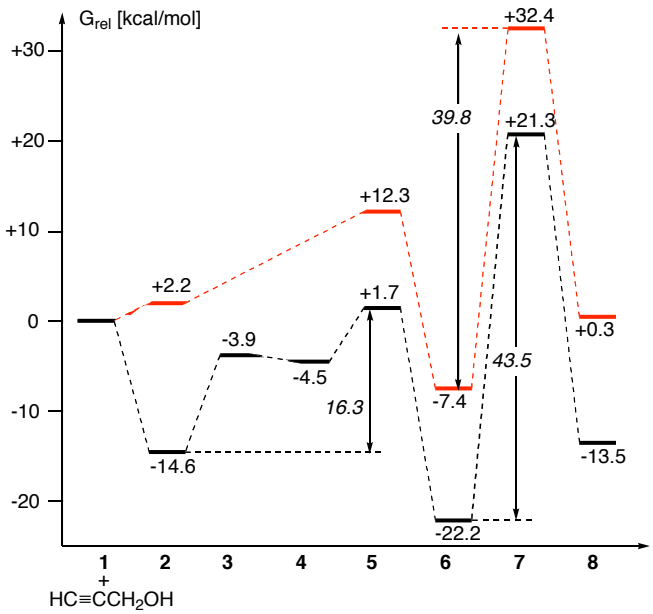

Figure 1. Free energy diagram (kcal/mol) for the reaction of **1** with a propargyl alcohol. Di-Ru (red) and mono-Ru reactions (black) are color-coded throughout this chapter.

The 3-D structures of the stationary points in the di-Ru and the mono-Ru systems are shown in Figures 2 and 3, respectively. The Ru^1-Ru^2 distance is elongated significantly upon π-complexation (2.684 -> 2.855 Å). While the distance changes less significantly (i.e., ranges from 2.814 – 2.855 Å) in the following process, it becomes longer when the Ru^1 center back-donates

electron to the substrate as in the π-complex and vinylidene/allenylidene complexes (this occurs irrespective of the absence or the presence of solvent molecules). The structures around the reactive site are not significantly different between di- and mono-Ru systems.

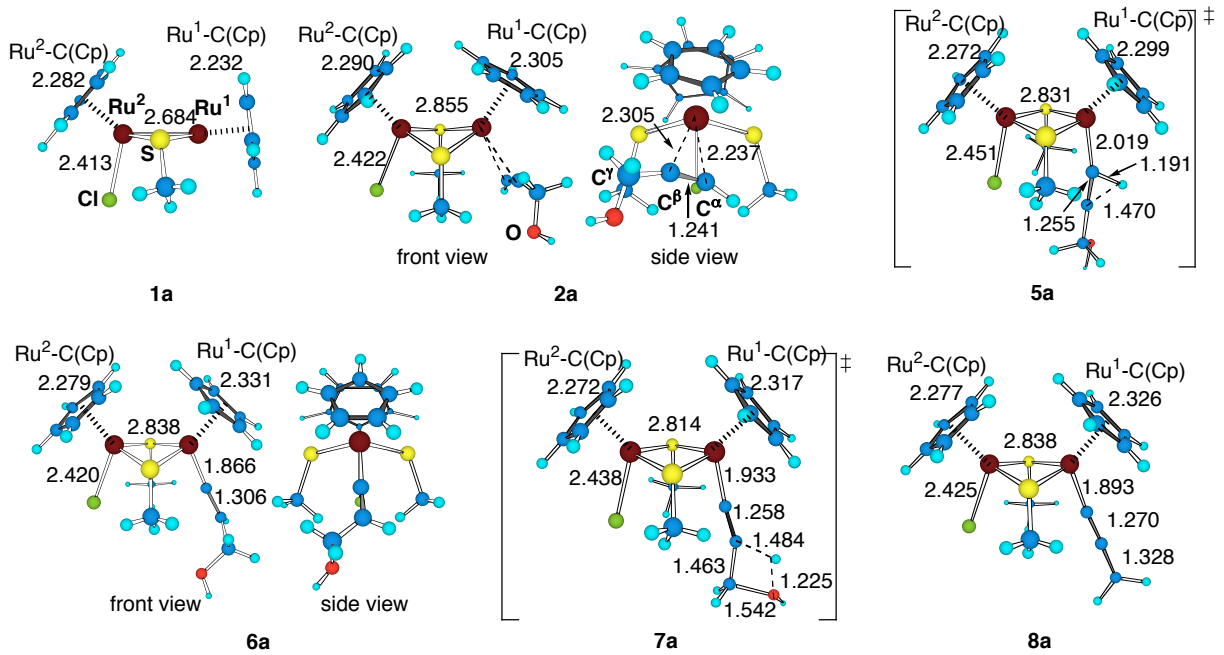

Figure 2. Structures of stationary points in the reaction of **1a** with propargyl alcohol. Numbers refer to distances (Å).

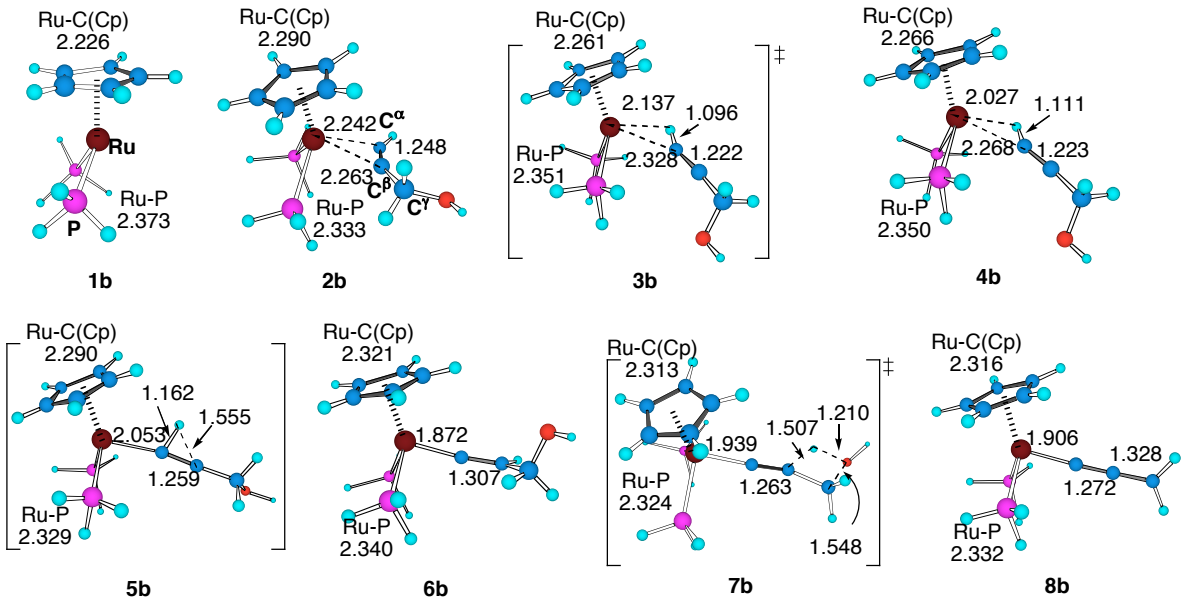

Figure 3. Structures of stationary points in the reaction of **1b** with propargyl alcohol. Numbers refer to distances (Å).

From an energetic point of view, it must be pointed out that energies of the π-complex (**2a**), vinylidene complex (**6a**) and allenylidene complex (**8a**) relative to **1a** are much higher than those of the corresponding mono-Ru complexes (**2b**, **6b** and **8b**) relative to **1b** (Figure 1). To get an insight into the difference, complexes **2** and **8** were separated into two fragments and their deformation energies and interaction energies were calculated according to Schemes 3 and 4. As the result, the weaker complexation energies (ΔE) in the di-Ru system were found to originate from the larger deformation energy of the [Ru] fragment (DEF_{Ru}) and the smaller interaction energy between the [Ru] fragment and the acetylene or allenylidene ligands (INT). The former reason is due to the much stronger Ru^1-Ru^2 bonding in **1a** than in **2a** and **8a** (Figure 2), which stabilizes the coordinatively unsaturated Ru^1 center.

Scheme 3. Fragment Analysis of Ru/Propargyl Alcohol π-Complex **2**[a]

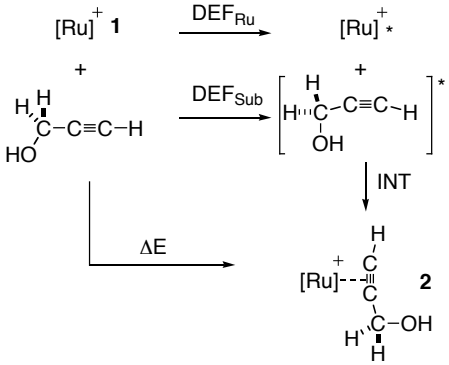

	a	b
DEF_{Ru}	+16.8	+4.9
DEF_{Sub}	+9.3	+12.8
INT	-39.4	-46.1
ΔE	-13.3	-28.4

[a] Formulae with asterisks refer to the parts taken from the complex **2**. Numbers (kcal/mol) are based on the electronic energies.

Scheme 4. Fragment Analysis of Ru-Allenylidene Complex **8**[a]

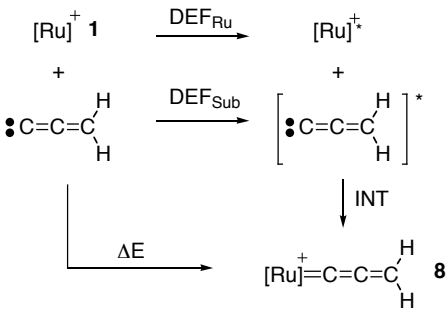

	a	b
DEF_{Ru}	+14.8	+6.4
DEF_{Sub}	+0.4	+0.3
INT	-83.5	-88.1
ΔE	-68.3	-81.4

[a] Formulae with asterisks refer to the parts taken from the complex **8**. Numbers (kcal/mol) are based on electronic energies.

The second reason originates from the back-donation ability of the [Ru] fragments. For the π-complexes **2a** and **2b**, the C^{α}-C^{β} bond length (**2a**: 1.241 Å, **2b**: 1.248 Å) as well as the C^{β}-C^{α}-H (**2a**: 155.8°, **2b**: 154.7°) and C^{α}-C^{β}-C^{γ} (**2a**: 161.3°, **2b**: 154.6°) bond angles indicate weaker back-donation in the di-Ru system (Figures 2, 3). Natural charge of the propargyl alcohol (**2a**: +0.15, **2b**: +0.07) also supports this conjecture. For the vinylidene and allenylidene complexes (**6**, **8**), while the geometry of the Ru-C^{α}-C^{β}-C^{γ} moiety is similar for the di-Ru and the mono-Ru systems, weaker back-donation in the di-Ru system is indicated by natural charges at the C^{α} atom (**6a**: +0.24, **6b**: +0.18; **8a**: +0.11, **8b**: +0.05) and (in the case of allenylidene complex) the $C^{\gamma}H_2$ moiety (**7a**: +0.27, **7b**: +0.25). As discussed later, the stability of a coordinatively unsaturated species **1a** and the weaker back-donation in the di-Ru system are critical factors for its unique catalytic activity.

7-3-2. Solvation with One MeOH Molecule

Next, chemical models including one MeOH molecule were studied. A hydrogen-bonded complex of propargyl alcohol with one MeOH molecule was allowed to react with di- and mono-Ru complexes (Scheme 5 and Figure 4). In this case, π-complexation (**1** -> **9**), π-bond to σ-bond slippage to the σ-complex (**9** -> **11**) and 1,2-proton migration (**11** -> **13**) proceed in essentially the same way as the MeOH-free model (Scheme 2). However, the presence of a MeOH molecule opened up a low-energy six-centered path for dehydration of the vinylidene complex **13** (instead of the four-centered path without methanol): The activity of protons at the β-position of vinylidene complexes being well-documented,[22] **13** is easily deprotonated by MeOH via TS **14** (di-Ru: +14.0 kcal/mol; mono-Ru: +17.5 kcal/mol). The resulting Ru-alkynyl complex **15,** with a very small barrier, looses its propargylic hydroxy group as protonated by $MeOH_2^+$ to afford the allenylidene complex **17** (or **8**).

Scheme 5. Reaction Pathway for Di- and Mono-ruthenium Allenylidene Complex Formation from **1** and Propargyl Alcohol in the Presence of One MeOH Molecule.[a]

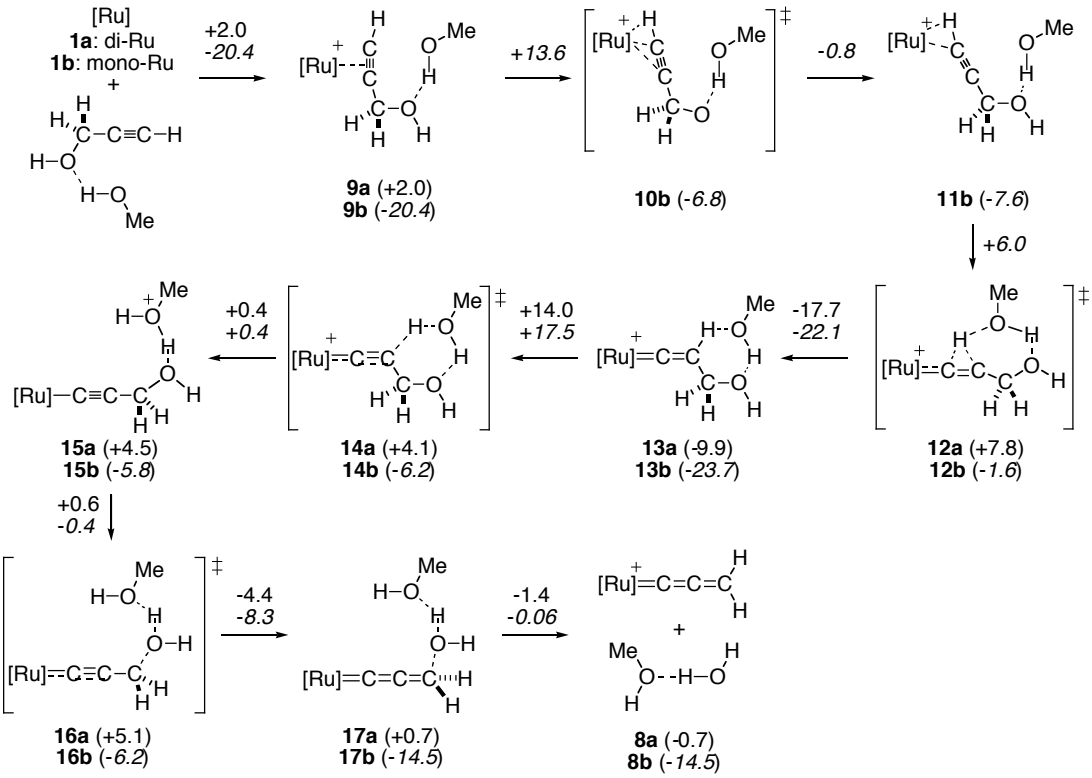

[a] Free energies (kcal/mol) are relative to [**1** + $HCCCH_2OH$---MeOH] (diruthenium in roman and monoruthenium in italic). Energy changes are shown above arrows.

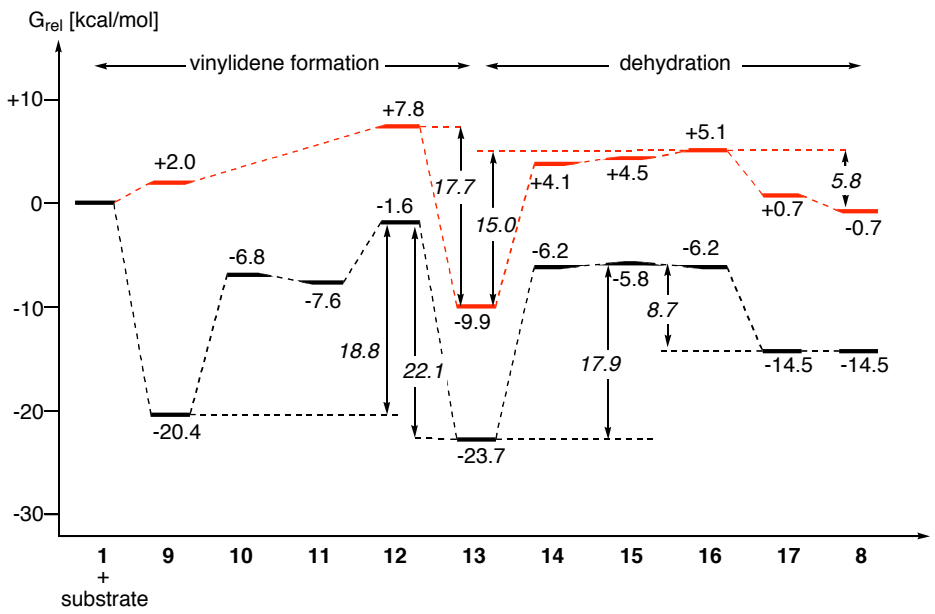

Figure 4. Free energy profile (kcal/mol) for the reaction of **1** with propargyl alcohol in the presence of one MeOH molecule. Di-Ru (red) and mono-Ru reactions (black) are color-coded.

The structures of stationary points from **1** to **13** are very similar to their counterparts in the solvent-free reaction pathway (Figures 2, 3). Figures 5 and 6 show TSs and intermediates for the dehydration of the γ-hydroxy vinylidene complex **13**. Upon deprotonation of the β-position that gives the Ru-alkynyl complex (**13** -> **14** -> **15**), the Ru-C$^{\alpha}$ bond becomes longer (di-Ru: 1.869 -> 1.976 -> 1.998 Å, mono-Ru: 1.878 -> 1.992 -> 2.015 Å), which indicates the decrease of back-donation during this process. To the contrary, in the process of γ-dehyroxylation of the Ru-alkynyl complex (**15** -> **16** -> **17**), it becomes shorter again (di-Ru: 1.998 -> 1.953 -> 1.914 Å, mono-Ru: 2.015 -> 1.975 -> 1.917 Å) reflecting the increase of back-donation.

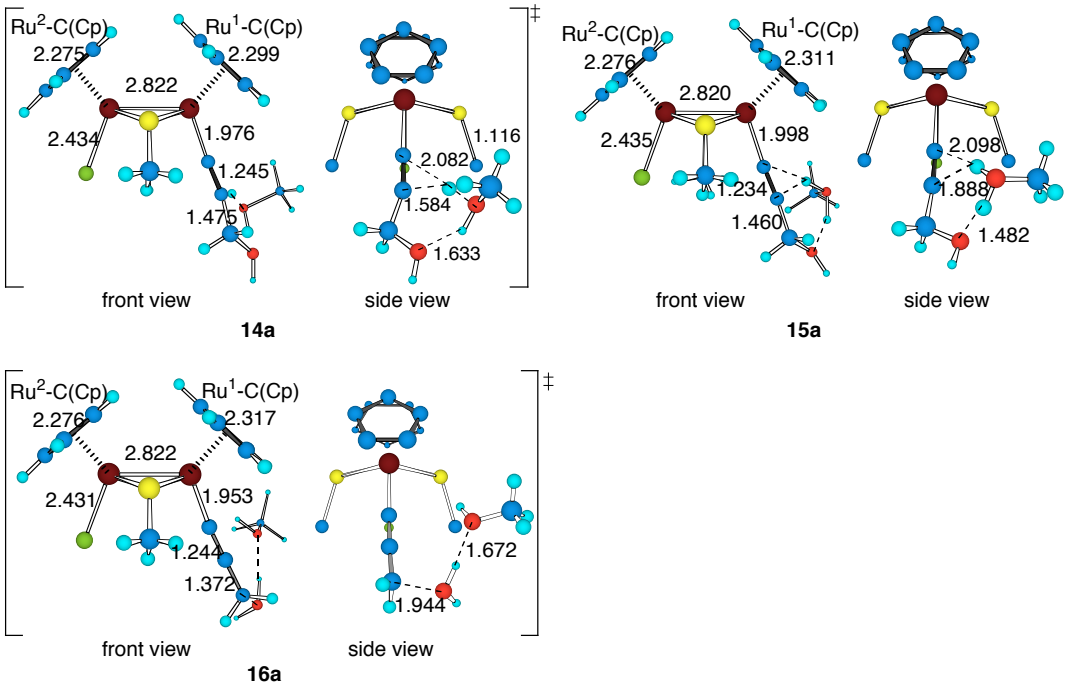

Figure 5. Structures of stationary points in the dehydration of di-Ru/vinylidene complex **13a**. Numbers refer to bond length (Å).

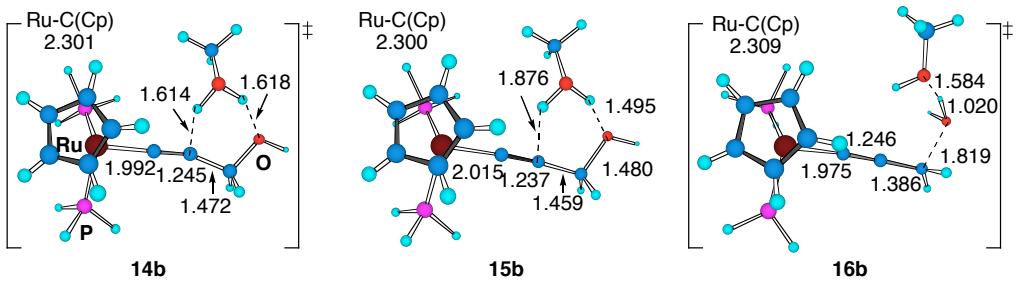

Figure 6. Structures of stationary points in the dehydration of mono-Ru/vinylidene complex **13b**. Numbers refer to bond length (Å).

In Figure 4, one can see that the activation free energies for both the vinylidene formation (di-Ru: +7.8 kcal/mol (**1a** -> **12a**); mono-Ru: +18.8 kcal/mol (**9b** -> **12 b**)) and the dehydration (di-Ru: +15.0 kcal/mol (**13a** -> **16a**); mono-Ru: +17.9 kcal/mol (**13b** -> **15b**)) are lower for the di-Ru system than for the mono-Ru system. It is also notable that their reverse reactions require less activation barriers for the di-Ru system than for the mono-Ru system: The activation energies for the water addition to the allenylidene complex (**8** -> **16**) are +5.8 and +8.3 kcal/mol for the di-Ru and mono-Ru systems, and those for the hydrogen migration from the vinylidene complexes (**13** -> **12**) are +17.7 and +22.1 kcal/mol for di-Ru and mono-Ru systems, respectively.

We consider that the lower activation barriers in the di-Ru system are due to its lower back-donation ability (vide supra): All of the above processes involve loss (or weakening) of back-bonding on the way from the reactant to the next transition state. For example, in the vinylidene formation step (**9** -> **13**), the TS **12** does not involve back-donation either to the C^{α}-C^{β} π^{*} orbital (as in **9**) or to the C^{α} vacant 2p orbital (as in **13**). In addition, in the vinylidene-allenylidene transformation (**13** -> **8**), the C^{α} atom of the intermediary Ru-alkynyl complexes (**14**-**16**) does not accept back-donation from Ru, judging from the much longer Ru-C^{α} bond lengths in **14**-**16** than in **8** and **13** (and natural population analysis; see below). Thus, in the mono-Ru sytems where back-bonding is stronger, more activation energy is necessary to disturb the back-donative bonding.

Analysis of natural charges also supports the above discussion (Figure 7). In the mono-Ru system (Figure 7a), charges of Ru, Cp and PH_3 (shown by blue, pink and gree lines, respectively) change in a parallel way except for the first π-complexation (this is also the case for the di-Ru system). Thus, the total charge of the $CpRu(PH_3)_2$ fragment (denoted as [Ru]) serves as a good indicator of the Ru oxidation state. The positive charge of [Ru] is large at π-complex **9**,

vinylidene complex **13** and allenylidene complex **8** and becomes smaller between them, indicating the presence or the absence of back-donation, respectively.

Figure 7b shows how the natural charges of two Ru atoms change in a complementary way. The interaction of two Ru centers is demonstrated clearly by the parallel change of charges of the [Ru^1] and the [Ru^2] fragments (note that [Ru^i] refers to $CpRu^i(SMe)$). Interestingly, the [Ru^1] fragment is less positive than the [Ru^2] fragment throughout the reaction pathway (except for the initial complex **1**), while the valence formalim in Scheme 1 indicates a positive charge at the [Ru^1] moiety. This suggests that the Ru-Ru moiety can be formally represented by two resonance structures as shown in Chart 1.

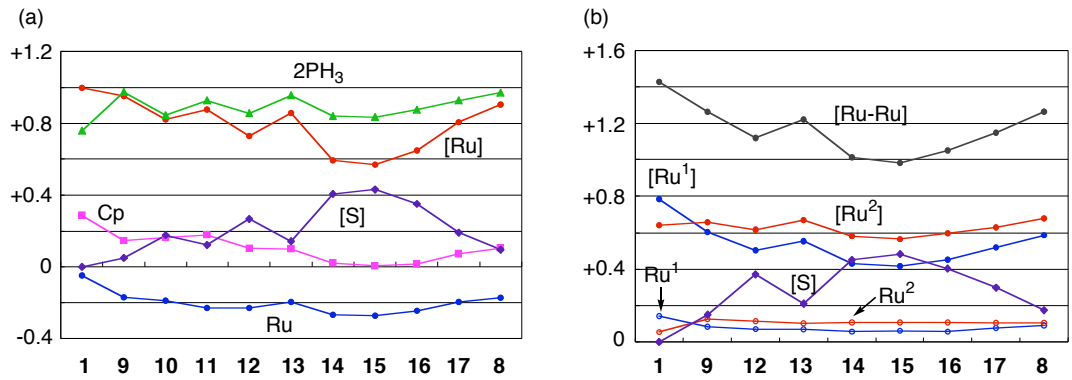

Figure 7. Changes of natural charges through the reaction of **1** with propargyl alcohol in the presence of one MeOH molecule. (a) Mono-Ru system. Ru, [Ru] and [S] refer to the Ru atom itself, the $CpRu(PH_3)_2$ fragment and [propargyl alcohol + MeOH], respectively. (b) Di-Ru system. Ru^i, [Ru^i] and [S] refer to the Ru^i atom and the $CpRu^i(SMe)$ fragment (SMe means half of the sum of two SMe charges) and [prapargyl alcohol + MeOH], respectively. [Ru-Ru] refers to {[Ru^1] + [Ru^2]}.

Chart 1.

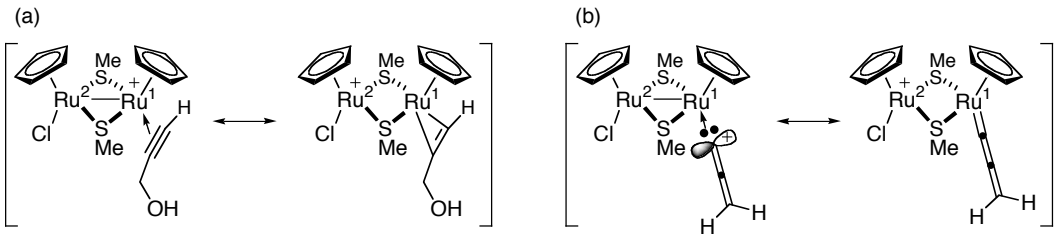

7-3-3. Solvation with Two MeOH Molecules

In the previous model, one MeOH molecule plays two roles in the dehydration steps (Scheme 5): It deprotonates the β-position of the vinylidene complex **13** as a base, and the resulting conjugate acid promotes subsequent dehydroxylation of the alkynyl complex **15**. In the actual experiment performed in MeOH, however, it looks more likely that more than one MeOH molecules perform these two different reactions. Therefore, we included two MeOH molecules in the next stage.

The reaction pathway and energetics are shown in Scheme 6 and Figure 8, respectively. First, Ru complex **1** forms a π-complex (**18**) with an alcohol trimer [propargyl alcohol--2MeOH]. Through an unstable σ-complex **20**, deprotonation of the acetylenic hydrogen takes place via TS **21** to give a Ru-alkynyl complex **22** *in a single step,* without forming a vinylidene intermediate (*cf.* Scheme 5). As shown in Figure 9, as one of the two MeOH molecules deprotonates the acetylenic C-H bond through TS **21** of linear C---H---O geometry, the other MeOH concurrently forms stronger hydrogen bonding with the propargylic hydroxy group (changes of C-H distance are: 1.976 -> 1.836 Å (di-Ru), 1.908 -> 1.835 Å (mono-Ru)).

The activation barriers for this step (di-Ru: 4.3 kcal/mol, mono-Ru: 12.5 kcal/mol) are lower than that for the 1,2-migration in the one-MeOH model (Figure 4). We ascribe the lower activation energy for the di-Ru complex again to the weaker back-donation. The Ru-alkynyl complex **22** undergoes dehydroxylation ($\Delta G^{\ddagger}$ = 6.9 kcal/mol for di-Ru, 4.5 kcal/mol for mono-Ru) to give the final product. As similar to the one-MeOH model, the free energy diagram shows that both forward and reverse reactions of the di-Ru system are more feasible than those of the mono-Ru system (Figure 8).

Scheme 6. Reaction Pathway for Allenylidene Complex Formation from **1** and Propargyl Alcohol in the Presence of Two MeOH Molecules.[a]

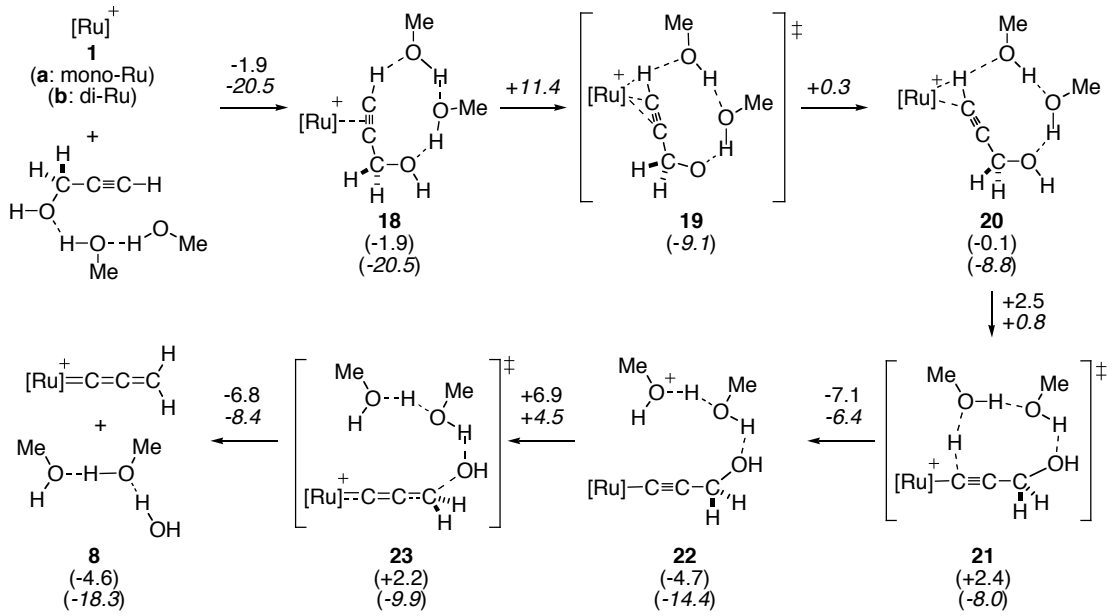

[a] Free energies (kcal/mol) are relative to [**1** + $HCCCH_2OH$-$(MeOH)_2$] (diruthenium in roman and monoruthenium in italic). Energy changes are shown above arrows.

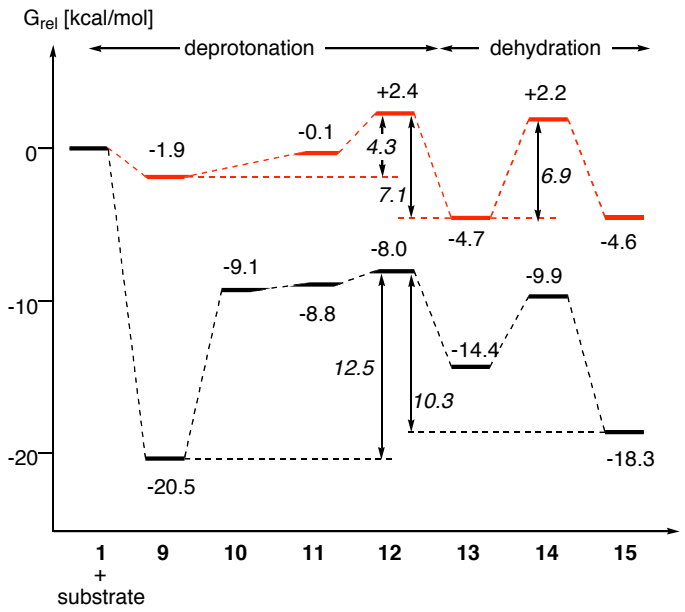

Figure 8. Free energy profile (kcal/mol) for the allenylidene complex formation from **1** and propargyl alcohol in the presence of two MeOH molecules. Di-Ru (red) and mono-Ru reactions (black) are color-coded.

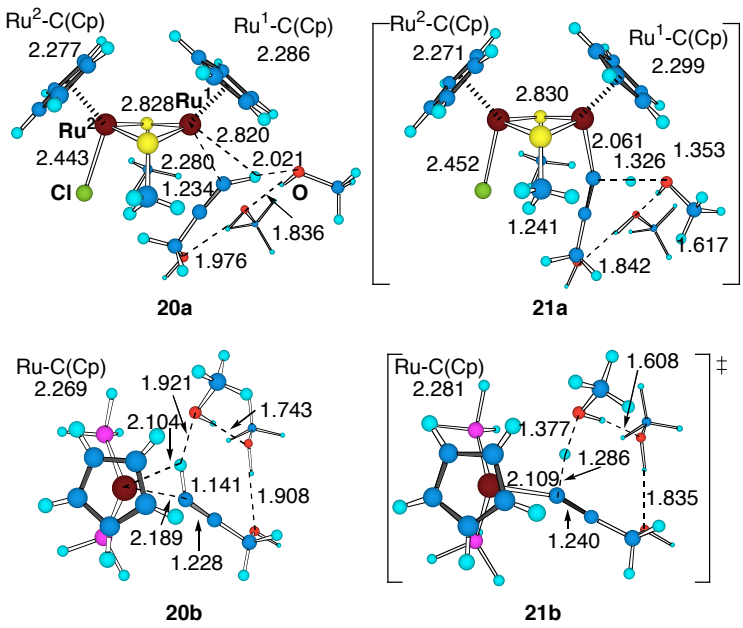

Figure 9. Structures of σ-complex **20** and deprotonation TS **21**. Numbers refer to bond lengths (Å).

7-4. Catalyst Turnover Step

In addition to the above energetic argument of the one-way process, one must consider the catalyst turnover step (i.e., dissociative exchange of the product with the substrate; see Scheme 1) when the feasibility of the *catalytic* cycle is concerned. The free energy changes for the dissociation of the di-Ru π-complexes **2a**, **9a** and **18a** are very small (eq 3), which indicates that this process is very easy. On the other hand, in the case of the mono-Ru complexes **2b**, **9b** and **18b** it requires free energy barriers as much as 15-20 kcal/mol (eq 4). This indicates that the mono-Ru complex has a difficulty in working as a catalyst.

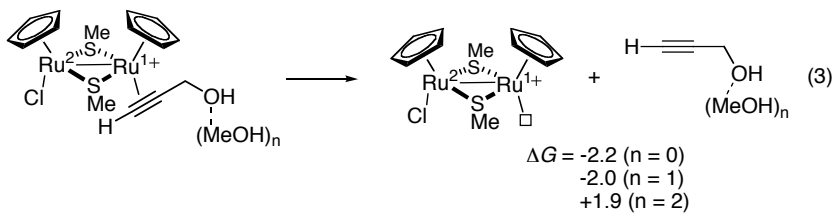

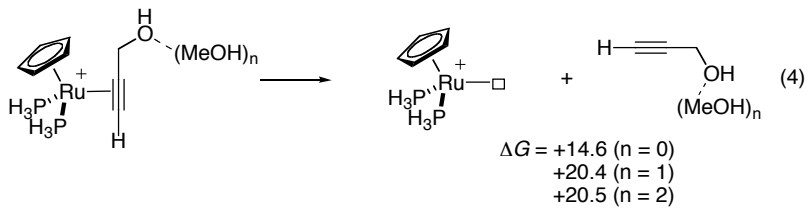

The favorable energetics for the di-Ru system originates from its weaker back-donation ability as well as the stability of the coordinatively unsaturated species **1a**, which benefit from much stronger Ru-Ru bond (2.684 Å) than other complexes (> 2.8 Å) (vide supra). In light of the resonance description of the Ru-Ru bond in Chart 1, this concept can be illustrated as follows (Scheme 7).

Scheme 7. Schematic Representation of Dissociation of C-C Triple Bond from Diruthenium Complex

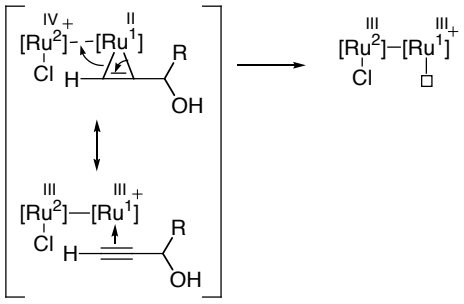

7-5. Summary

The present theoretical study has revealed the pathway of the nucleophilic substitution of a propargyl alcohol catalyzed by a thiolate-bridged diruthenium complex that features a cationic Ru-allenylidene complex as a key intermediate. It was found that solvent molecule(s) play an important role as a base and an acid to facilitate proton transfer during the transformation of the substrate on the metal center. A concrete answer to the essential question on the uniqueness of the diruthenium system is now given (Scheme 8). There are two critical factors: First, the high stability of the coordinatively unsaturated Ru complex **I** enables smooth catalyst turnover, i.e., a dissociative exchange of the product (in **VI**) with the substrate that regenerates **II**. Upon product

dissociation from **VI** to **I**, the energy loss due to the coordinative unsaturation can be compensated by the stronger Ru-Ru interaction, which is unavailable by the mono-Ru system. Second, the weaker back-donation ability of the di-Ru system that is inherent to the Ru^{III} (Ru^{II} in the mono-Ru system) center facilitates transformations of the substrate into the product (**II** -> **VI**). Because each of these processes involves weakening of back-donation from the reactant to the transition state, the di-Ru system that has less back-donation than the mono-Ru system requires less activation barriers than the latter.

Scheme 8. Bimetallic Mechanism of Propargylic Substitution Reaction that is Near Symmetric for Broken Line in the Center

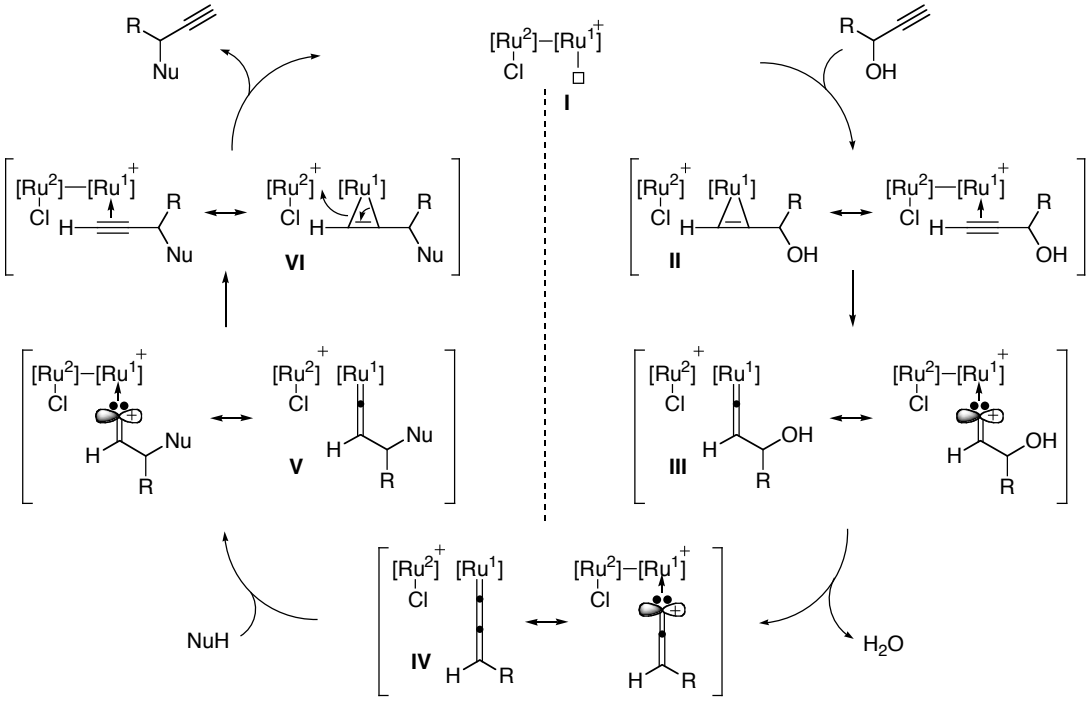

Finally, we wish to make a comparison of the present reaction with the dirhodium-catalyzed C-H insertion between a diazo compound and an alkane,[9] in terms of the bimetallic effects. The roles of the spectator metal centers in these two catalytic reactions are opposite: In the Ru catalysis, the spectator Ru^2 atom acts as an *acceptor* for the Ru^1 atom in the critical ligand exchange step. On the other hand, in the Rh catalysis, the Rh^2 acts as a *donor* to the Rh^1, which facilitates the Rh^1-carbene σ-bond cleavage in the C-H insertion step (Scheme 9). Studies on

these reactions have suggested that control of a metal-metal bond in appropriate distance and flexibility is essential for a design of a bimetallic catalysis.

Scheme 9. C-H Insertion of Alkane with Dirhodium Carbene Complex

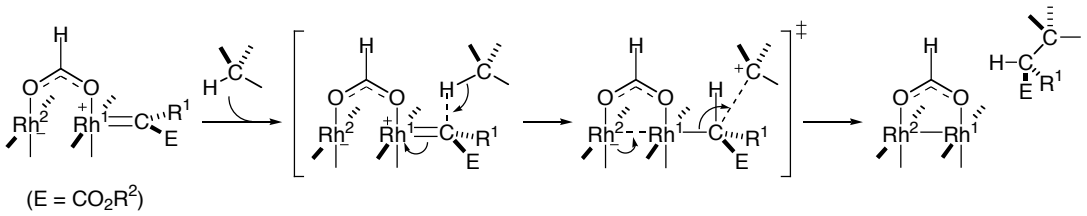

References and Notes

1. For example: *Catalysis by Di- and Polynuclear Metal Cluster Complexes*; Adams, R. D., Cotton, F. A., Eds.; WILEY-VCH: New York, 1998.
2. For example: Broussard, M. E.; Juma, B.; Train, S. G.; Peng, W.-J.; Laneman, S. A.; Stanley, G. G. *Science* **1993**, *260*, 1784-1788; Stoichiometric reaction: Takemori, T.; Inagaki, A.; Suzuki, H. *J. Am. Chem. Soc.* **2001**, *123*, 1762-1763.
3. Nishibayashi, Y.; Wakiji, I.; Hidai, M. *J. Am. Chem. Soc.* **2000**, *122*, 11019-11020; Nishibayashi, Y.; Wakiji, I.; Ishii, Y.; Uemura, S.; Hidai, M. *J. Am. Chem. Soc.* **2001**, *123*, 3393-3394; Inada, Y.; Nishibayashi, Y.; Hidai, M.; Uemura, S. *J. Am. Chem. Soc.* **2002**, *124*, 15172-15173; Nishibayashi, Y.; Inada, Y.; Yoshikawa, M.; Hidai, M.; Uemura, S. *Angew. Chem., Int. Ed.* **2003**, *42*, 1495-1498. Nishibayashi, Y.; Onodera, G.; Inada, Y.; Hidai, M.; Uemura, S. *Organometallics* **2003**, *22*, 873-876.
4. Selegue, J. P. *Organometallics* **1982**, *1*, 217-218.
5. Collman, J. P.; Hegedus, L. S.; Norton, J. R.; Finke, R. G. *Principles and Applications of Organotransition Metal Chemistry*, 2nd ed.; Wiley-Interscience: New York, 1987.
6. The reaction where both of two Ru atoms directly interacts with a substrate: Nishibayashi, Y.; Yamanashi, M.; Wakiji, I.; Hidai, M. *Angew. Chem., Int. Ed.* **2000**, *39*, 2909-2911.
7. Nakamura, E.; Mori, S. *Angew. Chem., Int. Ed.* **2000**, *39*, 3750-3771.
8. Yamanaka, M.; Nakamura, E. *J. Am. Chem. Soc.* **2001**, *123*, 1703-1708.
9. Nakamura, E.; Yoshikai, N.; Yamanaka, M. *J. Am. Chem. Soc.* **2002**, *124*, 7181-7192; Yoshikai, N.; Nakamura, E. *Adv. Synth. Catal.* **2003**, *345*, 1159-1171.
10. (a) Werner, H. *Chem. Commun.* **1997**, 903-910. (b) Touchard, D.; Dixneuf, P. H. *Coord. Chem. Rev.* **1998**, *178-180*, 409-429. (c) Bruce, M. I. *Chem. Rev.* **1998**, *98*, 2797-2858. (d) Cadierno, V.; Gamasa, M. P.; Gimeno, J. *Eur. J. Inorg. Chem.* **2001**, 571-591. (e) Touchard, D.; Dixneuf, P. H. *Coord. Chem. Rev.* **2004**, *248*, 1585-1601. (f) Cadierno, V.; Gamasa, M. P.; Gimeno, J. *Coord. Chem. Rev.* **2004**, *248*, 1627-1657.

11. For recent studies: Cadierno, V.; Conejero, S.; Gamasa, M. P.; Gimeno, J. *Organometallics* **2002**, *21*, 3837-3840; Cadierno, V.; Gamasa, M. P.; Gimeno, J.; Pélez-Carreno, E.; García-Granda, S. *J. Organomet. Chem.* **2003**, *670*, 75-83; Cadierno, V.; Conejero, S.; Gamasa, M. P.; Gimeno, J. *J. Dalton Trans.* **2003**, 3060-3066.
12. Recently, Gimeno et al. reported a cationic mononuclear Ru^{II} complex that catalyzes substitution reaction of a propargylic alcohol with an aliphatic alcohol, while an evidence for a Ru-allenylidene intermediate is not obtained yet: Cadierno, V.; Díez, J.; García-Garrido, S. E.; Gimeno, J. *Chem. Commun.* **2004**, 2716-2717.
13. Trost, B. M.; Flygare, J. A. *J. Am. Chem. Soc.* **1992**, *114*, 5476-5477; Maddock, S. M.; Finn, M. G. *Angew. Chem., Int. Ed.* **2001**, *40*, 2138-2141; Yeh, K.-L.; Liu, B.; Lo, H.-L.; Huang, H.-L.; Liu, R.-S. *J. Am. Chem. Soc.* **2002**, *124*, 6510-6511; Datta, S.; Chang, C.-L.; Yeh, K.-L.; Liu, R.-S. *J. Am. Chem. Soc.* **2003**, *125*, 9294-9295.
14. Nishibayashi, Y.; Imajima, H.; Onodera, G.; Hidai, M.; Uemura, S. *Organometallics* **2004**, *23*, 26-30; Nishibayashi, Y.; Imajima, H.; Onodera, G.; Inada, Y.; Hidai, M.; Uemura, S. *Organometallics* **2004**, *23*, 5100-5103.
15. Gaussian 98, revision A.9, Frisch, M. J.; Trucks, G. W.; Schlegel, H. B.; Scuseria, G. E.; Robb, M. A.; Cheeseman, J. R.; Zakrzewski, V. G.; Montogomery, J. A., Jr.; Stratmann, R. E.; Burant, J. C.; Dapprich, S.; Millam, J. M.; Daniels, A. D.; Kudin, K. N.; Strain, M. C.; Farkas, O.; Tomasi, J.; Barone, V.; Cossi, M.; Cammi, R.; Mennucci, B.; Pomelli, C.; Adamo, C.; Clifford, S.; Ochterski, J.; Petersson, G. A.; Ayala, P. Y.; Cui, Q.; Morokuma, K.; Malick, D. K.; Rabuck, A. D.; Raghavachari, K.; Foresman, J. B.; Cioslowski, J.; Ortiz, J. V.; Baboul, A. G.; Stefanov, B. B.; Liu, G.; Liashenko, A.; Piskorz, P.; Komaromi, I.; Gomperts, R.; Martin, R. L.; Fox, D. J.; Keith, T.; Al-Laham, M. A.; Peng, C. Y.; Nanayakkara, A.; Challacombe, M.; Gill, P. M. W.; Johnson, B.; Chen, W.; Wong, M. W.; Andres, J. L.; Gonzalez, C.; Head-Gordon, M.; Pople, J. A. Gaussian. Inc.: Pittsburg, PA, 1998; Gaussian 03, Revision C.02, Frisch, M. J.; Trucks, G. W.; Schlegel, H. B.; Scuseria, G. E.; Robb, M. A.; Cheeseman, J. R.; Montgomery, Jr., J. A.; Vreven, T.; Kudin, K. N.; Burant, J. C.; Millam, J. M.; Iyengar, S. S.; Tomasi, J.; Barone, V.; Mennucci, B.; Cossi, M.; Scalmani, G.; Rega, N.; Petersson, G. A.; Nakatsuji, H.; Hada, M.; Ehara, M.; Toyota, K.; Fukuda, R.; Hasegawa, J.; Ishida, M.; Nakajima, T.; Honda, Y.; Kitao, O.; Nakai, H.; Klene, M.; Li, X.; Knox, J. E.; Hratchian, H. P.; Cross, J. B.; Adamo, C.; Jaramillo, J.; Gomperts, R.; Stratmann, R. E.; Yazyev, O.; Austin, A. J.; Cammi, R.; Pomelli, C.; Ochterski, J. W.; Ayala, P. Y.; Morokuma, K.; Voth, G. A.; Salvador, P.; Dannenberg, J. J.; Zakrzewski, V. G.; Dapprich, S.; Daniels, A. D.; Strain, M. C.; Farkas, O.; Malick, D. K.; Rabuck, A. D.; Raghavachari, K.; Foresman, J. B.; Ortiz, J. V.; Cui, Q.; Baboul, A. G.; Clifford, S.; Cioslowski, J.; Stefanov, B. B.; Liu, G.; Liashenko, A.; Piskorz, P.; Komaromi, I.; Martin, R. L.; Fox, D. J.;

Keith, T.; Al-Laham, M. A.; Peng, C. Y.; Nanayakkara, A.; Challacombe, M.; Gill, P. M. W.; Johnson, B.; Chen, W.; Wong, M. W.; Gonzalez, C.; Pople, J. A. Gaussian, Inc.: Wallingford CT, 2004.

16. (a) Becke, A. D. *J. Chem. Phys.* **1993**, *98*, 5648-5652. (b) Lee, C.; Yang, W.; Parr, R. G.; *Phys. Rev. B* **1988**, *37*, 785-789.
17. Wadt, W. R.; Hay, P. J. *J. Chem. Phys.* **1985**, *82*, 299-310.
18. Hehre, W. J.; Radom, L.; Schleyer, P. v R.; Pople, J. A. *Ab Initio Molecular Orbital Theory*; John Wiley & Sons, Inc.: New York, 1986. References cited therein.
19. Errors of calculated bond lengths such as Ru-Ru, Ru-Cl, Ru-S and Ru-Cp are within 3%.
20. (a) Fukui, K. *Acc. Chem. Res.* **1981**, *14*, 363-368. (b) Gonzalez, C.; Schlegel, H. B. *J. Chem. Phys.* **1989**, *90*, 2154-2161. Gonzalez, C.; Schlegel, H. B. *J. Phys. Chem.* **1990**, *94*, 5523-5527.
21. Reed, A. E.; Weinstock, R. B.; Weinhold, F. *J. Chem. Phys.* **1985**, *83*, 735-746. NBO Version 3.1 in the Gaussian 98 package implemented by Glendening, E. D.; Reed, A. E.; Carpenter, J. E.; Weinhold, F.; University of Wisconsin: Madison, WI, 1990.
22. Bruce, M. I. *Chem. Rev.* **1991**, *91*, 197-257.
23. Wakatsuki, Y.; Koga, N.; Yamazaki, H.; Morokuma, K. *J. Am. Chem. Soc.* **1994**, *116*, 8105-8111.

CHAPTER 8

Summary and Outlook

Transition metal catalysis has owed its development largely to experimental trials and errors. While the development of theoretical methods as well as computational facility has made a significant contribution to the mechanistic understanding of elementary and catalytic reactions of transition metal complexes, the current situation is such that most of theoretical studies just follow experiments, and rarely give new ideas that give a valuable feedback to experimentalists. However, if one considers to design a multi-metallic catalysis, there are far more possibilities of metal/metal and metal/ligand combinations than in a monometallic catalysis, and therefore a close interplay between theory and experiments should become important. The present theoretical/experimental work was carried out to elucidate multi-metallic effects in several organic and organometallic transformations, which will further contribute to catalysis design.

The most typical catalysis with transition metal/main group metal combination would be a transition metal (Ni, Pd, Cu)-catalyzed cross-coupling reaction between an aryl or a vinyl halide with a main group organometallic reagent. This reaction was studied in Chapters 2-4 with a special focus on the process of activation of a C(sp^2)-halogen bond (oxidative addition). First, we studied the mechanism of the oldest cross-coupling reaction – substitution of an alkenyl bromide with a lithium organocuprate (Chapter 2). In addition to a typical three-centered mechanism, we found a new, eliminative mode of C-Br bond cleavage where the Cu and the Li atoms act as a nucleophile and a Lewis acid, respectively. In Chapter 3, the generality of the bimetallic eliminative mechanism of C(sp^2)-X bond cleavage was investigated. Thus, we carried out theoretical study of oxidative addition of aryl/vinyl halides to Ni^0/Pd^0-bisphosphine complexes with or without coordination of magnesium chloride to show that the bimetallic C(sp^2)-X bond

activation is a generally viable mechanism (particularly for X = F). The above basic studies lead to a new design of a cross-coupling reaction (Chapter 4). The combination of a nickel salt, a phosphorus ligand bearing a hydroxy group in close proximity and an organomagnesium reagent was proven to be highly effective for C-F bond activation/C-C bond formation reaction of aryl fluorides.

In Chapters 5-7 we carried out mechanistic studies on catalytic reactions of transition metal clusters with a metal-metal bond, where the only one metal center act as an active site. Chapters 5 and 6 cover the C-H bond insertion reaction between a diazo compound and an alkane catalyzed by dirhodium tetracarboxylate: In the former chapter we focused our attention on the fundamental mechanism as well as the bimetallic cooperation. The spectator Rh atom was found to act as a mobile ligand (in other words, an electron acceptor) to the active site Rh atom. In the latter chapter, we extended the studies to stereoselectivity issues. Diastereo- and enantioselectivities of various cyclization reactions via intramolecular C-H insertion have been successfully explained. In Chapter 7 is studied the propargylic substitution reaction catalyzed by a thiolate-bridged diruthenium complex. The product-substrate ligand exchange step was found to be the most critical step that differentiates a bimetallic and a monometallic complexes. Contrary to the dirhodium catalysis, the spectator Ru atom works as an acceptor from the active site.

In summary, the present study has revealed several types of multi-metallic cooperation at the molecular level, and demonstrated that elaborate control of metal atoms in their spatial alignment is essential for the multi-metallic effect to be exerted efficiently. In future, not only mechanistic studies of known reactions but also computational/experimental trial and error will provide unprecedented reactivity and selectivity in chemical transformations.

Appendix: Energies and Cartesian Coordinates

Chapter 2

1
E(RB+HF-LYP) = -569.516483828 A.U. after 9 cycles

Center Number	Atomic Number	Atomic Type	Coordinates (Angstroms) X	Y	Z
1	29	0	.000000	.000000	1.911935
2	3	0	.000000	1.628017	.000006
3	3	0	.000000	-1.628017	.000006
4	29	0	.000000	.000000	-1.911650
5	6	0	.000000	1.968492	-2.044609
6	6	0	.000000	-1.968492	-2.044609
7	1	0	.000000	2.076705	-3.138470
8	1	0	.000000	-2.076705	-3.138470
9	1	0	-.891184	2.538155	-1.717788
10	1	0	-.891184	-2.538155	-1.717788
11	1	0	.891184	-2.538155	-1.717788
12	1	0	.891184	2.538155	-1.717788
13	6	0	.000000	1.968466	2.044381
14	6	0	.000000	-1.968466	2.044381
15	1	0	.000000	2.078318	3.138009
16	1	0	.000000	-2.078318	3.138009
17	1	0	-.891168	2.537864	1.716631
18	1	0	-.891168	-2.537864	1.716631
19	1	0	.891168	-2.537864	1.716631
20	1	0	.891168	2.537864	1.716631

2
E(RB+HF-LYP) = -2651.86401217 A.U. after 8 cycles

Center Number	Atomic Number	Atomic Type	Coordinates (Angstroms) X	Y	Z
1	6	0	-.442206	-2.092518	.000000
2	6	0	.457436	-1.116639	.000000
3	1	0	-.110050	-3.127663	.000000
4	1	0	-1.511144	-1.905538	.000000
5	1	0	1.529813	-1.274620	.000000
6	35	0	.000000	.730365	.000000

1···2
E(RB+HF-LYP) = -3221.38690756 A.U. after 8 cycles

Center Number	Atomic Number	Atomic Type	Coordinates (Angstroms) X	Y	Z
1	29	0	-.396636	2.123892	.280922
2	3	0	-.037933	-.201078	1.262696
3	3	0	-1.967024	.831081	-1.171879
4	29	0	-2.026092	-1.297952	.123420
5	6	0	-1.235786	-1.848291	1.840873
6	1	0	-1.887986	-2.700380	2.082805
7	1	0	-1.340694	-1.169120	2.706817
8	1	0	-.214962	-2.271659	1.874881
9	6	0	-2.966050	-.937756	-1.577495
10	1	0	-3.464166	-1.906875	-1.722096
11	1	0	-3.794779	-.203074	-1.594882
12	1	0	-2.383349	-.793387	-2.507976
13	6	0	3.482982	1.036386	-.445781
14	6	0	3.512367	-.287853	-.390893
15	35	0	1.930344	-1.370528	-.388353
16	1	0	4.420942	1.586375	-.444860
17	1	0	2.560033	1.606539	-.483392
18	6	0	.519379	1.711417	1.975408
19	6	0	-1.250750	2.767426	-1.380876
20	1	0	.830172	2.720640	2.283680
21	1	0	-.100174	1.346913	2.814829
22	1	0	1.459884	1.128964	1.980588
23	1	0	-.839352	3.786004	-1.421942
24	1	0	-.967070	2.322091	-2.354077
25	1	0	-2.347549	2.920453	-1.400694
26	1	0	4.408121	-.895272	-.347093

TS_{1-3}
E(RB+HF-LYP) = -3221.37210010 A.U. after 9 cycles

Center Number	Atomic Number	Atomic Type	Coordinates (Angstroms) X	Y	Z
1	29	0	0.596436	1.433788	0.438247
2	3	0	-0.321184	-0.981199	0.830653
3	3	0	-1.723030	1.615597	-0.310777
4	29	0	-2.630695	-0.708743	-0.146971
5	6	0	-1.839455	-2.399043	0.486770
6	1	0	-2.691498	-3.077158	0.332214
7	1	0	-1.596590	-2.517121	1.561013
8	1	0	-1.015100	-2.857174	-0.089197
9	6	0	-3.609091	0.876963	-0.798624
10	1	0	-4.587019	0.420810	-1.009108
11	1	0	-3.844149	1.700283	-0.095463
12	1	0	-3.312355	1.342872	-1.757302
13	6	0	2.584603	1.278942	-0.832911
14	6	0	2.642546	0.264209	0.051311
15	35	0	2.112583	-1.525372	-0.423530
16	1	0	3.023929	2.237446	-0.568437
17	1	0	2.221514	1.157923	-1.847182
18	6	0	0.286740	0.499528	2.210758
19	6	0	-0.123340	2.917160	-0.740787
20	1	0	0.752393	1.273785	2.838952
21	1	0	-0.746086	0.417927	2.586794
22	1	0	0.809470	-0.432208	2.505861
23	1	0	0.688807	3.654880	-0.704243
24	1	0	-0.273021	2.704932	-1.812987
25	1	0	-1.006137	3.503637	-0.409686
26	1	0	3.109580	0.301165	1.026575

3
E(RB+HF-LYP) = -3221.37797512 A.U. after 29 cycles

Center Number	Atomic Number	Atomic Type	Coordinates (Angstroms) X	Y	Z
1	29	0	.740043	1.422322	.221710
2	3	0	-.274510	-1.060637	.608260
3	3	0	-1.677364	1.505257	.135746
4	29	0	-2.621656	-.778817	-.173425
5	6	0	-1.741865	-2.515831	.138788
6	1	0	-2.597297	-3.187683	-.025938
7	1	0	-1.388781	-2.786063	1.154513
8	1	0	-.972987	-2.860760	-.574391
9	6	0	-3.615339	.896350	-.473299
10	1	0	-4.611697	.496972	-.713114
11	1	0	-3.802770	1.580663	.378192
12	1	0	-3.349308	1.524680	-1.341858
13	6	0	2.475816	1.311772	-.850160
14	6	0	2.477061	.377760	.179816
15	35	0	2.187337	-1.520234	-.204229
16	1	0	3.019750	2.244826	-.714740
17	1	0	2.236453	1.038550	-1.873394
18	6	0	-.213675	.756628	1.925307
19	6	0	-.289324	2.933324	-.659811
20	1	0	.333886	1.486252	2.543845
21	1	0	-1.279091	.947904	2.142970
22	1	0	-.002086	-.206721	2.427647
23	1	0	.459844	3.724098	-.783275
24	1	0	-.676569	2.733447	-1.671129
25	1	0	-1.104819	3.430710	-.094675
26	1	0	3.045045	.485754	1.097219

TS_{3-4}
E(RB+HF-LYP) = -3221.34373671 A.U. after 12 cycles

Center Number	Atomic Number	Atomic Type	Coordinates (Angstroms) X	Y	Z
1	6	0	-3.557256	-0.859054	0.404995
2	6	0	-2.545671	-0.212155	0.998847
3	1	0	-4.392163	-1.242108	0.993024
4	1	0	-3.590683	-1.046334	-0.666420
5	35	0	-1.709281	1.537310	-0.532305
6	1	0	-2.506833	0.181729	2.008669
7	6	0	0.010099	-0.914483	1.818467
8	29	0	-1.078192	-1.068792	0.081048
9	1	0	-0.544504	-1.632585	2.433824
10	1	0	1.068387	-1.217223	1.837640
11	1	0	-0.052019	0.055583	2.335980
12	6	0	-0.316048	-2.236700	-1.373733
13	3	0	1.333523	-1.643278	-0.227669
14	1	0	0.167580	-3.190426	-1.091177
15	1	0	0.311526	-1.760237	-2.145076
16	1	0	-1.227095	-2.542796	-1.902904
17	3	0	0.517170	1.206728	0.469351
18	29	0	2.826024	0.336446	0.005617
19	6	0	2.368971	2.190456	0.489982
20	6	0	3.415999	-1.493590	-0.437668
21	1	0	3.374709	2.634646	0.510578
22	1	0	1.963132	2.407566	1.498076
23	1	0	1.807373	2.812981	-0.229991
24	1	0	4.504103	-1.343775	-0.487944
25	1	0	3.294234	-2.299203	0.314000
26	1	0	3.151323	-1.922845	-1.421261

TS_{3-5}
E(RB+HF-LYP) = -3221.34922948 A.U. after 10 cycles

Center Number	Atomic Number	Atomic Type	Coordinates (Angstroms) X	Y	Z
1	6	0	-2.189523	.780716	1.749598
2	6	0	-2.408793	.562965	.431989
3	1	0	-2.990578	1.048887	2.441215
4	1	0	-1.223294	.595770	2.224716
5	35	0	-1.871650	-1.930936	-.415202
6	1	0	-3.374473	.529180	-.059712
7	6	0	-.618461	1.286671	-1.784182
8	29	0	-.949296	1.708735	.115944
9	1	0	-1.550844	1.608850	-2.256324
10	1	0	.199102	1.868837	-2.234608
11	1	0	-.492638	.212479	-1.929762
12	6	0	.390769	3.127784	.536802
13	3	0	1.405416	1.537894	-.547330
14	1	0	.956900	3.576881	-.298773
15	1	0	1.100966	2.892034	1.345368
16	1	0	-.242545	3.938744	.916713
17	6	0	3.298368	.832977	-.953587
18	3	0	.371027	-2.011922	.220669
19	1	0	3.499041	1.812691	-.478444
20	1	0	2.897935	1.033242	-1.965915
21	1	0	4.298895	.418615	-1.141931
22	29	0	2.561985	-.645769	.124622
23	6	0	2.156052	-2.211036	1.247326
24	1	0	3.118806	-2.288447	1.772629
25	1	0	2.031873	-3.202906	.770496
26	1	0	1.410814	-2.146497	2.062312

4
E(RB+HF-LYP) = -3221.40656091 A.U. after 12 cycles

Center Number	Atomic Number	Atomic Type	Coordinates (Angstroms) X	Y	Z
1	6	0	1.829755	2.490122	-.803805
2	6	0	1.456250	1.317893	-1.350733
3	1	0	1.922395	3.404245	-1.395709
4	1	0	2.091776	2.587391	.250057
5	35	0	.670517	.470465	1.775584
6	1	0	1.244501	1.338190	-2.424724
7	6	0	1.853750	-1.208948	-2.200400
8	29	0	1.406907	-.451783	-.455069
9	1	0	2.708483	-.637814	-2.565249
10	1	0	2.077572	-2.270535	-2.121180
11	1	0	.964526	-1.025763	-2.806660
12	6	0	1.371719	-2.328349	.237412
13	3	0	-.689475	-1.439062	.870677
14	1	0	.741425	-3.008523	-.350126
15	1	0	1.126902	-2.405871	1.309213
16	1	0	2.402906	-2.683460	.146740
17	3	0	-.466953	1.666599	-.144040
18	29	0	-2.386848	-.019686	-.341142
19	6	0	-2.417212	1.873325	-.894196
20	6	0	-2.592646	-1.915188	.186813
21	1	0	-3.462675	1.957465	-1.224735
22	1	0	-1.826080	2.200314	-1.768644
23	1	0	-2.323958	2.661368	-.119427
24	1	0	-3.624390	-2.084189	-.153307
25	1	0	-2.006826	-2.701098	-.325301
26	1	0	-2.626765	-2.181130	1.263277

TS_{4-5}
E(RB+HF-LYP) = -3221.39184136 A.U. after 12 cycles

Center Number	Atomic Number	Atomic Type	Coordinates (Angstroms) X	Y	Z
1	6	0	1.815020	2.458400	.473293
2	6	0	1.401975	1.715350	-.570836
3	1	0	1.507724	3.500580	.580513
4	1	0	2.483807	2.072616	1.239475
5	35	0	.439739	-.674388	1.865869
6	1	0	.764930	2.174187	-1.328414
7	6	0	2.699487	.630536	-1.821062
8	29	0	1.355894	-.224727	-.586643
9	1	0	3.555780	.137626	-1.353794
10	1	0	2.340916	.100210	-2.705028
11	1	0	2.953370	1.655952	-2.075164
12	6	0	1.241461	-2.133274	-1.238146
13	3	0	-.680227	-1.714365	-.196876
14	1	0	.740415	-2.259443	-2.210756
15	1	0	.890254	-2.948282	-.575477
16	1	0	2.294658	-2.395522	-1.411583
17	3	0	-.520727	1.356399	.958634
18	29	0	-2.307373	.268992	-.454590
19	6	0	-2.286980	2.151588	.160700
20	6	0	-2.584862	-1.575810	-1.092681
21	1	0	-3.269158	2.477074	-.211458
22	1	0	-1.574856	2.874833	-.276970
23	1	0	-2.339908	2.363404	1.248834
24	1	0	-3.603132	-1.487464	-1.498842
25	1	0	-1.984437	-1.960230	-1.936237
26	1	0	-2.672091	-2.392496	-.347655

5
E(RB+HF-LYP) = -3103.57107551 A.U. after 9 cycles

Center Number	Atomic Number	Atomic Type	Coordinates (Angstroms) X	Y	Z
1	29	0	-2.413127	-.394886	.000132
2	3	0	-.157026	-1.596150	-.004524
3	3	0	-1.075028	1.763114	-.001020
4	29	0	1.341927	1.060554	.001261
5	35	0	2.176988	-1.111675	-.001523
6	6	0	.694239	2.892409	.003047
7	1	0	1.642407	3.445779	.006328
8	1	0	.155995	3.258272	.896323
9	1	0	.161034	3.260171	-.892467
10	6	0	-2.072423	-2.336305	.005148
11	6	0	-3.105238	1.452596	-.005128
12	1	0	-3.114999	-2.684480	.012360
13	1	0	-1.623846	-2.817357	.895652
14	1	0	-1.634453	-2.821864	-.888189
15	1	0	-4.179849	1.221320	-.011157
16	1	0	-2.965125	2.095560	-.895465
17	1	0	-2.974253	2.093759	.887786

6
E(RB+HF-LYP) = -117.907556178 A.U. after 7 cycles

Center Number	Atomic Number	Atomic Type	Coordinates (Angstroms) X	Y	Z
1	6	0	-1.283135	.220350	-.000002
2	6	0	-.133770	-.455420	-.000029
3	1	0	-2.245236	-.285016	.000077
4	1	0	-1.305930	1.308600	-.000009
5	1	0	-.163956	-1.546185	.000023
6	6	0	1.235047	.162879	-.000006
7	1	0	1.812473	-.150773	-.880220
8	1	0	1.181605	1.256813	-.000290
9	1	0	1.812191	-.150292	.880639

3·$2Me_2O$
E(RB+HF-LYP) = -3531.46592459 A.U. after 1 cycles

Center Number	Atomic Number	Atomic Type	Coordinates (Angstroms) X	Y	Z
1	29	0	0.224087	-1.550845	-0.126618
2	3	0	-1.036046	0.956883	0.054385
3	3	0	2.170655	0.000961	-0.151509
4	29	0	0.805363	1.774114	-1.471620
5	6	0	-1.076309	1.699321	-2.038887
6	1	0	-0.963760	2.107835	-3.056310
7	1	0	-1.840805	2.338661	-1.564447
8	1	0	-1.536862	0.708200	-2.187613
9	6	0	2.708098	2.003157	-1.041476
10	1	0	2.941577	2.883174	-1.662319
11	1	0	2.951629	2.309767	-0.009975
12	1	0	3.458186	1.252555	-1.350560
13	6	0	-1.077635	-2.969640	-0.852299
14	6	0	-1.626922	-2.333107	0.251603
15	35	0	-3.071270	-1.036866	0.034557
16	1	0	-0.600607	-3.939298	-0.723610
17	1	0	-1.353396	-2.698730	-1.866900
18	6	0	0.403779	-0.299791	1.495455
19	6	0	1.756808	-1.888769	-1.416247
20	1	0	0.841983	-1.025343	2.199417
21	1	0	1.046809	0.595003	1.564185
22	1	0	-0.543807	-0.004653	1.973146
23	1	0	1.999703	-2.958349	-1.323437
24	1	0	1.364953	-1.746284	-2.432242
25	1	0	2.739964	-1.383652	-1.416211
26	1	0	-1.665714	-2.769047	1.243821
27	6	0	4.785798	0.331864	1.474185
28	8	0	3.754902	-0.512598	0.971988
29	6	0	3.834458	-1.837201	1.492928
30	1	0	5.773924	-0.082814	1.232696
31	1	0	4.698933	0.444467	2.563929
32	1	0	4.672012	1.302738	0.991201
33	1	0	3.710305	-1.832256	2.584669
34	1	0	4.802871	-2.290171	1.240857
35	1	0	3.030424	-2.410949	1.030816
36	6	0	-2.596055	2.131345	2.383656
37	8	0	-1.788125	2.351278	1.231300
38	6	0	-1.296276	3.689452	1.149450
39	1	0	-3.461291	2.807686	2.380057
40	1	0	-2.015459	2.290369	3.302467

41	1	0	-2.943123	1.097678	2.341571
42	1	0	-0.679876	3.926515	2.026989
43	1	0	-2.131437	4.399625	1.087262
44	1	0	-0.689215	3.750023	0.244806

TS$_{3-4}$ · 2Me$_2$O
E(RB+HF-LYP) = -3531.43719786 A.U. after 13 cycles

Center Number	Atomic Number	Atomic Type	Coordinates (Angstroms) X	Y	Z
1	6	0	-0.585064	-3.817169	-0.085829
2	6	0	-0.882857	-2.729154	0.648574
3	1	0	-0.433719	-4.786455	0.390327
4	1	0	-0.485966	-3.786535	-1.168482
5	35	0	-2.484040	-1.357891	-0.564886
6	1	0	-1.185285	-2.708523	1.690377
7	6	0	0.449517	-0.540590	1.595407
8	29	0	0.409135	-1.553590	-0.167627
9	1	0	0.928751	-1.223764	2.307325
10	1	0	0.995699	0.413766	1.606313
11	1	0	-0.569519	-0.334286	1.936663
12	6	0	1.674808	-1.168075	-1.681219
13	3	0	2.130866	0.372101	-0.165988
14	1	0	2.697784	-1.558021	-1.571896
15	1	0	1.744636	-0.156568	-2.114667
16	1	0	1.211550	-1.761114	-2.483082
17	3	0	-1.618345	0.990103	-0.206740
18	29	0	0.467190	2.314827	-1.011506
19	6	0	-1.314811	2.335303	-1.843598
20	6	0	2.304539	2.563348	-0.355218
21	1	0	-1.104764	3.001055	-2.694767
22	1	0	-2.161048	2.815218	-1.319792
23	1	0	-1.699210	1.410529	-2.309460
24	1	0	2.393859	3.653431	-0.485186
25	1	0	2.547897	2.391765	0.707922
26	1	0	3.133647	2.151249	-0.959985
27	6	0	5.017131	0.561809	0.885676
28	8	0	3.826022	-0.208619	0.735695
29	6	0	4.008422	-1.562758	1.145669
30	1	0	5.823154	0.149542	0.263563
31	1	0	5.339033	0.568599	1.935784
32	1	0	4.787649	1.578395	0.566277
33	1	0	4.299271	-1.605671	2.203896
34	1	0	4.782286	-2.049599	0.536977
35	1	0	3.056180	-2.074477	1.004363
36	6	0	-3.583846	1.233112	2.056114
37	8	0	-2.452151	1.768093	1.371116
38	6	0	-2.039791	3.034544	1.883546
39	1	0	-4.446562	1.904962	1.954350
40	1	0	-3.356120	1.094834	3.121549
41	1	0	-3.807073	0.268943	1.597340
42	1	0	-1.756106	2.944783	2.940590
43	1	0	-2.847441	3.771918	1.784316
44	1	0	-1.177408	3.351729	1.294246

TS$_{3-5}$ · 2Me$_2$O
E(RB+HF-LYP) = -3531.44333047 A.U. after 7 cycles

Center Number	Atomic Number	Atomic Type	Coordinates (Angstroms) X	Y	Z
1	6	0	0.433525	-2.889716	1.573276
2	6	0	0.422036	-2.858058	0.219923
3	1	0	0.545194	-3.820906	2.132689
4	1	0	0.442059	-1.983202	2.180595
5	35	0	2.385367	-1.540341	-0.969156
6	1	0	0.597606	-3.702741	-0.436572
7	6	0	-1.212222	-1.143155	-1.495517
8	29	0	-1.142868	-1.820243	0.358567
9	1	0	-0.702725	-1.864943	-2.132757
10	1	0	-2.258879	-1.038730	-1.801928
11	1	0	-0.657960	-0.198217	-1.558084
12	6	0	-2.842037	-1.228269	1.232414
13	3	0	-2.226732	0.510980	-0.064497
14	1	0	-3.715573	-1.249594	0.566484
15	1	0	-2.845746	-0.279328	1.796936
16	1	0	-3.004858	-2.005176	1.990346
17	6	0	-1.471914	2.540330	0.321117
18	3	0	2.146109	0.508199	0.285861
19	1	0	-2.501315	2.544677	0.722997
20	1	0	-1.551203	2.526659	-0.779805
21	1	0	-1.090406	3.547566	0.553057
22	29	0	-0.062406	1.511525	1.232434
23	6	0	1.393295	0.775838	2.334351
24	1	0	0.866078	0.664180	3.295372
25	1	0	2.217282	1.479925	2.541287
26	1	0	1.859307	-0.213361	2.175694
27	6	0	-3.824170	1.531723	-2.392171
28	8	0	-3.903651	0.918398	-1.105959
29	6	0	-5.089860	1.288328	-0.403327
30	1	0	-3.790621	2.625268	-2.302138
31	1	0	-4.686747	1.240741	-3.005633
32	1	0	-2.908006	1.173753	-2.865718
33	1	0	-5.978658	0.994024	-0.976367
34	1	0	-5.113964	2.371215	-0.222290
35	1	0	-5.080866	0.754461	0.548531
36	6	0	4.253887	1.700893	-1.411754
37	8	0	3.313823	1.918307	-0.358188
38	6	0	3.329237	3.256393	0.131120
39	1	0	5.276379	1.883984	-1.055364
40	1	0	4.038230	2.367963	-2.257146
41	1	0	4.145278	0.660477	-1.721467
42	1	0	3.095084	3.963217	-0.676394
43	1	0	4.313270	3.502103	0.552946
44	1	0	2.566702	3.323733	0.908661

1-Bromocyclooctene
E(RB+HF-LYP) = -2886.53736142 A.U. after 7 cycles

Center Number	Atomic Number	Atomic Type	Coordinates (Angstroms) X	Y	Z
1	6	0	-.072224	-1.223951	.370934
2	6	0	.540179	-.039757	.296197
3	6	0	.074208	1.372719	.542743
4	1	0	.520540	-2.095969	.105242
5	35	0	2.422245	-.069894	-.210986
6	6	0	-1.506383	-1.534323	.753075
7	6	0	-1.440235	1.635390	.612010
8	1	0	.490589	1.996694	-.258737
9	1	0	.549845	1.736716	1.465020
10	6	0	-2.530739	-1.354476	-.397376
11	1	0	-1.825676	-.957836	1.627520
12	1	0	-1.522424	-2.583463	1.069977
13	1	0	-2.044454	-1.606861	-1.349045
14	6	0	-3.178764	.034532	-.498666
15	1	0	-3.337311	-2.087277	-.262767
16	1	0	-1.874044	1.159845	1.498100
17	6	0	-2.238338	1.242233	-.658346
18	1	0	-1.545704	2.713837	.784083
19	1	0	-3.807134	.198890	.389611
20	1	0	-3.867918	.017544	-1.353866
21	1	0	-2.854774	2.097463	-.961616
22	1	0	-1.546317	1.062510	-1.492423

3 (1-bromocyclooctene)
E(RB+HF-LYP) = -3456.04546398 A.U. after 1 cycles

Center Number	Atomic Number	Atomic Type	Coordinates (Angstroms) X	Y	Z
1	6	0	-1.710245	-0.436488	-0.948284
2	6	0	-1.444369	0.538623	0.007969
3	6	0	-2.151493	0.985683	1.274276
4	1	0	-1.309276	-0.259041	-1.943798
5	35	0	-0.359527	2.083175	-0.710606
6	6	0	-2.777979	-1.520687	-0.908352
7	6	0	-3.393729	0.196656	1.730957
8	1	0	-2.465156	2.027875	1.129500
9	1	0	-1.420599	1.010264	2.091615
10	6	0	-4.210405	-1.039167	-1.254905
11	1	0	-2.791583	-2.040580	0.054870
12	1	0	-2.464033	-2.271177	-1.641420
13	1	0	-4.156656	-0.159252	-1.910793
14	6	0	-5.100842	-0.733836	-0.042328
15	1	0	-4.704767	-1.824645	-1.840792
16	1	0	-3.168449	-0.870988	1.831459
17	6	0	-4.667374	0.419769	0.875261
18	1	0	-3.594540	0.546238	2.751085
19	6	0	0.996126	-0.469246	1.889788
20	1	0	-5.201261	-1.648948	0.560726
21	1	0	-6.109565	-0.508023	-0.413562
22	1	0	-5.504184	0.621118	1.555647
23	29	0	-0.019997	-0.966326	0.148134
24	1	0	-4.548623	1.334361	0.276734
25	6	0	0.581937	-2.721577	-0.696087
26	3	0	2.245699	-1.792122	0.286118
27	6	0	4.345511	-1.919712	-0.044664
28	3	0	1.742303	1.067808	0.451167
29	29	0	3.940699	0.008264	-0.009133
30	6	0	3.633017	1.954971	0.069344
31	1	0	0.227636	-0.966469	2.504100
32	1	0	1.948804	-0.920804	2.218401
33	1	0	1.026197	0.557350	2.305996
34	1	0	1.168392	-3.449095	-0.095989
35	1	0	1.093445	-2.637019	-1.668337
36	1	0	-0.351288	-3.259325	-0.901251
37	1	0	3.994310	-2.523504	-0.900142
38	1	0	4.176504	-2.522100	0.870329
39	1	0	5.440464	-1.899212	-0.147610
40	1	0	4.666016	2.317689	-0.038343
41	1	0	3.288346	2.420691	1.014700
42	1	0	3.078030	2.440288	-0.752624

Chapter 3

$2a_{vb}$

SCF Done: E(RB+HF-LYP) = -3584.93781345 A.U. after 18 cycles

Center Number	Atomic Number	Atomic Type	Coordinates (Angstroms) X	Y	Z
1	6	0	-1.151208	-1.836160	0.541747
2	6	0	-1.592839	-0.536141	0.848534
3	1	0	-1.802667	-0.208121	1.861726
4	1	0	-1.414326	-2.310460	-0.400613
5	35	0	-2.769595	0.410108	-0.400667
6	1	0	-0.933461	-2.516996	1.365255
7	28	0	0.265754	-0.472676	0.298290
8	15	0	1.147732	1.555896	0.379694
9	15	0	2.206034	-1.278291	-0.391744
10	6	0	3.011088	1.351638	0.187132
11	6	0	3.315809	0.194903	-0.782237
12	1	0	0.879367	2.493747	-0.651910
13	1	0	1.111123	2.486091	1.450818
14	1	0	3.038294	-1.999515	0.505779
15	1	0	2.463685	-2.090499	-1.526407
16	1	0	3.491517	2.278601	-0.141725
17	1	0	3.401594	1.116678	1.185044
18	1	0	4.376765	-0.073666	-0.756687
19	1	0	3.079242	0.495778	-1.810386

$2a_{vc}$

SCF Done: E(RB+HF-LYP) = -1471.25731391 A.U. after 9 cycles

Center Number	Atomic Number	Atomic Type	Coordinates (Angstroms) X	Y	Z
1	28	0	0.247961	-0.371959	-0.243714
2	15	0	-0.801974	1.572124	-0.267575
3	15	0	-1.656232	-1.385109	0.243893
4	6	0	-2.649998	1.209194	-0.191870
5	6	0	-2.906352	-0.039677	0.671479
6	1	0	-0.663134	2.457456	0.833689
7	1	0	-0.789468	2.571722	-1.274927
8	1	0	-2.371786	-2.092372	-0.759561
9	1	0	-1.915789	-2.304536	1.293201
10	6	0	2.156564	-0.216809	-0.606573
11	17	0	3.049397	0.697721	0.663326
12	6	0	1.819106	-1.566098	-0.395265
13	1	0	2.405046	0.174562	-1.588712
14	1	0	2.050879	-2.057200	0.547021
15	1	0	1.739087	-2.220832	-1.262715
16	1	0	-3.219717	2.067605	0.177957
17	1	0	-2.971820	1.023837	-1.224212
18	1	0	-3.937620	-0.390648	0.563455
19	1	0	-2.751152	0.199121	1.730881

$2a_{vf}$

SCF Done: E(RB+HF-LYP) = -1110.88718376 A.U. after 9 cycles

Center Number	Atomic Number	Atomic Type	Coordinates (Angstroms) X	Y	Z
1	28	0	0.545777	-0.234770	-0.150018
2	15	0	-0.700531	1.571947	-0.111048
3	15	0	-1.261899	-1.487421	0.079865
4	6	0	-2.500819	1.020142	-0.228689
5	6	0	-2.687723	-0.324028	0.497864
6	1	0	-0.752349	2.366150	1.066432
7	1	0	-0.725383	2.659101	-1.024869
8	1	0	-1.807861	-2.158407	-1.048581
9	1	0	-1.525701	-2.527529	1.010353
10	6	0	2.464007	0.190602	-0.307748
11	9	0	2.915185	0.873383	0.806016
12	6	0	2.284172	-1.194367	-0.233017
13	1	0	2.744699	0.713379	-1.220584
14	1	0	2.492267	-1.722057	0.695504
15	1	0	2.351269	-1.781768	-1.146756
16	1	0	-3.186131	1.779014	0.162342
17	1	0	-2.719508	0.902131	-1.297381
18	1	0	-3.660398	-0.768376	0.263620
19	1	0	-2.650692	-0.170505	1.583556

$2a_{vo}$

SCF Done: E(RB+HF-LYP) = -1126.17565116 A.U. after 8 cycles

Center Number	Atomic Number	Atomic Type	Coordinates (Angstroms) X	Y	Z
1	6	0	2.209169	-0.535215	-0.466166
2	8	0	2.972252	-0.005348	0.568993
3	6	0	1.648371	-1.807730	-0.310952
4	1	0	2.473164	-0.149422	-1.455005
5	1	0	1.787981	-2.348831	0.622899
6	1	0	1.471971	-2.415118	-1.196299
7	6	0	3.249075	1.372265	0.443173
8	1	0	2.332355	1.976727	0.523706
9	1	0	3.734870	1.600798	-0.518880
10	1	0	3.929873	1.637725	1.255872
11	28	0	0.209510	-0.440801	-0.151142
12	15	0	-0.652099	1.570083	-0.209442
13	15	0	-1.787942	-1.292146	0.226017
14	6	0	-2.528169	1.364766	-0.299691
15	6	0	-2.963334	0.151050	0.538830
16	1	0	-0.558834	2.440943	0.913036
17	1	0	-0.494232	2.589003	-1.189252
18	1	0	-2.486302	-1.957430	-0.819766
19	1	0	-2.213426	-2.169481	1.260231
20	1	0	-3.051380	2.273532	0.015075
21	1	0	-2.769464	1.196489	-1.356750
22	1	0	-4.005632	-0.117002	0.337955
23	1	0	-2.885306	0.387420	1.607415

$2a_{vs}$

SCF Done: E(RB+HF-LYP) = -1449.16156263 A.U. after 10 cycles

Center Number	Atomic Number	Atomic Type	Coordinates (Angstroms) X	Y	Z
1	6	0	-1.888352	-0.705896	0.670664
2	16	0	-3.076305	-0.097162	-0.534755
3	6	0	-1.263660	-1.951682	0.449203
4	1	0	-2.091489	-0.386839	1.693840
5	1	0	-1.418185	-2.489726	-0.485116
6	1	0	-0.999621	-2.573983	1.303516
7	6	0	-2.992473	1.704047	-0.262009
8	1	0	-2.016349	2.104213	-0.552697
9	1	0	-3.192450	1.952601	0.785142
10	1	0	-3.768294	2.159604	-0.883878
11	28	0	0.038477	-0.479515	0.196111
12	15	0	0.841499	1.570564	0.266611
13	15	0	2.038502	-1.243826	-0.308850
14	6	0	2.722557	1.414654	0.269772
15	6	0	3.154049	0.242236	-0.628067
16	1	0	0.673439	2.471637	-0.821923
17	1	0	0.691929	2.548870	1.286448
18	1	0	2.803970	-1.933010	0.670875
19	1	0	2.415194	-2.070917	-1.400069
20	1	0	3.206341	2.347757	-0.036373
21	1	0	3.014992	1.219250	1.308997
22	1	0	4.212053	0.000777	-0.484035
23	1	0	3.019277	0.509540	-1.683549

$3a_{vb}$

SCF Done: E(RB+HF-LYP) = -3584.91344995 A.U. after 19 cycles

Center Number	Atomic Number	Atomic Type	Coordinates (Angstroms) X	Y	Z
1	6	0	-1.763846	0.864756	1.985130
2	6	0	-1.572223	1.199293	0.686446
3	1	0	-1.797347	2.153561	0.219829
4	1	0	-1.784097	-0.168067	2.319177
5	35	0	-2.116883	-0.492389	-0.766921
6	1	0	-1.944439	1.630771	2.738826
7	28	0	-0.066683	0.164554	0.414150
8	15	0	1.472738	1.446125	-0.634825
9	15	0	1.489857	-1.439379	0.704237
10	6	0	3.122686	0.565423	-0.401806
11	6	0	2.927981	-0.961063	-0.409251
12	1	0	1.889607	2.776766	-0.357809
13	1	0	2.170462	-1.642096	1.934009
14	1	0	1.352087	-2.808373	0.365993
15	1	0	3.851012	0.867809	-1.160803
16	1	0	3.512036	0.889198	0.571336
17	1	0	3.850146	-1.476244	-0.121774
18	1	0	2.662243	-1.301092	-1.417534
19	1	0	1.469798	1.592214	-2.049525

$3a_{vc}$

SCF Done: E(RB+HF-LYP) = -1471.22354226 A.U. after 10 cycles

Center Number	Atomic Number	Atomic Type	Coordinates (Angstroms) X	Y	Z
1	6	0	-2.445367	0.177836	1.604892
2	6	0	-2.083693	0.816613	0.469493
3	1	0	-2.350188	1.824009	0.165636
4	1	0	-2.374462	-0.901753	1.702878
5	17	0	-2.200449	-0.484801	-1.284706

6	1	0	-2.849275	0.727659	2.454042
7	28	0	-0.461136	-0.019343	0.213522
8	15	0	1.065741	1.577722	-0.232822
9	15	0	1.200335	-1.544958	0.363057
10	6	0	2.751709	0.776050	0.028918
11	6	0	2.713740	-0.708389	-0.374359
12	1	0	1.299945	2.815942	0.424239
13	1	0	1.728932	-1.991837	1.602810
14	1	0	1.253521	-2.796378	-0.299364
15	1	0	3.538283	1.307282	-0.516225
16	1	0	2.976050	0.868824	1.098735
17	1	0	3.638256	-1.217876	-0.084390
18	1	0	2.615252	-0.800066	-1.462855
19	1	0	1.233637	2.083301	-1.551328

$3a_{vf}$

SCF Done: E(RB+HF-LYP) = -1110.82715329 A.U. after 11 cycles

Center Number	Atomic Number	Atomic Type	Coordinates (Angstroms) X	Y	Z
1	6	0	-2.827782	0.342134	1.245729
2	6	0	-2.353117	0.524296	-0.002128
3	1	0	-2.705501	1.267733	-0.710115
4	1	0	-2.543930	-0.515881	1.849555
5	9	0	-2.212544	-0.926465	-0.916348
6	1	0	-3.497301	1.072575	1.694884
7	28	0	-0.603672	-0.169460	-0.183090
8	15	0	0.726287	1.567314	-0.237799
9	15	0	1.208553	-1.521430	0.256398
10	6	0	2.420955	1.020365	0.372488
11	6	0	2.703203	-0.425155	-0.074539
12	1	0	0.566327	2.766855	0.502624
13	1	0	1.493003	-1.933187	1.586025
14	1	0	1.650463	-2.717783	-0.367691
15	1	0	3.212915	1.696467	0.034975
16	1	0	2.388243	1.075133	1.467546
17	1	0	3.602417	-0.816497	0.411258
18	1	0	2.875975	-0.456924	-1.157335
19	1	0	1.090943	2.186455	-1.466372

$3a_{vo}$

SCF Done: E(RB+HF-LYP) = -1126.11167883 A.U. after 10 cycles

Center Number	Atomic Number	Atomic Type	Coordinates (Angstroms) X	Y	Z
1	6	0	2.420781	-1.378687	1.164747
2	6	0	1.982314	-1.101234	-0.085381
3	1	0	2.240873	-1.706412	-0.949704
4	1	0	2.189562	-0.751899	2.022833
5	8	0	2.138448	0.526808	-0.751757
6	1	0	3.011353	-2.272342	1.358158
7	28	0	0.401673	-0.040763	-0.257421
8	15	0	-1.237795	-1.490611	-0.295657
9	15	0	-1.163336	1.609451	0.260211
10	6	0	-2.779661	-0.693269	0.426891
11	6	0	-2.839285	0.785948	0.006203
12	1	0	-1.229262	-2.729175	0.391991
13	1	0	-1.315288	2.044250	1.605442
14	1	0	-1.438527	2.873225	-0.328759
15	1	0	-3.692385	-1.222535	0.135060
16	1	0	-2.689511	-0.770053	1.517438
17	1	0	-3.631134	1.316185	0.544126
18	1	0	-3.063753	0.863425	-1.064961
19	1	0	-1.763500	-1.980449	-1.523806
20	6	0	2.858174	1.451542	0.040840
21	1	0	3.577047	1.962951	-0.612750
22	1	0	3.410383	0.927639	0.835102
23	1	0	2.202729	2.203676	0.503585

$3a_{vs}$

SCF Done: E(RB+HF-LYP) = -1449.12420749 A.U. after 10 cycles

Center Number	Atomic Number	Atomic Type	Coordinates (Angstroms) X	Y	Z
1	6	0	2.004000	-1.640436	1.362636
2	6	0	1.619465	-1.475951	0.077779
3	1	0	1.757136	-2.262049	-0.662566
4	1	0	1.948607	-0.840106	2.098552
5	16	0	2.154800	0.424980	-0.984104
6	1	0	2.384520	-2.596011	1.723331
7	28	0	0.236046	-0.187164	-0.061131
8	15	0	-1.633610	-1.408872	-0.345958
9	15	0	-1.108813	1.608588	0.440652
10	6	0	-3.101845	-0.357878	0.189688
11	6	0	-2.835303	1.123222	-0.133540
12	1	0	-1.964596	-2.638707	0.279385
13	1	0	-1.403162	2.007246	1.773782
14	1	0	-1.025527	2.916723	-0.100045
15	1	0	-4.035593	-0.697286	-0.269571
16	1	0	-3.203158	-0.492555	1.273744
17	1	0	-3.603246	1.766320	0.307595
18	1	0	-2.857752	1.281875	-1.218665
19	1	0	-2.057733	-1.780182	-1.651305
20	6	0	3.045412	1.370881	0.304555
21	1	0	3.924106	1.828903	-0.159195
22	1	0	3.378481	0.681993	1.088975
23	1	0	2.417808	2.149975	0.746217

$4a_{vb}$

SCF Done: E(RB+HF-LYP) = -3584.94722529 A.U. after 18 cycles

Center Number	Atomic Number	Atomic Type	Coordinates (Angstroms) X	Y	Z
1	28	0	-0.141771	0.265602	-0.056637
2	15	0	1.793106	1.225175	-0.157918
3	15	0	0.982722	-1.727087	0.179821
4	6	0	3.170832	0.012904	0.249631
5	6	0	2.788047	-1.400990	-0.230296
6	1	0	2.187424	1.755255	-1.407112
7	1	0	2.092809	2.334508	0.658738
8	1	0	1.063385	-2.335723	1.454858
9	1	0	0.695365	-2.880703	-0.579605
10	6	0	-0.882250	1.985565	-0.351055
11	35	0	-2.262719	-0.752545	-0.003867
12	6	0	-0.904342	3.036584	0.474102
13	1	0	-1.397961	2.039683	-1.312793
14	1	0	-0.423427	3.032354	1.452183
15	1	0	-1.459194	3.944130	0.230566
16	1	0	4.129472	0.332907	-0.171470
17	1	0	3.274603	0.024338	1.341584
18	1	0	3.457414	-2.156043	0.193189
19	1	0	2.873744	-1.464192	-1.321803

$4a_{vc}$

SCF Done: E(RB+HF-LYP) = -1471.26144763 A.U. after 10 cycles

Center Number	Atomic Number	Atomic Type	Coordinates (Angstroms) X	Y	Z
1	28	0	-0.542240	-0.078676	-0.042997
2	15	0	0.874862	1.543254	-0.167625
3	15	0	1.269832	-1.494187	0.191811
4	6	0	2.613727	0.956616	0.236274
5	6	0	2.803029	-0.497637	-0.239092
6	1	0	1.029364	2.162587	-1.428161
7	1	0	0.733438	2.695454	0.632154
8	1	0	1.595075	-2.022284	1.463940
9	1	0	1.437800	-2.671604	-0.567128
10	6	0	-1.884172	1.224360	-0.339274
11	17	0	-2.033359	-1.734182	-0.024097
12	6	0	-2.287134	2.206647	0.471536
13	1	0	-2.413467	1.035299	-1.275853
14	1	0	-1.807936	2.422989	1.426113
15	1	0	-3.162483	2.816006	0.240402
16	1	0	3.373931	1.619178	-0.190350
17	1	0	2.709336	1.011095	1.327672
18	1	0	3.716840	-0.932929	0.176827
19	1	0	2.894812	-0.527700	-1.331516

$4a_{vf}$

SCF Done: E(RB+HF-LYP) = -1110.87125201 A.U. after 9 cycles

Center Number	Atomic Number	Atomic Type	Coordinates (Angstroms) X	Y	Z
1	28	0	-0.632695	-0.467523	-0.053605
2	15	0	0.236192	1.533235	-0.166520
3	15	0	1.593436	-1.233407	0.196083
4	6	0	2.068004	1.523095	0.246295
5	6	0	2.706982	0.210643	-0.249314
6	1	0	0.206546	2.184159	-1.421562
7	1	0	-0.253930	2.588796	0.630884
8	1	0	2.097794	-1.601112	1.468871
9	1	0	2.175435	-2.291342	-0.539915
10	6	0	-2.319240	0.317470	-0.330831
11	9	0	-1.388186	-2.063772	-0.038562
12	6	0	-3.001012	1.135414	0.475704
13	1	0	-2.792672	-0.077725	-1.232578
14	1	0	-2.586832	1.536162	1.400734
15	1	0	-4.036233	1.414320	0.269919
16	1	0	2.584084	2.397141	-0.164001
17	1	0	2.139534	1.586302	1.339131
18	1	0	3.720611	0.091796	0.145404
19	1	0	2.781988	0.218946	-1.343479

$4a_{vo}$
SCF Done: E(RB+HF-LYP) = -1126.14331299 A.U. after 11 cycles

Center Number	Atomic Number	Atomic Type	Coordinates (Angstroms) X	Y	Z
1	28	0	-0.500320	-0.114845	-0.050303
2	15	0	0.992091	1.500018	-0.150791
3	15	0	1.355684	-1.559836	0.172086
4	6	0	2.717592	0.879875	0.257847
5	6	0	2.888140	-0.563867	-0.256647
6	1	0	1.191702	2.154801	-1.390060
7	1	0	0.885065	2.646817	0.665959
8	1	0	1.714440	-2.103073	1.431548
9	1	0	1.547245	-2.735858	-0.589311
10	6	0	-1.820772	1.198046	-0.350583
11	8	0	-1.647461	-1.504731	0.036457
12	6	0	-2.229423	2.183489	0.456312
13	1	0	-2.338691	1.049341	-1.304284
14	1	0	-1.772301	2.378773	1.426462
15	1	0	-3.073656	2.827662	0.201786
16	1	0	3.495954	1.539544	-0.139280
17	1	0	2.801580	0.899425	1.351471
18	1	0	3.804811	-1.015896	0.134645
19	1	0	2.964715	-0.565880	-1.350813
20	6	0	-3.039686	-1.454185	-0.024881
21	1	0	-3.422131	-1.035373	-0.974632
22	1	0	-3.492218	-0.866369	0.791443
23	1	0	-3.429610	-2.483294	0.050187

$4a_{vs}$
SCF Done: E(RB+HF-LYP) = -1449.14421401 A.U. after 8 cycles

Center Number	Atomic Number	Atomic Type	Coordinates (Angstroms) X	Y	Z
1	28	0	-0.276148	0.046269	-0.021276
2	15	0	1.418634	1.440440	-0.138047
3	15	0	1.289947	-1.617807	0.231265
4	6	0	3.050529	0.553241	0.156999
5	6	0	2.933692	-0.905334	-0.326527
6	1	0	1.640854	2.094914	-1.372414
7	1	0	1.520063	2.566576	0.708069
8	1	0	1.618363	-2.097046	1.523507
9	1	0	1.257548	-2.862794	-0.435289
10	6	0	-1.401114	1.535649	-0.337820
11	16	0	-1.946648	-1.402745	0.005461
12	6	0	-1.709591	2.531795	0.500757
13	1	0	-1.840423	1.535229	-1.340315
14	1	0	-1.317290	2.587721	1.516003
15	1	0	-2.405508	3.326060	0.223161
16	1	0	3.890895	1.065499	-0.322254
17	1	0	3.228484	0.576785	1.239096
18	1	0	3.780815	-1.506841	0.017961
19	1	0	2.928474	-0.940322	-1.422612
20	6	0	-3.585330	-0.585901	-0.122770
21	1	0	-3.706316	-0.077254	-1.083853
22	1	0	-3.733446	0.136718	0.682060
23	1	0	-4.341822	-1.373060	-0.046845

$5a_{vb}$
SCF Done: E(RB+HF-LYP) = -4705.60028160 A.U. after 10 cycles

Center Number	Atomic Number	Atomic Type	Coordinates (Angstroms) X	Y	Z
1	6	0	0.351297	-2.122123	-1.386349
2	6	0	-0.141454	-2.148930	-0.062397
3	1	0	-0.070785	-3.006543	0.599918
4	1	0	-0.173106	-1.590793	-2.177180
5	35	0	-2.036753	-1.451604	0.270656
6	1	0	0.959242	-2.962338	-1.724280
7	28	0	1.248440	-0.872148	-0.165648
8	15	0	1.768953	0.172443	1.747600
9	15	0	2.924158	0.224762	-1.169225
10	6	0	3.376273	1.105523	1.450495
11	6	0	3.446667	1.601023	-0.005451
12	1	0	0.943908	1.195349	2.274942
13	1	0	2.063944	-0.461601	2.980158
14	1	0	4.167976	-0.409361	-1.422703
15	1	0	2.817673	0.914534	-2.397871
16	1	0	3.491606	1.935005	2.154867
17	1	0	4.187973	0.394331	1.647925
18	1	0	4.446173	1.977993	-0.243925
19	1	0	2.732211	2.416132	-0.162598
20	12	0	-2.154937	1.111679	-0.239024
21	17	0	-4.244494	1.748066	0.182899
22	17	0	-0.224382	2.070310	-0.897556

$5a_{vc}$
SCF Done: E(RB+HF-LYP) = -2591.91831509 A.U. after 8 cycles

Center Number	Atomic Number	Atomic Type	Coordinates (Angstroms) X	Y	Z
1	6	0	-0.262041	2.358018	-1.130705
2	6	0	0.260008	2.277040	0.180228
3	1	0	0.145598	3.053763	0.930063
4	1	0	0.281219	1.952464	-1.981348
5	17	0	2.044309	1.696870	0.388889
6	1	0	-0.928483	3.188842	-1.363810
7	28	0	-1.072504	0.943597	-0.042254
8	15	0	-1.492253	-0.340721	1.743571
9	15	0	-2.671978	-0.154757	-1.158753
10	6	0	-3.012163	-1.375082	1.338841
11	6	0	-3.053275	-1.700169	-0.165270
12	1	0	-0.577915	-1.338219	2.161852
13	1	0	-1.835876	0.126843	3.036356
14	1	0	-3.970166	0.393210	-1.327877
15	1	0	-2.526955	-0.682612	-2.461632
16	1	0	-3.043927	-2.288754	1.940246
17	1	0	-3.882850	-0.769488	1.619412
18	1	0	-4.016017	-2.138609	-0.446138
19	1	0	-2.267342	-2.419938	-0.417821
20	12	0	2.416235	-0.656450	-0.249691
21	17	0	4.532290	-1.108379	0.257383
22	17	0	0.630831	-1.738343	-1.094551

$5a_{vf}$
SCF Done: E(RB+HF-LYP) = -2231.57053933 A.U. after 9 cycles

Center Number	Atomic Number	Atomic Type	Coordinates (Angstroms) X	Y	Z
1	6	0	0.063501	2.620156	-0.679766
2	6	0	-0.968376	1.791707	-1.149703
3	1	0	-1.328851	1.733775	-2.171217
4	1	0	-0.023694	3.087753	0.298423
5	9	0	-2.170630	1.737303	-0.285393
6	1	0	0.685233	3.140021	-1.406737
7	28	0	0.534689	0.717262	-0.542932
8	15	0	0.571610	-1.513010	-0.870578
9	15	0	2.607571	0.590749	0.301243
10	6	0	2.346736	-2.047318	-0.547780
11	6	0	2.950153	-1.225007	0.604160
12	1	0	-0.145359	-2.454572	-0.099828
13	1	0	0.327355	-2.085472	-2.139054
14	1	0	3.754615	0.974656	-0.439199
15	1	0	2.970977	1.179392	1.532255
16	1	0	2.393778	-3.119957	-0.335873
17	1	0	2.906681	-1.871969	-1.474582
18	1	0	4.019741	-1.427725	0.716368
19	1	0	2.458414	-1.476841	1.550613
20	12	0	-1.880379	-0.047429	0.522083
21	17	0	-3.204110	-1.629022	-0.368129
22	17	0	-0.615287	0.109476	2.406542

$5a_{vo}$
SCF Done: E(RB+HF-LYP) = -2246.86407878 A.U. after 7 cycles

Center Number	Atomic Number	Atomic Type	Coordinates (Angstroms) X	Y	Z
1	6	0	-0.304634	2.608039	-0.274123
2	6	0	-1.222110	1.660561	-0.772426
3	1	0	-1.558368	1.648551	-1.809055
4	1	0	-0.372195	2.931468	0.762300
5	8	0	-2.241952	1.170587	0.123150
6	1	0	0.168465	3.303819	-0.965395
7	28	0	0.555475	0.849360	-0.471862
8	15	0	1.027436	-1.230948	-1.174353
9	15	0	2.623077	0.998109	0.368395
10	6	0	2.858511	-1.504066	-0.826287
11	6	0	3.275514	-0.754457	0.450683
12	1	0	0.473793	-2.439089	-0.692172
13	1	0	0.949627	-1.543946	-2.551613
14	1	0	3.693402	1.664414	-0.284480
15	1	0	2.881627	1.473937	1.673342
16	1	0	3.078559	-2.573128	-0.748280
17	1	0	3.410479	-1.118585	-1.692248
18	1	0	4.360768	-0.784133	0.589399
19	1	0	2.805004	-1.210072	1.328872
20	12	0	-1.513235	-0.661547	0.550671
21	17	0	-2.694100	-2.240923	-0.551829
22	17	0	-0.179586	-0.767477	2.399731
23	6	0	-3.547068	1.734965	-0.074007
24	1	0	-3.909758	1.507243	-1.082251

25	1	0	-3.499894	2.818000	0.076629
26	1	0	-4.206692	1.278428	0.665824

5a$_{vs}$

SCF Done: E(RB+HF-LYP) = -2569.84167820 A.U. after 7 cycles

Center Number	Atomic Number	Atomic Type	Coordinates (Angstroms) X	Y	Z
1	6	0	1.068396	-1.331860	1.599630
2	6	0	1.081769	-1.954642	0.323240
3	1	0	0.918093	-3.024388	0.208965
4	1	0	1.706706	-0.481173	1.834755
5	16	0	2.000055	-1.225786	-1.053927
6	1	0	0.809637	-1.944734	2.464555
7	28	0	-0.559180	-0.912180	0.577045
8	15	0	-2.072974	-1.094112	-1.085342
9	15	0	-1.895447	0.552196	1.588245
10	6	0	-3.604511	-0.157176	-0.519139
11	6	0	-3.218229	1.047865	0.357724
12	1	0	-1.842415	-0.560258	-2.370681
13	1	0	-2.661505	-2.319277	-1.487520
14	1	0	-2.668757	0.105303	2.690692
15	1	0	-1.522869	1.804524	2.127802
16	1	0	-4.209604	0.161705	-1.373036
17	1	0	-4.204735	-0.870695	0.059005
18	1	0	-4.096422	1.466501	0.859204
19	1	0	-2.768490	1.831605	-0.260234
20	12	0	1.255043	1.140322	-0.407209
21	17	0	2.784159	2.035761	0.990152
22	17	0	-0.327734	2.094608	-1.725911
23	6	0	3.767637	-1.370564	-0.555346
24	1	0	4.007491	-2.424662	-0.397700
25	1	0	3.959050	-0.786115	0.345791
26	1	0	4.366204	-0.977867	-1.381792

6a$_{vb}$

SCF Done: E(RB+HF-LYP) = -4705.59318728 A.U. after 10 cycles

Center Number	Atomic Number	Atomic Type	Coordinates (Angstroms) X	Y	Z
1	6	0	0.361331	-1.913625	-1.932718
2	6	0	0.248021	-2.163738	-0.596894
3	1	0	0.206562	-3.116564	-0.082071
4	1	0	0.003796	-0.986849	-2.380769
5	35	0	-2.061053	-1.514620	0.514877
6	1	0	0.655246	-2.695584	-2.634233
7	28	0	1.356956	-0.742881	-0.468019
8	15	0	1.552312	-0.168216	1.671484
9	15	0	3.110310	0.670650	-0.928327
10	6	0	3.061789	0.929998	1.858291
11	6	0	3.267776	1.766509	0.581510
12	1	0	0.524809	0.609714	2.245696
13	1	0	1.726784	-1.090857	2.728105
14	1	0	4.432451	0.181233	-1.068921
15	1	0	3.129233	1.605950	-1.984837
16	1	0	2.976947	1.572708	2.739938
17	1	0	3.919125	0.265358	2.020525
18	1	0	4.229406	2.288134	0.604575
19	1	0	2.477123	2.518905	0.488065
20	12	0	-2.277068	0.862875	-0.194857
21	17	0	-4.135701	2.076742	0.049952
22	17	0	-0.240029	1.632338	-0.983037

6a$_{vc}$

SCF Done: E(RB+HF-LYP) = -2591.91099876 A.U. after 12 cycles

Center Number	Atomic Number	Atomic Type	Coordinates (Angstroms) X	Y	Z
1	6	0	-0.252402	2.389961	-1.360844
2	6	0	-0.142669	2.346865	0.001530
3	1	0	-0.175115	3.157588	0.720024
4	1	0	0.218084	1.645567	-2.001401
5	17	0	2.062732	1.680520	0.847368
6	1	0	-0.635127	3.277295	-1.866684
7	28	0	-1.152810	0.866811	-0.231813
8	15	0	-1.382069	-0.206480	1.710609
9	15	0	-2.786515	-0.494797	-1.092994
10	6	0	-2.816756	-1.406197	1.553412
11	6	0	-2.919442	-1.925945	0.107172
12	1	0	-0.330865	-1.037754	2.155417
13	1	0	-1.670156	0.427335	2.941240
14	1	0	-4.135007	-0.070004	-1.185122
15	1	0	-2.698905	-1.152445	-2.338694
16	1	0	-2.720242	-2.234180	2.262394
17	1	0	-3.723125	-0.850334	1.822838
18	1	0	-3.842848	-2.494359	-0.040306
19	1	0	-2.076432	-2.587587	-0.120142
20	12	0	2.545513	-0.378509	-0.150509
21	17	0	4.517925	-1.406610	0.033053
22	17	0	0.645146	-1.198537	-1.181864

6a$_{vf}$

SCF Done: E(RB+HF-LYP) = -2231.54841054 A.U. after 10 cycles

Center Number	Atomic Number	Atomic Type	Coordinates (Angstroms) X	Y	Z
1	6	0	0.354943	2.466087	-0.950327
2	6	0	0.241584	2.184091	0.372195
3	1	0	0.329985	2.841601	1.226627
4	1	0	0.569015	1.693054	-1.691802
5	9	0	1.728465	0.995448	1.185478
6	1	0	0.340833	3.489123	-1.326495
7	28	0	-0.962202	0.949104	-0.154249
8	15	0	-1.312124	-0.265705	1.647490
9	15	0	-2.654247	-0.201436	-1.202671
10	6	0	-2.832767	-1.322421	1.360424
11	6	0	-2.927559	-1.711143	-0.127654
12	1	0	-0.330191	-1.214521	1.996847
13	1	0	-1.552623	0.272584	2.931821
14	1	0	-3.968229	0.318558	-1.308570
15	1	0	-2.558328	-0.765242	-2.492733
16	1	0	-2.824150	-2.211728	1.998341
17	1	0	-3.700388	-0.718516	1.653133
18	1	0	-3.884154	-2.194810	-0.347250
19	1	0	-2.126384	-2.411198	-0.388291
20	12	0	2.486419	-0.250491	0.076060
21	17	0	4.637202	-0.863298	0.023375
22	17	0	0.758764	-1.155498	-1.206598

6a$_{vo}$

SCF Done: E(RB+HF-LYP) = -2246.80659592 A.U. after 9 cycles

Center Number	Atomic Number	Atomic Type	Coordinates (Angstroms) X	Y	Z
1	6	0	-0.929522	-0.344539	2.227602
2	6	0	-0.561219	0.785454	1.571717
3	1	0	-0.704868	1.801381	1.918649
4	1	0	-0.883750	-1.339501	1.775687
5	8	0	-1.577358	1.502178	-0.299365
6	1	0	-1.300661	-0.321322	3.253138
7	28	0	0.869998	-0.071973	0.859069
8	15	0	1.451047	1.432057	-0.612067
9	15	0	2.856324	-1.179579	0.472631
10	6	0	3.241733	1.134010	-1.071180
11	6	0	3.521567	-0.381959	-1.088437
12	1	0	0.794730	1.367447	-1.853383
13	1	0	1.406356	2.823478	-0.384164
14	1	0	3.963335	-1.059565	1.348769
15	1	0	2.983425	-2.554725	0.179303
16	1	0	3.489431	1.585752	-2.037408
17	1	0	3.859931	1.627303	-0.310996
18	1	0	4.588375	-0.586194	-1.220561
19	1	0	2.986013	-0.855131	-1.919383
20	12	0	-2.198568	-0.294590	-0.495565
21	17	0	-4.358597	-0.916634	-0.441474
22	17	0	-0.382363	-1.700833	-0.966791
23	6	0	-2.391325	2.622210	-0.053282
24	1	0	-2.062328	3.161995	0.853657
25	1	0	-3.451988	2.363215	0.086694
26	1	0	-2.327899	3.337485	-0.888714

6a$_{vs}$

SCF Done: E(RB+HF-LYP) = -2569.78622331 A.U. after 10 cycles

Center Number	Atomic Number	Atomic Type	Coordinates (Angstroms) X	Y	Z
1	6	0	-0.916585	-0.589793	2.023389
2	6	0	-0.550019	0.605264	1.486573
3	1	0	-0.721895	1.568867	1.949258
4	1	0	-0.842502	-1.543725	1.494733
5	16	0	-1.828860	1.848838	-0.618023
6	1	0	-1.317311	-0.664143	3.035452
7	28	0	0.953013	-0.150321	0.771686
8	15	0	1.806665	1.558103	-0.306659
9	15	0	2.945873	-1.276626	0.453647
10	6	0	3.604193	1.195222	-0.689464
11	6	0	3.791867	-0.317392	-0.914674
12	1	0	1.247526	1.815570	-1.574097
13	1	0	1.850542	2.876670	0.195363
14	1	0	3.960974	-1.321822	1.441156
15	1	0	3.047128	-2.607670	-0.004142
16	1	0	3.949963	1.766729	-1.556664
17	1	0	4.190316	1.527203	0.176224

18	1	0	4.852182	-0.575985	-0.993218
19	1	0	3.302870	-0.625995	-1.845649
20	12	0	-2.126556	-0.526227	-0.574410
21	17	0	-4.085314	-1.564827	-0.186201
22	17	0	-0.121094	-1.579343	-1.214343
23	6	0	-3.320506	2.465312	0.275377
24	1	0	-3.505192	3.498391	-0.030365
25	1	0	-3.152094	2.446349	1.357364
26	1	0	-4.199292	1.858898	0.045904

$7a_{vb}$

SCF Done: E(RB+HF-LYP) = -4705.63358059 A.U. after 1 cycles

Center Number	Atomic Number	Atomic Type	Coordinates (Angstroms) X	Y	Z
1	6	0	1.520503	-2.389733	-1.061745
2	6	0	0.617429	-1.406412	-1.224644
3	1	0	0.586221	-0.915669	-2.202458
4	1	0	1.628891	-2.936650	-0.127650
5	35	0	0.473835	1.910433	-0.451314
6	1	0	2.197087	-2.680112	-1.866950
7	28	0	-0.583718	-0.729469	0.120035
8	15	0	-2.176130	-0.829869	-1.372774
9	15	0	-2.118686	0.271957	1.501407
10	6	0	-3.777855	-0.146588	-0.682876
11	6	0	-3.474050	0.916328	0.389332
12	1	0	-1.948335	-0.074239	-2.541642
13	1	0	-2.574023	-2.050904	-1.958545
14	1	0	-2.838792	-0.471160	2.467507
15	1	0	-1.753070	1.380754	2.286504
16	1	0	-4.408153	0.255833	-1.482139
17	1	0	-4.314016	-0.994023	-0.239001
18	1	0	-4.376762	1.181482	0.947902
19	1	0	-3.083727	1.829003	-0.073773
20	12	0	2.139134	0.090298	0.098944
21	17	0	4.368113	0.126382	-0.135036
22	17	0	0.930771	-1.039370	1.875508

$7a_{vc}$

SCF Done: E(RB+HF-LYP) = -2591.95176784 A.U. after 13 cycles

Center Number	Atomic Number	Atomic Type	Coordinates (Angstroms) X	Y	Z
1	6	0	1.604351	2.143751	-1.151644
2	6	0	0.704187	1.722317	-0.246560
3	1	0	0.681541	2.251851	0.711892
4	1	0	1.711038	1.682538	-2.130807
5	17	0	0.506753	-0.814874	1.918619
6	1	0	2.282775	2.970665	-0.935992
7	28	0	-0.510862	0.244340	-0.479351
8	15	0	-2.052076	1.512004	0.407619
9	15	0	-2.109842	-1.400511	-0.566629
10	6	0	-3.694761	0.619080	0.487777
11	6	0	-3.451606	-0.895020	0.630431
12	1	0	-1.794228	1.888470	1.741668
13	1	0	-2.390190	2.769006	-0.136576
14	1	0	-2.829420	-1.651511	-1.758719
15	1	0	-1.800866	-2.724023	-0.199627
16	1	0	-4.312909	1.007511	1.303244
17	1	0	-4.217657	0.835650	-0.451531
18	1	0	-4.376723	-1.459785	0.481707
19	1	0	-3.070469	-1.128913	1.630737
20	12	0	2.147885	-0.269078	0.320753
21	17	0	4.371047	-0.108321	0.559952
22	17	0	1.010575	-1.033698	-1.691398

$7a_{vf}$

SCF Done: E(RB+HF-LYP) = -2231.58457168 A.U. after 13 cycles

Center Number	Atomic Number	Atomic Type	Coordinates (Angstroms) X	Y	Z
1	6	0	-1.568034	2.148197	1.104391
2	6	0	-0.665176	1.736675	0.200493
3	1	0	-0.628956	2.261417	-0.760337
4	1	0	-1.671200	1.681336	2.081045
5	9	0	-0.662171	-0.583632	-1.480632
6	1	0	-2.249472	2.973817	0.892030
7	28	0	0.487671	0.211217	0.335306
8	15	0	2.151366	1.477335	-0.250106
9	15	0	1.916136	-1.572154	0.144209
10	6	0	3.712348	0.460011	-0.454701
11	6	0	3.340560	-0.966276	-0.904389
12	1	0	2.018086	2.134526	-1.494107
13	1	0	2.573414	2.572403	0.533090
14	1	0	2.571843	-2.153334	1.254043
15	1	0	1.484215	-2.741096	-0.511056
16	1	0	4.404309	0.936786	-1.156172
17	1	0	4.204045	0.435264	0.525180
18	1	0	4.207937	-1.631817	-0.860040
19	1	0	2.979878	-0.957375	-1.939305
20	12	0	-2.145304	-0.306326	-0.432591
21	17	0	-4.341417	-0.184910	-0.868485
22	17	0	-1.057194	-1.070781	1.602456

$7a_{vo}$

SCF Done: E(RB+HF-LYP) = -2246.86102313 A.U. after 1 cycles

Center Number	Atomic Number	Atomic Type	Coordinates (Angstroms) X	Y	Z
1	6	0	-1.297796	-1.801229	1.623484
2	6	0	-0.684643	-0.617039	1.785658
3	1	0	-0.984329	0.010631	2.632085
4	1	0	-1.046123	-2.486548	0.813740
5	8	0	-0.991550	1.428303	0.149049
6	1	0	-2.079950	-2.141201	2.303665
7	28	0	0.496036	0.317842	0.627661
8	15	0	2.067875	-1.179791	0.894936
9	15	0	1.993283	1.457773	-0.740341
10	6	0	3.288339	-1.010588	-0.508187
11	6	0	3.591800	0.478826	-0.761687
12	1	0	2.887689	-1.167283	2.048656
13	1	0	1.710538	-2.540260	0.872880
14	1	0	1.626152	1.535823	-2.098425
15	1	0	2.459581	2.781564	-0.565006
16	1	0	4.204396	-1.578496	-0.315832
17	1	0	2.790142	-1.450784	-1.378792
18	1	0	4.138800	0.611063	-1.699781
19	1	0	4.220226	0.881490	0.042093
20	12	0	-2.015561	-0.132310	-0.484663
21	17	0	-4.265015	-0.160343	-0.574053
22	17	0	-0.372887	-1.183482	-1.801801
23	6	0	-1.420529	2.477557	0.994686
24	1	0	-2.343093	2.913308	0.591483
25	1	0	-0.659892	3.270127	1.050591
26	1	0	-1.630070	2.132396	2.018574

$7a_{vs}$

SCF Done: E(RB+HF-LYP) = -2569.84168407 A.U. after 10 cycles

Center Number	Atomic Number	Atomic Type	Coordinates (Angstroms) X	Y	Z
1	6	0	1.068113	-1.341704	1.594288
2	6	0	1.082698	-1.956203	0.313955
3	1	0	0.919711	-3.025334	0.193035
4	1	0	1.704525	-0.491144	1.834844
5	16	0	2.001705	-1.218969	-1.058336
6	1	0	0.810056	-1.960548	2.455151
7	28	0	-0.559469	-0.917092	0.573786
8	15	0	-2.070385	-1.086184	-1.092517
9	15	0	-1.898982	0.537153	1.595304
10	6	0	-3.601052	-0.148267	-0.525213
11	6	0	-3.214537	1.048033	0.363431
12	1	0	-1.835780	-0.547470	-2.375034
13	1	0	-2.660922	-2.308300	-1.500982
14	1	0	-2.678962	0.075423	2.686919
15	1	0	-1.530066	1.782298	2.153783
16	1	0	-4.200944	0.180018	-1.379194
17	1	0	-4.206601	-0.864254	0.044220
18	1	0	-4.093501	1.465552	0.864493
19	1	0	-2.759297	1.835240	-0.246099
20	12	0	1.253855	1.143610	-0.403214
21	17	0	2.777854	2.033689	1.003174
22	17	0	-0.324679	2.101978	-1.723944
23	6	0	3.768784	-1.365224	-0.558426
24	1	0	4.008994	-2.419996	-0.405905
25	1	0	3.958801	-0.785367	0.345968
26	1	0	4.368089	-0.968035	-1.382183

$8a_{vo}$

SCF Done: E(RB+HF-LYP) = -2246.80844473 A.U. after 10 cycles

Center Number	Atomic Number	Atomic Type	Coordinates (Angstroms) X	Y	Z
1	6	0	1.427425	0.983732	-1.910692
2	6	0	0.730370	1.637776	-0.815247
3	1	0	0.686713	2.727908	-0.706099
4	1	0	0.776705	0.423743	-2.587439
5	8	0	1.208671	1.136146	0.576409
6	1	0	2.071440	1.665148	-2.476170
7	28	0	-0.629797	0.726110	0.131434
8	15	0	-2.237279	0.530680	-1.312360
9	15	0	-1.948244	-0.398380	1.687810

10	6	0	-3.261261	-0.925812	-0.756424
11	6	0	-3.525115	-0.828651	0.757801
12	1	0	-1.930180	0.228815	-2.654441
13	1	0	-1.506367	-1.645405	2.172859
14	1	0	-2.494710	0.109203	2.892829
15	1	0	-4.198654	-0.998555	-1.317234
16	1	0	-2.653866	-1.808981	-0.980609
17	1	0	-3.962860	-1.757402	1.134919
18	1	0	-4.240115	-0.023777	0.966806
19	1	0	-3.206425	1.541754	-1.523649
20	6	0	1.585828	2.079047	1.600948
21	1	0	2.643254	2.322630	1.470167
22	1	0	1.430988	1.596374	2.567617
23	1	0	0.971366	2.981980	1.528488
24	12	0	2.221126	-0.562881	-0.576543
25	17	0	4.260295	-0.922473	0.345243
26	17	0	0.325794	-2.000477	-0.389420

8a$_{vs}$

SCF Done: E(RB+HF-LYP) = -2569.80087392 A.U. after 10 cycles

Center Number	Atomic Number	Atomic Type	Coordinates (Angstroms) X	Y	Z
1	6	0	-0.901171	0.154462	-1.727940
2	6	0	-0.518979	-0.756078	-0.768121
3	1	0	-0.770246	-1.810006	-0.876682
4	1	0	-0.749787	1.227390	-1.605038
5	16	0	-0.786981	-0.212083	1.271366
6	1	0	-1.205990	-0.192804	-2.713957
7	28	0	1.057650	-0.059274	-0.028960
8	15	0	2.739452	-1.336996	-0.778343
9	15	0	2.571053	1.526453	0.595421
10	6	0	4.281353	-0.259896	-0.741517
11	6	0	4.248926	0.689675	0.469770
12	1	0	2.867601	-1.928396	-2.059569
13	1	0	2.782824	2.675474	-0.206694
14	1	0	2.681125	2.164347	1.853572
15	1	0	5.192294	-0.866398	-0.739056
16	1	0	4.275541	0.318371	-1.673534
17	1	0	5.059779	1.422272	0.412608
18	1	0	4.385683	0.122304	1.398519
19	1	0	3.188913	-2.459651	-0.034331
20	6	0	-0.996424	-1.954313	1.842788
21	1	0	-1.050674	-1.920448	2.933333
22	1	0	-0.130375	-2.548194	1.544970
23	1	0	-1.920513	-2.370944	1.435984
24	12	0	-2.869860	0.336353	-0.256200
25	17	0	-4.098107	-1.564287	-0.245682
26	17	0	-3.168375	2.570081	-0.215069

2a$_{pb}$

SCF Done: E(RB+HF-LYP) = -3738.56908647 A.U. after 11 cycles

Center Number	Atomic Number	Atomic Type	Coordinates (Angstroms) X	Y	Z
1	28	0	-0.463975	0.210389	-0.163478
2	15	0	-1.597892	-1.130905	1.188423
3	15	0	-2.357780	0.923623	-1.060712
4	6	0	-3.405579	-0.616518	1.047403
5	6	0	-3.724767	-0.191715	-0.397294
6	1	0	-1.711012	-2.520610	0.912981
7	1	0	-1.503688	-1.265391	2.600249
8	1	0	-2.882456	2.199206	-0.713646
9	1	0	-2.742312	0.976393	-2.427912
10	6	0	1.206448	1.078213	-0.959726
11	6	0	1.500712	0.116567	0.068224
12	6	0	1.377499	2.466127	-0.648034
13	35	0	2.042015	-1.695933	-0.494156
14	6	0	1.978881	0.562830	1.341320
15	6	0	2.082621	1.908726	1.603521
16	1	0	-4.081559	-1.409979	1.381938
17	1	0	-3.539202	0.234656	1.726661
18	1	0	-4.707259	0.287070	-0.460263
19	1	0	-3.747752	-1.073375	-1.049885
20	6	0	1.782994	2.873216	0.600576
21	1	0	1.186617	0.773657	-2.002780
22	1	0	1.211774	3.196442	-1.437151
23	1	0	2.251840	-0.175011	2.089615
24	1	0	2.417239	2.237979	2.584008
25	1	0	1.910793	3.930276	0.817422

2a$_{pc}$

SCF Done: E(RB+HF-LYP) = -1624.88858583 A.U. after 8 cycles

Center Number	Atomic Number	Atomic Type	Coordinates (Angstroms) X	Y	Z
1	28	0	0.200216	-0.078308	-0.205792
2	15	0	1.544533	1.305116	0.876088
3	15	0	1.921403	-1.365425	-0.730717
4	6	0	3.205168	0.425159	1.018922
5	6	0	3.472470	-0.409348	-0.246520
6	1	0	1.959935	2.526666	0.279623
7	1	0	1.436439	1.814205	2.198776
8	1	0	2.148410	-2.583376	-0.031868
9	1	0	2.334884	-1.849349	-2.001718
10	6	0	-1.583276	-0.717139	-0.958505
11	6	0	-1.711206	0.497299	-0.198933
12	6	0	-2.059337	-1.931819	-0.366690
13	17	0	-1.812685	2.062858	-1.098565
14	6	0	-2.321750	0.460253	1.095776
15	6	0	-2.715169	-0.739602	1.639064
16	1	0	4.023390	1.127909	1.206397
17	1	0	3.132425	-0.233179	1.893586
18	1	0	4.333059	-1.071765	-0.108458
19	1	0	3.701515	0.253602	-1.090214
20	6	0	-2.589065	-1.950510	0.901354
21	1	0	-1.454285	-0.670728	-2.036926
22	1	0	-2.021294	-2.843338	-0.959221
23	1	0	-2.464934	1.393112	1.632869
24	1	0	-3.149733	-0.759050	2.635226
25	1	0	-2.946246	-2.881798	1.332319

2a$_{pf}$

SCF Done: E(RB+HF-LYP) = -1264.52332985 A.U. after 1 cycles

Center Number	Atomic Number	Atomic Type	Coordinates (Angstroms) X	Y	Z
1	28	0	-0.110602	0.063211	-0.242276
2	15	0	-1.501152	-1.513189	0.383149
3	15	0	-1.732686	1.559422	-0.217829
4	6	0	-3.102440	-0.645209	0.874901
5	6	0	-3.335518	0.582885	-0.022238
6	1	0	-2.007656	-2.444492	-0.565468
7	1	0	-1.405940	-2.440970	1.457319
8	1	0	-1.863127	2.460058	0.876884
9	1	0	-2.158544	2.486871	-1.209311
10	6	0	1.696184	0.728357	-0.938729
11	6	0	1.757474	-0.665979	-0.630470
12	6	0	2.314377	1.634184	-0.019840
13	9	0	1.602403	-1.571856	-1.658137
14	6	0	2.448160	-1.121723	0.527894
15	6	0	2.986091	-0.208912	1.407062
16	1	0	-3.960329	-1.324734	0.843180
17	1	0	-2.974012	-0.328521	1.917550
18	1	0	-4.146643	1.207126	0.366509
19	1	0	-3.624698	0.260498	-1.030391
20	6	0	2.921355	1.184366	1.131609
21	1	0	1.484098	1.046611	-1.956869
22	1	0	2.321565	2.693764	-0.264932
23	1	0	2.535882	-2.192646	0.687434
24	1	0	3.486498	-0.558005	2.306424
25	1	0	3.381589	1.889923	1.817707

2a$_{po}$

SCF Done: E(RB+HF-LYP) = -1279.80742776 A.U. after 1 cycles

Center Number	Atomic Number	Atomic Type	Coordinates (Angstroms) X	Y	Z
1	28	0	-0.284305	0.085065	-0.178479
2	15	0	-1.552716	-1.370946	0.858249
3	15	0	-2.048804	1.242778	-0.803319
4	6	0	-3.289474	-0.634765	0.894379
5	6	0	-3.548228	0.171213	-0.390822
6	1	0	-1.833374	-2.632997	0.264196
7	1	0	-1.486257	-1.856047	2.194497
8	1	0	-2.415250	2.441061	-0.126063
9	1	0	-2.451268	1.690080	-2.093724
10	6	0	1.516481	0.736340	-0.913366
11	6	0	1.694412	-0.452159	-0.125241
12	6	0	1.889309	1.994600	-0.344670
13	8	0	1.739208	-1.706202	-0.751878
14	6	0	2.236914	-0.329594	1.193612
15	6	0	2.538648	0.905344	1.721487
16	1	0	-4.056322	-1.403138	1.037645
17	1	0	-3.325851	0.029974	1.766662
18	1	0	-4.462674	0.767352	-0.306187
19	1	0	-3.679850	-0.511637	-1.239589
20	6	0	2.369908	2.082918	0.942612
21	1	0	1.393678	0.649665	-1.991201
22	1	0	1.806670	2.887822	-0.960326
23	1	0	2.404284	-1.242117	1.760958
24	1	0	2.927029	0.980620	2.734155
25	1	0	2.643842	3.048435	1.359366
26	6	0	3.018974	-2.023412	-1.293427
27	1	0	3.793791	-2.031356	-0.513802

28	1	0	3.314084	-1.308563	-2.074602
29	1	0	2.935484	-3.021760	-1.730889

2a$_{ps}$

SCF Done: E(RB+HF-LYP) = -1602.79556928 A.U. after 8 cycles

Center Number	Atomic Number	Atomic Type	Coordinates (Angstroms) X	Y	Z
1	28	0	-0.424192	0.113476	-0.168387
2	15	0	-1.618000	-1.400868	0.900042
3	15	0	-2.257116	1.102444	-0.880280
4	6	0	-3.398427	-0.779001	0.874242
5	6	0	-3.686222	-0.050771	-0.450666
6	1	0	-1.801490	-2.699145	0.350640
7	1	0	-1.542649	-1.823049	2.255382
8	1	0	-2.712012	2.303013	-0.266284
9	1	0	-2.643947	1.463574	-2.200480
10	6	0	1.313116	0.917339	-0.916935
11	6	0	1.578910	-0.124832	0.044347
12	6	0	1.543699	2.281666	-0.551299
13	16	0	1.881997	-1.820400	-0.496462
14	6	0	2.006345	0.272821	1.358931
15	6	0	2.168869	1.598380	1.686833
16	1	0	-4.115014	-1.589904	1.040489
17	1	0	-3.494507	-0.080066	1.714543
18	1	0	-4.641659	0.482220	-0.409529
19	1	0	-3.751461	-0.777556	-1.270033
20	6	0	1.948046	2.618120	0.718421
21	1	0	1.248595	0.662957	-1.972982
22	1	0	1.410369	3.052553	-1.307585
23	1	0	2.215374	-0.506494	2.087481
24	1	0	2.491446	1.870307	2.689017
25	1	0	2.119309	3.658288	0.983027
26	6	0	3.687352	-1.773742	-0.854271
27	1	0	4.254058	-1.492788	0.037718
28	1	0	3.907956	-1.075329	-1.666159
29	1	0	3.977673	-2.783047	-1.161072

3a$_{pb}$

SCF Done: E(RB+HF-LYP) = -3738.56154828 A.U. after 10 cycles

Center Number	Atomic Number	Atomic Type	Coordinates (Angstroms) X	Y	Z
1	28	0	-0.380336	0.048846	0.183516
2	15	0	-1.525459	-0.963923	-1.446877
3	15	0	-2.229632	0.213291	1.424399
4	6	0	-3.225606	-1.328720	-0.714350
5	6	0	-3.646761	-0.213799	0.258644
6	1	0	-1.920336	-0.291339	-2.638727
7	1	0	-1.287869	-2.217055	-2.076446
8	1	0	-2.510119	-0.681448	2.493209
9	1	0	-2.781534	1.365149	2.045661
10	6	0	1.685495	-0.380683	1.299598
11	6	0	1.513227	-0.011474	-0.052250
12	6	0	2.425716	-1.546436	1.586797
13	35	0	1.036410	2.059362	-0.340047
14	6	0	2.203142	-0.684105	-1.084599
15	6	0	2.942693	-1.810564	-0.765532
16	1	0	-3.979888	-1.468212	-1.495468
17	1	0	-3.133921	-2.280383	-0.176233
18	1	0	-4.551102	-0.493196	0.809140
19	1	0	-3.871925	0.704557	-0.297562
20	6	0	3.045154	-2.256271	0.568712
21	1	0	1.338099	0.261139	2.101091
22	1	0	2.550168	-1.852796	2.622740
23	1	0	2.112730	-0.339893	-2.109744
24	1	0	3.440886	-2.363072	-1.558629
25	1	0	3.637881	-3.137016	0.799224

3a$_{pc}$

SCF Done: E(RB+HF-LYP) = -1624.87293301 A.U. after 10 cycles

Center Number	Atomic Number	Atomic Type	Coordinates (Angstroms) X	Y	Z
1	28	0	0.301283	-0.345340	-0.023575
2	15	0	1.286951	1.483458	-0.839569
3	15	0	2.193709	-0.916894	1.048540
4	6	0	2.956199	1.597694	0.031426
5	6	0	3.521224	0.193020	0.305882
6	1	0	1.715475	1.574424	-2.194503
7	1	0	0.887314	2.843413	-0.733983
8	1	0	2.394742	-0.652607	2.430666
9	1	0	2.886075	-2.156224	1.028511
10	6	0	-1.871481	-0.631287	1.063031
11	6	0	-1.583003	-0.320342	-0.280348
12	6	0	-2.817381	0.155557	1.746219
13	17	0	-0.870199	-1.926246	-1.341554
14	6	0	-2.343995	0.632706	-0.987229
15	6	0	-3.288645	1.372896	-0.293817
16	1	0	3.670276	2.199062	-0.540280
17	1	0	2.774868	2.119395	0.979327
18	1	0	4.407300	0.244733	0.946880
19	1	0	3.824488	-0.280716	-0.635908
20	6	0	-3.519912	1.150214	1.078087
21	1	0	-1.420983	-1.495526	1.540083
22	1	0	-3.030424	-0.058333	2.790896
23	1	0	-2.156411	0.800824	-2.042859
24	1	0	-3.851179	2.142231	-0.817599
25	1	0	-4.272020	1.733812	1.601226

3a$_{pf}$

SCF Done: E(RB+HF-LYP) = -1264.48298270 A.U. after 10 cycles

Center Number	Atomic Number	Atomic Type	Coordinates (Angstroms) X	Y	Z
1	28	0	0.369935	-0.475177	-0.261263
2	15	0	1.037688	1.590065	-0.174913
3	15	0	2.485578	-1.178168	0.339653
4	6	0	2.787245	1.622789	0.514930
5	6	0	3.550051	0.355849	0.085948
6	1	0	1.210598	2.350766	-1.364794
7	1	0	0.440735	2.625885	0.587528
8	1	0	2.804466	-1.469155	1.694526
9	1	0	3.354058	-2.151519	-0.224161
10	6	0	-2.017653	-0.808443	0.980843
11	6	0	-1.569134	-0.433977	-0.298900
12	6	0	-3.174647	-0.214870	1.494066
13	9	0	-0.879204	-1.721359	-1.086815
14	6	0	-2.364335	0.385725	-1.123856
15	6	0	-3.520730	0.945956	-0.594913
16	1	0	3.327988	2.525812	0.214302
17	1	0	2.690735	1.648459	1.607271
18	1	0	4.502143	0.273375	0.619238
19	1	0	3.778403	0.398397	-0.986203
20	6	0	-3.931467	0.663866	0.717847
21	1	0	-1.458027	-1.537263	1.561377
22	1	0	-3.498718	-0.471658	2.500228
23	1	0	-2.046671	0.605759	-2.138326
24	1	0	-4.114222	1.614475	-1.215000
25	1	0	-4.841792	1.104020	1.113804

3a$_{po}$

SCF Done: E(RB+HF-LYP) = -1279.76443148 A.U. after 1 cycles

Center Number	Atomic Number	Atomic Type	Coordinates (Angstroms) X	Y	Z
1	28	0	-0.417000	0.341714	-0.234308
2	15	0	-1.164294	-1.706594	-0.225258
3	15	0	-2.569365	1.064245	0.329107
4	6	0	-2.927624	-1.732506	0.424102
5	6	0	-3.653512	-0.442502	0.001211
6	1	0	-1.322658	-2.422800	-1.443552
7	1	0	-0.590826	-2.769471	0.515614
8	1	0	-2.936803	1.320538	1.679986
9	1	0	-3.408159	2.064991	-0.233863
10	6	0	2.004829	0.234081	1.148404
11	6	0	1.518305	0.195495	-0.175939
12	6	0	3.184832	-0.444607	1.478883
13	8	0	0.832541	1.665608	-0.804784
14	6	0	2.282110	-0.466389	-1.167469
15	6	0	3.451985	-1.123682	-0.817435
16	1	0	-3.476005	-2.619366	0.090798
17	1	0	-2.859527	-1.782079	1.517838
18	1	0	-4.621879	-0.354197	0.503222
19	1	0	-3.845212	-0.455489	-1.078945
20	6	0	3.917132	-1.125301	0.509481
21	1	0	1.449334	0.757273	1.923400
22	1	0	3.528759	-0.429771	2.511440
23	1	0	1.938402	-0.459259	-2.197924
24	1	0	4.017372	-1.643522	-1.588522
25	1	0	4.837747	-1.639330	0.770087
26	6	0	1.048701	2.848378	-0.055135
27	1	0	1.865981	2.712293	0.666871
28	1	0	0.148042	3.167079	0.489527
29	1	0	1.335426	3.637696	-0.761422

3a$_{ps}$

SCF Done: E(RB+HF-LYP) = -1602.77564056 A.U. after 11 cycles

Center Number	Atomic Number	Atomic Type	Coordinates (Angstroms) X	Y	Z
1	28	0	-0.415099	0.333876	0.081697

2	15	0	-1.350878	-1.143605	-1.322556
3	15	0	-2.393427	0.437280	1.220337
4	6	0	-3.041341	-1.591843	-0.618791
5	6	0	-3.663221	-0.375571	0.089160
6	1	0	-1.734525	-0.758249	-2.638278
7	1	0	-0.892738	-2.438754	-1.680678
8	1	0	-2.618903	-0.316655	2.405224
9	1	0	-3.136520	1.577060	1.625970
10	6	0	1.748797	-0.459227	1.411338
11	6	0	1.497343	0.070816	0.128183
12	6	0	2.702740	-1.466189	1.588265
13	16	0	0.811643	2.161558	0.237725
14	6	0	2.297689	-0.361111	-0.948843
15	6	0	3.269501	-1.340410	-0.753247
16	1	0	-3.712980	-1.982026	-1.390154
17	1	0	-2.870764	-2.398449	0.105134
18	1	0	-4.567858	-0.660264	0.635853
19	1	0	-3.951101	0.383168	-0.649144
20	6	0	3.471411	-1.907415	0.510903
21	1	0	1.217485	-0.064272	2.273396
22	1	0	2.869245	-1.876662	2.581799
23	1	0	2.135863	0.038503	-1.945315
24	1	0	3.863022	-1.679114	-1.599952
25	1	0	4.232418	-2.669673	0.654157
26	6	0	1.538734	2.636300	-1.380293
27	1	0	0.985923	2.199765	-2.215073
28	1	0	2.592770	2.349079	-1.439856
29	1	0	1.459801	3.725863	-1.440955

4a$_{pb}$

SCF Done: E(RB+HF-LYP) = -3738.60625861 A.U. after 10 cycles

Center Number	Atomic Number	Atomic Type	Coordinates (Angstroms) X	Y	Z
1	28	0	0.387444	0.097488	-0.007520
2	15	0	0.827047	-2.029477	-0.037061
3	15	0	2.660862	0.438839	0.013120
4	6	0	2.657272	-2.333071	-0.335305
5	6	0	3.487983	-1.218786	0.331145
6	1	0	0.567408	-2.760453	1.145259
7	1	0	0.209219	-2.892574	-0.965537
8	1	0	3.294971	0.876000	-1.173565
9	1	0	3.315338	1.294864	0.923724
10	6	0	-2.125433	-0.629617	1.217504
11	35	0	-0.069892	2.401544	-0.009985
12	6	0	-1.460453	-0.396897	0.005928
13	6	0	-3.490302	-0.937311	1.236461
14	6	0	-2.186907	-0.499435	-1.188484
15	6	0	-3.550244	-0.807622	-1.170391
16	1	0	2.963717	-3.325013	0.012428
17	1	0	2.799202	-2.310493	-1.422695
18	1	0	4.527159	-1.243001	-0.011068
19	1	0	3.498919	-1.357027	1.419082
20	6	0	-4.206692	-1.027190	0.042533
21	1	0	-1.589247	-0.551750	2.161386
22	1	0	-3.992144	-1.102325	2.187609
23	1	0	-1.698803	-0.316124	-2.143356
24	1	0	-4.100805	-0.870455	-2.106722
25	1	0	-5.267134	-1.266168	0.056235

4a$_{pc}$

SCF Done: E(RB+HF-LYP) = -1624.92027567 A.U. after 10 cycles

Center Number	Atomic Number	Atomic Type	Coordinates (Angstroms) X	Y	Z
1	28	0	0.378359	0.427478	-0.008715
2	15	0	0.801783	-1.697216	-0.054826
3	15	0	2.665895	0.753324	0.013527
4	6	0	2.629999	-2.015431	-0.348970
5	6	0	3.469451	-0.914609	0.329237
6	1	0	0.531006	-2.434672	1.120747
7	1	0	0.180431	-2.546596	-0.993206
8	1	0	3.311552	1.186677	-1.168594
9	1	0	3.326551	1.599718	0.929182
10	6	0	-2.125116	-0.336368	1.212772
11	17	0	-0.060295	2.605844	0.009918
12	6	0	-1.467834	-0.065478	0.005776
13	6	0	-3.494980	-0.622181	1.230809
14	6	0	-2.203634	-0.104863	-1.185974
15	6	0	-3.571351	-0.392307	-1.168628
16	1	0	2.925636	-3.012921	-0.007836
17	1	0	2.776526	-1.986035	-1.435582
18	1	0	4.510621	-0.950004	-0.005681
19	1	0	3.470728	-1.058344	1.416481
20	6	0	-4.221381	-0.651593	0.040144
21	1	0	-1.579714	-0.306200	2.154150
22	1	0	-3.992307	-0.817436	2.178549
23	1	0	-1.719880	0.113030	-2.135636
24	1	0	-4.130846	-0.406563	-2.101603
25	1	0	-5.285427	-0.874016	0.052921

4a$_{pf}$

SCF Done: E(RB+HF-LYP) = -1264.53170739 A.U. after 9 cycles

Center Number	Atomic Number	Atomic Type	Coordinates (Angstroms) X	Y	Z
1	28	0	-0.349966	-0.620327	-0.037352
2	15	0	-0.825158	1.514900	-0.016433
3	15	0	-2.692111	-0.962061	-0.025173
4	6	0	-2.658980	1.824611	-0.273031
5	6	0	-3.472130	0.694644	0.388591
6	1	0	-0.552105	2.234472	1.170573
7	1	0	-0.232901	2.403351	-0.938865
8	1	0	-3.381163	-1.311114	-1.213909
9	1	0	-3.383755	-1.835989	0.845492
10	6	0	2.150444	0.031026	1.217823
11	9	0	0.101799	-2.326840	-0.044967
12	6	0	1.475459	-0.111967	-0.001003
13	6	0	3.522941	0.300443	1.247943
14	6	0	2.200213	0.034437	-1.190770
15	6	0	3.572168	0.302863	-1.163384
16	1	0	-2.962350	2.807106	0.102682
17	1	0	-2.827214	1.824709	-1.356939
18	1	0	-4.525199	0.742850	0.095372
19	1	0	-3.432629	0.793024	1.480250
20	6	0	4.237615	0.437290	0.056921
21	1	0	1.612604	-0.087609	2.156404
22	1	0	4.033327	0.398375	2.203942
23	1	0	1.700621	-0.080095	-2.150709
24	1	0	4.121861	0.402843	-2.097134
25	1	0	5.304395	0.646121	0.078963

4a$_{po}$

SCF Done: E(RB+HF-LYP) = -1279.80273686 A.U. after 10 cycles

Center Number	Atomic Number	Atomic Type	Coordinates (Angstroms) X	Y	Z
1	28	0	0.396981	0.465214	-0.026054
2	15	0	0.989809	-1.663566	-0.021367
3	15	0	2.713723	0.907211	-0.009076
4	6	0	2.835751	-1.867129	-0.304160
5	6	0	3.595044	-0.705762	0.368034
6	1	0	0.782206	-2.418045	1.159432
7	1	0	0.445860	-2.587564	-0.941024
8	1	0	3.342920	1.804277	0.884383
9	1	0	3.382379	1.329011	-1.185944
10	6	0	-2.077929	-0.349921	1.218822
11	8	0	0.043894	2.231715	-0.029304
12	6	0	-1.410872	-0.127259	0.004123
13	6	0	-3.421208	-0.740925	1.244763
14	6	0	-2.128329	-0.322544	-1.186597
15	6	0	-3.470994	-0.713000	-1.165122
16	1	0	3.197499	-2.838492	0.048232
17	1	0	2.989070	-1.837442	-1.389949
18	1	0	4.645644	-0.692420	0.061868
19	1	0	3.574322	-0.825086	1.458169
20	6	0	-4.122636	-0.923846	0.051925
21	1	0	-1.553756	-0.204854	2.162008
22	1	0	-3.919294	-0.900485	2.199122
23	1	0	-1.643360	-0.155874	-2.146994
24	1	0	-4.008906	-0.850954	-2.101081
25	1	0	-5.166238	-1.228474	0.069984
26	6	0	-1.202870	2.862674	-0.027749
27	1	0	-1.809907	2.626330	0.862501
28	1	0	-1.817017	2.618731	-0.911118
29	1	0	-1.036766	3.953205	-0.033228

4a$_{ps}$

SCF Done: E(RB+HF-LYP) = -1602.80398296 A.U. after 10 cycles

Center Number	Atomic Number	Atomic Type	Coordinates (Angstroms) X	Y	Z
1	28	0	0.450524	0.312447	-0.039849
2	15	0	1.122389	-1.792381	-0.004656
3	15	0	2.678774	0.861911	-0.089381
4	6	0	2.985085	-1.912000	-0.222124
5	6	0	3.651757	-0.667507	0.395203
6	1	0	0.906581	-2.515126	1.193179
7	1	0	0.647386	-2.767242	-0.910579
8	1	0	3.278981	1.868150	0.699569
9	1	0	3.282790	1.196222	-1.326273
10	6	0	-2.001637	-0.594886	1.209575
11	16	0	-0.118345	2.443930	0.051508
12	6	0	-1.345729	-0.330348	-0.003418
13	6	0	-3.313446	-1.081169	1.230516

14	6	0	-2.042643	-0.580612	-1.196644
15	6	0	-3.354360	-1.065564	-1.178824
16	1	0	3.389618	-2.834966	0.205339
17	1	0	3.173555	-1.942758	-1.302224
18	1	0	4.704286	-0.595350	0.103713
19	1	0	3.616540	-0.723786	1.489913
20	6	0	-3.995724	-1.317232	0.035745
21	1	0	-1.494246	-0.406174	2.153785
22	1	0	-3.802999	-1.271439	2.183649
23	1	0	-1.566478	-0.384389	-2.155601
24	1	0	-3.876268	-1.244341	-2.116917
25	1	0	-5.015748	-1.693195	0.050636
26	6	0	-1.932513	2.721088	-0.016465
27	1	0	-2.438987	2.244872	0.825733
28	1	0	-2.359016	2.341493	-0.947439
29	1	0	-2.089321	3.803053	0.034312

5a$_{pf}$

SCF Done: E(RB+HF-LYP) = -2385.20255108 A.U. after 11 cycles

Center Number	Atomic Number	Atomic Type	Coordinates (Angstroms) X	Y	Z
1	28	0	-0.524189	0.344174	0.037049
2	15	0	0.939161	1.014328	-1.510843
3	15	0	-0.920037	2.504190	0.577012
4	6	0	0.669387	2.869478	-1.679130
5	6	0	0.409321	3.493909	-0.297553
6	1	0	2.350180	0.969126	-1.418183
7	1	0	0.838135	0.589392	-2.855590
8	1	0	-2.087035	3.202205	0.168751
9	1	0	-0.851536	3.022111	1.890683
10	6	0	-1.800148	-0.852983	1.087261
11	6	0	-1.008942	-1.565137	0.131847
12	6	0	-3.191287	-0.686539	0.785409
13	9	0	0.097621	-2.376882	0.690194
14	6	0	-1.593404	-2.153205	-1.029714
15	6	0	-2.917512	-1.907376	-1.297561
16	1	0	1.527883	3.337274	-2.171243
17	1	0	-0.200795	3.011607	-2.331638
18	1	0	0.141926	4.551325	-0.386818
19	1	0	1.308524	3.427306	0.325736
20	6	0	-3.728054	-1.174441	-0.381619
21	1	0	-1.444362	-0.741499	2.108527
22	1	0	-3.825055	-0.198441	1.521741
23	1	0	-0.973805	-2.759903	-1.682921
24	1	0	-3.361366	-2.305070	-2.206049
25	1	0	-4.785209	-1.043510	-0.593218
26	12	0	1.697331	-1.197261	0.566425
27	17	0	3.170436	-2.008003	-0.923208
28	17	0	1.739576	0.251547	2.316021

5a$_{po}$

SCF Done: E(RB+HF-LYP) = -2400.49526512 A.U. after 13 cycles

Center Number	Atomic Number	Atomic Type	Coordinates (Angstroms) X	Y	Z
1	28	0	-0.220937	-0.730183	-0.036893
2	15	0	-1.532806	0.265653	-1.524967
3	15	0	-1.991893	-1.860423	0.770315
4	6	0	-3.209084	-0.588203	-1.393636
5	6	0	-3.495997	-0.996961	0.061505
6	1	0	-1.944818	1.620438	-1.573276
7	1	0	-1.259283	0.133023	-2.907630
8	1	0	-2.282771	-3.210229	0.431965
9	1	0	-2.333614	-1.948531	2.140132
10	6	0	1.453608	-1.319383	0.987086
11	6	0	1.767181	-0.355804	-0.031219
12	6	0	1.794853	-2.689934	0.750058
13	8	0	1.995809	1.009165	0.357836
14	6	0	2.398766	-0.790294	-1.243361
15	6	0	2.650339	-2.125135	-1.449900
16	1	0	-3.996879	0.065264	-1.781162
17	1	0	-3.171041	-1.473968	-2.039324
18	1	0	-4.391338	-1.623584	0.121747
19	1	0	-3.663769	-0.108976	0.681341
20	6	0	2.359484	-3.086362	-0.438779
21	1	0	1.253411	-0.978710	2.000464
22	1	0	1.618438	-3.412634	1.543384
23	1	0	2.664576	-0.041834	-1.985381
24	1	0	3.100254	-2.449094	-2.384561
25	1	0	2.611518	-4.129985	-0.603951
26	6	0	3.306741	1.303535	0.883123
27	1	0	4.067080	0.991179	0.162236
28	1	0	3.452878	0.785333	1.835678
29	1	0	3.349649	2.384536	1.026073
30	12	0	0.211612	1.974476	0.359967
31	17	0	0.270726	3.713894	-1.076412
32	17	0	-1.016534	1.573675	2.238382

5a$_{ps}$

SCF Done: E(RB+HF-LYP) = -2723.47266789 A.U. after 8 cycles

Center Number	Atomic Number	Atomic Type	Coordinates (Angstroms) X	Y	Z
1	28	0	-0.030286	-0.785256	0.169350
2	15	0	-1.388364	-1.658408	-1.398317
3	15	0	-1.698036	-0.811009	1.637919
4	6	0	-2.919453	-2.228990	-0.463474
5	6	0	-3.251540	-1.270458	0.694132
6	1	0	-1.951896	-0.892888	-2.443266
7	1	0	-1.115885	-2.828964	-2.152986
8	1	0	-1.626563	-1.848232	2.605822
9	1	0	-2.202489	0.189130	2.504630
10	6	0	1.781847	-0.236717	0.957179
11	6	0	1.859618	-0.302584	-0.479630
12	6	0	2.335689	-1.329842	1.698997
13	16	0	1.469849	1.161743	-1.477572
14	6	0	2.575320	-1.376114	-1.105864
15	6	0	3.082366	-2.404213	-0.349882
16	1	0	-3.776105	-2.332155	-1.136350
17	1	0	-2.685951	-3.228009	-0.074608
18	1	0	-4.004875	-1.705485	1.358495
19	1	0	-3.646302	-0.328607	0.298886
20	6	0	2.940341	-2.392023	1.066916
21	1	0	1.610645	0.704861	1.472899
22	1	0	2.299005	-1.286767	2.784761
23	1	0	2.691775	-1.366909	-2.186195
24	1	0	3.604315	-3.226044	-0.832193
25	1	0	3.359883	-3.205344	1.652909
26	6	0	2.835844	2.331667	-1.075501
27	1	0	3.791358	1.854431	-1.304108
28	1	0	2.785033	2.634942	-0.028575
29	1	0	2.697162	3.206357	-1.716589
30	12	0	-0.566160	1.886733	-0.027765
31	17	0	-2.562796	1.937957	-1.104966
32	17	0	0.277563	3.162929	1.644831

6a$_{pf}$

SCF Done: E(RB+HF-LYP) = -2385.19399641 A.U. after 10 cycles

Center Number	Atomic Number	Atomic Type	Coordinates (Angstroms) X	Y	Z
1	28	0	-0.501418	0.607874	0.000313
2	15	0	1.086174	0.743257	-1.567109
3	15	0	0.031941	2.741061	0.649590
4	6	0	1.757592	2.496132	-1.529801
5	6	0	1.720378	3.050413	-0.094369
6	1	0	2.263429	-0.039733	-1.523246
7	1	0	0.785618	0.570752	-2.937297
8	1	0	-0.684423	3.883654	0.211484
9	1	0	0.215783	3.126502	1.994668
10	6	0	-2.125268	-0.412256	0.963166
11	6	0	-1.548565	-0.883745	-0.239242
12	6	0	-3.529739	-0.196537	0.983801
13	9	0	-0.403599	-2.401313	0.117029
14	6	0	-2.326729	-1.260963	-1.348043
15	6	0	-3.688824	-1.017956	-1.292486
16	1	0	2.771922	2.528551	-1.938893
17	1	0	1.119282	3.097980	-2.187904
18	1	0	1.985799	4.111924	-0.077050
19	1	0	2.433035	2.512656	0.540672
20	6	0	-4.294142	-0.483504	-0.131104
21	1	0	-1.559239	-0.410355	1.892123
22	1	0	-4.000691	0.127839	1.908545
23	1	0	-1.857942	-1.680747	-2.231933
24	1	0	-4.300860	-1.232558	-2.165208
25	1	0	-5.369469	-0.332480	-0.109908
26	12	0	1.305805	-1.921815	0.612662
27	17	0	3.116262	-2.644815	-0.512939
28	17	0	1.333164	-0.215486	2.165951

6a$_{po}$

SCF Done: E(RB+HF-LYP) = -2400.45393960 A.U. after 11 cycles

Center Number	Atomic Number	Atomic Type	Coordinates (Angstroms) X	Y	Z
1	28	0	-1.060629	0.413841	-0.212816
2	15	0	-1.429099	-0.648083	1.668989
3	15	0	-2.985924	-0.516779	-1.076208
4	6	0	-3.120679	-1.448270	1.568038
5	6	0	-3.396874	-1.900092	0.120497
6	1	0	-0.593114	-1.738710	1.980885
7	1	0	-1.457350	-0.032427	2.941246
8	1	0	-4.213248	0.191878	-1.117391
9	1	0	-3.094127	-1.168077	-2.324093

10	6	0	0.478464	1.725361	-1.209307
11	6	0	0.305182	1.549333	0.181300
12	6	0	0.643704	3.033690	-1.717079
13	8	0	1.721925	0.081636	1.043918
14	6	0	0.363491	2.641347	1.061901
15	6	0	0.524251	3.916989	0.533670
16	1	0	-3.207034	-2.289465	2.263179
17	1	0	-3.852567	-0.691862	1.877313
18	1	0	-4.431065	-2.238297	0.005042
19	1	0	-2.737771	-2.732744	-0.148595
20	6	0	0.665575	4.117845	-0.852513
21	1	0	0.588438	0.873031	-1.879428
22	1	0	0.806783	3.174179	-2.782805
23	1	0	0.244078	2.496656	2.131291
24	1	0	0.520452	4.773729	1.203587
25	1	0	0.808023	5.122451	-1.240072
26	6	0	2.697437	0.686410	1.864416
27	1	0	2.458393	0.555157	2.932192
28	1	0	2.755846	1.769125	1.670347
29	1	0	3.699880	0.265962	1.692714
30	12	0	2.113329	-1.352870	-0.153583
31	17	0	4.120651	-2.350509	-0.298763
32	17	0	0.204566	-1.931817	-1.345480

6a$_{ps}$

SCF Done: E(RB+HF-LYP) = -2723.43469233 A.U. after 10 cycles

Center Number	Atomic Number	Atomic Type	Coordinates (Angstroms) X	Y	Z
1	28	0	-1.152260	0.547094	-0.270654
2	15	0	-1.946716	-0.142900	1.664610
3	15	0	-3.016159	-0.358796	-1.296014
4	6	0	-3.664971	-0.835994	1.386350
5	6	0	-3.746547	-1.497513	-0.002584
6	1	0	-1.264981	-1.204882	2.289258
7	1	0	-2.132209	0.694984	2.786801
8	1	0	-4.137417	0.438944	-1.637400
9	1	0	-2.992232	-1.177870	-2.444240
10	6	0	0.614311	1.464674	-1.289655
11	6	0	0.316208	1.573767	0.085474
12	6	0	1.065038	2.606864	-1.989460
13	16	0	1.672674	-0.189163	1.742502
14	6	0	0.532852	2.773728	0.778145
15	6	0	0.982788	3.882196	0.068676
16	1	0	-3.937764	-1.545166	2.174261
17	1	0	-4.363515	0.007485	1.449643
18	1	0	-4.776833	-1.774294	-0.245697
19	1	0	-3.134995	-2.405535	-0.027576
20	6	0	1.247813	3.802979	-1.311979
21	1	0	0.606988	0.500565	-1.801838
22	1	0	1.323845	2.521780	-3.041786
23	1	0	0.323877	2.842524	1.841040
24	1	0	1.113882	4.828868	0.587613
25	1	0	1.615667	4.677534	-1.840859
26	6	0	3.332518	0.600833	1.896485
27	1	0	3.618597	0.628919	2.950986
28	1	0	3.276127	1.626398	1.517088
29	1	0	4.090428	0.051267	1.333795
30	12	0	1.927372	-1.783026	-0.026128
31	17	0	3.914896	-2.432708	-0.849914
32	17	0	-0.179271	-2.291470	-0.864022

7a$_{pb}$

SCF Done: E(RB+HF-LYP) = -4859.29212852 A.U. after 11 cycles

Center Number	Atomic Number	Atomic Type	Coordinates (Angstroms) X	Y	Z
1	28	0	1.199629	0.177353	0.550478
2	15	0	2.488375	1.291896	-0.797555
3	15	0	2.945969	-1.306774	0.789493
4	6	0	4.186348	0.506904	-0.901224
5	6	0	4.068051	-1.010937	-0.672313
6	1	0	2.044866	1.333353	-2.133384
7	1	0	2.773818	2.658031	-0.592420
8	1	0	3.842222	-1.241093	1.884300
9	1	0	2.708443	-2.693434	0.770596
10	6	0	-0.607786	2.275611	1.262068
11	6	0	-0.181085	1.476137	0.183001
12	6	0	-1.632410	3.206623	1.100022
13	35	0	-3.701043	-1.275473	-0.273690
14	6	0	-0.814208	1.649887	-1.062097
15	6	0	-1.860612	2.574569	-1.216749
16	1	0	4.663305	0.734504	-1.859890
17	1	0	4.796352	0.967265	-0.114421
18	1	0	5.052740	-1.468969	-0.539581
19	1	0	3.580560	-1.490502	-1.527660
20	6	0	-2.265075	3.356112	-0.140139
21	1	0	-0.154424	2.151415	2.241729
22	1	0	-1.951952	3.807795	1.947785
23	1	0	-0.501127	1.065215	-1.924976
24	1	0	-2.350873	2.671536	-2.181749
25	1	0	-3.073814	4.072152	-0.256702
26	12	0	-1.337259	-0.978445	-0.084749
27	17	0	0.371493	-1.667090	-1.547275
28	17	0	-0.154470	-0.987999	2.034018

7a$_{pc}$

SCF Done: E(RB+HF-LYP) = -2745.61167498 A.U. after 11 cycles

Center Number	Atomic Number	Atomic Type	Coordinates (Angstroms) X	Y	Z
1	28	0	0.784132	0.175157	0.553706
2	15	0	1.839002	1.634193	-0.658347
3	15	0	2.795299	-0.926141	0.766520
4	6	0	3.665690	1.228224	-0.747884
5	6	0	3.859637	-0.294674	-0.630657
6	1	0	1.431988	1.690253	-2.005381
7	1	0	1.823568	3.008671	-0.341778
8	1	0	3.633803	-0.751505	1.894723
9	1	0	2.858822	-2.326753	0.648302
10	6	0	-1.444270	1.816765	1.291688
11	6	0	-0.827185	1.181010	0.195807
12	6	0	-2.636291	2.520839	1.130269
13	17	0	-3.561306	-2.110656	-0.496473
14	6	0	-1.445514	1.284158	-1.064669
15	6	0	-2.658322	1.976089	-1.219532
16	1	0	4.109256	1.621561	-1.668141
17	1	0	4.146563	1.741989	0.093490
18	1	0	4.915110	-0.549635	-0.496043
19	1	0	3.499620	-0.798109	-1.534136
20	6	0	-3.249720	2.598856	-0.126095
21	1	0	-1.004239	1.738980	2.282106
22	1	0	-3.100085	2.997727	1.990309
23	1	0	-0.990714	0.823417	-1.939403
24	1	0	-3.128907	2.018176	-2.198140
25	1	0	-4.187161	3.135472	-0.242497
26	12	0	-1.448712	-1.419454	-0.226274
27	17	0	0.395782	-1.674353	-1.661355
28	17	0	-0.344914	-1.315554	1.930297

7a$_{pf}$

SCF Done: E(RB+HF-LYP) = -2385.24343596 A.U. after 10 cycles

Center Number	Atomic Number	Atomic Type	Coordinates (Angstroms) X	Y	Z
1	28	0	-0.555183	-0.147920	0.571300
2	15	0	-1.338803	-1.848384	-0.521288
3	15	0	-2.732631	0.568518	0.794983
4	6	0	-3.210773	-1.795863	-0.576717
5	6	0	-3.685798	-0.331791	-0.534218
6	1	0	-0.955282	-1.910885	-1.874236
7	1	0	-1.060532	-3.173848	-0.126582
8	1	0	-3.503803	0.305724	1.954162
9	1	0	-3.062954	1.922569	0.602936
10	6	0	1.960960	-1.298935	1.305054
11	6	0	1.205172	-0.856434	0.201566
12	6	0	3.265986	-1.759243	1.139144
13	9	0	2.826743	2.555764	-0.775834
14	6	0	1.802782	-0.901006	-1.071915
15	6	0	3.126456	-1.343589	-1.232504
16	1	0	-3.590956	-2.316879	-1.461271
17	1	0	-3.570041	-2.341360	0.304491
18	1	0	-4.767662	-0.271424	-0.382173
19	1	0	-3.442528	0.177454	-1.472562
20	6	0	3.855152	-1.777947	-0.130872
21	1	0	1.536305	-1.258322	2.304438
22	1	0	3.834200	-2.089008	2.005587
23	1	0	1.247745	-0.584478	-1.953396
24	1	0	3.574305	-1.342305	-2.222708
25	1	0	4.878371	-2.122510	-0.252321
26	12	0	1.287937	1.772837	-0.437208
27	17	0	-0.639140	1.583331	-1.781459
28	17	0	0.326429	1.620077	1.787552

7a$_{po}$

SCF Done: E(RB+HF-LYP) = -2400.51672776 A.U. after 11 cycles

Center Number	Atomic Number	Atomic Type	Coordinates (Angstroms) X	Y	Z
1	28	0	-0.675214	0.239824	0.484620
2	15	0	-2.060314	1.379166	-0.746029
3	15	0	-2.508247	-1.129897	1.027826
4	6	0	-3.582757	0.351661	-1.088473
5	6	0	-4.014119	-0.383777	0.194000
6	1	0	-2.585821	2.600649	-0.262944

7	1	0	-1.647451	1.792602	-2.025836
8	1	0	-2.503864	-2.461309	0.562667
9	1	0	-2.997228	-1.371365	2.333811
10	6	0	1.426933	1.449257	-1.133565
11	6	0	0.646480	1.541979	0.029562
12	6	0	2.501865	2.321496	-1.345314
13	8	0	0.632218	-0.915381	1.301218
14	6	0	0.939324	2.557876	0.952272
15	6	0	2.007392	3.435625	0.735477
16	1	0	-4.396864	0.960802	-1.494854
17	1	0	-3.283540	-0.369723	-1.857043
18	1	0	-4.774112	-1.139633	-0.024419
19	1	0	-4.452789	0.323630	0.908237
20	6	0	2.795927	3.314550	-0.410225
21	1	0	1.194282	0.703282	-1.892109
22	1	0	3.104201	2.223037	-2.245296
23	1	0	0.341733	2.670337	1.855473
24	1	0	2.223211	4.212699	1.465466
25	1	0	3.628241	3.993368	-0.575905
26	6	0	1.253377	-0.581965	2.531335
27	1	0	0.518661	-0.594422	3.349712
28	1	0	1.713661	0.413684	2.492670
29	1	0	2.035904	-1.316158	2.760779
30	12	0	1.422341	-1.795426	-0.229888
31	17	0	3.428948	-2.792815	-0.182428
32	17	0	-0.291077	-1.811163	-1.793350

7a$_{ps}$

SCF Done: E(RB+HF-LYP) = -2723.49524556 A.U. after 11 cycles

Center Number	Atomic Number	Atomic Type	Coordinates (Angstroms) X	Y	Z
1	28	0	-0.736506	0.376131	0.530567
2	15	0	-1.973482	1.399143	-0.962293
3	15	0	-2.663566	-0.770799	1.126037
4	6	0	-3.548714	0.435135	-1.242638
5	6	0	-4.079967	-0.083192	0.105190
6	1	0	-2.429815	2.712496	-0.698056
7	1	0	-1.462163	1.588290	-2.259241
8	1	0	-2.734234	-2.160929	0.902630
9	1	0	-3.203243	-0.735472	2.432015
10	6	0	1.465231	1.228705	-1.196740
11	6	0	0.701293	1.498081	-0.049722
12	6	0	2.576476	2.016257	-1.523715
13	16	0	0.561189	-0.950156	1.867085
14	6	0	1.050718	2.609189	0.734511
15	6	0	2.149378	3.406921	0.398974
16	1	0	-4.301222	1.033283	-1.766723
17	1	0	-3.265821	-0.403202	-1.887691
18	1	0	-4.866403	-0.829475	-0.040683
19	1	0	-4.513637	0.739561	0.686418
20	6	0	2.921675	3.107082	-0.725779
21	1	0	1.189379	0.414312	-1.866915
22	1	0	3.164186	1.775395	-2.406055
23	1	0	0.476151	2.852561	1.626339
24	1	0	2.405308	4.260498	1.022943
25	1	0	3.780597	3.722179	-0.980228
26	6	0	2.155609	-0.174900	2.380291
27	1	0	2.823226	-0.976278	2.703681
28	1	0	1.963046	0.499980	3.216902
29	1	0	2.616182	0.380776	1.563713
30	12	0	1.173642	-1.942795	-0.304380
31	17	0	3.239441	-2.744395	-0.645544
32	17	0	-0.702768	-1.995277	-1.652346

8a$_{po}$

SCF Done: E(RB+HF-LYP) = -2400.44819231 A.U. after 10 cycles

Center Number	Atomic Number	Atomic Type	Coordinates (Angstroms) X	Y	Z
1	28	0	-1.048639	0.068861	0.244924
2	15	0	-2.803554	1.362501	0.392591
3	15	0	-2.373280	-1.730410	-0.254233
4	6	0	-4.260732	0.362857	-0.255759
5	6	0	-4.113595	-1.124471	0.119446
6	1	0	-3.322701	1.799424	1.642571
7	1	0	-3.002115	2.584372	-0.297576
8	1	0	-2.515915	-2.156110	-1.597484
9	1	0	-2.409317	-3.014556	0.339659
10	6	0	0.890185	0.736584	-1.265466
11	6	0	0.543966	1.125982	0.059519
12	6	0	1.448638	1.687681	-2.137365
13	8	0	0.807588	-0.209142	1.076526
14	6	0	0.916144	2.406548	0.533146
15	6	0	1.490466	3.308223	-0.349762
16	1	0	-5.213341	0.765546	0.103023
17	1	0	-4.248280	0.476728	-1.346700
18	1	0	-4.870639	-1.728028	-0.390899
19	1	0	-4.264799	-1.256661	1.198073
20	6	0	1.758262	2.965659	-1.688810
21	1	0	0.608445	-0.250195	-1.642935
22	1	0	1.658971	1.397856	-3.163665
23	1	0	0.706960	2.699353	1.556675
24	1	0	1.736810	4.305112	0.007929
25	1	0	2.224707	3.685521	-2.353380
26	6	0	0.950211	0.092361	2.475429
27	1	0	0.935260	-0.859163	3.013505
28	1	0	0.114579	0.709975	2.815683
29	1	0	1.903063	0.602858	2.646899
30	12	0	2.264197	-1.154472	-0.016642
31	17	0	1.352791	-2.912399	-1.124046
32	17	0	4.270761	-0.617792	0.840554

8a$_{ps}$

SCF Done: E(RB+HF-LYP) = -2723.44616557 A.U. after 11 cycles

Center Number	Atomic Number	Atomic Type	Coordinates (Angstroms) X	Y	Z
1	28	0	-1.276337	0.057294	-0.150792
2	15	0	-3.018998	-1.324736	-0.338971
3	15	0	-2.653249	1.777078	0.324076
4	6	0	-4.512049	-0.341067	0.258093
5	6	0	-4.371662	1.145710	-0.114790
6	1	0	-3.499693	-1.757156	-1.606062
7	1	0	-3.263544	-2.551606	0.331919
8	1	0	-2.874251	2.199226	1.661177
9	1	0	-2.708341	3.065939	-0.263570
10	6	0	0.718900	-0.187113	1.403338
11	6	0	0.431881	-0.803262	0.155234
12	6	0	1.150221	-0.974252	2.487520
13	16	0	0.532952	0.515232	-1.424754
14	6	0	0.704485	-2.180833	-0.010922
15	6	0	1.152097	-2.929496	1.068480
16	1	0	-5.447157	-0.754682	-0.132657
17	1	0	-4.536232	-0.452508	1.349213
18	1	0	-5.153012	1.742918	0.365898
19	1	0	-4.481794	1.274672	-1.198667
20	6	0	1.370557	-2.336181	2.323857
21	1	0	0.600290	0.886925	1.533725
22	1	0	1.342792	-0.494213	3.443158
23	1	0	0.529612	-2.663326	-0.965821
24	1	0	1.331197	-3.993351	0.936530
25	1	0	1.735049	-2.936015	3.152132
26	6	0	0.933204	-0.698947	-2.747552
27	1	0	0.078630	-1.356637	-2.916779
28	1	0	1.833123	-1.263369	-2.493369
29	1	0	1.114325	-0.107859	-3.648801
30	12	0	2.733482	0.863474	-0.115714
31	17	0	2.687848	2.844822	0.947005
32	17	0	4.219524	-0.609592	-0.938613

9a$_{vb}$

SCF Done: E(RB+HF-LYP) = -4860.66376738 A.U. after 9 cycles

Center Number	Atomic Number	Atomic Type	Coordinates (Angstroms) X	Y	Z
1	6	0	1.085969	2.646218	0.546875
2	6	0	0.518093	2.241884	-0.682833
3	1	0	0.671418	2.755062	-1.627043
4	1	0	0.540208	2.539224	1.481139
5	35	0	-1.462079	1.764003	-0.681871
6	1	0	1.829748	3.444304	0.532932
7	28	0	1.725575	0.904537	-0.090446
8	15	0	2.034124	-0.842414	-1.469941
9	15	0	3.245782	0.021136	1.293586
10	6	0	3.477326	-1.836909	-0.782051
11	6	0	3.488447	-1.758842	0.755609
12	1	0	1.054586	-1.843544	-1.661595
13	1	0	2.423276	-0.713026	-2.825646
14	1	0	4.589113	0.481805	1.317650
15	1	0	3.080370	-0.120900	2.689951
16	1	0	3.438368	-2.876082	-1.122973
17	1	0	4.393744	-1.392872	-1.190089
18	1	0	4.406933	-2.189895	1.166695
19	1	0	2.638430	-2.312590	1.169124
20	12	0	-1.561151	-0.827914	0.060603
21	17	0	-1.823581	-2.127076	-1.787660
22	17	0	-0.178673	-1.149853	1.860095
23	6	0	-4.662683	-0.872696	0.106918
24	6	0	-3.707122	-0.187790	2.201620
25	8	0	-3.462622	-0.655266	0.866255
26	1	0	-4.356319	-1.268181	-0.861823
27	1	0	-5.203863	0.073226	-0.014894
28	1	0	-5.297347	-1.600912	0.624441
29	1	0	-2.737746	-0.111689	2.694872
30	1	0	-4.338804	-0.908732	2.732898
31	1	0	-4.201113	0.790547	2.172156

9a$_{vc}$
SCF Done: E(RB+HF-LYP) = -2746.98295359 A.U. after 9 cycles

Center Number	Atomic Number	Atomic Type	Coordinates (Angstroms) X	Y	Z
1	6	0	-1.012045	-2.729860	-0.526110
2	6	0	-0.370301	-1.918442	-1.490848
3	1	0	-0.503361	-2.022477	-2.563023
4	1	0	-0.496848	-3.032600	0.382450
5	17	0	1.457627	-1.591305	-1.241743
6	1	0	-1.791247	-3.411876	-0.868314
7	28	0	-1.583132	-0.858745	-0.467262
8	15	0	-1.854307	1.280401	-1.102468
9	15	0	-3.087798	-0.525713	1.150798
10	6	0	-3.287357	1.967092	-0.091873
11	6	0	-3.297296	1.330489	1.309736
12	1	0	-0.868796	2.275884	-0.917186
13	1	0	-2.245604	1.661851	-2.409155
14	1	0	-4.439756	-0.942820	1.025501
15	1	0	-2.906719	-0.911417	2.498525
16	1	0	-3.236857	3.058497	-0.028107
17	1	0	-4.209232	1.713376	-0.629833
18	1	0	-4.205783	1.596338	1.859664
19	1	0	-2.434453	1.677718	1.888723
20	12	0	1.698423	0.528943	0.133987
21	17	0	2.020760	2.294927	-1.260497
22	17	0	0.391119	0.368105	2.010069
23	6	0	4.799636	0.382903	0.080403
24	6	0	3.827034	-0.932009	1.839670
25	8	0	3.597549	-0.012631	0.761249
26	1	0	4.507321	1.103936	-0.683323
27	1	0	5.274625	-0.492815	-0.377595
28	1	0	5.487977	0.849778	0.793992
29	1	0	2.862542	-1.112068	2.315306
30	1	0	4.519160	-0.485232	2.562434
31	1	0	4.245193	-1.868222	1.451527

9a$_{vf}$
SCF Done: E(RB+HF-LYP) = -2386.62983012 A.U. after 9 cycles

Center Number	Atomic Number	Atomic Type	Coordinates (Angstroms) X	Y	Z
1	6	0	-0.586673	-2.127619	-1.685947
2	6	0	0.081412	-0.932915	-2.011711
3	1	0	0.140282	-0.475139	-2.993503
4	1	0	-0.137254	-2.827939	-0.985124
5	9	0	1.447878	-0.809789	-1.435700
6	1	0	-1.262700	-2.562024	-2.421298
7	28	0	-1.331730	-0.556399	-0.777665
8	15	0	-1.726634	1.607632	-0.323163
9	15	0	-3.075950	-1.107501	0.509700
10	6	0	-3.394131	1.664661	0.549661
11	6	0	-3.547528	0.436581	1.464938
12	1	0	-0.927965	2.363240	0.561748
13	1	0	-1.905938	2.608351	-1.307410
14	1	0	-4.332667	-1.482300	-0.034948
15	1	0	-3.034696	-2.078186	1.537440
16	1	0	-3.512365	2.594301	1.115411
17	1	0	-4.167067	1.655303	-0.229033
18	1	0	-4.558987	0.371718	1.878519
19	1	0	-2.844185	0.501173	2.303024
20	12	0	1.652563	0.317566	0.188420
21	17	0	1.944787	2.494053	-0.432491
22	17	0	0.436138	-0.597479	1.919676
23	6	0	4.739390	0.221859	-0.073938
24	6	0	3.872100	-1.581545	1.249666
25	8	0	3.585370	-0.365472	0.545533
26	1	0	4.410002	1.153559	-0.534657
27	1	0	5.146535	-0.460033	-0.830432
28	1	0	5.499930	0.429565	0.687605
29	1	0	2.938449	-1.911280	1.706387
30	1	0	4.619806	-1.389534	2.028003
31	1	0	4.248275	-2.340404	0.552671

10a$_{vb}$
SCF Done: E(RB+HF-LYP) = -4860.65470507 A.U. after 11 cycles

Center Number	Atomic Number	Atomic Type	Coordinates (Angstroms) X	Y	Z
1	6	0	-1.056366	2.519498	-1.444841
2	6	0	-0.919854	2.429673	-0.090797
3	1	0	-0.992851	3.210238	0.657772
4	1	0	-0.578359	1.806364	-2.115882
5	35	0	1.535317	1.898190	0.743108
6	1	0	-1.490543	3.402673	-1.915918
7	28	0	-1.811702	0.875309	-0.333354
8	15	0	-1.863194	-0.241458	1.598220
9	15	0	-3.348662	-0.626105	-1.146654
10	6	0	-3.153573	-1.597885	1.465217
11	6	0	-3.247972	-2.093025	0.009998
12	1	0	-0.708398	-0.937035	2.021437
13	1	0	-2.209533	0.385051	2.816857
14	1	0	-4.739626	-0.349448	-1.131972
15	1	0	-3.280578	-1.231080	-2.419774
16	1	0	-2.918534	-2.422987	2.144354
17	1	0	-4.111127	-1.169779	1.785506
18	1	0	-4.095092	-2.773403	-0.121353
19	1	0	-2.333720	-2.628113	-0.268324
20	12	0	1.620036	-0.530574	0.038150
21	17	0	1.731616	-2.071630	1.737737
22	17	0	0.044708	-0.982091	-1.642983
23	6	0	4.634886	-0.238080	-0.288708
24	6	0	3.666070	-1.821904	-1.803800
25	8	0	3.443282	-0.686530	-0.952719
26	1	0	4.362899	0.648786	0.285496
27	1	0	5.391940	0.022942	-1.036998
28	1	0	5.015865	-1.018960	0.379160
29	1	0	2.710590	-2.054642	-2.275426
30	1	0	4.015869	-2.676969	-1.214030
31	1	0	4.407217	-1.562758	-2.568558

10a$_{vc}$
SCF Done: E(RB+HF-LYP) = -2746.97278587 A.U. after 9 cycles

Center Number	Atomic Number	Atomic Type	Coordinates (Angstroms) X	Y	Z
1	6	0	0.962114	2.891221	0.489563
2	6	0	0.822007	2.387447	-0.773278
3	1	0	0.923538	2.886219	-1.729994
4	1	0	0.426304	2.463113	1.335658
5	17	0	-1.487630	1.741524	-1.347876
6	1	0	1.440269	3.856354	0.662853
7	28	0	1.677787	0.981582	-0.024852
8	15	0	1.754571	-0.713748	-1.481857
9	15	0	3.159811	-0.181751	1.283309
10	6	0	3.001594	-1.971180	-0.857336
11	6	0	3.049339	-1.950029	0.681756
12	1	0	0.595273	-1.489721	-1.707406
13	1	0	2.164077	-0.533506	-2.822731
14	1	0	4.557454	0.051146	1.222078
15	1	0	3.045338	-0.326095	2.682666
16	1	0	2.760297	-2.972278	-1.227316
17	1	0	3.977920	-1.693827	-1.272863
18	1	0	3.875499	-2.560811	1.059022
19	1	0	2.115527	-2.345751	1.095456
20	12	0	-1.766144	-0.250571	-0.090147
21	17	0	-2.000702	-2.188135	-1.296686
22	17	0	-0.273150	-0.330950	1.718398
23	6	0	-4.736735	0.424866	-0.001122
24	6	0	-3.981407	-0.798809	1.916245
25	8	0	-3.616746	0.044944	0.812870
26	1	0	-4.355031	1.094543	-0.773005
27	1	0	-5.472903	0.952174	0.616403
28	1	0	-5.192475	-0.460199	-0.459436
29	1	0	-3.068004	-0.993196	2.479865
30	1	0	-4.408864	-1.739788	1.551423
31	1	0	-4.706546	-0.275449	2.550021

10a$_{vf}$
SCF Done: E(RB+HF-LYP) = -2386.60903586 A.U. after 11 cycles

Center Number	Atomic Number	Atomic Type	Coordinates (Angstroms) X	Y	Z
1	6	0	-0.382465	-2.939973	-0.337797
2	6	0	-0.390137	-2.016153	-1.326162
3	1	0	-0.324826	-2.150550	-2.397853
4	1	0	-0.117947	-2.674779	0.687121
5	9	0	1.398872	-0.839053	-1.459021
6	1	0	-0.535679	-4.001782	-0.534458
7	28	0	-1.465116	-1.037043	-0.256826
8	15	0	-1.659944	0.887437	-1.332039
9	15	0	-3.119371	-0.327734	1.182054
10	6	0	-3.043669	1.873980	-0.539271
11	6	0	-3.140637	1.529620	0.958901
12	1	0	-0.563079	1.778329	-1.307044
13	1	0	-1.979824	0.957132	-2.706842
14	1	0	-4.489900	-0.649306	1.008010
15	1	0	-3.060185	-0.466545	2.585126
16	1	0	-2.884837	2.946888	-0.684750
17	1	0	-3.973813	1.605325	-1.054482
18	1	0	-4.028108	1.983547	1.410718
19	1	0	-2.258184	1.901382	1.490665
20	12	0	1.714967	0.349392	-0.085585
21	17	0	1.915321	2.585340	-0.592340
22	17	0	0.259660	-0.096478	1.737950

23	6	0	4.304763	-1.222506	-0.380017
24	6	0	4.435510	0.385712	1.399928
25	8	0	3.596574	-0.321545	0.482010
26	1	0	3.557916	-1.649949	-1.048724
27	1	0	4.785662	-2.005845	0.218221
28	1	0	5.061814	-0.677015	-0.956836
29	1	0	3.786621	1.014430	2.010980
30	1	0	5.149913	1.014377	0.856018
31	1	0	4.970544	-0.327577	2.038296

$11a_{vb}$

SCF Done: E(RB+HF-LYP) = -4860.68719306 A.U. after 1 cycles

Center Number	Atomic Number	Atomic Type	Coordinates (Angstroms) X	Y	Z
1	6	0	1.716302	3.219085	1.225308
2	6	0	1.050395	2.226410	0.629558
3	1	0	0.072413	2.413816	0.178409
4	1	0	2.699507	3.088669	1.677187
5	35	0	-2.960837	1.733676	-0.639318
6	1	0	1.281634	4.214814	1.325213
7	28	0	1.533244	0.391724	0.685525
8	15	0	2.939714	0.993622	-0.815173
9	15	0	2.451716	-1.745719	0.545796
10	6	0	4.079468	-0.421025	-1.288336
11	6	0	3.376471	-1.773987	-1.078333
12	1	0	2.354274	1.394795	-2.030541
13	1	0	3.835965	2.058424	-0.599036
14	1	0	3.459902	-2.149443	1.459452
15	1	0	1.709357	-2.943028	0.517981
16	1	0	4.431676	-0.311074	-2.319247
17	1	0	4.956072	-0.339945	-0.633519
18	1	0	4.092564	-2.600076	-1.127024
19	1	0	2.612678	-1.931356	-1.845440
20	12	0	-1.613162	-0.211936	-0.085629
21	17	0	-0.127357	-1.169648	-1.624783
22	17	0	-0.327136	-0.168839	1.976455
23	6	0	-4.288554	-1.757924	-0.217506
24	6	0	-2.547480	-2.991501	0.872008
25	8	0	-2.972235	-1.724550	0.357626
26	1	0	-4.509264	-0.744463	-0.554031
27	1	0	-5.011581	-2.069319	0.545123
28	1	0	-4.311287	-2.455952	-1.062946
29	1	0	-1.570828	-2.838635	1.332310
30	1	0	-2.472869	-3.725977	0.061503
31	1	0	-3.260597	-3.339165	1.628629

$11a_{vc}$

SCF Done: E(RB+HF-LYP) = -2746.98295359 A.U. after 9 cycles

Center Number	Atomic Number	Atomic Type	Coordinates (Angstroms) X	Y	Z
1	6	0	-1.012045	-2.729860	-0.526110
2	6	0	-0.370301	-1.918442	-1.490848
3	1	0	-0.503361	-2.022477	-2.563023
4	1	0	-0.496848	-3.032600	0.382450
5	17	0	1.457627	-1.591305	-1.241743
6	1	0	-1.791247	-3.411876	-0.868314
7	28	0	-1.583132	-0.858745	-0.467262
8	15	0	-1.854307	1.280401	-1.102468
9	15	0	-3.087798	-0.525713	1.150798
10	6	0	-3.287357	1.967092	-0.091873
11	6	0	-3.297296	1.330489	1.309736
12	1	0	-0.868796	2.275884	-0.917186
13	1	0	-2.245604	1.661851	-2.409155
14	1	0	-4.439756	-0.942820	1.025501
15	1	0	-2.906719	-0.911417	2.498525
16	1	0	-3.236857	3.058497	-0.028107
17	1	0	-4.209232	1.713376	-0.629833
18	1	0	-4.205783	1.596338	1.859664
19	1	0	-2.434453	1.677718	1.888723
20	12	0	1.698423	0.528943	0.133987
21	17	0	2.020760	2.294927	-1.260497
22	17	0	0.391119	0.368105	2.010069
23	6	0	4.799636	0.382903	0.080403
24	6	0	3.827034	-0.932009	1.839670
25	8	0	3.597549	-0.012631	0.761249
26	1	0	4.507321	1.103936	-0.683323
27	1	0	5.274625	-0.492815	-0.377595
28	1	0	5.487977	0.849778	0.793992
29	1	0	2.862542	-1.112068	2.315306
30	1	0	4.519160	-0.485232	2.562434
31	1	0	4.245193	-1.868222	1.451527

$11a_{vf}$

SCF Done: E(RB+HF-LYP) = -2386.64049931 A.U. after 11 cycles

Center Number	Atomic Number	Atomic Type	Coordinates (Angstroms) X	Y	Z
1	6	0	1.583550	3.404659	0.119093
2	6	0	0.835874	2.335904	-0.167948
3	1	0	-0.095791	2.430078	-0.733302
4	1	0	2.522168	3.347098	0.670467
5	9	0	-2.127350	1.656315	-1.444885
6	1	0	1.261898	4.410924	-0.155034
7	28	0	1.121601	0.596729	0.545250
8	15	0	2.674080	0.519624	-0.929436
9	15	0	1.758935	-1.552832	1.184546
10	6	0	3.662446	-1.070092	-0.793716
11	6	0	2.781145	-2.203781	-0.238896
12	1	0	2.218841	0.531629	-2.261732
13	1	0	3.672991	1.510920	-0.995451
14	1	0	2.641208	-1.735625	2.281168
15	1	0	0.860217	-2.601448	1.456445
16	1	0	4.100597	-1.342030	-1.759686
17	1	0	4.491464	-0.858695	-0.106706
18	1	0	3.388564	-3.066079	0.052860
19	1	0	2.056307	-2.529078	-0.991105
20	12	0	-1.808189	0.156054	-0.522722
21	17	0	-0.657473	-1.718785	-1.296482
22	17	0	-0.889053	0.621484	1.700430
23	6	0	-4.787155	0.509776	-0.247024
24	6	0	-4.122099	-1.663661	0.555713
25	8	0	-3.734093	-0.455250	-0.097723
26	1	0	-4.338654	1.359691	-0.762569
27	1	0	-5.165785	0.808098	0.738247
28	1	0	-5.599406	0.079651	-0.845092
29	1	0	-3.245450	-2.313208	0.568098
30	1	0	-4.931849	-2.148263	-0.003097
31	1	0	-4.451853	-1.454150	1.580787

$2b_{vb}$

SCF Done: E(RB+HF-LYP) = -3542.39511025 A.U. after 15 cycles

Center Number	Atomic Number	Atomic Type	Coordinates (Angstroms) X	Y	Z
1	46	0	-0.242626	-0.426744	-0.253617
2	15	0	-1.317436	1.700601	-0.353527
3	15	0	-2.356664	-1.271596	0.443362
4	6	0	-3.164907	1.372480	-0.177645
5	6	0	-3.438120	0.227162	0.813271
6	1	0	-1.133865	2.635897	0.698886
7	1	0	-1.360025	2.662041	-1.397384
8	1	0	-3.195516	-1.954945	-0.477078
9	1	0	-2.692098	-2.073113	1.565875
10	6	0	1.841661	-0.512621	-0.788760
11	35	0	2.988711	0.494975	0.417502
12	6	0	1.436925	-1.809298	-0.462324
13	1	0	2.004949	-0.189897	-1.810803
14	1	0	1.688014	-2.250755	0.497205
15	1	0	1.215833	-2.506366	-1.268539
16	1	0	-3.701600	2.277662	0.124267
17	1	0	-3.526766	1.097649	-1.176394
18	1	0	-4.500027	-0.039375	0.810823
19	1	0	-3.184859	0.545861	1.832185

$2b_{vc}$

SCF Done: E(RB+HF-LYP) = -1428.71522415 A.U. after 7 cycles

Center Number	Atomic Number	Atomic Type	Coordinates (Angstroms) X	Y	Z
1	46	0	0.232804	-0.313896	-0.199151
2	15	0	-1.043562	1.700738	-0.230777
3	15	0	-1.825930	-1.411765	0.279009
4	6	0	-2.855604	1.184600	-0.194620
5	6	0	-3.067331	-0.055136	0.691918
6	1	0	-1.013778	2.569931	0.891588
7	1	0	-1.124257	2.727854	-1.207755
8	1	0	-2.538630	-2.086423	-0.748215
9	1	0	-2.150897	-2.333878	1.308360
10	6	0	2.360078	-0.153087	-0.561291
11	17	0	3.234740	0.794559	0.679247
12	6	0	2.060660	-1.500181	-0.345385
13	1	0	2.552769	0.248771	-1.550099
14	1	0	2.292036	-1.977386	0.602256
15	1	0	1.963407	-2.157698	-1.206466
16	1	0	-3.496145	2.008130	0.137255
17	1	0	-3.132171	0.955149	-1.231394
18	1	0	-4.096464	-0.418866	0.606265
19	1	0	-2.899877	0.204372	1.744740

$2b_{vf}$

SCF Done: E(RB+HF-LYP) = -1068.34738610 A.U. after 8 cycles

Center Number	Atomic Number	Atomic Type	Coordinates (Angstroms) X	Y	Z
1	46	0	0.494565	-0.185893	-0.122406
2	15	0	-0.974804	1.675764	-0.087433
3	15	0	-1.466821	-1.535982	0.101539
4	6	0	-2.723095	0.984707	-0.236858
5	6	0	-2.868760	-0.345939	0.521714
6	1	0	-1.121271	2.441369	1.100485
7	1	0	-1.101224	2.775655	-0.977822
8	1	0	-2.033102	-2.171470	-1.036928
9	1	0	-1.790164	-2.577137	1.012747
10	6	0	2.636112	0.250084	-0.275118
11	9	0	3.081438	0.935578	0.824770
12	6	0	2.481668	-1.128134	-0.212638
13	1	0	2.845835	0.797107	-1.190489
14	1	0	2.695786	-1.658833	0.710596
15	1	0	2.512050	-1.705500	-1.132105
16	1	0	-3.466430	1.709182	0.111565
17	1	0	-2.901156	0.825913	-1.307940
18	1	0	-3.845643	-0.797655	0.320488
19	1	0	-2.808764	-0.168807	1.602963

$2b_{vo}$

SCF Done: E(RB+HF-LYP) = -1083.63767162 A.U. after 7 cycles

Center Number	Atomic Number	Atomic Type	Coordinates (Angstroms) X	Y	Z
1	46	0	0.206223	-0.381668	-0.133004
2	15	0	-0.876160	1.712751	-0.194632
3	15	0	-1.952576	-1.329530	0.232827
4	6	0	-2.727537	1.351363	-0.281840
5	6	0	-3.103710	0.127814	0.570287
6	1	0	-0.865178	2.564142	0.945116
7	1	0	-0.832719	2.769844	-1.145657
8	1	0	-2.656021	-1.931234	-0.847051
9	1	0	-2.451391	-2.219482	1.223779
10	6	0	2.452012	-0.467720	-0.419021
11	8	0	3.171078	0.142707	0.585442
12	6	0	1.944615	-1.746265	-0.230799
13	1	0	2.648332	-0.074577	-1.418835
14	1	0	2.080876	-2.245897	0.724345
15	1	0	1.773884	-2.379775	-1.096230
16	6	0	3.307210	1.543450	0.444764
17	1	0	2.333193	2.044666	0.542314
18	1	0	3.745602	1.808442	-0.529836
19	1	0	3.976758	1.878665	1.240258
20	1	0	-3.313925	2.225593	0.019677
21	1	0	-2.954198	1.155999	-1.337641
22	1	0	-4.150521	-0.147736	0.405284
23	1	0	-2.994073	0.366242	1.635834

$2b_{vs}$

SCF Done: E(RB+HF-LYP) = -1406.62151545 A.U. after 8 cycles

Center Number	Atomic Number	Atomic Type	Coordinates (Angstroms) X	Y	Z
1	46	0	-0.020210	-0.429912	-0.171181
2	15	0	-1.024197	1.720987	-0.235700
3	15	0	-2.188977	-1.260965	0.316460
4	6	0	-2.887877	1.424258	-0.251414
5	6	0	-3.277198	0.241599	0.651447
6	1	0	-0.940651	2.596248	0.882025
7	1	0	-0.969806	2.748959	-1.216097
8	1	0	-2.955166	-1.888143	-0.703031
9	1	0	-2.644349	-2.100292	1.368278
10	6	0	2.144870	-0.675317	-0.611359
11	16	0	3.285043	0.053999	0.563559
12	6	0	1.571120	-1.924924	-0.349681
13	1	0	2.308728	-0.369523	-1.644132
14	1	0	1.713183	-2.407769	0.614474
15	1	0	1.322352	-2.585252	-1.177443
16	6	0	3.063031	1.833339	0.230371
17	1	0	2.047395	2.150791	0.484981
18	1	0	3.267021	2.065348	-0.819583
19	1	0	3.783080	2.368957	0.855484
20	1	0	-3.432613	2.327738	0.041360
21	1	0	-3.156834	1.205051	-1.292448
22	1	0	-4.338011	-0.001427	0.531295
23	1	0	-3.121407	0.507241	1.704644

$3b_{vb}$

SCF Done: E(RB+HF-LYP) = -3542.36329855 A.U. after 16 cycles

Center Number	Atomic Number	Atomic Type	Coordinates (Angstroms) X	Y	Z
1	46	0	-0.027212	0.096487	0.259887
2	15	0	1.733754	1.465083	-0.710885
3	15	0	1.702323	-1.534304	0.663311
4	6	0	3.337112	0.575032	-0.279164
5	6	0	3.179131	-0.953840	-0.346030
6	1	0	1.898452	1.572132	-2.119532
7	1	0	2.145849	2.795398	-0.425449
8	1	0	2.327306	-1.715769	1.926345
9	1	0	1.691959	-2.904458	0.298934
10	6	0	-1.703251	1.319278	0.327879
11	35	0	-2.397344	-0.624712	-0.607127
12	6	0	-2.009798	1.471193	1.630396
13	1	0	-1.814040	2.084951	-0.432349
14	1	0	-2.056270	0.634090	2.319948
15	1	0	-2.233132	2.460357	2.028750
16	1	0	4.153080	0.902829	-0.931224
17	1	0	3.594413	0.881541	0.742392
18	1	0	4.099329	-1.448230	-0.017927
19	1	0	2.991536	-1.267977	-1.380106

$3b_{vc}$

SCF Done: E(RB+HF-LYP) = -1428.67264906 A.U. after 10 cycles

Center Number	Atomic Number	Atomic Type	Coordinates (Angstroms) X	Y	Z
1	46	0	-0.379206	-0.065976	0.075436
2	15	0	1.278709	1.598649	-0.450995
3	15	0	1.495977	-1.558136	0.461612
4	6	0	2.929681	0.849489	0.057107
5	6	0	2.988012	-0.658014	-0.246599
6	1	0	1.586317	1.963425	-1.790615
7	1	0	1.449099	2.899886	0.092490
8	1	0	1.987089	-1.857512	1.760488
9	1	0	1.718558	-2.846810	-0.086548
10	6	0	-2.182226	0.968782	0.137252
11	17	0	-2.557206	-0.892886	-0.855894
12	6	0	-2.603273	1.025479	1.412742
13	1	0	-2.342331	1.735192	-0.613217
14	1	0	-2.573932	0.165036	2.074114
15	1	0	-2.999411	1.956344	1.815614
16	1	0	3.761001	1.369549	-0.429539
17	1	0	3.027892	1.019241	1.136496
18	1	0	3.922122	-1.087711	0.129214
19	1	0	2.966108	-0.824773	-1.330604

$3b_{vf}$

SCF Done: E(RB+HF-LYP) = -1068.27503926 A.U. after 10 cycles

Center Number	Atomic Number	Atomic Type	Coordinates (Angstroms) X	Y	Z
1	46	0	-0.524090	-0.244346	-0.119177
2	15	0	0.799185	1.641890	-0.241923
3	15	0	1.644137	-1.478935	0.287013
4	6	0	2.531488	1.216312	0.343059
5	6	0	2.948261	-0.186505	-0.134747
6	1	0	1.090223	2.260197	-1.487106
7	1	0	0.561399	2.833017	0.486926
8	1	0	2.057027	-1.801451	1.608029
9	1	0	2.250455	-2.605054	-0.331377
10	6	0	-2.499990	0.449548	-0.185937
11	9	0	-2.352541	-1.295637	-0.366791
12	6	0	-3.079825	0.901567	0.932956
13	1	0	-2.782545	0.725836	-1.195935
14	1	0	-2.823528	0.535665	1.922454
15	1	0	-3.857768	1.659809	0.862768
16	1	0	3.255841	1.967597	0.011920
17	1	0	2.507272	1.248532	1.439330
18	1	0	3.921995	-0.457482	0.284889
19	1	0	3.051224	-0.195871	-1.226971

$3b_{vo}$

SCF Done: E(RB+HF-LYP) = -1083.55211516 A.U. after 9 cycles

Center Number	Atomic Number	Atomic Type	Coordinates (Angstroms) X	Y	Z
1	46	0	0.388294	-0.046101	-0.037792
2	15	0	-1.216496	1.548773	0.446757
3	15	0	-1.617035	-1.563578	-0.451161
4	6	0	-2.919212	0.928955	-0.044870
5	6	0	-3.063181	-0.575663	0.246469
6	1	0	-1.458383	1.940265	1.789810
7	1	0	-1.237445	2.849299	-0.114047
8	1	0	-2.074634	-1.721252	-1.787576
9	1	0	-2.025904	-2.854764	-0.015044
10	6	0	2.246493	0.919341	0.080659

11	8	0	2.336489	-0.874644	-0.273449
12	6	0	2.622683	1.800429	-0.860466
13	1	0	2.621796	0.946297	1.102103
14	1	0	2.285397	1.749021	-1.891224
15	1	0	3.337058	2.582640	-0.608306
16	1	0	-3.709873	1.496575	0.456667
17	1	0	-3.020155	1.113666	-1.121549
18	1	0	-4.017296	-0.948340	-0.139023
19	1	0	-3.060905	-0.749900	1.329873
20	6	0	2.735114	-1.649613	0.838623
21	1	0	2.765040	-1.066517	1.774307
22	1	0	3.750033	-2.031504	0.652693
23	1	0	2.063419	-2.506280	1.000906

$3b_{vs}$
SCF Done: E(RB+HF-LYP) = -1406.57117482 A.U. after 8 cycles

Center Number	Atomic Number	Atomic Type	Coordinates (Angstroms) X	Y	Z
1	46	0	0.205468	0.001659	-0.101458
2	15	0	-1.540576	1.480500	0.659351
3	15	0	-1.649116	-1.562115	-0.536370
4	6	0	-3.180919	0.717986	0.139859
5	6	0	-3.157548	-0.812004	0.304726
6	1	0	-1.808036	1.691837	2.040525
7	1	0	-1.766988	2.822898	0.258478
8	1	0	-2.181815	-1.757235	-1.839826
9	1	0	-1.797695	-2.908932	-0.115427
10	6	0	1.910946	1.195075	-0.313646
11	16	0	2.380696	-1.002713	-0.075317
12	6	0	2.067066	1.772817	-1.517563
13	1	0	2.262298	1.684868	0.593090
14	1	0	1.812048	1.270086	-2.446618
15	1	0	2.485725	2.775418	-1.603358
16	1	0	-4.014935	1.152867	0.699862
17	1	0	-3.326007	0.979962	-0.915671
18	1	0	-4.084491	-1.253093	-0.075359
19	1	0	-3.084561	-1.074223	1.367641
20	6	0	3.267572	-0.620842	1.492752
21	1	0	2.577858	-0.305459	2.278311
22	1	0	4.035027	0.143993	1.341183
23	1	0	3.751604	-1.549851	1.807838

$4b_{vb}$
SCF Done: E(RB+HF-LYP) = -3542.40044457 A.U. after 16 cycles

Center Number	Atomic Number	Atomic Type	Coordinates (Angstroms) X	Y	Z
1	46	0	-0.118705	0.248121	-0.080022
2	15	0	1.944729	1.232327	-0.172984
3	15	0	1.117422	-1.841045	0.166739
4	6	0	3.255293	-0.010735	0.329460
5	6	0	2.914455	-1.419601	-0.193303
6	1	0	2.418374	1.706196	-1.418190
7	1	0	2.262267	2.359385	0.615272
8	1	0	1.210546	-2.459290	1.436524
9	1	0	0.933732	-3.008340	-0.607287
10	6	0	-1.010784	2.056750	-0.311709
11	35	0	-2.377815	-0.831198	0.021921
12	6	0	-0.943813	3.097305	0.518802
13	1	0	-1.628806	2.092525	-1.208939
14	1	0	-0.359434	3.092601	1.437327
15	1	0	-1.523552	4.003409	0.333240
16	1	0	4.247365	0.304673	-0.010586
17	1	0	3.270740	-0.008950	1.426134
18	1	0	3.600454	-2.161198	0.227988
19	1	0	3.029070	-1.454223	-1.283515

$4b_{vc}$
SCF Done: E(RB+HF-LYP) = -1428.71342984 A.U. after 8 cycles

Center Number	Atomic Number	Atomic Type	Coordinates (Angstroms) X	Y	Z
1	46	0	-0.483331	-0.049902	-0.051005
2	15	0	1.091629	1.589312	-0.195989
3	15	0	1.418436	-1.570963	0.197271
4	6	0	2.769499	0.902930	0.278996
5	6	0	2.938493	-0.545993	-0.218838
6	1	0	1.332636	2.168681	-1.462618
7	1	0	1.008005	2.773839	0.566977
8	1	0	1.756017	-2.088269	1.470957
9	1	0	1.646077	-2.743367	-0.557152
10	6	0	-1.954824	1.324461	-0.284655
11	17	0	-2.137029	-1.765072	-0.005585
12	6	0	-2.218290	2.367178	0.502854
13	1	0	-2.597879	1.075306	-1.128446
14	1	0	-1.616601	2.629573	1.371314
15	1	0	-3.097624	2.991125	0.332892
16	1	0	3.575972	1.542491	-0.094911
17	1	0	2.811188	0.932498	1.374588
18	1	0	3.853015	-0.987182	0.189708
19	1	0	3.031698	-0.559671	-1.311514

$4b_{vf}$
SCF Done: E(RB+HF-LYP) = -1068.31320378 A.U. after 9 cycles

Center Number	Atomic Number	Atomic Type	Coordinates (Angstroms) X	Y	Z
1	46	0	-0.562040	-0.378169	-0.014421
2	15	0	0.442450	1.663505	-0.125518
3	15	0	1.750044	-1.249760	0.105280
4	6	0	2.258081	1.511803	0.310234
5	6	0	2.857707	0.218858	-0.274997
6	1	0	0.488576	2.327428	-1.374105
7	1	0	0.037008	2.758298	0.670273
8	1	0	2.289512	-1.700853	1.335183
9	1	0	2.317700	-2.248478	-0.719985
10	6	0	-2.439973	0.338322	-0.128218
11	9	0	-1.420603	-2.141336	0.021020
12	6	0	-2.973979	1.518795	0.186626
13	1	0	-3.056826	-0.496361	-0.461494
14	1	0	-2.404393	2.368609	0.558993
15	1	0	-4.049879	1.684312	0.104105
16	1	0	2.817817	2.390813	-0.026292
17	1	0	2.310517	1.491346	1.405552
18	1	0	3.877685	0.067390	0.091544
19	1	0	2.913151	0.292443	-1.367891

$4b_{vo}$
SCF Done: E(RB+HF-LYP) = -1083.58572046 A.U. after 8 cycles

Center Number	Atomic Number	Atomic Type	Coordinates (Angstroms) X	Y	Z
1	46	0	-0.435141	-0.083931	-0.054773
2	15	0	1.172907	1.551215	-0.184432
3	15	0	1.490875	-1.615942	0.183733
4	6	0	2.846834	0.854307	0.292679
5	6	0	3.009092	-0.587621	-0.227393
6	1	0	1.445602	2.156458	-1.435223
7	1	0	1.108043	2.729911	0.592340
8	1	0	1.847960	-2.142377	1.450261
9	1	0	1.740514	-2.785534	-0.572365
10	6	0	-1.889087	1.303517	-0.295692
11	8	0	-1.736667	-1.608903	0.049514
12	6	0	-2.178897	2.338232	0.496523
13	1	0	-2.515964	1.095606	-1.166479
14	1	0	-1.602492	2.584499	1.386918
15	1	0	-3.042856	2.977961	0.304506
16	1	0	3.661401	1.493020	-0.064712
17	1	0	2.882221	0.864526	1.388906
18	1	0	3.925337	-1.037828	0.167525
19	1	0	3.094472	-0.584569	-1.320921
20	6	0	-3.120173	-1.461030	-0.014793
21	1	0	-3.479244	-1.020701	-0.965486
22	1	0	-3.541124	-0.849111	0.802558
23	1	0	-3.577393	-2.463312	0.058155

$4b_{vs}$
SCF Done: E(RB+HF-LYP) = -1406.59840704 A.U. after 8 cycles

Center Number	Atomic Number	Atomic Type	Coordinates (Angstroms) X	Y	Z
1	46	0	-0.251183	0.051302	-0.041077
2	15	0	1.587130	1.481677	-0.162653
3	15	0	1.426328	-1.695858	0.207023
4	6	0	3.155727	0.530413	0.237079
5	6	0	3.062493	-0.916086	-0.283947
6	1	0	1.909652	2.084739	-1.402357
7	1	0	1.721859	2.631196	0.648882
8	1	0	1.743589	-2.220428	1.484134
9	1	0	1.471959	-2.912435	-0.511662
10	6	0	-1.513519	1.621519	-0.317713
11	16	0	-2.049043	-1.477540	0.041582
12	6	0	-1.745477	2.625077	0.531769
13	1	0	-2.032346	1.596223	-1.278461
14	1	0	-1.270039	2.696637	1.508715
15	1	0	-2.459438	3.417230	0.295957
16	1	0	4.041388	1.033218	-0.164727
17	1	0	3.248998	0.531574	1.329979
18	1	0	3.912512	-1.509397	0.068011
19	1	0	3.089838	-0.923758	-1.380318
20	6	0	-3.663741	-0.617752	-0.105863

21	1	0	-3.774166	-0.123293	-1.075638
22	1	0	-3.800783	0.119291	0.688042
23	1	0	-4.438669	-1.386357	-0.019804

$5b_{vb}$
SCF Done: E(RB+HF-LYP) = -4663.06296793 A.U. after 8 cycles

Center Number	Atomic Number	Atomic Type	Coordinates (Angstroms) X	Y	Z
1	46	0	0.451985	-0.811391	-0.691202
2	15	0	1.964691	-1.277254	1.172309
3	15	0	2.180784	0.691726	-1.433630
4	6	0	3.567830	-0.371423	0.785608
5	6	0	3.326069	0.945739	0.026049
6	1	0	1.690533	-0.863725	2.491770
7	1	0	2.484355	-2.560963	1.473831
8	1	0	3.082833	0.250175	-2.434199
9	1	0	2.023122	2.016262	-1.899325
10	6	0	-1.479588	-1.702193	-0.623045
11	35	0	-2.580784	-0.851549	0.786789
12	6	0	-1.369508	-1.054329	-1.859560
13	1	0	-1.126122	-1.664181	-2.729030
14	1	0	4.130338	-0.179073	1.704109
15	1	0	4.168607	-1.056408	0.174463
16	1	0	4.277046	1.382416	-0.295227
17	1	0	2.823303	1.666885	0.679729
18	17	0	-1.891592	2.641069	-1.182116
19	12	0	-0.919991	1.348907	0.382806
20	17	0	0.357430	1.871086	2.181492
21	1	0	-1.494355	-2.775948	-0.478847
22	1	0	-1.853849	-0.104599	-2.067156

$5b_{vc}$
SCF Done: E(RB+HF-LYP) = -2549.38167621 A.U. after 9 cycles

Center Number	Atomic Number	Atomic Type	Coordinates (Angstroms) X	Y	Z
1	46	0	0.277178	-1.005219	-0.370825
2	15	0	2.051876	-0.679945	1.280969
3	15	0	1.619272	0.428230	-1.768546
4	6	0	3.396965	0.318129	0.421896
5	6	0	2.823159	1.291888	-0.623499
6	1	0	1.858069	0.035932	2.479587
7	1	0	2.838246	-1.734517	1.808568
8	1	0	2.496284	-0.146974	-2.722750
9	1	0	1.166703	1.506417	-2.561645
10	6	0	-1.472615	-2.037020	0.277805
11	17	0	-2.443624	-0.995847	1.422456
12	6	0	-1.606710	-1.811529	-1.098127
13	1	0	-1.362138	-2.633584	-1.769162
14	1	0	3.996925	0.863270	1.156578
15	1	0	4.059765	-0.409396	-0.062863
16	1	0	3.631671	1.763704	-1.190949
17	1	0	2.251875	2.082234	-0.124058
18	17	0	-2.708868	1.785892	-1.350150
19	12	0	-1.347784	1.129481	0.315348
20	17	0	-0.015835	2.305013	1.719810
21	1	0	-1.297083	-3.001999	0.738222
22	1	0	-2.267556	-1.047865	-1.498523

$5b_{vf}$
SCF Done: E(RB+HF-LYP) = -2189.02799830 A.U. after 8 cycles

Center Number	Atomic Number	Atomic Type	Coordinates (Angstroms) X	Y	Z
1	46	0	-0.485120	-0.744935	-0.481797
2	15	0	-0.698649	1.617661	-0.881435
3	15	0	-2.690707	-0.574434	0.510324
4	6	0	-2.494347	2.035263	-0.519739
5	6	0	-3.004866	1.263638	0.709981
6	1	0	-0.034270	2.612202	-0.131384
7	1	0	-0.523367	2.195127	-2.157886
8	1	0	-3.884409	-0.982149	-0.138117
9	1	0	-3.016247	-1.052617	1.799565
10	6	0	1.258603	-1.872160	-1.006680
11	9	0	2.392988	-1.556550	-0.156991
12	6	0	0.320754	-2.755846	-0.474733
13	1	0	-0.260976	-3.368920	-1.157817
14	1	0	-2.612151	3.113786	-0.374312
15	1	0	-3.074701	1.761406	-1.409540
16	1	0	-4.066201	1.468378	0.881729
17	1	0	-2.457960	1.574786	1.607802
18	17	0	1.103970	0.213006	2.641973
19	12	0	1.927310	0.288148	0.537162
20	17	0	3.008684	1.831895	-0.699761
21	1	0	1.592619	-1.817778	-2.035562
22	1	0	0.432945	-3.123128	0.541250

$5b_{vo}$
SCF Done: E(RB+HF-LYP) = -2204.32346082 A.U. after 8 cycles

Center Number	Atomic Number	Atomic Type	Coordinates (Angstroms) X	Y	Z
1	6	0	0.628687	-2.672190	-0.074170
2	6	0	1.486632	-1.709812	-0.612401
3	1	0	1.816425	-1.708985	-1.649198
4	1	0	0.673453	-2.907645	0.985258
5	8	0	2.405983	-1.046005	0.259191
6	1	0	0.195294	-3.424535	-0.727939
7	46	0	-0.511435	-0.851390	-0.411618
8	15	0	-1.108176	1.346711	-1.172009
9	15	0	-2.741420	-0.925712	0.535024
10	6	0	-2.938896	1.544062	-0.791291
11	6	0	-3.308354	0.861419	0.537162
12	1	0	-0.597217	2.565685	-0.672406
13	1	0	-1.070646	1.687499	-2.543214
14	1	0	-3.871051	-1.558849	-0.047791
15	1	0	-3.011312	-1.295485	1.872730
16	1	0	-3.208363	2.604640	-0.768561
17	1	0	-3.490935	1.085672	-1.621256
18	1	0	-4.384520	0.936549	0.722578
19	1	0	-2.788651	1.346520	1.371528
20	12	0	1.540586	0.796454	0.536349
21	17	0	2.638734	2.212805	-0.852513
22	17	0	0.477717	1.146881	2.514548
23	6	0	3.785019	-1.409287	0.061950
24	1	0	4.107156	-1.139916	-0.949272
25	1	0	3.901881	-2.484268	0.230071
26	1	0	4.365341	-0.847151	0.794845

$5b_{vs}$
SCF Done: E(RB+HF-LYP) = -2527.30149419 A.U. after 9 cycles

Center Number	Atomic Number	Atomic Type	Coordinates (Angstroms) X	Y	Z
1	6	0	-1.432258	-1.533487	-1.377774
2	6	0	-1.463896	-1.905504	-0.021818
3	1	0	-1.344040	-2.941682	0.283089
4	1	0	-1.959440	-0.658786	-1.750096
5	16	0	-2.267153	-0.873614	1.232580
6	1	0	-1.227134	-2.303802	-2.119851
7	46	0	0.444208	-0.956904	-0.433890
8	15	0	2.097307	-0.873449	1.351311
9	15	0	1.980168	0.416176	-1.652686
10	6	0	3.601698	-0.012133	0.619311
11	6	0	3.210314	1.071428	-0.400748
12	1	0	1.891995	-0.150117	2.544700
13	1	0	2.729950	-2.006189	1.922578
14	1	0	2.839991	-0.179398	-2.610595
15	1	0	1.685549	1.589292	-2.384453
16	1	0	4.219586	0.420455	1.412068
17	1	0	4.198250	-0.794034	0.132780
18	1	0	4.100436	1.468399	-0.899302
19	1	0	2.705491	1.899499	0.108653
20	12	0	-1.139319	1.264653	0.285522
21	17	0	-2.526886	2.060097	-1.319214
22	17	0	0.313429	2.367138	1.641614
23	6	0	-4.036157	-0.853729	0.725607
24	1	0	-4.413141	-1.878523	0.691416
25	1	0	-4.151050	-0.358170	-0.239580
26	1	0	-4.575298	-0.290700	1.492342

$6b_{vb}$
SCF Done: E(RB+HF-LYP) = -4663.04243435 A.U. after 10 cycles

Center Number	Atomic Number	Atomic Type	Coordinates (Angstroms) X	Y	Z
1	46	0	-0.500736	-1.188555	-0.130544
2	15	0	-1.218279	0.275537	-1.830982
3	15	0	-2.653086	-0.683982	0.914995
4	6	0	-2.958641	0.844543	-1.426219
5	6	0	-3.195729	0.906926	0.094328
6	1	0	-0.536009	1.457687	-2.170943
7	1	0	-1.377706	-0.281042	-3.120760
8	1	0	-3.802186	-1.497638	0.754121
9	1	0	-2.795909	-0.388350	2.285833
10	6	0	1.269830	-1.934318	-0.658686
11	35	0	2.765077	0.218779	-0.720831
12	6	0	1.333844	-2.588780	0.523757
13	1	0	1.537496	-3.660160	0.554023
14	1	0	-3.140083	1.823162	-1.880402
15	1	0	-3.645681	0.129893	-1.894698

16	1	0	-4.246372	1.126174	0.308815
17	1	0	-2.585807	1.706358	0.530002
18	17	0	0.631859	0.267457	2.773830
19	12	0	1.111009	1.313985	0.810683
20	17	0	-0.044271	3.138843	0.099082
21	1	0	1.598374	-2.246094	-1.642323
22	1	0	1.303604	-2.072192	1.483463

$6b_{vc}$

SCF Done: E(RB+HF-LYP) = -2549.35965786 A.U. after 9 cycles

Center Number	Atomic Number	Atomic Type	Coordinates (Angstroms) X	Y	Z
1	46	0	-0.161450	-1.187638	-0.147301
2	15	0	-1.303806	0.162063	-1.704240
3	15	0	-2.106347	-0.812812	1.286662
4	6	0	-2.955241	0.652163	-0.959935
5	6	0	-2.885516	0.732663	0.576243
6	1	0	-0.790851	1.358740	-2.236492
7	1	0	-1.696331	-0.476184	-2.903143
8	1	0	-3.218890	-1.687645	1.360230
9	1	0	-1.993377	-0.499930	2.656435
10	6	0	1.561185	-1.776762	-0.953567
11	17	0	2.736959	0.364648	-1.243434
12	6	0	1.863276	-2.382579	0.219302
13	1	0	2.150888	-3.434472	0.238708
14	1	0	-3.274013	1.611800	-1.377242
15	1	0	-3.684845	-0.103722	-1.273597
16	1	0	-3.881995	0.903995	0.995458
17	1	0	-2.244804	1.570665	0.872788
18	17	0	1.369793	0.501301	2.463993
19	12	0	1.422739	1.434459	0.389306
20	17	0	0.064740	3.163276	-0.187621
21	1	0	1.761822	-2.081656	-1.972873
22	1	0	1.960918	-1.832230	1.155378

$6b_{vf}$

SCF Done: E(RB+HF-LYP) = -2188.99485221 A.U. after 8 cycles

Center Number	Atomic Number	Atomic Type	Coordinates (Angstroms) X	Y	Z
1	46	0	-0.945288	0.949292	-0.104468
2	15	0	-1.209828	-0.510411	1.688098
3	15	0	-2.718942	-0.345454	-1.183748
4	6	0	-2.695623	-1.595689	1.346307
5	6	0	-2.808903	-1.911756	-0.157233
6	1	0	-0.177466	-1.446530	1.889275
7	1	0	-1.418142	-0.124868	3.031498
8	1	0	-4.079745	0.049336	-1.212863
9	1	0	-2.641331	-0.871637	-2.491515
10	6	0	0.511914	2.143449	0.466584
11	9	0	1.768778	0.732912	1.217789
12	6	0	0.767326	2.526909	-0.804186
13	1	0	0.903232	3.577730	-1.059621
14	1	0	-2.640531	-2.519720	1.930954
15	1	0	-3.579023	-1.043667	1.690112
16	1	0	-3.727934	-2.468602	-0.364413
17	1	0	-1.962244	-2.528422	-0.479083
18	17	0	0.983225	-1.312004	-1.349864
19	12	0	2.607365	-0.407284	0.032559
20	17	0	4.802845	-0.844161	0.060178
21	1	0	0.605708	2.703822	1.386435
22	1	0	0.913397	1.811625	-1.615477

$6b_{vo}$

SCF Done: E(RB+HF-LYP) = -2204.25347352 A.U. after 8 cycles

Center Number	Atomic Number	Atomic Type	Coordinates (Angstroms) X	Y	Z
1	46	0	0.890397	-0.057704	0.893141
2	15	0	1.316978	1.459085	-0.794620
3	15	0	2.995753	-1.124342	0.246075
4	6	0	3.082283	1.200309	-1.360727
5	6	0	3.423063	-0.302708	-1.385476
6	1	0	0.586462	1.263465	-1.978063
7	1	0	1.221108	2.860906	-0.672539
8	1	0	4.197254	-0.939836	0.974065
9	1	0	3.173788	-2.488157	-0.076091
10	6	0	-0.774743	0.734245	1.611948
11	8	0	-1.623271	1.422861	-0.313310
12	6	0	-1.254186	-0.372790	2.224822
13	1	0	-1.738556	-0.312882	3.200410
14	1	0	3.242927	1.643833	-2.349367
15	1	0	3.733175	1.730122	-0.654392
16	1	0	4.475881	-0.457161	-1.640889
17	1	0	2.819986	-0.812432	-2.145901
18	17	0	-0.643174	-1.859283	-1.063829
19	12	0	-2.339223	-0.348581	-0.577229
20	17	0	-4.558366	-0.727318	-0.551246
21	1	0	-0.910499	1.757580	1.939490
22	1	0	-1.189454	-1.372793	1.789641
23	6	0	-2.441492	2.553282	-0.117554
24	1	0	-2.366168	3.234084	-0.980230
25	1	0	-2.119043	3.126992	0.770118
26	1	0	-3.502621	2.297785	0.018879

$6b_{vs}$

SCF Done: E(RB+HF-LYP) = -2527.23849462 A.U. after 10 cycles

Center Number	Atomic Number	Atomic Type	Coordinates (Angstroms) X	Y	Z
1	46	0	-0.263453	-1.045692	0.022934
2	15	0	-1.346508	-0.088800	-1.801377
3	15	0	-2.391926	-0.669127	1.223171
4	6	0	-3.143606	0.180082	-1.351895
5	6	0	-3.305242	0.548433	0.133912
6	1	0	-0.930956	1.158909	-2.307700
7	1	0	-1.442208	-0.805414	-3.016326
8	1	0	-3.372411	-1.677361	1.405122
9	1	0	-2.488714	-0.060951	2.491997
10	6	0	1.401679	-1.655338	-0.924228
11	16	0	2.665232	0.726571	-1.199223
12	6	0	1.952903	-2.432961	0.024997
13	1	0	2.413420	-3.388506	-0.232133
14	1	0	-3.572708	0.958193	-1.990956
15	1	0	-3.665922	-0.757428	-1.578167
16	1	0	-4.365658	0.602939	0.399077
17	1	0	-2.852796	1.527783	0.325435
18	17	0	-0.476749	3.071542	0.045618
19	12	0	1.106365	1.483196	0.466085
20	17	0	1.027870	0.177150	2.374729
21	1	0	1.462863	-1.816692	-1.993382
22	1	0	1.991127	-2.141029	1.073600
23	6	0	4.153508	0.191781	-0.260875
24	1	0	4.980301	0.069370	-0.964975
25	1	0	3.955032	-0.768324	0.227774
26	1	0	4.439364	0.925994	0.495941

$7b_{vb}$

SCF Done: E(RB+HF-LYP) = -4663.08027080 A.U. after 10 cycles

Center Number	Atomic Number	Atomic Type	Coordinates (Angstroms) X	Y	Z
1	46	0	-1.029472	-0.670105	0.282564
2	15	0	-2.523386	-0.714815	-1.443752
3	15	0	-2.626500	0.809512	1.359017
4	6	0	-3.994892	0.365230	-1.036689
5	6	0	-3.590693	1.503067	-0.081861
6	1	0	-2.017301	-0.192772	-2.650155
7	1	0	-3.113847	-1.905260	-1.919889
8	1	0	-3.647790	0.419877	2.259395
9	1	0	-2.161959	1.958769	2.026587
10	6	0	0.344220	-1.612172	-0.916705
11	35	0	4.164968	0.334282	-0.240991
12	6	0	1.333941	-2.402476	-0.475977
13	1	0	2.058465	-2.829206	-1.170968
14	1	0	-4.437593	0.759391	-1.957055
15	1	0	-4.742686	-0.285364	-0.567327
16	1	0	-4.472222	2.061732	0.247348
17	1	0	-2.910799	2.200409	-0.583722
18	17	0	0.674816	-0.341136	2.033021
19	12	0	1.779944	0.430890	-0.012296
20	17	0	0.302008	1.946243	-0.994567
21	1	0	0.281795	-1.411487	-1.987983
22	1	0	1.473264	-2.650962	0.572764

$7b_{vc}$

SCF Done: E(RB+HF-LYP) = -2549.39960101 A.U. after 9 cycles

Center Number	Atomic Number	Atomic Type	Coordinates (Angstroms) X	Y	Z
1	46	0	0.773356	0.646521	0.287518
2	15	0	2.578957	0.115219	-0.955895
3	15	0	1.111025	-1.545672	1.370215
4	6	0	3.295107	-1.519279	-0.395671
5	6	0	2.198766	-2.453305	0.149039
6	1	0	2.315727	-0.069824	-2.327042
7	1	0	3.700266	0.965338	-1.035362
8	1	0	1.870727	-1.654036	2.562376
9	1	0	0.114249	-2.496554	1.664945
10	6	0	0.728829	2.372754	-0.773109
11	17	0	-4.897146	-0.159133	-0.324311

12	6	0	1.549350	3.409252	-0.608132
13	1	0	1.371566	4.353523	-1.125179
14	1	0	3.841991	-1.992635	-1.217881
15	1	0	4.025007	-1.285086	0.388983
16	1	0	2.647359	-3.345685	0.596279
17	1	0	1.530043	-2.775830	-0.655870
18	17	0	-1.477556	1.153306	1.256073
19	12	0	-2.674868	-0.309101	-0.186535
20	17	0	-1.223035	-1.755364	-1.219511
21	1	0	-0.116166	2.418388	-1.461680
22	1	0	2.402745	3.392163	0.067181

$7b_{vf}$

SCF Done: E(RB+HF-LYP) = -2189.03171342 A.U. after 9 cycles

Center Number	Atomic Number	Atomic Type	Coordinates (Angstroms) X	Y	Z
1	46	0	0.496050	0.641580	0.446182
2	15	0	1.999898	0.971763	-1.230600
3	15	0	1.924416	-1.244232	1.063522
4	6	0	3.279986	-0.390188	-1.220632
5	6	0	2.709958	-1.665540	-0.574384
6	1	0	1.434437	0.918146	-2.520101
7	1	0	2.768655	2.149190	-1.359025
8	1	0	3.025486	-1.263989	1.956965
9	1	0	1.303557	-2.447046	1.447584
10	6	0	-0.784320	1.933598	-0.491209
11	9	0	-0.415015	-1.506406	-1.049175
12	6	0	-1.801640	2.550230	0.120492
13	1	0	-2.470837	3.204488	-0.440801
14	1	0	3.624430	-0.582983	-2.241818
15	1	0	4.139756	-0.015890	-0.651778
16	1	0	3.486783	-2.430081	-0.476795
17	1	0	1.885356	-2.064891	-1.173461
18	17	0	-1.318843	-0.190653	1.923184
19	12	0	-1.944659	-0.799601	-0.357200
20	17	0	-4.067587	-0.917765	-1.067442
21	1	0	-0.640240	2.107866	-1.559370
22	1	0	-2.023927	2.426901	1.176171

$7b_{vo}$

SCF Done: E(RB+HF-LYP) = -2204.30096549 A.U. after 9 cycles

Center Number	Atomic Number	Atomic Type	Coordinates (Angstroms) X	Y	Z
1	46	0	-0.528550	0.039883	-0.727782
2	15	0	-2.144545	-1.513823	-0.345327
3	15	0	-2.065079	1.602345	0.366235
4	6	0	-3.250024	-0.872773	1.013462
5	6	0	-3.601204	0.606716	0.776293
6	1	0	-3.051800	-1.891800	-1.362621
7	1	0	-1.756260	-2.787679	0.110886
8	1	0	-1.634228	2.055161	1.629787
9	1	0	-2.639532	2.803728	-0.112224
10	6	0	0.735871	-1.381275	-1.434995
11	8	0	1.230313	1.202938	-0.837834
12	6	0	1.331473	-2.359858	-0.741497
13	1	0	2.124362	-2.961844	-1.187557
14	1	0	-4.154944	-1.483076	1.101871
15	1	0	-2.674361	-0.985502	1.939246
16	1	0	-4.118170	1.022091	1.646514
17	1	0	-4.277374	0.705154	-0.081716
18	17	0	0.783065	-0.313752	2.240817
19	12	0	2.215352	0.058947	0.422700
20	17	0	4.465560	-0.085420	0.372221
21	1	0	1.033791	-1.165062	-2.462412
22	1	0	1.065342	-2.604822	0.285874
23	6	0	1.177692	2.606074	-0.966209
24	1	0	0.695917	2.899684	-1.909237
25	1	0	2.199491	3.009160	-0.970974
26	1	0	0.629215	3.084122	-0.136782

$7b_{vs}$

SCF Done: E(RB+HF-LYP) = -2527.29165571 A.U. after 9 cycles

Center Number	Atomic Number	Atomic Type	Coordinates (Angstroms) X	Y	Z
1	46	0	-0.597310	0.047539	-0.739251
2	15	0	-2.083595	-1.684295	-0.331819
3	15	0	-2.243551	1.415539	0.381105
4	6	0	-3.240740	-1.134359	1.025469
5	6	0	-3.705881	0.311342	0.778158
6	1	0	-2.963155	-2.153720	-1.336177
7	1	0	-1.589986	-2.918476	0.134061
8	1	0	-1.867343	1.905740	1.648639
9	1	0	-2.887252	2.571675	-0.117454
10	6	0	0.789144	-1.241636	-1.531394
11	16	0	1.195189	1.648127	-1.029906
12	6	0	1.368941	-2.297617	-0.936353
13	1	0	2.161199	-2.861880	-1.429405
14	1	0	-4.095843	-1.812199	1.114900
15	1	0	-2.660656	-1.196812	1.953102
16	1	0	-4.262110	0.692129	1.640073
17	1	0	-4.377281	0.353425	-0.088185
18	17	0	0.721746	-0.419014	2.217511
19	12	0	2.209362	-0.163719	0.430877
20	17	0	4.439218	-0.498150	0.460075
21	1	0	1.122404	-0.951961	-2.530676
22	1	0	1.084093	-2.651499	0.054973
23	6	0	0.910809	3.039904	0.146488
24	1	0	0.073070	3.655543	-0.193115
25	1	0	1.814923	3.654990	0.149369
26	1	0	0.725993	2.678149	1.160921

$8b_{vo}$

SCF Done: E(RB+HF-LYP) = -2204.25307776 A.U. after 7 cycles

Center Number	Atomic Number	Atomic Type	Coordinates (Angstroms) X	Y	Z
1	46	0	0.749004	-0.453870	0.257931
2	15	0	2.588515	-1.195381	-0.909404
3	15	0	2.244583	1.351230	1.092435
4	6	0	3.843287	0.194193	-0.944419
5	6	0	3.942056	0.898294	0.422346
6	1	0	3.364468	-2.272510	-0.415643
7	1	0	2.543521	-1.582930	-2.267650
8	1	0	2.027412	2.609073	0.486259
9	1	0	2.608565	1.821150	2.378735
10	6	0	-0.871147	-1.480459	-0.523139
11	8	0	-1.367589	-0.577673	0.805484
12	6	0	-1.360818	-1.048222	-1.749833
13	1	0	-1.031792	-2.500944	-0.179599
14	1	0	-0.952808	-0.166275	-2.241772
15	1	0	-1.788455	-1.805691	-2.403833
16	1	0	4.823594	-0.176502	-1.261038
17	1	0	3.496614	0.899757	-1.709033
18	1	0	4.585258	1.780114	0.345488
19	1	0	4.399281	0.226649	1.159562
20	6	0	-1.701475	-1.303527	2.002773
21	1	0	-1.192074	-2.273538	2.013906
22	1	0	-2.785922	-1.445595	2.026350
23	1	0	-1.377100	-0.716128	2.865858
24	12	0	-2.650962	0.462943	-0.483977
25	17	0	-4.760649	-0.083438	0.137504
26	17	0	-1.476434	2.415676	-0.801646

$8b_{vs}$

SCF Done: E(RB+HF-LYP) = -2527.25220829 A.U. after 7 cycles

Center Number	Atomic Number	Atomic Type	Coordinates (Angstroms) X	Y	Z
1	46	0	1.054467	-0.082628	0.110353
2	15	0	2.720711	-1.063981	-1.279270
3	15	0	2.932451	1.216741	1.060903
4	6	0	4.274134	-0.025716	-1.101254
5	6	0	4.484552	0.422456	0.356702
6	1	0	3.232413	-2.356014	-0.997342
7	1	0	2.652578	-1.203740	-2.685921
8	1	0	3.127866	2.561866	0.657873
9	1	0	3.333459	1.386724	2.409010
10	6	0	-0.770866	-0.722171	-0.689509
11	16	0	-1.087187	-0.017709	1.269501
12	6	0	-1.254468	-0.012983	-1.770137
13	1	0	-0.973580	-1.791654	-0.643066
14	1	0	-1.068738	1.052179	-1.897902
15	1	0	-1.601856	-0.565528	-2.642084
16	1	0	5.150847	-0.569352	-1.467061
17	1	0	4.139028	0.848423	-1.750001
18	1	0	5.340681	1.100307	0.426485
19	1	0	4.706025	-0.445950	0.989491
20	6	0	-1.285620	-1.670483	2.061250
21	1	0	-0.507150	-2.351271	1.712282
22	1	0	-2.277362	-2.061542	1.822969
23	1	0	-1.177491	-1.526731	3.138454
24	12	0	-3.174942	0.320818	-0.404355
25	17	0	-3.582405	2.535881	-0.486497
26	17	0	-4.333578	-1.599488	-0.070914

$2b_{pb}$

SCF Done: E(RB+HF-LYP) = -3696.02891184 A.U. after 8 cycles

Center Number	Atomic Number	Atomic Type	Coordinates (Angstroms) X	Y	Z

1	46	0	-0.480128	0.209313	-0.128765
2	15	0	-1.797954	-1.142048	1.327163
3	15	0	-2.500770	0.948457	-1.128309
4	6	0	-3.564917	-0.545463	1.045242
5	6	0	-3.825577	-0.198537	-0.430705
6	1	0	-1.979244	-2.526444	1.057290
7	1	0	-1.857417	-1.275917	2.743141
8	1	0	-3.077579	2.201712	-0.780601
9	1	0	-2.947122	0.972332	-2.479103
10	6	0	1.521182	1.058100	-0.933391
11	6	0	1.801636	0.074546	0.056241
12	6	0	1.682795	2.426937	-0.581368
13	35	0	2.184412	-1.745757	-0.525560
14	6	0	2.259847	0.460942	1.343817
15	6	0	2.387392	1.802061	1.649885
16	1	0	-4.289824	-1.287959	1.394891
17	1	0	-3.690996	0.349403	1.667770
18	1	0	-4.823501	0.236285	-0.550107
19	1	0	-3.793326	-1.110748	-1.039836
20	6	0	2.099749	2.793041	0.683362
21	1	0	1.435162	0.776768	-1.977509
22	1	0	1.500613	3.181676	-1.342189
23	1	0	2.509321	-0.305967	2.069682
24	1	0	2.724711	2.093358	2.641029
25	1	0	2.228928	3.842713	0.932020

2b$_{pc}$

SCF Done: E(RB+HF-LYP) = -1582.34918233 A.U. after 1 cycles

Center Number	Atomic Number	Atomic Type	Coordinates (Angstroms) X	Y	Z
1	46	0	0.234781	-0.073893	-0.172249
2	15	0	1.710544	1.397058	0.968501
3	15	0	2.119641	-1.390584	-0.756087
4	6	0	3.346668	0.459895	1.023816
5	6	0	3.602510	-0.329513	-0.271410
6	1	0	2.155968	2.595179	0.344983
7	1	0	1.739053	1.920922	2.291860
8	1	0	2.432676	-2.567208	-0.019686
9	1	0	2.623642	-1.878639	-1.994694
10	6	0	-1.852204	-0.761367	-0.902790
11	6	0	-2.032884	0.476718	-0.227402
12	6	0	-2.226529	-1.953768	-0.224879
13	17	0	-2.082250	1.982432	-1.188434
14	6	0	-2.596069	0.509416	1.074685
15	6	0	-2.928032	-0.673364	1.706849
16	1	0	4.181080	1.139766	1.225551
17	1	0	3.276859	-0.229955	1.874401
18	1	0	4.505754	-0.940815	-0.173153
19	1	0	3.768986	0.364122	-1.105334
20	6	0	-2.745493	-1.913940	1.055070
21	1	0	-1.674977	-0.777848	-1.973202
22	1	0	-2.122259	-2.900735	-0.748072
23	1	0	-2.767013	1.469479	1.550720
24	1	0	-3.346841	-0.643930	2.709110
25	1	0	-3.035159	-2.834173	1.554503

2b$_{pf}$

SCF Done: E(RB+HF-LYP) = -1221.99257543 A.U. after 8 cycles

Center Number	Atomic Number	Atomic Type	Coordinates (Angstroms) X	Y	Z
1	46	0	0.230239	-0.144575	-0.319165
2	15	0	2.068321	-1.549644	0.156950
3	15	0	1.635601	1.727109	0.038859
4	6	0	3.547940	-0.377751	0.181462
5	6	0	3.195449	0.985473	0.800072
6	1	0	2.217485	-2.124986	1.450087
7	1	0	2.690888	-2.629811	-0.531586
8	1	0	2.227021	2.412033	-1.059408
9	1	0	1.540274	2.879230	0.869362
10	6	0	-1.969397	0.283613	-0.987431
11	6	0	-2.710711	0.897377	0.047801
12	6	0	-1.821234	-1.129004	-0.946742
13	9	0	-2.874490	2.238609	-0.009917
14	6	0	-3.274074	0.191076	1.084929
15	6	0	-3.114009	-1.213225	1.113280
16	1	0	4.394101	-0.828408	0.710918
17	1	0	3.853060	-0.245851	-0.864456
18	1	0	4.041538	1.674772	0.708805
19	1	0	2.987043	0.867228	1.870955
20	6	0	-2.405796	-1.863212	0.119913
21	1	0	-1.752560	0.857013	-1.883379
22	1	0	-1.457238	-1.656809	-1.823335
23	1	0	-3.837270	0.716147	1.849449
24	1	0	-3.566539	-1.780745	1.921801
25	1	0	-2.306226	-2.944916	0.134790

2b$_{po}$

SCF Done: E(RB+HF-LYP) = -1237.28147326 A.U. after 9 cycles

Center Number	Atomic Number	Atomic Type	Coordinates (Angstroms) X	Y	Z
1	46	0	0.491177	-0.261741	-0.301741
2	15	0	2.545359	-1.261030	0.275689
3	15	0	1.504327	1.858753	-0.054986
4	6	0	3.780447	0.166432	0.217309
5	6	0	3.173295	1.478377	0.742507
6	1	0	2.787285	-1.708120	1.605667
7	1	0	3.371597	-2.248294	-0.335217
8	1	0	1.962334	2.577928	-1.195026
9	1	0	1.193626	3.022833	0.705525
10	6	0	-1.724352	-0.301233	-1.084046
11	6	0	-2.627567	0.285116	-0.150731
12	6	0	-1.327424	-1.648876	-0.911431
13	8	0	-2.984841	1.571557	-0.439382
14	6	0	-3.094375	-0.446624	0.930549
15	6	0	-2.677329	-1.788336	1.096849
16	1	0	4.691152	-0.080907	0.773180
17	1	0	4.064985	0.282155	-0.836358
18	1	0	3.875118	2.306676	0.597964
19	1	0	2.985675	1.396934	1.820792
20	6	0	-1.816663	-2.387531	0.199959
21	1	0	-1.557761	0.221478	-2.021238
22	1	0	-0.827710	-2.169020	-1.723544
23	1	0	-3.784920	-0.012760	1.644523
24	1	0	-3.060965	-2.352838	1.943008
25	1	0	-1.522927	-3.426057	0.323479
26	6	0	-3.893972	2.221034	0.432154
27	1	0	-3.487633	2.305128	1.449085
28	1	0	-4.857856	1.695898	0.474250
29	1	0	-4.045049	3.220572	0.019804

2b$_{ps}$

SCF Done: E(RB+HF-LYP) = -1560.25705385 A.U. after 7 cycles

Center Number	Atomic Number	Atomic Type	Coordinates (Angstroms) X	Y	Z
1	46	0	-0.439984	0.125802	-0.130710
2	15	0	-1.798934	-1.466496	0.979886
3	15	0	-2.420820	1.188376	-0.882405
4	6	0	-3.541428	-0.750697	0.875937
5	6	0	-3.792280	-0.039015	-0.464643
6	1	0	-2.037102	-2.737408	0.388735
7	1	0	-1.855412	-1.933406	2.323097
8	1	0	-2.933743	2.335645	-0.214415
9	1	0	-2.888159	1.572973	-2.170965
10	6	0	1.619805	0.919990	-0.885760
11	6	0	1.866920	-0.139849	0.039495
12	6	0	1.850263	2.264210	-0.487897
13	16	0	2.033921	-1.842594	-0.536289
14	6	0	2.309770	0.198796	1.353333
15	6	0	2.507966	1.516152	1.717749
16	1	0	-4.295492	-1.527677	1.040217
17	1	0	-3.629499	-0.033560	1.701973
18	1	0	-4.769889	0.454440	-0.457357
19	1	0	-3.805065	-0.772984	-1.280415
20	6	0	2.284609	2.559136	0.789535
21	1	0	1.483499	0.689603	-1.938647
22	1	0	1.697728	3.058254	-1.214834
23	1	0	2.503692	-0.605964	2.057050
24	1	0	2.850718	1.751427	2.722236
25	1	0	2.465633	3.590275	1.081015
26	6	0	3.833522	-1.894822	-0.920712
27	1	0	4.431327	-1.680389	-0.030520
28	1	0	4.087189	-1.187552	-1.715109
29	1	0	4.052550	-2.910647	-1.263200

3b$_{pb}$

SCF Done: E(RB+HF-LYP) = -3696.01522037 A.U. after 8 cycles

Center Number	Atomic Number	Atomic Type	Coordinates (Angstroms) X	Y	Z
1	46	0	0.451956	-0.211356	0.126304
2	15	0	1.583122	1.621387	-0.988867
3	15	0	2.618019	-0.822476	0.988368
4	6	0	3.325767	1.619611	-0.271747
5	6	0	3.841511	0.191494	-0.021523
6	1	0	1.906380	1.579711	-2.374282
7	1	0	1.342667	3.022007	-0.953494
8	1	0	3.049630	-0.472537	2.297023
9	1	0	3.284126	-2.075574	0.947529
10	6	0	-1.992656	0.346537	1.342602
11	6	0	-1.678957	0.115225	-0.006716

12	6	0	-2.765089	1.468089	1.676301
13	35	0	-1.392390	-2.003330	-0.500016
14	6	0	-2.235646	0.913105	-1.022647
15	6	0	-3.011395	2.009763	-0.666615
16	1	0	4.018108	2.165036	-0.921145
17	1	0	3.270387	2.168617	0.676647
18	1	0	4.822063	0.219746	0.464835
19	1	0	3.966925	-0.335792	-0.975408
20	6	0	-3.273690	2.299391	0.682045
21	1	0	-1.658272	-0.343350	2.110376
22	1	0	-2.990343	1.663080	2.722046
23	1	0	-2.035420	0.683324	-2.063730
24	1	0	-3.417053	2.648578	-1.447649
25	1	0	-3.891687	3.153101	0.945099

$3b_{pc}$

SCF Done: E(RB+HF-LYP) = -1582.32566896 A.U. after 7 cycles

Center Number	Atomic Number	Atomic Type	Coordinates (Angstroms) X	Y	Z
1	46	0	0.369935	-0.441260	-0.029376
2	15	0	1.158408	1.762138	-0.548984
3	15	0	2.667268	-0.931875	0.621112
4	6	0	2.914637	1.850984	0.123350
5	6	0	3.660318	0.516720	-0.057983
6	1	0	1.393765	2.188789	-1.885509
7	1	0	0.677519	3.015634	-0.086331
8	1	0	3.103305	-0.896844	1.973941
9	1	0	3.525380	-1.990744	0.222676
10	6	0	-2.190850	-0.254280	1.234379
11	6	0	-1.796570	-0.356510	-0.108852
12	6	0	-3.145433	0.706376	1.587812
13	17	0	-1.250701	-2.268159	-0.662470
14	6	0	-2.441755	0.392256	-1.108331
15	6	0	-3.395817	1.331373	-0.732268
16	1	0	3.474591	2.667199	-0.344376
17	1	0	2.826954	2.088357	1.190990
18	1	0	4.649689	0.566286	0.408082
19	1	0	3.813824	0.313832	-1.125183
20	6	0	-3.747135	1.503280	0.615165
21	1	0	-1.765475	-0.916341	1.981770
22	1	0	-3.433327	0.805944	2.631729
23	1	0	-2.174560	0.250651	-2.150221
24	1	0	-3.873399	1.936734	-1.499289
25	1	0	-4.502846	2.232049	0.893480

$3b_{pf}$

SCF Done: E(RB+HF-LYP) = -1221.93344345 A.U. after 8 cycles

Center Number	Atomic Number	Atomic Type	Coordinates (Angstroms) X	Y	Z
1	46	0	0.339599	-0.499768	-0.017422
2	15	0	1.043735	1.694225	-0.075606
3	15	0	2.817913	-1.055962	0.082260
4	6	0	2.875226	1.774073	0.321622
5	6	0	3.632746	0.595318	-0.316294
6	1	0	1.001745	2.426889	-1.290120
7	1	0	0.548070	2.725107	0.760234
8	1	0	3.428336	-1.315927	1.338980
9	1	0	3.677891	-1.901099	-0.670280
10	6	0	-2.386296	-0.115730	1.225614
11	6	0	-1.775500	-0.418321	0.000771
12	6	0	-3.609592	0.555743	1.219621
13	9	0	-1.123468	-2.048547	0.010954
14	6	0	-2.417372	-0.141078	-1.214144
15	6	0	-3.640215	0.530654	-1.190648
16	1	0	3.307469	2.727896	0.001878
17	1	0	2.960191	1.728614	1.414422
18	1	0	4.681154	0.602818	-0.002460
19	1	0	3.620654	0.689269	-1.409365
20	6	0	-4.244203	0.888173	0.018867
21	1	0	-1.907365	-0.391957	2.159857
22	1	0	-4.072789	0.812050	2.170110
23	1	0	-1.961442	-0.435358	-2.154297
24	1	0	-4.127312	0.767930	-2.134096
25	1	0	-5.200410	1.403077	0.025670

$3b_{po}$

SCF Done: E(RB+HF-LYP) = -1237.21142410 A.U. after 9 cycles

Center Number	Atomic Number	Atomic Type	Coordinates (Angstroms) X	Y	Z
1	46	0	-0.378554	0.342233	-0.124710
2	15	0	-1.234693	-1.801684	0.092651
3	15	0	-2.818458	1.057285	0.012228
4	6	0	-3.061687	-1.726625	0.515356
5	6	0	-3.747494	-0.565009	-0.226409
6	1	0	-1.258286	-2.675356	-1.025560
7	1	0	-0.784736	-2.755126	1.038640
8	1	0	-3.403334	1.469378	1.241701
9	1	0	-3.630536	1.884782	-0.810242
10	6	0	2.311422	-0.018966	1.152883
11	6	0	1.713778	0.140015	-0.108665
12	6	0	3.515430	-0.726569	1.262034
13	8	0	1.096364	1.829709	-0.529630
14	6	0	2.346790	-0.385351	-1.252720
15	6	0	3.540230	-1.085282	-1.119078
16	1	0	-3.560605	-2.675266	0.291867
17	1	0	-3.128496	-1.571972	1.599396
18	1	0	-4.790427	-0.471525	0.091769
19	1	0	-3.753943	-0.761054	-1.305935
20	6	0	4.138614	-1.263160	0.137446
21	1	0	1.831985	0.371097	2.046293
22	1	0	3.958704	-0.858783	2.247189
23	1	0	1.905272	-0.227558	-2.232255
24	1	0	4.016260	-1.491399	-2.009376
25	1	0	5.074756	-1.806255	0.230116
26	6	0	1.351967	2.810471	0.452098
27	1	0	2.144053	2.490078	1.147027
28	1	0	0.461327	3.075708	1.041781
29	1	0	1.703530	3.711725	-0.069565

$3b_{ps}$

SCF Done: E(RB+HF-LYP) = -1560.22775004 A.U. after 1 cycles

Center Number	Atomic Number	Atomic Type	Coordinates (Angstroms) X	Y	Z
1	46	0	-0.422663	0.326649	0.088824
2	15	0	-1.379300	-1.714800	-0.760402
3	15	0	-2.766932	0.877605	0.684315
4	6	0	-3.172094	-1.784609	-0.194859
5	6	0	-3.819696	-0.388444	-0.231100
6	1	0	-1.557865	-1.932391	-2.154265
7	1	0	-0.981114	-3.041514	-0.455359
8	1	0	-3.285736	0.697440	1.996513
9	1	0	-3.522078	2.044732	0.393972
10	6	0	2.082545	-0.456904	1.402049
11	6	0	1.693320	0.033171	0.136680
12	6	0	3.070159	-1.434820	1.509303
13	16	0	1.141846	2.158895	0.234123
14	6	0	2.360467	-0.450593	-1.006540
15	6	0	3.362457	-1.415184	-0.881904
16	1	0	-3.751710	-2.492832	-0.795577
17	1	0	-3.160557	-2.165577	0.834071
18	1	0	-4.835405	-0.426564	0.175140
19	1	0	-3.897721	-0.037518	-1.267828
20	6	0	3.722349	-1.918065	0.370629
21	1	0	1.629750	-0.047230	2.301053
22	1	0	3.349497	-1.802353	2.494406
23	1	0	2.074708	-0.103847	-1.994731
24	1	0	3.854665	-1.786290	-1.778670
25	1	0	4.505549	-2.665759	0.459656
26	6	0	1.856478	2.589321	-1.396524
27	1	0	1.192708	2.320318	-2.220800
28	1	0	2.831004	2.109983	-1.533135
29	1	0	1.984837	3.675932	-1.391440

$4b_{pb}$

SCF Done: E(RB+HF-LYP) = -3696.05882607 A.U. after 7 cycles

Center Number	Atomic Number	Atomic Type	Coordinates (Angstroms) X	Y	Z
1	46	0	0.363673	0.081393	0.002410
2	15	0	0.961977	-2.136662	0.004992
3	15	0	2.760999	0.510507	-0.009893
4	6	0	2.798500	-2.286730	-0.344707
5	6	0	3.586127	-1.144400	0.325521
6	1	0	0.807600	-2.879299	1.199008
7	1	0	0.400266	-3.069866	-0.892803
8	1	0	3.396815	0.918640	-1.206761
9	1	0	3.449610	1.364054	0.880309
10	6	0	-2.275578	-0.684867	1.218953
11	35	0	-0.264867	2.502273	-0.012852
12	6	0	-1.608681	-0.462967	0.009262
13	6	0	-3.627090	-1.048050	1.222052
14	6	0	-2.302527	-0.618840	-1.195664
15	6	0	-3.653301	-0.982349	-1.188210
16	1	0	3.178652	-3.263731	-0.028334
17	1	0	2.907509	-2.232227	-1.434719
18	1	0	4.630490	-1.154908	-0.001868
19	1	0	3.585709	-1.275868	1.414376
20	6	0	-4.318637	-1.199250	0.019592
21	1	0	-1.756894	-0.557323	2.165830
22	1	0	-4.137382	-1.207539	2.169489
23	1	0	-1.804890	-0.438252	-2.145024

24	1	0	-4.184868	-1.090106	-2.131239
25	1	0	-5.368753	-1.480182	0.023445

4b$_{pc}$

SCF Done: E(RB+HF-LYP) = -1582.37147709 A.U. after 8 cycles

Center Number	Atomic Number	Atomic Type	Coordinates (Angstroms) X	Y	Z
1	46	0	0.341697	0.374693	-0.001123
2	15	0	0.872076	-1.848855	-0.002138
3	15	0	2.758339	0.740049	-0.012100
4	6	0	2.703974	-2.057655	-0.344439
5	6	0	3.525248	-0.940996	0.328779
6	1	0	0.686906	-2.587959	1.189427
7	1	0	0.282929	-2.758749	-0.905770
8	1	0	3.413709	1.123878	-1.206612
9	1	0	3.473604	1.570395	0.879428
10	6	0	-2.307543	-0.341118	1.217811
11	17	0	-0.211808	2.687460	-0.009171
12	6	0	-1.639595	-0.124783	0.008242
13	6	0	-3.672642	-0.649820	1.221696
14	6	0	-2.343239	-0.230517	-1.195872
15	6	0	-3.707392	-0.539918	-1.187258
16	1	0	3.050917	-3.046267	-0.025962
17	1	0	2.819533	-2.007732	-1.433975
18	1	0	4.570281	-0.986499	0.006694
19	1	0	3.514952	-1.071380	1.417695
20	6	0	-4.374868	-0.751765	0.020330
21	1	0	-1.779440	-0.250748	2.163761
22	1	0	-4.184717	-0.805280	2.168796
23	1	0	-1.842905	-0.051303	-2.143990
24	1	0	-4.247655	-0.608872	-2.128925
25	1	0	-5.435325	-0.990640	0.024836

4b$_{pf}$

SCF Done: E(RB+HF-LYP) = -1221.97191345 A.U. after 9 cycles

Center Number	Atomic Number	Atomic Type	Coordinates (Angstroms) X	Y	Z
1	46	0	-0.319867	-0.526415	-0.009250
2	15	0	-0.872311	1.680586	0.012092
3	15	0	-2.759321	-0.914519	-0.021471
4	6	0	-2.705355	1.888737	-0.321050
5	6	0	-3.516830	0.763995	0.350002
6	1	0	-0.689306	2.422972	1.203058
7	1	0	-0.294594	2.599830	-0.890533
8	1	0	-3.434248	-1.269262	-1.216045
9	1	0	-3.493725	-1.747200	0.855730
10	6	0	2.329072	0.125190	1.218792
11	9	0	0.194444	-2.420842	-0.039460
12	6	0	1.647943	-0.027628	0.006476
13	6	0	3.704072	0.384942	1.227955
14	6	0	2.353676	0.092027	-1.195524
15	6	0	3.728161	0.351511	-1.183540
16	1	0	-3.055404	2.873302	0.006434
17	1	0	-2.828431	1.845728	-1.410087
18	1	0	-4.566592	0.812571	0.044311
19	1	0	-3.490302	0.881295	1.440173
20	6	0	4.406404	0.499978	0.027561
21	1	0	1.798755	0.025863	2.162688
22	1	0	4.224392	0.492836	2.177322
23	1	0	1.842227	-0.033080	-2.146644
24	1	0	4.267988	0.433121	-2.124609
25	1	0	5.474740	0.701174	0.035488

4b$_{po}$

SCF Done: E(RB+HF-LYP) = -1237.24401143 A.U. after 8 cycles

Center Number	Atomic Number	Atomic Type	Coordinates (Angstroms) X	Y	Z
1	46	0	0.369264	0.397635	-0.001466
2	15	0	1.044726	-1.805303	0.010466
3	15	0	2.784902	0.885505	-0.014558
4	6	0	2.883955	-1.909676	-0.342514
5	6	0	3.638478	-0.749988	0.336102
6	1	0	0.925479	-2.570900	1.196664
7	1	0	0.519301	-2.761242	-0.887854
8	1	0	3.438877	1.292588	-1.204124
9	1	0	3.468296	1.750661	0.871788
10	6	0	-2.253971	-0.431173	1.218445
11	8	0	-0.055014	2.357033	-0.025204
12	6	0	-1.579738	-0.207219	0.010070
13	6	0	-3.600022	-0.814093	1.224984
14	6	0	-2.277695	-0.390101	-1.191892
15	6	0	-3.623154	-0.773243	-1.185105
16	1	0	3.292664	-2.877388	-0.033378
17	1	0	2.993031	-1.843616	-1.431969
18	1	0	4.687576	-0.738461	0.024005
19	1	0	3.624911	-0.880020	1.425114
20	6	0	-4.288630	-0.986937	0.023399
21	1	0	-1.737995	-0.294761	2.166217
22	1	0	-4.108971	-0.975407	2.173127
23	1	0	-1.780340	-0.220205	-2.144199
24	1	0	-4.150652	-0.902601	-2.128007
25	1	0	-5.334183	-1.284989	0.028415
26	6	0	-1.346747	2.887906	-0.031080
27	1	0	-1.940679	2.617076	0.859352
28	1	0	-1.940856	2.597171	-0.915213
29	1	0	-1.261804	3.988730	-0.043926

4b$_{ps}$

SCF Done: E(RB+HF-LYP) = -1560.25741627 A.U. after 10 cycles

Center Number	Atomic Number	Atomic Type	Coordinates (Angstroms) X	Y	Z
1	46	0	0.410905	0.277173	-0.014185
2	15	0	1.207924	-1.925997	0.007931
3	15	0	2.766381	0.871181	-0.040820
4	6	0	3.059930	-1.918190	-0.296499
5	6	0	3.716338	-0.695058	0.370306
6	1	0	1.106040	-2.687557	1.197998
7	1	0	0.770589	-2.925136	-0.891647
8	1	0	3.388416	1.262830	-1.251471
9	1	0	3.395176	1.811668	0.806869
10	6	0	-2.179103	-0.658860	1.217917
11	16	0	-0.259412	2.538357	0.006195
12	6	0	-1.522945	-0.398948	0.006385
13	6	0	-3.488161	-1.153800	1.230091
14	6	0	-2.203262	-0.655905	-1.192463
15	6	0	-3.512008	-1.150774	-1.179593
16	1	0	3.524308	-2.847582	0.048755
17	1	0	3.194237	-1.871248	-1.384098
18	1	0	4.768835	-0.614746	0.080227
19	1	0	3.685365	-0.798661	1.461730
20	6	0	-4.159330	-1.401165	0.031588
21	1	0	-1.678282	-0.462877	2.163111
22	1	0	-3.982688	-1.342338	2.180863
23	1	0	-1.721390	-0.458425	-2.147204
24	1	0	-4.025464	-1.337277	-2.120702
25	1	0	-5.176983	-1.783560	0.041177
26	6	0	-2.086557	2.725071	-0.027303
27	1	0	-2.554691	2.266292	0.846184
28	1	0	-2.519822	2.291794	-0.931361
29	1	0	-2.288656	3.801156	-0.016294

5b$_{pb}$

SCF Done: E(RB+HF-LYP) = -4816.69743732 A.U. after 9 cycles

Center Number	Atomic Number	Atomic Type	Coordinates (Angstroms) X	Y	Z
1	46	0	-0.113869	-0.773809	0.250187
2	15	0	-1.467905	-1.782190	-1.522544
3	15	0	-2.083134	-0.749705	1.573239
4	6	0	-3.047971	-2.275766	-0.626678
5	6	0	-3.483324	-1.244235	0.429099
6	1	0	-1.987296	-0.955909	-2.545345
7	1	0	-1.301626	-2.951396	-2.312675
8	1	0	-2.114536	-1.789184	2.537518
9	1	0	-2.745358	0.224587	2.360353
10	6	0	2.106687	-0.176219	-0.294790
11	35	0	1.753264	1.471612	-1.293607
12	6	0	1.993651	-0.140387	1.116484
13	6	0	2.515595	-1.249949	1.833671
14	6	0	3.146686	-2.292205	1.176833
15	6	0	3.301177	-2.264417	-0.225723
16	1	0	-3.859452	-2.437822	-1.342949
17	1	0	-2.838194	-3.241575	-0.149660
18	1	0	-4.330055	-1.627745	1.007642
19	1	0	-3.800593	-0.316357	-0.059790
20	6	0	2.797446	-1.210210	-0.966575
21	1	0	1.715625	0.767184	1.643143
22	1	0	2.446815	-1.240801	2.917760
23	1	0	3.557161	-3.121227	1.746042
24	1	0	3.819802	-3.073276	-0.732207
25	1	0	2.914493	-1.171465	-2.044187
26	17	0	0.006074	3.007435	1.990901
27	12	0	-0.708107	1.849710	0.190724
28	17	0	-2.466065	2.047035	-1.223903

5b$_{pc}$

SCF Done: E(RB+HF-LYP) = -2703.01668790 A.U. after 9 cycles

Center	Atomic	Atomic	Coordinates (Angstroms)

Number	Number	Type	X	Y	Z
1	46	0	-0.133118	-0.633668	-0.270135
2	15	0	1.079038	-2.181966	1.168643
3	15	0	1.769170	-0.576124	-1.661839
4	6	0	2.556297	-2.668664	0.106008
5	6	0	3.107659	-1.499799	-0.728511
6	1	0	1.734061	-1.644212	2.300547
7	1	0	0.798351	-3.459267	1.725642
8	1	0	1.603870	-1.386138	-2.814285
9	1	0	2.562486	0.422563	-2.281452
10	6	0	-2.225007	0.356694	0.613124
11	17	0	-1.533520	1.662477	1.628206
12	6	0	-2.170884	0.492035	-0.791793
13	6	0	-2.881512	-0.466372	-1.556596
14	6	0	-3.635896	-1.456060	-0.942020
15	6	0	-3.724075	-1.516681	0.461084
16	1	0	3.353527	-3.086591	0.728641
17	1	0	2.204073	-3.472170	-0.553250
18	1	0	3.873447	-1.859149	-1.423802
19	1	0	3.572137	-0.754420	-0.073017
20	6	0	-3.023434	-0.614256	1.246267
21	1	0	-1.771555	1.387379	-1.258451
22	1	0	-2.859985	-0.382430	-2.639263
23	1	0	-4.189643	-2.167184	-1.548070
24	1	0	-4.338631	-2.275088	0.936867
25	1	0	-3.077246	-0.644708	2.329212
26	17	0	0.254049	3.385350	-1.356461
27	12	0	0.831263	1.836336	0.179863
28	17	0	2.570140	1.543002	1.598319

5b$_{pf}$

SCF Done: E(RB+HF-LYP) = -2342.66363722 A.U. after 10 cycles

Center Number	Atomic Number	Atomic Type	Coordinates (Angstroms) X	Y	Z
1	46	0	0.044636	-0.634103	-0.019904
2	15	0	-1.632083	0.018361	-1.548775
3	15	0	-1.495464	-2.416262	0.721375
4	6	0	-2.840316	-1.420064	-1.555698
5	6	0	-3.101568	-1.938693	-0.130026
6	1	0	-2.532818	1.099960	-1.407542
7	1	0	-1.384626	0.178480	-2.931016
8	1	0	-1.434476	-3.791984	0.367541
9	1	0	-1.966155	-2.615400	2.041920
10	6	0	2.105415	0.424641	0.179118
11	9	0	1.774284	1.724897	0.668023
12	6	0	2.066651	-0.643161	1.102970
13	6	0	2.811031	-1.807106	0.762911
14	6	0	3.535642	-1.868848	-0.412233
15	6	0	3.570809	-0.762184	-1.293538
16	1	0	-3.778663	-1.120428	-2.033921
17	1	0	-2.396932	-2.210808	-2.173402
18	1	0	-3.799668	-2.781231	-0.152994
19	1	0	-3.558153	-1.151540	0.481754
20	6	0	2.887337	0.400325	-0.994001
21	1	0	1.694791	-0.483691	2.110811
22	1	0	2.824635	-2.635658	1.465226
23	1	0	4.105772	-2.761612	-0.650711
24	1	0	4.157014	-0.815871	-2.206116
25	1	0	2.925108	1.280626	-1.626827
26	17	0	-1.206084	1.643078	2.494733
27	12	0	-0.253156	2.063156	0.487781
28	17	0	-0.507831	3.554276	-1.187716

5b$_{po}$

SCF Done: E(RB+HF-LYP) = -2357.95913700 A.U. after 7 cycles

Center Number	Atomic Number	Atomic Type	Coordinates (Angstroms) X	Y	Z
1	46	0	0.349298	-0.807924	0.073698
2	15	0	1.641911	0.327341	1.666311
3	15	0	2.419506	-1.608579	-0.957782
4	6	0	3.392626	-0.280152	1.345948
5	6	0	3.669494	-0.455350	-0.158093
6	1	0	1.876759	1.716616	1.810967
7	1	0	1.500608	0.045714	3.045755
8	1	0	3.076653	-2.853468	-0.742734
9	1	0	2.810513	-1.470369	-2.313251
10	6	0	-2.066087	-0.406877	-0.396003
11	8	0	-1.930820	0.858353	-1.017467
12	6	0	-1.592449	-1.540399	-1.092427
13	6	0	-1.898433	-2.818912	-0.563249
14	6	0	-2.651921	-2.943422	0.593303
15	6	0	-3.133413	-1.796871	1.257558
16	1	0	4.115501	0.411846	1.789996
17	1	0	3.497729	-1.239720	1.867601
18	1	0	4.690125	-0.819172	-0.314075
19	1	0	3.570962	0.505291	-0.676577
20	6	0	-2.850565	-0.531955	0.770282
21	1	0	-1.182533	-1.427938	-2.091118
22	1	0	-1.556205	-3.702081	-1.095111
23	1	0	-2.888168	-3.929876	0.981595
24	1	0	-3.724603	-1.902754	2.162438
25	1	0	-3.196901	0.364318	1.275401
26	17	0	1.270448	2.388805	-1.778277
27	12	0	-0.294790	1.862324	-0.212299
28	17	0	-1.193796	3.075547	1.486344
29	6	0	-3.140903	1.420227	-1.575588
30	1	0	-3.856697	1.650232	-0.782535
31	1	0	-3.569925	0.711819	-2.290003
32	1	0	-2.841936	2.336189	-2.086597

5b$_{ps}$

SCF Done: E(RB+HF-LYP) = -2680.93318267 A.U. after 8 cycles

Center Number	Atomic Number	Atomic Type	Coordinates (Angstroms) X	Y	Z
1	46	0	0.408905	-0.859938	-0.049098
2	15	0	1.693041	-0.132324	1.778762
3	15	0	2.454076	-1.201056	-1.320710
4	6	0	3.432693	-0.657554	1.292221
5	6	0	3.723662	-0.390419	-0.195938
6	1	0	1.951187	1.164945	2.289573
7	1	0	1.561416	-0.769142	3.036583
8	1	0	3.085767	-2.460432	-1.524696
9	1	0	2.848731	-0.634414	-2.557742
10	6	0	-2.098803	-0.584411	-0.528689
11	16	0	-1.916313	0.924085	-1.518726
12	6	0	-1.591304	-1.778211	-1.095996
13	6	0	-1.780342	-2.992798	-0.402345
14	6	0	-2.497025	-3.022863	0.788905
15	6	0	-3.031504	-1.839220	1.319299
16	1	0	4.167298	-0.144505	1.921444
17	1	0	3.509047	-1.730100	1.510936
18	1	0	4.733998	-0.729441	-0.446281
19	1	0	3.664665	0.682945	-0.405949
20	6	0	-2.821385	-0.622498	0.681634
21	1	0	-1.209811	-1.782583	-2.111624
22	1	0	-1.398534	-3.912005	-0.837782
23	1	0	-2.659822	-3.968112	1.298883
24	1	0	-3.596264	-1.863692	2.246691
25	1	0	-3.196966	0.294535	1.121433
26	17	0	1.746109	2.720262	-1.057909
27	12	0	-0.024780	1.844945	0.068924
28	17	0	-1.264428	2.707016	1.775095
29	6	0	-3.430043	1.883878	-1.130885
30	1	0	-3.386386	2.285624	-0.117214
31	1	0	-4.308870	1.251832	-1.277443
32	1	0	-3.447723	2.708545	-1.847950

6b$_{pb}$

SCF Done: E(RB+HF-LYP) = -4816.68865171 A.U. after 10 cycles

Center Number	Atomic Number	Atomic Type	Coordinates (Angstroms) X	Y	Z
1	46	0	0.091682	-0.924475	0.105127
2	15	0	-1.306064	-1.012641	-1.834671
3	15	0	-1.772065	-2.007041	1.255449
4	6	0	-2.846469	-1.972795	-1.352076
5	6	0	-3.236283	-1.737386	0.119425
6	1	0	-1.817977	0.095678	-2.537742
7	1	0	-0.846770	-1.770830	-2.938394
8	1	0	-1.845117	-3.405619	1.477702
9	1	0	-2.283044	-1.579386	2.499013
10	6	0	1.922443	-0.104149	-0.309873
11	35	0	1.248581	2.136583	-0.858589
12	6	0	2.185584	-0.251647	1.070570
13	6	0	3.309254	-1.030831	1.445629
14	6	0	4.140991	-1.573528	0.482098
15	6	0	3.881857	-1.352159	-0.887437
16	1	0	-3.676160	-1.701482	-2.011590
17	1	0	-2.624277	-3.032819	-1.524248
18	1	0	-4.075216	-2.382493	0.398840
19	1	0	-3.550635	-0.696767	0.256589
20	17	0	-0.641840	1.609682	2.716804
21	12	0	-0.922089	1.869522	0.484665
22	17	0	-2.899366	2.036360	-0.614058
23	6	0	2.793761	-0.598031	-1.299893
24	1	0	2.587790	-0.431214	-2.351527
25	1	0	1.656604	0.330770	1.820875
26	1	0	3.540845	-1.137212	2.502124
27	1	0	5.013667	-2.149125	0.776292
28	1	0	4.533259	-1.792640	-1.638165

6b$_{pc}$

SCF Done: E(RB+HF-LYP) = -2703.00511557 A.U. after 9 cycles

Center Number	Atomic Number	Atomic Type	Coordinates (Angstroms) X	Y	Z
1	46	0	0.291758	-0.713450	0.178898
2	15	0	-1.179264	-1.351330	-1.590483
3	15	0	-1.381802	-1.701868	1.662379
4	6	0	-2.620309	-2.266395	-0.805875
5	6	0	-2.930269	-1.746686	0.610037
6	1	0	-1.798446	-0.489887	-2.516839
7	1	0	-0.695091	-2.325932	-2.495597
8	1	0	-1.337276	-3.034160	2.146691
9	1	0	-1.845381	-1.077040	2.839287
10	6	0	1.961862	0.239549	-0.518298
11	17	0	1.022950	2.098040	-1.391649
12	6	0	2.290946	0.409385	0.845089
13	6	0	3.526524	-0.126913	1.290450
14	6	0	4.389360	-0.737575	0.398424
15	6	0	4.052875	-0.826018	-0.970141
16	1	0	-3.505006	-2.179707	-1.443454
17	1	0	-2.342534	-3.326622	-0.771731
18	1	0	-3.707678	-2.358461	1.078483
19	1	0	-3.300456	-0.716909	0.552513
20	17	0	-0.645971	2.269543	2.178650
21	12	0	-0.970739	2.002304	-0.047692
22	17	0	-2.976533	1.753899	-1.076222
23	6	0	2.857695	-0.315414	-1.451675
24	1	0	2.591735	-0.383131	-2.500772
25	1	0	1.717791	1.066340	1.494937
26	1	0	3.809972	0.012123	2.330338
27	1	0	5.344368	-1.124560	0.741173
28	1	0	4.732297	-1.317794	-1.661795

6b$_{pf}$

SCF Done: E(RB+HF-LYP) = -2342.64457607 A.U. after 8 cycles

Center Number	Atomic Number	Atomic Type	Coordinates (Angstroms) X	Y	Z
1	46	0	0.276324	-0.731647	0.090785
2	15	0	-1.238298	-0.601595	-1.709396
3	15	0	-1.239779	-2.431365	1.007550
4	6	0	-2.486318	-1.981668	-1.476312
5	6	0	-2.811406	-2.194474	0.013388
6	1	0	-2.056567	0.528603	-1.933068
7	1	0	-0.800717	-0.818076	-3.035481
8	1	0	-1.055652	-3.832362	0.885390
9	1	0	-1.732100	-2.413936	2.330046
10	6	0	1.851309	0.444399	-0.350543
11	9	0	0.922911	2.156026	-0.361890
12	6	0	2.401304	0.232352	0.924783
13	6	0	3.748080	-0.188251	0.995336
14	6	0	4.505959	-0.302904	-0.160597
15	6	0	3.940140	0.005896	-1.413330
16	1	0	-3.396739	-1.762802	-2.043073
17	1	0	-2.043998	-2.889415	-1.904128
18	1	0	-3.492196	-3.042130	0.138933
19	1	0	-3.307761	-1.308106	0.425004
20	17	0	-0.881738	1.107629	2.430511
21	12	0	-0.755905	2.204330	0.418896
22	17	0	-2.518204	3.018851	-0.738219
23	6	0	2.617624	0.414570	-1.524023
24	1	0	2.175405	0.659658	-2.483159
25	1	0	1.848691	0.489157	1.825332
26	1	0	4.196178	-0.357653	1.970829
27	1	0	5.548095	-0.602475	-0.101385
28	1	0	4.541146	-0.086158	-2.314555

6b$_{po}$

SCF Done: E(RB+HF-LYP) = -2357.90658349 A.U. after 9 cycles

Center Number	Atomic Number	Atomic Type	Coordinates (Angstroms) X	Y	Z
1	46	0	0.005984	-0.807558	0.284569
2	15	0	-1.099790	-0.752222	-1.775707
3	15	0	-2.085328	-1.816108	1.153952
4	6	0	-2.802110	-1.503852	-1.548107
5	6	0	-3.339477	-1.270156	-0.124371
6	1	0	-1.351476	0.438695	-2.483558
7	1	0	-0.561979	-1.530791	-2.826062
8	1	0	-2.364240	-3.205444	1.230378
9	1	0	-2.703019	-1.421411	2.359033
10	6	0	1.843740	-0.152548	-0.255495
11	8	0	1.155674	1.880319	-0.671995
12	6	0	2.470810	-0.174813	1.000781
13	6	0	3.778491	-0.684377	1.094605
14	6	0	4.460343	-1.089819	-0.047436
15	6	0	3.838841	-0.993648	-1.302851
16	1	0	-3.488681	-1.083806	-2.289330
17	1	0	-2.709057	-2.576812	-1.754455
18	1	0	-4.295507	-1.785766	0.010178
19	1	0	-3.506332	-0.199060	0.036760
20	17	0	-0.516969	1.262077	2.420709
21	12	0	-0.512327	2.028109	0.236744
22	17	0	-2.484058	2.532854	-0.791784
23	6	0	2.538146	-0.512674	-1.421307
24	1	0	2.065528	-0.436764	-2.395128
25	1	0	1.976532	0.236935	1.876580
26	1	0	4.264444	-0.713880	2.066651
27	1	0	5.478570	-1.460725	0.026291
28	1	0	4.371324	-1.308319	-2.197339
29	6	0	2.283505	2.712507	-0.760253
30	1	0	3.071069	2.228818	-1.357556
31	1	0	2.712764	2.954233	0.225317
32	1	0	2.027824	3.659308	-1.261667

7b$_{pb}$

SCF Done: E(RB+HF-LYP) = -4816.74044792 A.U. after 8 cycles

Center Number	Atomic Number	Atomic Type	Coordinates (Angstroms) X	Y	Z
1	46	0	1.205207	0.195365	0.556441
2	15	0	2.720680	0.845357	-0.993791
3	15	0	2.602156	-1.802873	0.825419
4	6	0	4.128214	-0.384539	-1.054465
5	6	0	3.632155	-1.807113	-0.736577
6	1	0	2.229567	0.881576	-2.313482
7	1	0	3.374238	2.093706	-0.943109
8	1	0	3.593865	-1.939299	1.828749
9	1	0	2.078528	-3.110145	0.858584
10	6	0	0.137961	1.865054	0.052195
11	35	0	-4.134175	-1.141477	-0.208588
12	6	0	0.094655	2.940563	0.945879
13	6	0	-0.742321	4.029210	0.683910
14	6	0	-1.532208	4.053310	-0.468335
15	6	0	-1.479477	2.987509	-1.364957
16	1	0	4.620579	-0.347873	-2.031922
17	1	0	4.861323	-0.056800	-0.307189
18	1	0	4.477085	-2.498506	-0.661775
19	1	0	2.967969	-2.168363	-1.529081
20	17	0	-0.656127	-0.578131	2.029352
21	12	0	-1.760471	-1.189386	0.003196
22	17	0	-0.185864	-1.980152	-1.491548
23	6	0	-0.636199	1.895968	-1.114138
24	1	0	-0.596265	1.078179	-1.831133
25	1	0	0.688471	2.929097	1.856075
26	1	0	-0.780908	4.856377	1.388651
27	1	0	-2.185961	4.898896	-0.663414
28	1	0	-2.091598	2.994476	-2.263149

7b$_{pc}$

SCF Done: E(RB+HF-LYP) = -2703.05980136 A.U. after 11 cycles

Center Number	Atomic Number	Atomic Type	Coordinates (Angstroms) X	Y	Z
1	46	0	0.739163	0.335165	0.570055
2	15	0	2.006727	1.455047	-0.935059
3	15	0	2.683509	-1.136782	0.842826
4	6	0	3.725008	0.717214	-0.987580
5	6	0	3.685094	-0.794575	-0.699359
6	1	0	1.547981	1.367793	-2.263895
7	1	0	2.243430	2.842396	-0.849597
8	1	0	3.654993	-0.977158	1.862454
9	1	0	2.591174	-2.542392	0.850080
10	6	0	-0.786756	1.595457	0.056867
11	17	0	-3.746037	-2.529683	-0.369064
12	6	0	-1.188673	2.582524	0.963298
13	6	0	-2.322512	3.354376	0.693163
14	6	0	-3.054233	3.150759	-0.479604
15	6	0	-2.645988	2.176640	-1.388971
16	1	0	4.193412	0.921917	-1.955996
17	1	0	4.313497	1.239754	-0.223426
18	1	0	4.700423	-1.194727	-0.618434
19	1	0	3.174306	-1.326885	-1.508930
20	17	0	-0.823555	-1.021041	1.967349
21	12	0	-1.623534	-1.882764	-0.107453
22	17	0	0.150891	-2.115045	-1.566726
23	6	0	-1.504725	1.404545	-1.130080
24	1	0	-1.189989	0.658740	-1.857580
25	1	0	-0.641924	2.740657	1.889210
26	1	0	-2.637435	4.111090	1.407671
27	1	0	-3.938886	3.748581	-0.680686
28	1	0	-3.208965	2.008308	-2.303377

7b$_{pf}$

SCF Done: E(RB+HF-LYP) = -2342.69116221 A.U. after 7 cycles

Center Number	Atomic Number	Atomic Type	Coordinates (Angstroms) X	Y	Z
1	46	0	0.503624	-0.319965	-0.595448
2	15	0	1.379207	-1.834183	0.847977
3	15	0	2.791468	0.499920	-0.842652
4	6	0	3.239625	-1.649382	0.901805
5	6	0	3.655471	-0.185214	0.668304
6	1	0	0.971838	-1.670145	2.185963
7	1	0	1.191957	-3.224921	0.704823
8	1	0	3.671365	0.118156	-1.885923
9	1	0	3.097220	1.873477	-0.788307
10	6	0	-1.355220	-1.023206	-0.098748
11	9	0	-2.791375	2.883191	0.641021
12	6	0	-2.097584	-1.704324	-1.072132
13	6	0	-3.419733	-2.070352	-0.811015
14	6	0	-4.012892	-1.759679	0.416625
15	6	0	-3.275746	-1.089789	1.389230
16	1	0	3.627976	-2.022382	1.855339
17	1	0	3.641809	-2.294851	0.111232
18	1	0	4.743569	-0.105343	0.583150
19	1	0	3.332195	0.443662	1.504747
20	17	0	-0.560651	1.504485	-1.901141
21	12	0	-1.240732	2.114791	0.328277
22	17	0	0.622387	1.977803	1.716495
23	6	0	-1.941225	-0.732272	1.140976
24	1	0	-1.373837	-0.230452	1.923284
25	1	0	-1.661199	-1.930535	-2.041172
26	1	0	-3.992168	-2.589675	-1.575850
27	1	0	-5.045790	-2.036701	0.608155
28	1	0	-3.726300	-0.837710	2.345486

7b$_{po}$

SCF Done: E(RB+HF-LYP) = -2357.96033568 A.U. after 7 cycles

Center Number	Atomic Number	Atomic Type	Coordinates (Angstroms) X	Y	Z
1	46	0	-0.687872	0.202663	0.468732
2	15	0	-2.372041	1.248046	-0.630183
3	15	0	-2.336956	-1.600190	0.852919
4	6	0	-3.662629	-0.024052	-1.075659
5	6	0	-3.941448	-0.962536	0.113001
6	1	0	-3.115349	2.263774	0.014570
7	1	0	-2.111023	1.895486	-1.853092
8	1	0	-2.143512	-2.821705	0.175042
9	1	0	-2.798042	-2.115444	2.087832
10	6	0	1.264987	1.744346	-1.199657
11	6	0	0.534391	1.762837	-0.004828
12	6	0	2.202928	2.750059	-1.463099
13	8	0	0.973668	-0.881435	1.229159
14	6	0	0.722678	2.810966	0.903640
15	6	0	1.658892	3.816035	0.632366
16	1	0	-4.582907	0.458731	-1.421291
17	1	0	-3.244466	-0.589632	-1.916362
18	1	0	-4.591785	-1.786328	-0.195861
19	1	0	-4.462511	-0.418789	0.910446
20	6	0	2.401918	3.785596	-0.548569
21	1	0	1.112235	0.949885	-1.927164
22	1	0	2.775413	2.719098	-2.386996
23	1	0	0.154952	2.849240	1.830586
24	1	0	1.804771	4.621332	1.348706
25	1	0	3.129413	4.565668	-0.756346
26	6	0	1.614526	-0.460667	2.422299
27	1	0	0.948072	-0.592377	3.287095
28	1	0	1.910297	0.595345	2.368986
29	1	0	2.517239	-1.062948	2.588192
30	12	0	1.782721	-1.799886	-0.265015
31	17	0	3.864458	-2.625832	-0.098092
32	17	0	0.195237	-1.977524	-1.924680

7b$_{ps}$

SCF Done: E(RB+HF-LYP) = -2680.94725689 A.U. after 8 cycles

Center Number	Atomic Number	Atomic Type	Coordinates (Angstroms) X	Y	Z
1	46	0	0.649266	-0.470521	0.516524
2	15	0	1.931640	-1.568444	-1.062419
3	15	0	2.746798	0.658714	1.095264
4	6	0	3.477973	-0.561874	-1.343278
5	6	0	4.070662	-0.094518	-0.002309
6	1	0	2.424050	-2.874425	-0.829089
7	1	0	1.415063	-1.751504	-2.359959
8	1	0	2.880084	2.042637	0.865908
9	1	0	3.369231	0.586823	2.363193
10	6	0	-1.687010	-1.208768	-1.268951
11	6	0	-0.982799	-1.540186	-0.103629
12	6	0	-2.837918	-1.920707	-1.629898
13	16	0	-0.681984	1.042990	1.867518
14	6	0	-1.425010	-2.618800	0.673784
15	6	0	-2.567951	-3.335969	0.303920
16	1	0	4.214706	-1.127885	-1.922920
17	1	0	3.161708	0.301138	-1.939326
18	1	0	4.888346	0.612732	-0.170296
19	1	0	4.486168	-0.947011	0.548653
20	6	0	-3.280616	-2.985126	-0.844539
21	1	0	-1.348851	-0.399570	-1.914207
22	1	0	-3.382125	-1.637471	-2.527361
23	1	0	-0.892840	-2.899630	1.579711
24	1	0	-2.902304	-4.167456	0.920288
25	1	0	-4.172649	-3.538329	-1.125708
26	6	0	-2.377583	0.397046	2.211219
27	1	0	-2.974708	1.232400	2.583132
28	1	0	-2.309462	-0.377476	2.977613
29	1	0	-2.843795	-0.014270	1.316131
30	12	0	-1.020441	2.199516	-0.295278
31	17	0	-3.074498	3.005186	-0.709016
32	17	0	0.884093	2.311320	-1.581185

8b$_{po}$

SCF Done: E(RB+HF-LYP) = -2357.90276961 A.U. after 8 cycles

Center Number	Atomic Number	Atomic Type	Coordinates (Angstroms) X	Y	Z
1	46	0	0.001376	-0.658650	-0.503759
2	15	0	-0.613619	-1.668169	1.542552
3	15	0	-2.162638	-1.443642	-1.362249
4	6	0	-2.457331	-1.969014	1.424427
5	6	0	-2.856102	-2.497197	0.033277
6	1	0	-0.141596	-2.973189	1.835074
7	1	0	-0.488251	-1.111881	2.833436
8	1	0	-3.192657	-0.495165	-1.547238
9	1	0	-2.474481	-2.283130	-2.461236
10	6	0	2.557575	0.324520	1.065059
11	6	0	1.930470	0.077145	-0.163625
12	6	0	3.861991	-0.128372	1.229325
13	8	0	0.864858	1.555827	-0.717468
14	6	0	2.611708	-0.482784	-1.247448
15	6	0	3.918694	-0.956450	-1.042573
16	1	0	-2.787350	-2.665049	2.202543
17	1	0	-2.940141	-1.004883	1.622813
18	1	0	-3.945228	-2.570464	-0.045245
19	1	0	-2.451819	-3.506429	-0.113558
20	6	0	4.544722	-0.777707	0.186412
21	1	0	2.022330	0.824085	1.866452
22	1	0	4.354649	0.025330	2.186246
23	1	0	2.141203	-0.567354	-2.225916
24	1	0	4.444793	-1.431144	-1.866948
25	1	0	5.566794	-1.114039	0.332548
26	6	0	1.217964	2.152717	-1.964988
27	1	0	0.453891	1.962977	-2.727080
28	1	0	2.181824	1.758513	-2.306407
29	1	0	1.324170	3.234766	-1.819823
30	17	0	-0.556526	2.030683	2.591558
31	12	0	-0.756555	2.023130	0.334051
32	17	0	-2.520294	2.540539	-0.984815

8b$_{ps}$

SCF Done: E(RB+HF-LYP) = -2680.89880877 A.U. after 9 cycles

Center Number	Atomic Number	Atomic Type	Coordinates (Angstroms) X	Y	Z
1	46	0	-1.269747	-0.130840	0.203423
2	15	0	-3.045391	1.495467	-0.029436
3	15	0	-3.019436	-1.805904	-0.108530
4	6	0	-4.544912	0.527537	-0.625691
5	6	0	-4.635346	-0.855544	0.044270
6	1	0	-3.611670	2.149945	1.097546
7	1	0	-3.125538	2.610403	-0.902675
8	1	0	-3.215101	-2.414889	-1.375290
9	1	0	-3.346017	-2.947408	0.666476
10	6	0	1.041938	0.441245	-1.349457
11	6	0	0.650759	0.812330	-0.036782
12	6	0	1.598044	1.397416	-2.213581
13	16	0	0.804551	-0.800876	1.337249
14	6	0	0.903237	2.127346	0.403882
15	6	0	1.468341	3.054461	-0.466938
16	1	0	-5.467193	1.093216	-0.460001
17	1	0	-4.425297	0.411611	-1.710209
18	1	0	-5.467488	-1.427828	-0.377713
19	1	0	-4.830982	-0.742396	1.117993
20	6	0	1.818617	2.701406	-1.776993
21	1	0	0.876339	-0.573982	-1.707773
22	1	0	1.873039	1.097964	-3.221422
23	1	0	0.628436	2.431938	1.407379
24	1	0	1.637905	4.069698	-0.117411
25	1	0	2.275350	3.432219	-2.436918
26	6	0	1.280746	0.206119	2.797912

27	1	0	0.416323	0.759094	3.169339
28	1	0	2.111505	0.872160	2.554883
29	1	0	1.599442	-0.511982	3.557900
30	17	0	4.486069	0.388983	0.939045
31	12	0	2.954298	-0.880844	-0.113041
32	17	0	2.904448	-2.666885	-1.483121

$9b_{vb}$

SCF Done: E(RB+HF-LYP) = -4818.11819518 A.U. after 9 cycles

Center Number	Atomic Number	Atomic Type	Coordinates (Angstroms) X	Y	Z
1	46	0	-1.582209	-0.917411	0.103593
2	15	0	-2.452490	0.419884	-1.702804
3	15	0	-2.770681	0.590517	1.533398
4	6	0	-3.577664	1.715196	-0.924037
5	6	0	-3.101596	2.111077	0.485393
6	1	0	-1.625900	1.217238	-2.524333
7	1	0	-3.316029	-0.052057	-2.724859
8	1	0	-4.070046	0.333497	2.045649
9	1	0	-2.238179	1.182105	2.701813
10	6	0	-0.151008	-2.395668	-0.330184
11	35	0	1.582788	-1.611873	-0.949429
12	6	0	-0.395029	-2.454951	1.050395
13	1	0	-0.414468	-3.168709	-1.042782
14	1	0	0.280411	-2.015788	1.778040
15	1	0	-1.034909	-3.258281	1.414228
16	17	0	1.641493	0.382906	2.623022
17	12	0	1.604426	0.811657	0.391343
18	17	0	0.575776	2.462456	-0.809091
19	6	0	4.675193	0.452728	0.659466
20	6	0	4.077811	1.734192	-1.278483
21	8	0	3.611673	1.019653	-0.123424
22	1	0	4.216601	-0.004682	1.536141
23	1	0	5.363305	1.246267	0.972144
24	1	0	5.214321	-0.296933	0.068229
25	1	0	3.201276	2.166630	-1.761053
26	1	0	4.594661	1.047007	-1.959188
27	1	0	4.762108	2.531391	-0.966360
28	1	0	-3.649447	2.599497	-1.564696
29	1	0	-4.578662	1.268691	-0.872824
30	1	0	-3.830697	2.772172	0.965443
31	1	0	-2.149043	2.648667	0.419390

$9b_{vc}$

SCF Done: E(RB+HF-LYP) = -2704.43748411 A.U. after 15 cycles

Center Number	Atomic Number	Atomic Type	Coordinates (Angstroms) X	Y	Z
1	46	0	-1.472149	-0.940947	-0.270378
2	15	0	-2.322209	0.951528	-1.496781
3	15	0	-2.629191	-0.001878	1.602626
4	6	0	-3.397932	1.933406	-0.300862
5	6	0	-2.906377	1.797844	1.151395
6	1	0	-1.477715	1.958154	-2.013926
7	1	0	-3.209683	0.880953	-2.601677
8	1	0	-3.939931	-0.382400	1.995736
9	1	0	-2.094285	0.132566	2.904948
10	6	0	-0.037878	-2.171839	-1.205598
11	17	0	1.561274	-1.296564	-1.484683
12	6	0	-0.286135	-2.714854	0.064341
13	1	0	-0.316011	-2.637677	-2.143828
14	1	0	0.401535	-2.577946	0.893435
15	1	0	-0.939889	-3.584018	0.119254
16	17	0	2.017909	-0.748793	2.388305
17	12	0	1.788733	0.436779	0.464953
18	17	0	0.754806	2.426662	0.020627
19	6	0	4.831848	-0.093989	0.207921
20	6	0	4.126020	1.784996	-1.107257
21	8	0	3.738779	0.750061	-0.190253
22	1	0	4.437726	-0.800730	0.938306
23	1	0	5.617822	0.516061	0.667288
24	1	0	5.231485	-0.622307	-0.665671
25	1	0	3.237227	2.384346	-1.304765
26	1	0	4.505193	1.339193	-2.034598
27	1	0	4.902379	2.409529	-0.650736
28	1	0	-3.436920	2.987192	-0.593364
29	1	0	-4.414960	1.532357	-0.394071
30	1	0	-3.610174	2.275453	1.841074
31	1	0	-1.934076	2.290674	1.263050

$9b_{vf}$

SCF Done: E(RB+HF-LYP) = -2344.08226150 A.U. after 8 cycles

Center Number	Atomic Number	Atomic Type	Coordinates (Angstroms) X	Y	Z
1	46	0	-1.383223	-0.826706	-0.598570
2	15	0	-2.240688	1.342141	-1.188133
3	15	0	-2.769916	-0.628998	1.356336
4	6	0	-3.423506	1.853012	0.186798
5	6	0	-3.034641	1.220614	1.534952
6	1	0	-1.406477	2.476868	-1.284939
7	1	0	-3.057681	1.625739	-2.313339
8	1	0	-4.106465	-1.096779	1.474421
9	1	0	-2.363874	-0.960828	2.670547
10	6	0	0.300988	-1.506082	-1.652925
11	9	0	1.475912	-0.708505	-1.301910
12	6	0	-0.040928	-2.517536	-0.752684
13	1	0	0.278972	-1.552230	-2.734795
14	1	0	0.535424	-2.678052	0.154132
15	1	0	-0.596564	-3.369909	-1.137830
16	17	0	2.385687	-1.495202	1.948920
17	12	0	1.894255	0.180861	0.488960
18	17	0	0.777158	2.156591	0.804072
19	6	0	4.873393	-0.104526	-0.296923
20	6	0	3.984710	2.047029	-0.877678
21	8	0	3.745569	0.782198	-0.245035
22	1	0	4.596047	-1.001421	0.257577
23	1	0	5.738777	0.373106	0.176642
24	1	0	5.108406	-0.351014	-1.339505
25	1	0	3.084776	2.646268	-0.737603
26	1	0	4.187654	1.900506	-1.945714
27	1	0	4.839979	2.541134	-0.402396
28	1	0	-3.465713	2.942965	0.274487
29	1	0	-4.421802	1.512221	-0.114858
30	1	0	-3.792087	1.439968	2.294689
31	1	0	-2.079309	1.632751	1.879498

$10b_{vb}$

SCF Done: E(RB+HF-LYP) = -4818.10195107 A.U. after 9 cycles

Center Number	Atomic Number	Atomic Type	Coordinates (Angstroms) X	Y	Z
1	46	0	1.723280	0.794260	0.330180
2	15	0	1.871817	-0.245981	-1.776184
3	15	0	2.846211	-1.208042	1.153244
4	6	0	2.692825	-1.920732	-1.562634
5	6	0	2.449741	-2.487947	-0.152124
6	1	0	0.724132	-0.525999	-2.539819
7	1	0	2.677038	0.346146	-2.777794
8	1	0	4.254132	-1.346817	1.261754
9	1	0	2.484945	-1.868955	2.345270
10	6	0	0.801923	2.541141	0.126084
11	35	0	-1.476774	1.863847	-0.869975
12	6	0	0.782417	2.646526	1.478900
13	1	0	0.963159	3.308920	-0.621024
14	1	0	0.267064	1.924612	2.111755
15	1	0	1.172057	3.537745	1.972459
16	17	0	-0.689207	-0.709945	2.233162
17	12	0	-1.641519	-0.492033	0.133597
18	17	0	-1.228154	-2.203479	-1.365705
19	6	0	-4.622165	-0.388750	-0.574574
20	6	0	-4.148951	-1.653156	1.403383
21	8	0	-3.691258	-0.645676	0.486743
22	1	0	-4.206617	0.422311	-1.174373
23	1	0	-5.583215	-0.077538	-0.149192
24	1	0	-4.754216	-1.284763	-1.191747
25	1	0	-3.383808	-1.747446	2.174685
26	1	0	-4.282397	-2.607838	0.881423
27	1	0	-5.096815	-1.332891	1.850893
28	1	0	2.315159	-2.613971	-2.319840
29	1	0	3.765461	-1.781138	-1.742836
30	1	0	3.030099	-3.403986	-0.001620
31	1	0	1.388302	-2.733138	-0.033140

$10b_{vc}$

SCF Done: E(RB+HF-LYP) = -2704.41961112 A.U. after 8 cycles

Center Number	Atomic Number	Atomic Type	Coordinates (Angstroms) X	Y	Z
1	46	0	1.644153	0.891904	0.039753
2	15	0	1.778225	-0.710646	-1.679773
3	15	0	2.625242	-0.845725	1.441131
4	6	0	2.471654	-2.300697	-0.962044
5	6	0	2.163126	-2.419716	0.541809
6	1	0	0.643685	-1.126066	-2.399280
7	1	0	2.662670	-0.470124	-2.757912
8	1	0	4.016897	-1.034928	1.642066
9	1	0	2.192759	-1.111431	2.756778
10	6	0	0.773577	2.530687	-0.660728
11	17	0	-1.377684	1.693600	-1.408359
12	6	0	0.743345	2.993232	0.615374
13	1	0	0.952760	3.059358	-1.588703
14	1	0	0.185059	2.488254	1.403508
15	1	0	1.157871	3.972001	0.859077

16	17	0	-0.982987	0.129217	2.229160
17	12	0	-1.777538	-0.156817	0.075876
18	17	0	-1.433447	-2.239752	-0.875410
19	6	0	-4.647818	-0.079013	-0.945503
20	6	0	-4.476893	-0.716003	1.357121
21	8	0	-3.851120	-0.050816	0.247843
22	1	0	-4.113587	0.501055	-1.699272
23	1	0	-5.621083	0.383433	-0.745071
24	1	0	-4.781314	-1.110934	-1.289217
25	1	0	-3.795267	-0.624726	2.203526
26	1	0	-4.647285	-1.772559	1.119162
27	1	0	-5.429104	-0.223607	1.585498
28	1	0	2.057938	-3.157450	-1.501704
29	1	0	3.554588	-2.288904	-1.133818
30	1	0	2.673093	-3.288370	0.970683
31	1	0	1.084738	-2.551765	0.684608

$10b_{vf}$

SCF Done: E(RB+HF-LYP) = -2344.05611890 A.U. after 8 cycles

Center Number	Atomic Number	Atomic Type	Coordinates (Angstroms) X	Y	Z
1	46	0	-1.426088	-0.989827	-0.179967
2	15	0	-1.557093	0.944192	-1.482603
3	15	0	-2.965910	0.156126	1.341604
4	6	0	-2.796379	2.100193	-0.683721
5	6	0	-2.771938	1.952350	0.849101
6	1	0	-0.399828	1.744356	-1.604408
7	1	0	-1.979951	0.923718	-2.830896
8	1	0	-4.378573	0.022604	1.329484
9	1	0	-2.786808	0.217282	2.739875
10	6	0	-0.214257	-2.162385	-1.203028
11	9	0	1.388626	-0.871365	-1.382500
12	6	0	-0.078328	-3.042062	-0.190142
13	1	0	-0.196845	-2.330881	-2.271101
14	1	0	0.191591	-2.722828	0.816821
15	1	0	-0.155934	-4.116108	-0.360684
16	17	0	0.626207	-0.102846	1.993982
17	12	0	1.788311	0.307487	-0.002982
18	17	0	1.944852	2.519334	-0.657983
19	6	0	4.547374	-0.641044	-0.747887
20	6	0	4.486592	0.363790	1.432247
21	8	0	3.747617	-0.279829	0.386570
22	1	0	3.869244	-1.109896	-1.461481
23	1	0	5.324754	-1.350020	-0.438960
24	1	0	5.006751	0.250126	-1.191896
25	1	0	3.786280	0.540387	2.250109
26	1	0	4.899452	1.315596	1.078832
27	1	0	5.293798	-0.296263	1.771395
28	1	0	-2.583541	3.133915	-0.974157
29	1	0	-3.786891	1.843468	-1.078467
30	1	0	-3.542994	2.578772	1.308588
31	1	0	-1.800121	2.268757	1.244714

$11b_{vb}$

SCF Done: E(RB+HF-LYP) = -4818.13898527 A.U. after 9 cycles

Center Number	Atomic Number	Atomic Type	Coordinates (Angstroms) X	Y	Z
1	46	0	1.466838	0.318469	0.685375
2	15	0	2.911363	0.794850	-0.982204
3	15	0	2.209978	-2.022105	0.403312
4	6	0	3.850301	-0.742804	-1.486275
5	6	0	2.998825	-2.011092	-1.292629
6	1	0	2.301997	1.238194	-2.172035
7	1	0	3.917931	1.772515	-0.845589
8	1	0	3.280229	-2.510986	1.197985
9	1	0	1.415958	-3.183830	0.373745
10	6	0	1.069042	2.308299	0.716609
11	35	0	-2.523109	1.885388	-0.987144
12	6	0	1.871316	3.226902	1.251679
13	1	0	0.079197	2.543749	0.323655
14	1	0	2.865830	3.005617	1.635682
15	1	0	1.536934	4.259694	1.364386
16	17	0	-0.580183	-0.157014	2.026083
17	12	0	-1.763322	-0.261530	-0.104264
18	17	0	-0.689697	-1.821897	-1.461774
19	6	0	-4.748258	-1.038327	-0.147070
20	6	0	-3.399314	-2.530721	1.153832
21	8	0	-3.491120	-1.252168	0.513685
22	1	0	-4.707094	-0.039146	-0.582013
23	1	0	-5.560330	-1.099812	0.586600
24	1	0	-4.894249	-1.790258	-0.931913
25	1	0	-2.435018	-2.565808	1.662236
26	1	0	-3.460907	-3.334330	0.411057
27	1	0	-4.207389	-2.632102	1.887712
28	1	0	4.190807	-0.653079	-2.523278
29	1	0	4.744709	-0.780088	-0.851995
30	1	0	3.608092	-2.904994	-1.459024
31	1	0	2.162792	-2.030990	-1.999449

$11b_{vc}$

SCF Done: E(RB+HF-LYP) = -2704.45899720 A.U. after 7 cycles

Center Number	Atomic Number	Atomic Type	Coordinates (Angstroms) X	Y	Z
1	46	0	-1.252583	0.455123	-0.575573
2	15	0	-2.825515	0.389676	1.040019
3	15	0	-1.695337	-1.961139	-0.842971
4	6	0	-3.585941	-1.317004	1.134391
5	6	0	-2.570451	-2.408583	0.749068
6	1	0	-2.336140	0.627468	2.339083
7	1	0	-3.940018	1.253050	1.036237
8	1	0	-2.643644	-2.396057	-1.805961
9	1	0	-0.751309	-2.994901	-0.986578
10	6	0	-1.107836	2.435237	-0.152567
11	17	0	2.300381	1.965631	1.607029
12	6	0	-1.991468	3.354451	-0.537425
13	1	0	-0.176798	2.686097	0.356848
14	1	0	-2.930274	3.115118	-1.034280
15	1	0	-1.783715	4.417110	-0.400359
16	17	0	0.898169	0.518482	-1.833263
17	12	0	1.953571	0.105345	0.324188
18	17	0	1.051399	-1.838383	1.238969
19	6	0	5.005231	-0.197190	0.503393
20	6	0	4.032087	-1.557014	-1.213229
21	8	0	3.853822	-0.454730	-0.315985
22	1	0	4.756247	0.657479	1.132967
23	1	0	5.862358	0.039715	-0.137527
24	1	0	5.231544	-1.073899	1.122163
25	1	0	3.129494	-1.624086	-1.821894
26	1	0	4.175327	-2.487150	-0.651304
27	1	0	4.898454	-1.368627	-1.857975
28	1	0	-3.991610	-1.493966	2.136180
29	1	0	-4.431975	-1.315644	0.435939
30	1	0	-3.069317	-3.379959	0.674509
31	1	0	-1.779314	-2.488553	1.501907

$11b_{vf}$

SCF Done: E(RB+HF-LYP) = -2344.09297073 A.U. after 7 cycles

Center Number	Atomic Number	Atomic Type	Coordinates (Angstroms) X	Y	Z
1	46	0	1.044759	0.601147	0.494926
2	15	0	2.707536	0.424043	-1.020920
3	15	0	1.676797	-1.689267	1.183895
4	6	0	3.611787	-1.198221	-0.795432
5	6	0	2.666090	-2.300243	-0.282378
6	1	0	2.282628	0.400294	-2.363514
7	1	0	3.745317	1.374481	-1.113355
8	1	0	2.592993	-1.910759	2.245447
9	1	0	0.794165	-2.757001	1.432873
10	6	0	0.690007	2.426170	-0.328717
11	9	0	-1.945417	1.365151	-1.693685
12	6	0	1.428242	3.511954	-0.108619
13	1	0	-0.230692	2.413309	-0.915870
14	1	0	2.351234	3.507388	0.469094
15	1	0	1.104197	4.486895	-0.478023
16	17	0	-1.164027	0.636143	1.632001
17	12	0	-1.883515	-0.070844	-0.616583
18	17	0	-0.958287	-2.143046	-1.118641
19	6	0	-4.718748	0.807258	-0.282879
20	6	0	-4.413247	-1.415285	0.589979
21	8	0	-3.898172	-0.371030	-0.239091
22	1	0	-4.186648	1.515452	-0.918890
23	1	0	-4.844141	1.218078	0.726388
24	1	0	-5.696719	0.557758	-0.711097
25	1	0	-3.724968	-2.257372	0.500990
26	1	0	-5.409056	-1.711067	0.238918
27	1	0	-4.469365	-1.082451	1.633744
28	1	0	4.090984	-1.497601	-1.733630
29	1	0	4.410253	-1.008380	-0.067322
30	1	0	3.234172	-3.203288	-0.037752
31	1	0	1.922559	-2.560602	-1.043185

Chapter 5

1
E(RB+HF-LYP) = -975.812266935 A.U.

Center Number	Atomic Number	Atomic Type	Coordinates (Angstroms) X	Y	Z
1	45	0	.000000	.000000	1.199783
2	45	0	.000000	.000000	-1.199783
3	6	0	.000000	2.622295	.000000
4	6	0	-2.622295	.000000	.000000
5	6	0	.000000	-2.622295	.000000
6	6	0	2.622295	.000000	.000000
7	1	0	.000000	3.720534	.000000
8	1	0	-3.720534	.000000	.000000
9	1	0	.000000	-3.720534	.000000
10	1	0	3.720534	.000000	.000000
11	8	0	.000000	2.066448	1.138346
12	8	0	-2.066448	.000000	1.138346
13	8	0	.000000	-2.066448	1.138346
14	8	0	2.066448	.000000	1.138346
15	8	0	.000000	2.066448	-1.138346
16	8	0	-2.066448	.000000	-1.138346
17	8	0	.000000	-2.066448	-1.138346
18	8	0	2.066448	.000000	-1.138346

2
E(RB+HF-LYP) = -1124.57943240 A.U.

Center Number	Atomic Number	Atomic Type	Coordinates (Angstroms) X	Y	Z
1	6	0	-2.761979	-0.067446	0.000000
2	6	0	2.447201	-0.737786	0.000000
3	6	0	-0.158137	-0.400152	2.625928
4	6	0	-0.158137	-0.400152	-2.625928
5	6	0	0.152110	3.046702	0.000000
6	8	0	-2.070471	0.997595	0.000000
7	8	0	2.046837	0.469036	0.000000
8	8	0	-2.362261	-1.264589	0.000000
9	8	0	1.755418	-1.791886	0.000000
10	8	0	-0.008381	0.735396	2.076364
11	8	0	-0.008381	0.735396	-2.076364
12	45	0	0.000000	0.806209	0.000000
13	45	0	-0.315902	-1.614084	0.000000
14	8	0	-0.305075	-1.526089	2.075622
15	8	0	-0.305075	-1.526089	-2.075622
16	1	0	-3.852101	0.078352	0.000000
17	1	0	3.538680	-0.871505	0.000000
18	1	0	-0.158889	-0.395142	3.725754
19	1	0	-0.158889	-0.395142	-3.725754
20	1	0	-0.322013	3.371251	0.925073
21	1	0	-0.322013	3.371251	-0.925073
22	7	0	1.471230	3.361785	0.000000
23	7	0	2.589279	3.483667	0.000000

TS-3
E(RB+HF-LYP) = -1124.55296676 A.U.

Center Number	Atomic Number	Coordinates (Angstroms) X	Y	Z
1	6	-2.796273	-0.030123	0.0
2	6	2.398816	-0.787630	0.0
3	6	-0.197798	-0.361116	2.625081
4	6	-0.197798	-0.361116	-2.625081
5	6	0.075006	2.822105	0.0
6	8	-2.080943	1.022992	0.0
7	8	2.025794	0.432224	0.0
8	8	-2.428025	-1.232429	0.0
9	8	1.683954	-1.820393	0.0
10	8	-0.011244	0.772401	2.074374
11	8	-0.011244	0.772401	-2.074374
12	45	0.0	0.842995	0.0
13	45	-0.385871	-1.600198	0.0
14	8	-0.374769	-1.482883	2.082161
15	8	-0.374769	-1.482883	-2.082161
16	1	-3.880845	0.152500	0.0
17	1	3.488024	-0.937374	0.0
18	1	-0.202437	-0.344229	3.724950
19	1	-0.202437	-0.344229	-3.724950
20	1	-0.151276	3.385430	0.911439
21	1	-0.151276	3.385430	-0.911439
22	7	1.993065	3.387998	0.0
23	7	3.055892	3.073783	0.0

5
E(RB+HF-LYP) = -1015.03194966 A.U.

Center Number	Atomic Number	Coordinates (Angstroms) X	Y	Z
1	6	0.0	-2.624169	0.110947
2	6	0.000000	2.624169	0.110947
3	1	0.0	-3.723747	0.089249
4	1	0.000000	3.723747	0.089249
5	6	-2.624079	0.000000	0.190703
6	6	2.624079	-0.000000	0.190703
7	1	-3.723502	0.000000	0.171811
8	1	3.723502	-0.000000	0.171811
9	6	0.000000	0.000000	-3.013037
10	1	0.0	0.926123	-3.600459
11	1	-0.000000	-0.926123	-3.600459
12	8	0.0	-2.072394	-1.039305
13	8	0.000000	2.072394	-1.039305
14	8	0.0	-2.083779	1.246090
15	8	0.000000	2.083779	1.246090
16	8	-2.077657	0.000000	-0.960826
17	8	2.077657	-0.000000	-0.960826
18	45	0.000000	0.000000	-1.106724
19	45	-0.000000	-0.000000	1.375242
20	8	-2.074971	0.000000	1.319911
21	8	2.074971	-0.000000	1.319911

6a
E(RB+HF-LYP) = -1055.54998313 A.U.

Center Number	Atomic Number	Atomic Type	Coordinates (Angstroms) X	Y	Z
1	45	0	0.375772	-1.562921	0.000000
2	45	0	0.000000	0.891017	0.000000
3	6	0	-2.397588	-0.774659	0.000000
4	6	0	2.794132	-0.021002	0.000000
5	8	0	-2.026649	0.444979	0.000000
6	8	0	2.083699	1.036938	0.000000
7	6	0	-0.168179	2.793745	0.000000
8	8	0	-1.684311	-1.807982	0.000000
9	8	0	2.419258	-1.219432	0.000000
10	6	0	0.187659	-0.307840	2.623979
11	6	0	0.187659	-0.307840	-2.623979
12	8	0	0.011845	0.828435	2.071311
13	8	0	0.011845	0.828435	-2.071311
14	8	0	0.357839	-1.430371	2.083986
15	8	0	0.357839	-1.430371	-2.083986
16	6	0	-3.323584	3.852219	0.000000
17	1	0	-3.487389	-0.920602	0.000000
18	1	0	3.878677	0.160789	0.000000
19	1	0	-0.151165	3.382258	-0.924447
20	1	0	-0.151165	3.382258	0.924447
21	1	0	0.187505	-0.285618	3.723592
22	1	0	0.187505	-0.285618	-3.723592
23	1	0	-2.610185	3.019857	0.000000
24	1	0	-2.796227	4.810429	0.000000
25	1	0	-3.949406	3.779577	0.893649
26	1	0	-3.949406	3.779577	-0.893649

TS-7a
E(RB+HF-LYP) = -1055.54051090 A.U.

Center Number	Atomic Number	Atomic Type	Coordinates (Angstroms) X	Y	Z
1	45	0	.217232	-1.583154	.000000
2	45	0	.000000	.867356	.000000
3	6	0	-2.516833	-.563262	.000000
4	6	0	.112511	-.348637	2.626625
5	6	0	.112511	-.348637	-2.626625
6	6	0	2.724031	-.150522	.000000
7	1	0	-3.614385	-.642171	.000000
8	1	0	.117904	-.338797	3.727012
9	1	0	.117904	-.338797	-3.727012
10	1	0	3.819676	-.049840	.000000
11	8	0	-2.062497	.628162	.000000
12	8	0	.004292	.793857	2.078621
13	8	0	.004292	.793857	-2.078621
14	8	0	2.083578	.946813	.000000
15	6	0	-.084478	2.973586	.000000
16	1	0	.244466	3.471276	-.912997
17	1	0	.244466	3.471276	.912997
18	8	0	-1.877332	-1.645014	.000000
19	8	0	.212175	-1.479741	2.080506
20	8	0	.212175	-1.479741	-2.080506
21	8	0	2.274314	-1.328451	.000000
22	1	0	-1.326775	2.899034	.000000
23	6	0	-1.961146	3.989789	.000000
24	1	0	-1.437654	4.938748	.000000

25	1	0	-2.534285	3.824164	.912306
26	1	0	-2.534285	3.824164	-.912306

6b

E(RB+HF-LYP) = -1134.17773363 A.U.

Center Number	Atomic Number	Coordinates (Angstroms) X	Y	Z
1	45	1.084129	-1.581415	-0.000000
2	45	0.000000	0.644180	0.000000
3	6	-1.831537	-1.608947	-0.000000
4	6	2.918255	0.642497	0.000000
5	8	-1.838170	-0.333342	-0.000000
6	8	1.927643	1.440310	0.000000
7	6	-0.728120	2.533194	0.000000
8	8	-0.847450	-2.388702	-0.000000
9	8	2.919807	-0.616267	0.000000
10	6	0.542074	-0.453484	2.626757
11	6	0.542074	-0.453484	-2.626757
12	8	0.034942	0.576804	2.078184
13	8	0.034942	0.576804	-2.078184
14	8	1.036418	-1.475951	2.083995
15	8	1.036418	-1.475951	-2.083995
16	6	-3.153683	2.795212	0.000000
17	1	-2.828003	-2.076685	-0.000000
18	1	3.903825	1.131697	0.000000
19	1	-0.632974	3.138653	-0.908669
20	1	-0.632974	3.138653	0.908669
21	1	0.542493	-0.438347	3.727297
22	1	0.542493	-0.438347	-3.727297
23	1	-2.048416	2.291976	0.000000
24	1	-3.009816	3.877813	0.000000
25	6	-3.766358	2.285088	1.291785
26	6	-3.766358	2.285088	-1.291785
27	1	-3.774617	1.192249	-1.312190
28	1	-3.774617	1.192249	1.312190
29	1	-3.221982	2.647517	-2.169051
30	1	-3.221982	2.647517	2.169051
31	1	-4.801843	2.644976	-1.364484
32	1	-4.801843	2.644976	1.364484

TS-7b

E(RB+HF-LYP) = -1134.17741103 A.U.

Center Number	Atomic Number	Coordinates (Angstroms) X	Y	Z
1	45	1.032421	-1.623272	-0.000000
2	45	-0.000000	0.617868	0.000000
3	6	-1.887715	-1.588668	-0.000000
4	6	2.905751	0.575329	0.000000
5	8	-1.867265	-0.313805	-0.000000
6	8	1.932717	1.392289	0.000000
7	6	-0.768089	2.584464	0.000000
8	8	-0.920036	-2.389667	-0.000000
9	8	2.881115	-0.684959	0.000000
10	6	0.518524	-0.492366	2.627692
11	6	0.518524	-0.492366	-2.627692
12	8	0.033131	0.547455	2.080464
13	8	0.033131	0.547455	-2.080464
14	8	0.991161	-1.525121	2.082792
15	8	0.991161	-1.525121	-2.082792
16	6	-2.933946	2.985238	0.000000
17	1	-2.893060	-2.037561	-0.000000
18	1	3.903053	1.040478	0.000000
19	1	-0.595005	3.159499	-0.911041
20	1	-0.595005	3.159499	0.911041
21	1	0.521408	-0.480729	3.728422
22	1	0.521408	-0.480729	-3.728422
23	1	-1.891278	2.174362	0.000000
24	1	-2.672964	4.040983	0.000000
25	6	-3.578710	2.527430	1.293324
26	6	-3.578710	2.527430	-1.293324
27	1	-3.683832	1.439254	-1.317987
28	1	-3.683832	1.439254	1.317987
29	1	-3.003057	2.845057	-2.167278
30	1	-3.003057	2.845057	2.167278
31	1	-4.579208	2.975792	-1.364101
32	1	-4.579208	2.975792	1.364101

8

E(RB+HF-LYP) = -1346.29540069 A.U.

Center Number	Atomic Number	Coordinates (Angstroms) X	Y	Z
1	6	-0.009012	-2.342726	1.028012
2	6	-1.799485	2.203082	-0.963132
3	6	-1.209914	-1.210293	-2.319602
4	6	-0.594670	1.094281	2.380871
5	6	2.316609	0.899131	-0.987390
6	8	0.878037	-1.538316	0.535782
7	8	-0.519260	2.010911	-1.032512
8	8	-1.277672	-2.141875	1.094580
9	8	-2.669300	1.402726	-0.458633
10	8	-0.067384	-0.645204	-2.095836
11	8	0.414379	1.151563	1.569505
12	45	0.235237	0.253912	-0.271763
13	45	-2.030757	-0.387294	0.337253
14	8	-2.210803	-1.269907	-1.510809
15	8	-1.728922	0.531237	2.156774
16	1	0.363640	-3.288278	1.429145
17	1	-2.169280	3.143979	-1.377600
18	1	-1.332615	-1.682317	-3.297038
19	1	-0.461164	1.576969	3.351899
20	1	2.112236	1.143728	-2.023771
21	6	3.118395	-0.313896	-0.688708
22	8	3.280755	-1.252411	-1.453751
23	8	3.603656	-0.243205	0.597746
24	6	4.160740	-1.512576	1.117351
25	1	4.921408	-1.903492	0.438985
26	1	3.344045	-2.228476	1.217850
27	1	4.584265	-1.252569	2.085397
28	7	2.522468	1.969512	-0.184527
29	7	2.607817	2.822848	0.556083

TS-9

E(RB+HF-LYP) = -1352.42292403 A.U.

Center Number	Atomic Number	Atomic Type	Coordinates (Angstroms) X	Y	Z
1	6	0	-0.122621	-1.756302	1.871800
2	6	0	-1.769217	1.630358	-1.786580
3	6	0	-1.168784	-2.022483	-1.680936
4	6	0	-0.790948	1.898919	1.786599
5	6	0	2.117114	0.356736	-1.009085
6	8	0	0.791138	-1.209178	1.175846
7	8	0	-0.508089	1.464489	-1.722413
8	8	0	-1.370096	-1.592459	1.805113
9	8	0	-2.669371	1.097165	-1.086502
10	8	0	-0.047469	-1.425518	-1.646804
11	8	0	0.254028	1.675178	1.092778
12	45	0	0.215400	0.138655	-0.300639
13	45	0	-2.115729	-0.263134	0.391686
14	8	0	-2.201678	-1.796374	-0.996048
15	8	0	-1.894987	1.298757	1.748740
16	1	0	0.235223	-2.465178	2.632991
17	1	0	-2.105312	2.336577	-2.559890
18	1	0	-1.234151	-2.843040	-2.409832
19	1	0	-0.701721	2.725466	2.506343
20	1	0	2.193729	0.610856	-2.068077
21	6	0	3.212505	-0.539379	-0.552339
22	8	0	3.334426	-1.610341	-1.111491
23	8	0	3.917529	-0.120060	0.502464
24	6	0	4.886850	-1.063195	1.005437
25	1	0	5.589659	-1.344150	0.217324
26	1	0	4.378310	-1.955382	1.377256
27	1	0	5.399340	-0.544118	1.814563
28	7	0	2.694456	2.105500	-0.420758
29	7	0	2.552247	3.008686	0.204961

11

E(RB+HF-LYP) = -1242.90804506 A.U.

Center Number	Atomic Number	Coordinates (Angstroms) X	Y	Z
1	6	0.217254	1.475430	1.981003
2	6	-1.746275	-1.417700	-1.933518
3	6	-1.326534	-1.886636	1.710487
4	6	-0.310009	2.004002	-1.656560
5	6	2.100830	-1.103952	-0.683548
6	8	1.052981	0.725713	1.378902
7	8	-0.501098	-1.567880	-1.706768
8	8	-1.013094	1.619558	1.761311
9	8	-2.567948	-0.664473	-1.350618
10	8	-0.173857	-1.927002	1.170510
11	8	0.619542	1.148762	-1.502034
12	45	0.346415	-0.448459	-0.179696
13	45	-1.892879	0.524979	0.222307
14	8	-2.239397	-1.037723	1.543425
15	8	-1.442079	2.042346	-1.111111
16	1	0.642066	2.071257	2.801980
17	1	-2.141518	-2.036821	-2.751868
18	1	-1.533264	-2.707678	2.411567
19	1	-0.075871	2.811186	-2.365603
20	1	2.172638	-1.897418	-1.434731
21	6	3.379302	-0.604008	-0.171831

22	8	4.002225	-1.381112	0.534041
23	8	3.706446	0.648167	-0.460088
24	6	4.914505	1.140876	0.161600
25	1	5.767735	0.515915	-0.112378
26	1	4.796884	1.147988	1.247555
27	1	5.038035	2.153242	-0.220329

12a

E(RB+HF-LYP) = -1283.42754536 A.U.

Center Number	Atomic Number	Atomic Type	Coordinates (Angstroms) X	Y	Z
1	45	0	-0.246986	0.156419	-0.161443
2	45	0	2.188366	-0.092357	0.198397
3	8	0	-0.537845	-1.315410	1.270351
4	8	0	0.192266	1.616433	-1.568387
5	8	0	1.707051	-1.541181	1.616572
6	8	0	2.441003	1.378758	-1.251916
7	8	0	-0.198984	1.593093	1.329704
8	8	0	-0.019871	-1.318671	-1.624821
9	8	0	2.046254	1.374647	1.656990
10	8	0	2.221957	-1.548419	-1.274231
11	6	0	0.496720	-1.813212	1.822886
12	6	0	1.419292	1.883228	-1.785227
13	6	0	0.913142	1.871522	1.883603
14	6	0	1.130793	-1.820173	-1.835991
15	1	0	0.288294	-2.583484	2.579639
16	1	0	1.593495	2.661354	-2.542419
17	1	0	0.857364	2.648684	2.659024
18	1	0	1.156235	-2.592969	-2.617836
19	6	0	-2.132090	0.288586	-0.602092
20	1	0	-2.456149	1.077914	-1.288715
21	6	0	-3.197229	-0.581616	-0.098011
22	8	0	-3.959059	-0.073420	0.710045
23	8	0	-3.202987	-1.840344	-0.513024
24	6	0	-4.205857	-2.695087	0.082468
25	1	0	-5.204146	-2.282217	-0.079715
26	1	0	-4.017748	-2.795840	1.153704
27	1	0	-4.096413	-3.654406	-0.421103
28	6	0	-4.754472	3.522613	-0.072633
29	1	0	-4.580220	2.485152	0.224737
30	1	0	-3.856337	4.115548	0.122410
31	1	0	-5.589004	3.929061	0.505553
32	1	0	-4.997536	3.569365	-1.138452

TS-13a

E(RB+HF-LYP) = -1283.41185690 A.U.

Center Number	Atomic Number	Atomic Type	Coordinates (Angstroms) X	Y	Z
1	45	0	-0.249891	0.254197	-0.202379
2	45	0	2.080241	-0.382925	0.247633
3	6	0	-2.252126	0.799336	-0.665520
4	1	0	-2.377233	0.974695	-1.733451
5	6	0	-3.374684	0.089228	0.014314
6	8	0	-3.952005	0.447498	1.020312
7	8	0	-3.613520	-1.058494	-0.644684
8	6	0	-4.531928	-1.960921	-0.000989
9	1	0	-5.511566	-1.490148	0.114750
10	1	0	-4.149689	-2.249398	0.981227
11	1	0	-4.594126	-2.826498	-0.659911
12	6	0	-2.861681	2.855600	-0.180406
13	1	0	-2.064971	1.918314	-0.083648
14	1	0	-2.191935	3.589268	-0.628810
15	1	0	-3.053866	2.988111	0.882727
16	1	0	-3.769025	2.691056	-0.749181
17	6	0	0.150660	-1.328244	2.191167
18	6	0	1.671569	1.199042	-2.153859
19	6	0	1.233877	2.142984	1.419583
20	6	0	0.614939	-2.262201	-1.375166
21	8	0	-0.777993	-0.774015	1.523837
22	8	0	0.425389	1.244764	-1.902942
23	8	0	1.388278	-1.350395	1.951707
24	8	0	2.586570	0.635268	-1.496909
25	8	0	0.075836	1.975666	0.915087
26	8	0	-0.403138	-1.507034	-1.300961
27	8	0	2.240245	1.394638	1.330618
28	8	0	1.756016	-2.104026	-0.861232
29	1	0	-0.178150	-1.856836	3.098166
30	1	0	1.983328	1.726013	-3.068046
31	1	0	1.358428	3.065291	2.006103
32	1	0	0.473896	-3.176993	-1.969792

12b

E(RB+HF-LYP) = -1362.05178239 A.U.

Center Number	Atomic Number	Atomic Type	Coordinates (Angstroms) X	Y	Z
1	45	0	-2.218082	0.577514	0.403838
2	45	0	-0.027856	-0.307170	-0.329875
3	6	0	-0.583099	2.418429	-1.142434
4	6	0	-1.641324	-2.156281	1.204561
5	8	0	0.319936	1.523347	-1.242124
6	8	0	-0.510022	-2.087404	0.622003
7	6	0	1.741445	-0.900846	-0.870284
8	8	0	-1.693867	2.352274	-0.557283
9	8	0	-2.536845	-1.277120	1.295561
10	6	0	-0.091289	1.035252	2.277985
11	8	0	0.703898	0.446466	1.477274
12	8	0	-1.321781	1.255568	2.143051
13	6	0	-2.251171	-0.732023	-2.163720
14	8	0	-1.005376	-0.962210	-2.035987
15	8	0	-3.023504	-0.140307	-1.367090
16	6	0	4.299266	1.605593	0.662389
17	1	0	-0.344103	3.369453	-1.639736
18	1	0	-1.850099	-3.121119	1.689328
19	1	0	2.330332	-0.238900	-1.514350
20	6	0	2.361634	-2.195959	-0.580656
21	1	0	0.376059	1.393254	3.206757
22	1	0	-2.692822	-1.106906	-3.097914
23	1	0	4.245092	0.555119	0.349798
24	1	0	5.320240	1.790866	1.019523
25	1	0	3.618286	1.726515	1.513106
26	6	0	3.929050	2.559311	-0.479250
27	8	0	2.354948	-2.997094	-1.500578
28	8	0	2.829401	-2.391200	0.644613
29	6	0	3.372868	-3.706511	0.903943
30	1	0	4.174786	-3.932332	0.197161
31	1	0	2.584388	-4.457442	0.818422
32	1	0	3.755058	-3.660455	1.922460
33	1	0	2.907531	2.342529	-0.818324
34	1	0	4.588402	2.376292	-1.339311
35	6	0	4.024421	4.034595	-0.074420
36	1	0	5.043191	4.294850	0.239219
37	1	0	3.354093	4.257448	0.765272
38	1	0	3.751689	4.697453	-0.903917

TS-13b

E(RB+HF-LYP) = -1362.04434949 A.U.

Center Number	Atomic Number	Atomic Type	Coordinates (Angstroms) X	Y	Z
1	45	0	-2.343429	0.156059	0.313034
2	45	0	0.041129	-0.070873	-0.239385
3	6	0	-1.227727	2.325071	-1.267137
4	6	0	-1.075167	-2.239341	1.329635
5	8	0	-0.095985	1.744403	-1.252148
6	8	0	0.023236	-1.865403	0.812430
7	6	0	2.103919	-0.253767	-0.805914
8	8	0	-2.307672	1.957205	-0.734715
9	8	0	-2.194917	-1.659830	1.308883
10	6	0	-0.507020	1.319251	2.250530
11	8	0	0.475127	0.959614	1.523285
12	8	0	-1.736195	1.146911	2.048344
13	6	0	-1.795412	-1.216539	-2.167109
14	8	0	-0.552309	-1.058571	-1.963405
15	8	0	-2.766180	-0.845823	-1.451298
16	6	0	3.511343	1.191346	0.092767
17	1	0	-1.257812	3.276116	-1.820121
18	1	0	-1.035929	-3.198114	1.867921
19	1	0	2.266415	0.161871	-1.797548
20	6	0	2.762390	-1.563069	-0.586988
21	1	0	-0.233833	1.850036	3.175177
22	1	0	-2.051739	-1.747967	-3.095274
23	1	0	2.390815	0.571461	0.062876
24	1	0	4.271635	0.805299	-0.581263
25	1	0	3.725222	0.908885	1.125874
26	6	0	3.103661	2.630514	-0.140554
27	8	0	2.734098	-2.437349	-1.428773
28	8	0	3.306970	-1.700126	0.640469
29	6	0	3.810410	-3.014157	0.940122
30	1	0	4.570318	-3.311071	0.212516
31	1	0	2.993799	-3.739648	0.926067
32	1	0	4.240773	-2.939489	1.938883
33	1	0	2.259722	2.878312	0.510022
34	1	0	2.758228	2.756001	-1.172308
35	6	0	4.289579	3.572381	0.136614
36	1	0	5.136011	3.359510	-0.526242
37	1	0	4.638458	3.485616	1.171752
38	1	0	3.986193	4.611461	-0.028905

12c

E(RB+HF-LYP) = -1362.04971611 A.U.

| Center Number | Atomic Number | Atomic Type | Coordinates (Angstroms) X | Y | Z |

1	45	0	-2.326436	-0.047575	0.343087
2	45	0	0.065498	0.003126	-0.267834
3	8	0	-0.118888	2.071280	-0.486397
4	8	0	0.073354	-2.053277	0.027873
5	8	0	-2.335023	2.018834	0.056029
6	8	0	-2.141074	-2.099693	0.578968
7	8	0	0.489738	0.274574	1.751216
8	8	0	-1.720706	0.227028	2.320068
9	8	0	-0.543954	-0.247180	-2.241783
10	8	0	-2.751844	-0.325122	-1.667947
11	6	0	-1.265338	2.587493	-0.280952
12	6	0	-0.489110	0.317369	2.563400
13	6	0	-1.787855	-0.356336	-2.479217
14	6	0	-1.011371	-2.618760	0.372887
15	1	0	-1.315341	3.678409	-0.418420
16	1	0	-0.943917	-3.708449	0.507407
17	1	0	-0.210120	0.454037	3.619359
18	1	0	-2.047748	-0.495526	-3.539025
19	6	0	2.037756	-0.020104	-0.922012
20	1	0	2.165625	0.345050	-1.943817
21	6	0	2.878667	-1.212157	-0.647298
22	8	0	2.908333	-2.136142	-1.435187
23	8	0	3.498591	-1.204701	0.548267
24	6	0	4.188821	-2.423654	0.883404
25	1	0	4.950326	-2.653715	0.133559
26	1	0	3.478756	-3.251723	0.942120
27	1	0	4.646913	-2.239780	1.855127
28	1	0	2.515776	0.996487	-0.222117
29	6	0	3.421556	1.818920	-0.060965
30	1	0	4.335399	1.260913	-0.272066
31	6	0	3.253657	2.132244	1.412615
32	6	0	3.158623	2.945735	-1.036354
33	1	0	2.147599	3.341866	-0.912410
34	1	0	3.289062	2.628015	-2.075412
35	1	0	3.877427	3.753976	-0.842548
36	1	0	2.271764	2.567448	1.615104
37	1	0	4.026148	2.859268	1.702089
38	1	0	3.373892	1.234652	2.022737

TS-13c

E(RB+HF-LYP) = -1362.04944887 A.U.

Center Number	Atomic Number	Atomic Type	Coordinates (Angstroms) X	Y	Z
1	45	0	-2.331453	-0.090332	0.326913
2	45	0	0.056559	0.046762	-0.250401
3	6	0	-1.384381	2.566809	-0.377580
4	6	0	-0.904209	-2.597650	0.464283
5	8	0	-0.214181	2.095825	-0.551095
6	8	0	0.159655	-1.995645	0.118968
7	6	0	2.109410	0.102598	-0.887116
8	8	0	-2.432439	1.962493	-0.030904
9	8	0	-2.060165	-2.122328	0.633839
10	6	0	-0.551071	0.446258	2.559252
11	8	0	0.440657	0.424321	1.762658
12	8	0	-1.772213	0.277144	2.302515
13	6	0	-1.734303	-0.477773	-2.473118
14	8	0	-0.501325	-0.308013	-2.220304
15	8	0	-2.713553	-0.453186	-1.678143
16	6	0	3.456652	1.760756	-0.084155
17	1	0	-1.483663	3.648406	-0.556127
18	1	0	-0.793907	-3.678367	0.637606
19	1	0	2.188971	0.485959	-1.902434
20	6	0	2.899244	-1.132939	-0.674711
21	1	0	-0.298931	0.640757	3.612952
22	1	0	-1.971912	-0.670205	-3.529793
23	1	0	2.383745	0.985076	-0.106555
24	1	0	4.313659	1.188835	-0.433558
25	6	0	3.452701	1.962006	1.417571
26	6	0	3.100249	2.948769	-0.945441
27	8	0	2.966230	-2.007481	-1.513906
28	8	0	3.458244	-1.217678	0.554812
29	6	0	4.086172	-2.477674	0.850755
30	1	0	4.878760	-2.694129	0.129539
31	1	0	3.345228	-3.279945	0.822572
32	1	0	4.497246	-2.369584	1.854735
33	1	0	2.091078	3.307003	-0.725362
34	1	0	3.168902	2.718877	-2.012154
35	1	0	3.812042	3.757513	-0.728026
36	1	0	2.523371	2.424276	1.759844
37	1	0	4.289790	2.630404	1.666396
38	1	0	3.595801	1.015204	1.941396

14

E(RB+HF-LYP) = -2024.78646684 A.U.

Center Number	Atomic Number	Atomic Type	Coordinates (Angstroms) X	Y	Z
1	6	0	.000000	1.249757	-1.253259
2	6	0	.000000	-1.249757	-1.253259
3	8	0	.000000	1.427942	.007001
4	8	0	.000000	-1.427942	.007001
5	6	0	.000000	2.514875	-2.092905
6	6	0	.000000	-2.514875	-2.092905
7	6	0	.000000	.000000	-1.904482
8	1	0	.000000	.000000	-2.988663
9	1	0	-.880525	3.117475	-1.841785
10	1	0	.880525	3.117475	-1.841785
11	1	0	.880525	-3.117475	-1.841785
12	1	0	-.880525	-3.117475	-1.841785
13	1	0	.000000	-2.312927	-3.167336
14	1	0	.000000	2.312927	-3.167336
15	29	0	.000000	.000000	1.413279
16	6	0	.000000	.000000	3.233735
17	1	0	.000000	-.885755	3.885916
18	1	0	.000000	.885755	3.885916

TS-15

E(RB+HF-LYP) = -2065.30142225 A.U.

Center Number	Atomic Number	Atomic Type	Coordinates (Angstroms) X	Y	Z
1	6	0	-.929438	-1.811386	.000000
2	6	0	1.562850	-1.495162	.000000
3	8	0	-1.294755	-.592192	.000000
4	8	0	1.618889	-.222982	.000000
5	6	0	-2.062993	-2.824573	.000000
6	6	0	2.913429	-2.193582	.000000
7	6	0	.397306	-2.287151	.000000
8	1	0	.534353	-3.362719	.000000
9	1	0	-2.695548	-2.662368	.880625
10	1	0	-2.695548	-2.662368	-.880625
11	1	0	-1.710983	-3.859649	.000000
12	1	0	2.830103	-3.283702	.000000
13	1	0	3.485290	-1.878405	-.880534
14	1	0	3.485290	-1.878405	.880534
15	29	0	.000000	.919392	.000000
16	6	0	.008034	2.832597	.000000
17	1	0	.349418	3.344896	.900553
18	1	0	.349418	3.344896	-.900553
19	1	0	-1.211258	2.781837	.000000
20	6	0	-1.780968	3.998383	.000000
21	1	0	-2.367196	3.864455	-.910154
22	1	0	-2.367196	3.864455	.910154
23	1	0	-1.228531	4.931352	.000000

16

E(RB+HF-LYP) = -1488.85531850 A.U.

Center Number	Atomic Number	Atomic Type	Coordinates (Angstroms) X	Y	Z
1	1	0	2.160758	.000000	-2.937643
2	1	0	-2.160758	.000000	-2.937643
3	6	0	1.214053	.000000	-2.406848
4	6	0	-1.214053	.000000	-2.406848
5	6	0	1.176541	.000000	-1.008459
6	6	0	-1.176541	.000000	-1.008460
7	7	0	.000000	.000000	-.361318
8	6	0	.000000	.000000	-3.100510
9	1	0	.000000	.000001	-4.185970
10	6	0	-2.294926	.000000	-.065024
11	6	0	2.294926	.000000	-.065024
12	7	0	-2.003705	.000000	1.196324
13	7	0	2.003704	.000000	1.196324
14	1	0	-2.799558	.000000	1.829612
15	1	0	2.799558	.000000	1.829612
16	44	0	.000000	.000000	1.766430
17	6	0	.000000	.000000	3.633429
18	1	0	.000000	-.925184	4.222481
19	1	0	.000000	.925184	4.222480
20	1	0	3.325227	.000000	-.417559
21	1	0	-3.325227	.000000	-.417559
22	17	0	.000000	-2.461038	1.819828
23	17	0	.000000	2.461037	1.819827

TS-17

E(RB+HF-LYP) = -1529.32970239 A.U.

Center Number	Atomic Number	Atomic Type	Coordinates (Angstroms) X	Y	Z
1	1	0	0.096378	-3.912939	2.159913
2	1	0	0.096378	-3.912939	-2.159913
3	6	0	0.083072	-3.383146	1.212521

4	6	0	0.083072	-3.383146	-1.212521
5	6	0	0.060217	-1.985959	1.186653
6	6	0	0.060217	-1.985959	-1.186653
7	7	0	0.040211	-1.328156	0.000000
8	6	0	0.091295	-4.079077	0.000000
9	1	0	0.108872	-5.164321	0.000000
10	6	0	0.060217	-1.060312	-2.312301
11	6	0	0.060217	-1.060312	2.312301
12	7	0	0.052321	0.210431	-2.034908
13	7	0	0.052321	0.210431	2.034908
14	1	0	0.056282	0.819351	-2.853807
15	1	0	0.056282	0.819351	2.853807
16	44	0	0.052724	0.664237	0.000000
17	6	0	0.354913	2.784812	0.000000
18	1	0	0.781861	3.226418	0.900908
19	1	0	0.781861	3.226418	-0.900908
20	1	0	0.069380	-1.434825	3.335133
21	1	0	0.069380	-1.434825	-3.335133
22	17	0	-2.397130	0.930250	0.000000
23	17	0	2.511569	0.768033	0.000000
24	6	0	-1.236296	4.141419	0.000000
25	1	0	-0.881448	2.915225	0.000000
26	1	0	-1.841029	4.104788	-0.905599
27	1	0	-1.841029	4.104788	0.905599
28	1	0	-0.533985	4.967400	0.000000

11-C_s

E(RB+HF-LYP) = -1242.89778884 A.U.

Center Number	Atomic Number	Coordinates (Angstroms) X	Y	Z
1	6	-1.832978	-1.723156	-0.000000
2	6	2.901814	0.536185	0.000000
3	6	0.553460	-0.647004	2.622930
4	6	0.553460	-0.647004	-2.622930
5	6	-0.665101	2.334857	-0.000000
6	8	-1.830128	-0.450888	-0.000000
7	8	1.912519	1.340631	0.000000
8	8	-0.858230	-2.519725	-0.000000
9	8	2.892199	-0.720517	0.000000
10	8	0.059936	0.391486	2.074877
11	8	0.059936	0.391486	-2.074877
12	45	0.0	0.529158	0.0
13	45	1.060377	-1.715790	0.000000
14	8	1.037645	-1.667206	2.073103
15	8	1.037645	-1.667206	-2.073103
16	1	-2.834854	-2.177614	-0.000000
17	1	3.887845	1.023073	0.000000
18	1	0.545729	-0.629738	3.722168
19	1	0.545729	-0.629738	-3.722168
20	1	0.111518	3.108318	0.000000
21	6	-2.016192	2.975291	-0.000000
22	8	-2.142039	4.189265	-0.000000
23	8	-3.028689	2.106527	-0.000000
24	6	-4.343941	2.687318	-0.000000
25	1	-4.485164	3.305659	-0.890731
26	1	-4.485164	3.305659	0.890731
27	1	-5.032103	1.843047	-0.000000

Chapter 6

TS1a-1

E(RB+HF-LYP) = -1474.16442336 A.U. after 10 cycles

Center Number	Atomic Number	Atomic Type	Coordinates (Angstroms) X	Y	Z
1	45	0	-0.003410	-0.056100	-0.014608
2	45	0	2.445242	0.122725	0.008083
3	6	0	-2.169772	-0.163867	-0.038878
4	6	0	-2.741473	-0.973420	1.079618
5	6	0	-2.867152	1.093737	-0.477089
6	8	0	-3.348039	1.263381	-1.580437
7	8	0	-2.847706	1.992484	0.507767
8	6	0	-3.383629	3.286709	0.174207
9	1	0	-4.429912	3.201900	-0.129656
10	1	0	-2.802961	3.733102	-0.636602
11	1	0	-3.291775	3.875319	1.086299
12	6	0	-2.909059	-1.684784	-1.549041
13	1	0	-2.120939	-0.828091	-1.152755
14	1	0	-2.449928	-1.742579	-2.538895
15	1	0	-3.907811	-1.255451	-1.590344
16	6	0	1.068541	2.367940	-1.188919
17	6	0	1.388791	-2.308265	1.183387
18	6	0	1.329505	-1.154602	-2.352965
19	6	0	1.140114	1.203062	2.333373
20	8	0	-0.041211	1.797544	-0.948359
21	8	0	0.209775	-1.915769	0.910743
22	8	0	2.233707	1.960876	-0.932456
23	8	0	2.482768	-1.728609	0.952541
24	8	0	0.161507	-0.998115	-1.869524
25	8	0	0.022175	0.874104	1.833286
26	8	0	2.433533	-0.820829	-1.851247
27	8	0	2.297321	1.046929	1.850917
28	1	0	0.993951	3.345203	-1.687899
29	1	0	1.452946	-3.285256	1.685176
30	1	0	1.367771	-1.647623	-3.335786
31	1	0	1.086234	1.688737	3.318280
32	8	0	-2.906763	-0.458446	2.169485
33	6	0	-3.094131	-2.435734	0.797506
34	1	0	-2.622195	-3.053185	1.567325
35	6	0	-2.697609	-2.857014	-0.620790
36	1	0	-4.179689	-2.515810	0.944633
37	1	0	-3.293774	-3.710202	-0.969525
38	1	0	-1.645682	-3.155168	-0.650793

TS1a-2

E(RB+HF-LYP) = -1474.16243003 A.U. after 13 cycles

Center Number	Atomic Number	Atomic Type	Coordinates (Angstroms) X	Y	Z
1	45	0	0.029715	-0.075574	-0.012204
2	45	0	2.478623	0.065656	-0.007922
3	6	0	-2.164491	-0.154613	-0.027297
4	6	0	-2.739790	-0.944422	1.106230
5	6	0	-2.803439	1.133965	-0.456671
6	8	0	-3.232354	1.373248	-1.569201
7	8	0	-2.794942	1.993890	0.564762
8	6	0	-3.254100	3.323180	0.259317
9	1	0	-4.286740	3.300519	-0.097802
10	1	0	-2.613783	3.772496	-0.503524
11	1	0	-3.181180	3.871261	1.198100
12	6	0	-2.987166	-1.565788	-1.593802
13	1	0	-2.081054	-0.870494	-1.052871
14	1	0	-2.208853	-2.118633	-2.127960
15	1	0	-3.505542	-0.848124	-2.224462
16	6	0	1.128529	2.361873	-1.132936
17	6	0	1.397637	-2.380095	1.110907
18	6	0	1.322909	-1.133422	-2.391185
19	6	0	1.209478	1.104689	2.356641
20	8	0	0.012671	1.805336	-0.889965
21	8	0	0.223255	-1.964713	0.852864
22	8	0	2.289941	1.926842	-0.905321
23	8	0	2.497882	-1.806988	0.893111
24	8	0	0.161559	-0.967876	-1.895389
25	8	0	0.082911	0.799990	1.860793
26	8	0	2.436466	-0.833938	-1.888303
27	8	0	2.359685	0.949963	1.856670
28	1	0	1.064984	3.353091	-1.605139
29	1	0	1.451020	-3.371575	1.584444
30	1	0	1.345870	-1.600475	-3.387028
31	1	0	1.172134	1.564795	3.354490
32	8	0	-2.905811	-0.450446	2.203800
33	6	0	-3.070480	-2.391423	0.754424
34	1	0	-2.123809	-2.943223	0.684381
35	6	0	-3.798328	-2.374350	-0.598895
36	1	0	-3.670738	-2.827091	1.556423
37	1	0	-4.790189	-1.925655	-0.478212
38	1	0	-3.941991	-3.390605	-0.986157

TS1b-1

E(RB+HF-LYP) = -1434.85230099 A.U. after 11 cycles

Center Number	Atomic Number	Atomic Type	Coordinates (Angstroms) X	Y	Z
1	45	0	-0.096814	0.083873	-0.032356
2	45	0	2.340950	-0.125098	0.025269
3	6	0	-2.318315	0.224817	-0.087568
4	6	0	-2.938322	-0.522548	1.046624
5	6	0	-2.863153	1.575494	-0.467904
6	8	0	-3.301704	1.781378	-1.587287
7	6	0	-2.761440	2.639351	0.600586
8	1	0	-1.706778	2.896809	0.744863
9	1	0	-3.138514	2.271369	1.558301
10	1	0	-3.315989	3.517397	0.262536
11	6	0	-3.183696	-1.088581	-1.495068
12	1	0	-2.206877	-0.371086	-1.193460
13	1	0	-2.754784	-1.275080	-2.483889
14	1	0	-4.115575	-0.534530	-1.557128
15	6	0	1.361968	2.305725	-1.194237
16	6	0	0.897036	-2.352393	1.190285
17	6	0	1.071621	-1.223057	-2.349795
18	6	0	1.187548	1.179472	2.320895
19	8	0	0.172460	1.920539	-0.966723
20	8	0	-0.198018	-1.777493	0.891507
21	8	0	2.443094	1.715846	-0.921675
22	8	0	2.072672	-1.954085	0.976753
23	8	0	-0.064994	-0.886281	-1.880879
24	8	0	0.038335	1.035563	1.800050
25	8	0	2.205849	-1.062788	-1.831869
26	8	0	2.308161	0.821371	1.862941
27	1	0	1.451875	3.280804	-1.694236
28	1	0	0.794724	-3.322532	1.697585
29	1	0	1.046948	-1.717529	-3.331962
30	1	0	1.199631	1.683372	3.297691
31	8	0	-3.059425	-0.033208	2.144527
32	8	0	-3.381666	-1.780434	0.787039
33	6	0	-3.129956	-2.253451	-0.537518
34	1	0	-3.908194	-2.986704	-0.768658
35	1	0	-2.150429	-2.739377	-0.565623

TS1b-2

E(RB+HF-LYP) = -1434.84428892 A.U. after 12 cycles

Center Number	Atomic Number	Atomic Type	Coordinates (Angstroms) X	Y	Z
1	45	0	-0.054643	0.057648	-0.022606
2	45	0	2.381338	-0.151289	-0.013943
3	6	0	-2.296499	0.179783	-0.038930
4	6	0	-2.913534	-0.598988	1.081102
5	6	0	-2.819734	1.552534	-0.350636
6	8	0	-3.275160	1.846725	-1.443671
7	6	0	-2.668649	2.550420	0.778065
8	1	0	-1.655912	2.965004	0.723177
9	1	0	-2.781256	2.087618	1.760907
10	1	0	-3.395043	3.353000	0.628500
11	6	0	-3.176069	-1.028767	-1.582211
12	1	0	-2.158724	-0.464081	-1.083173
13	1	0	-2.516658	-1.819283	-1.949775
14	1	0	-3.490519	-0.322542	-2.346346
15	6	0	1.381065	2.299921	-1.178372
16	6	0	0.958178	-2.392440	1.141423
17	6	0	1.070017	-1.213384	-2.380546
18	6	0	1.281837	1.120135	2.320598
19	8	0	0.195846	1.911664	-0.935303
20	8	0	-0.139214	-1.811245	0.872786
21	8	0	2.466689	1.704914	-0.935911
22	8	0	2.132484	-1.992417	0.913540
23	8	0	-0.056028	-0.880161	-1.885643
24	8	0	0.123534	0.987316	1.820419
25	8	0	2.214151	-1.061904	-1.881580
26	8	0	2.393367	0.766054	1.835904
27	1	0	1.463389	3.283165	-1.663759
28	1	0	0.863683	-3.370743	1.633969
29	1	0	1.025755	-1.694144	-3.368681
30	1	0	1.315696	1.609385	3.304425
31	8	0	-2.744637	-0.324247	2.241878
32	8	0	-3.700232	-1.648567	0.700860
33	6	0	-4.242277	-1.493307	-0.613166
34	1	0	-5.074305	-0.781371	-0.578896
35	1	0	-4.629823	-2.472670	-0.905822

TS5a

E(RB+HF-LYP) = -1450.88676593 A.U. after 13 cycles

Standard orientation:

Center Number	Atomic Number	Atomic Type	Coordinates (Angstroms) X	Y	Z
1	45	0	0.072788	0.102760	-0.055678
2	45	0	-2.348259	-0.262430	0.055161
3	6	0	2.222809	0.421805	-0.155438
4	6	0	2.671659	1.471601	0.816773
5	6	0	3.058996	-0.763782	-0.473997
6	8	0	3.459676	-0.992472	-1.599927
7	8	0	3.299977	-1.511262	0.606982
8	6	0	4.053680	-2.715913	0.371193
9	1	0	5.034824	-2.478018	-0.047342
10	1	0	3.512506	-3.368358	-0.318305
11	1	0	4.154090	-3.185208	1.349213
12	6	0	2.749694	2.279204	-1.295096
13	1	0	2.059833	1.082188	-1.196337
14	1	0	2.082073	2.816870	-1.968660
15	1	0	3.666810	1.898996	-1.742143
16	6	0	-0.835099	-2.456421	-1.063411
17	6	0	-1.456855	2.308354	1.063411
18	6	0	-1.402983	0.977904	-2.398582
19	6	0	-0.898254	-1.123718	2.386237
20	8	0	0.232090	-1.791969	-0.881964
21	8	0	-0.259836	1.999784	0.762147
22	8	0	-2.023054	-2.123944	-0.800407
23	8	0	-2.505192	1.628512	0.908770
24	8	0	-0.214083	0.939333	-1.943368
25	8	0	0.175348	-0.735037	1.834440
26	8	0	-2.462913	0.583376	-1.847084
27	8	0	-2.077864	-1.079642	1.935513
28	1	0	-0.696547	-3.451702	-1.509968
29	1	0	-1.585887	3.303204	1.515269
30	1	0	-1.507327	1.415345	-3.402498
31	1	0	-0.778266	-1.555640	3.390093
32	8	0	2.826661	1.355360	2.003390
33	7	0	2.801314	2.667390	0.038388
34	1	0	2.256518	3.465260	0.350764

TS7a-1

E(RB+HF-LYP) = -1282.20269877 A.U. after 20 cycles

Center Number	Atomic Number	Atomic Type	Coordinates (Angstroms) X	Y	Z
1	45	0	-0.299386	0.056090	-0.320663
2	45	0	2.043824	-0.078819	0.382313
3	6	0	-2.352606	0.200256	-0.975445
4	6	0	-3.300020	0.970487	-0.120407
5	1	0	-2.467292	0.406017	-2.039904
6	6	0	-3.513613	-1.540121	-0.739602
7	1	0	-2.357783	-1.046806	-0.888951
8	1	0	-3.111952	-2.552363	-0.846516
9	1	0	-4.227354	-1.296043	-1.522753
10	6	0	1.599958	-0.350003	-2.468558
11	6	0	0.132268	0.325698	2.529553
12	6	0	0.620813	-2.624026	0.315600
13	6	0	1.133966	2.574614	-0.251265
14	8	0	0.350184	-0.216465	-2.276239
15	8	0	-0.813051	0.294782	1.678655
16	8	0	2.531080	-0.348478	-1.618629
17	8	0	1.370943	0.207516	2.331140
18	8	0	-0.431228	-2.014631	-0.071703
19	8	0	-0.010621	2.095781	-0.518256
20	8	0	1.748901	-2.139512	0.580242
21	8	0	2.173399	1.967612	0.132034
22	1	0	1.900277	-0.486184	-3.517904
23	1	0	-0.182564	0.473087	3.572978
24	1	0	0.515385	-3.713314	0.430209
25	1	0	1.224194	3.663438	-0.372931
26	8	0	-3.351741	2.173146	-0.171312
27	8	0	-4.099694	0.258926	0.725895
28	6	0	-3.911420	-1.154098	0.667627
29	1	0	-4.859556	-1.619961	0.951839
30	1	0	-3.134495	-1.451353	1.380039

TS7a-2

E(RB+HF-LYP) = -1282.19566092 A.U. after 17 cycles

Center Number	Atomic Number	Atomic Type	Coordinates (Angstroms) X	Y	Z
1	45	0	-0.285356	-0.038258	-0.210439
2	45	0	2.118972	0.005697	0.253869
3	6	0	-2.379302	-0.033824	-0.702057
4	6	0	-3.298600	0.978117	-0.091161
5	1	0	-2.516752	-0.185129	-1.775102
6	6	0	-3.561367	-1.709058	-0.060140
7	1	0	-2.424924	-1.142444	-0.150656
8	1	0	-3.247176	-2.141199	0.894703
9	1	0	-3.566326	-2.445081	-0.863220
10	6	0	1.370622	-1.241602	-2.259682
11	6	0	0.459113	1.199721	2.300017
12	6	0	0.705551	-2.346335	1.238758
13	6	0	1.140226	2.290223	-1.192733
14	8	0	0.146888	-1.017705	-1.995900
15	8	0	-0.568812	0.910905	1.612527
16	8	0	2.387681	-0.957450	-1.572398

17	8	0	1.671859	0.971579	2.036389
18	8	0	-0.382705	-1.877286	0.768219
19	8	0	-0.020581	1.779092	-1.171948
20	8	0	1.856339	-1.842923	1.192739
21	8	0	2.212098	1.834086	-0.704809
22	1	0	1.557731	-1.752684	-3.215812
23	1	0	0.256869	1.714611	3.250440
24	1	0	0.614790	-3.317252	1.748285
25	1	0	1.215185	3.259312	-1.706581
26	8	0	-3.069404	2.157591	-0.118583
27	8	0	-4.424645	0.478798	0.511264
28	6	0	-4.784513	-0.816623	0.033549
29	1	0	-5.274639	-0.721254	-0.942888
30	1	0	-5.507621	-1.220841	0.747176

Chapter 7

1a

SCF Done: E(RB+HF-LYP) = -1911.16300452 A.U. after 18 cycles

Center Number	Atomic Number	Atomic Type	Coordinates (Angstroms) X	Y	Z
1	44	0	1.396687	-0.008694	-0.205131
2	44	0	-1.284857	0.008461	-0.086026
3	17	0	-1.658982	0.086842	2.296816
4	16	0	0.053090	-1.916897	0.107877
5	16	0	0.056679	1.927049	-0.019434
6	6	0	0.313787	-2.522546	1.824510
7	6	0	0.325952	2.627732	1.660075
8	6	0	3.087210	0.685651	-1.438695
9	6	0	3.309393	-1.176930	-0.077113
10	6	0	3.324483	1.137852	-0.107407
11	6	0	3.432834	-0.010225	0.742227
12	6	0	3.073923	-0.754978	-1.419772
13	1	0	1.133832	-3.245243	1.790461
14	1	0	0.517939	-1.707854	2.515877
15	1	0	-0.604431	-3.031242	2.128286
16	1	0	1.146559	3.346007	1.579611
17	1	0	0.534244	1.853341	2.395239
18	1	0	-0.590639	3.151513	1.941745
19	1	0	2.939381	1.308163	-2.311069
20	1	0	3.355833	-2.200403	0.269250
21	1	0	3.385498	2.168725	0.214059
22	1	0	3.588205	0.002781	1.813149
23	1	0	2.916632	-1.397706	-2.275729
24	6	0	-2.302372	0.848200	-1.929537
25	6	0	-3.533288	-0.308196	-0.344565
26	6	0	-3.167018	1.002172	-0.788212
27	6	0	-2.884553	-1.255559	-1.180145
28	6	0	-2.114904	-0.542094	-2.162887
29	1	0	-1.865588	1.654278	-2.504502
30	1	0	-4.140905	-0.535022	0.520895
31	1	0	-3.511549	1.934683	-0.362596
32	1	0	-2.946497	-2.331267	-1.081831
33	1	0	-1.525337	-0.985696	-2.953771

2a

SCF Done: E(RB+HF-LYP) = -2103.03326773 A.U. after 2 cycles

Center Number	Atomic Number	Atomic Type	Coordinates (Angstroms) X	Y	Z
1	44	0	-1.581989	0.141388	-0.125612
2	44	0	1.159987	-0.588699	0.191092
3	16	0	0.213561	0.894069	-1.441183
4	16	0	-0.527589	-0.345548	1.903093
5	6	0	0.634986	2.656363	-1.167347
6	6	0	-0.353080	1.074274	3.044029
7	17	0	-2.010225	2.399444	0.639656
8	1	0	-0.100233	3.234371	-1.732460
9	1	0	0.576893	2.926681	-0.116283
10	1	0	1.635490	2.844879	-1.562801
11	1	0	-1.337642	1.233066	3.490100
12	1	0	-0.047996	1.985947	2.535117
13	1	0	0.350787	0.780990	3.828824
14	6	0	-2.996432	-1.653811	0.016943
15	6	0	-2.837718	-0.511977	-1.986166
16	6	0	-3.714770	-0.425940	0.155512
17	6	0	-3.609415	0.279902	-1.094148
18	6	0	-2.444461	-1.700039	-1.299913
19	1	0	-2.893341	-2.413058	0.781623
20	1	0	-2.563720	-0.241045	-2.997442
21	1	0	-4.260115	-0.089578	1.026533
22	1	0	-4.026845	1.255035	-1.303054
23	1	0	-1.862963	-2.507842	-1.723278
24	6	0	1.619885	-2.729016	0.989482
25	6	0	2.622664	-1.940482	-0.940086
26	6	0	2.811797	-2.179439	0.467335
27	6	0	1.303785	-2.355106	-1.278561
28	6	0	0.669908	-2.811963	-0.083519
29	1	0	1.442625	-3.011071	2.018646
30	1	0	3.370385	-1.577140	-1.631797
31	1	0	3.709102	-1.962008	1.031624
32	1	0	0.859792	-2.312689	-2.264363
33	1	0	-0.328524	-3.215674	-0.002358
34	6	0	2.315276	0.937865	1.347556
35	6	0	2.872168	0.953940	0.238836
36	6	0	3.788092	1.322479	-0.866589
37	8	0	4.016805	2.717880	-0.779547
38	1	0	2.167865	1.217192	2.371778
39	1	0	4.719055	0.745247	-0.746033
40	1	0	3.347472	1.038168	-1.832543
41	1	0	4.777719	2.937994	-1.341475

5a

SCF Done: E(RB+HF-LYP) = -2103.01174034 A.U. after 2 cycles

Center Number	Atomic Number	Atomic Type	Coordinates (Angstroms) X	Y	Z
1	44	0	0.940706	1.081745	0.018931
2	44	0	-1.470156	-0.401023	-0.023542
3	17	0	-0.576819	-2.653241	0.348243
4	16	0	0.003631	-0.071751	-1.835757
5	16	0	-0.359428	0.399889	1.890462
6	6	0	1.006016	3.208192	0.939678
7	6	0	1.117571	2.946345	-1.341404
8	6	0	2.322685	2.758682	0.623506
9	6	0	2.393214	2.590290	-0.803317
10	6	0	0.257276	3.319924	-0.269976
11	1	0	0.633296	3.411085	1.935004
12	1	0	0.847278	2.912666	-2.388607
13	1	0	3.132846	2.620276	1.327076
14	1	0	3.268025	2.308945	-1.374215
15	1	0	-0.767364	3.653155	-0.357623
16	6	0	-3.527983	-0.433120	0.897701
17	6	0	-3.294790	-0.495711	-1.397185
18	6	0	-3.562699	-1.285392	-0.245581
19	6	0	-3.104655	0.866767	-0.972583
20	6	0	-3.254530	0.905746	0.440662
21	1	0	-3.697581	-0.739857	1.920793
22	1	0	-3.239947	-0.859326	-2.414492
23	1	0	-3.696164	-2.358713	-0.230456
24	1	0	-2.903962	1.708717	-1.621067
25	1	0	-3.181285	1.784315	1.067896
26	6	0	0.918311	-1.540783	-2.439707
27	6	0	0.404152	-0.851666	2.989378
28	6	0	2.167675	-0.495244	0.309458
29	6	0	2.667048	-1.638543	0.440833
30	6	0	3.292454	-2.953057	0.495940
31	8	0	3.839814	-3.270226	-0.767082
32	1	0	3.344464	-0.334699	0.392808
33	1	0	1.329342	-0.430572	3.390952
34	1	0	1.932618	-1.233812	-2.704612
35	1	0	0.580374	-1.786730	2.462363
36	1	0	0.928809	-2.336736	-1.698509
37	1	0	-0.303212	-1.010762	3.807588
38	1	0	0.393074	-1.870350	-3.340109
39	1	0	4.037305	-2.981516	1.307061
40	1	0	2.463583	-3.620474	0.793238
41	1	0	4.164027	-4.185266	-0.735380

6a

SCF Done: E(RB+HF-LYP) = -2103.04803614 A.U. after 1 cycles

Center Number	Atomic Number	Atomic Type	Coordinates (Angstroms) X	Y	Z
1	44	0	-0.985815	0.928662	0.051711
2	44	0	1.547592	-0.350559	-0.029188
3	17	0	1.232816	-2.728951	0.291678
4	16	0	0.298721	0.097270	1.901458
5	16	0	-0.049269	-0.366874	-1.735131
6	6	0	-0.457734	-1.362199	2.708830
7	6	0	-0.902650	-1.962510	-2.025023
8	6	0	-2.347648	-0.303692	0.382732
9	6	0	-3.361722	-1.084002	0.642119
10	6	0	-4.126285	-1.887712	-0.394704
11	8	0	-3.666718	-3.224849	-0.293541
12	1	0	-1.229729	-0.991416	3.389054
13	1	0	-0.856208	-2.068199	1.984700
14	1	0	0.336806	-1.840141	3.286928
15	1	0	-1.721367	-1.754159	-2.719636
16	1	0	-1.262895	-2.429458	-1.111908
17	1	0	-0.173828	-2.618437	-2.507211
18	1	0	-3.616355	-1.253891	1.690303
19	1	0	-3.957813	-1.467571	-1.396226
20	1	0	-5.198593	-1.804234	-0.169313
21	1	0	-4.287509	-3.802610	-0.766774
22	6	0	-1.122549	2.811947	-1.349922
23	6	0	-0.913085	3.109656	0.922107
24	6	0	-2.389556	2.520782	-0.756307
25	6	0	-2.258983	2.706954	0.659535
26	6	0	-0.214709	3.183190	-0.317214
27	1	0	-0.896864	2.755090	-2.406949
28	1	0	-0.500366	3.319725	1.900387
29	1	0	-3.294896	2.254183	-1.284594
30	1	0	-3.047210	2.603086	1.392837
31	1	0	0.813462	3.487592	-0.452809
32	6	0	3.385572	-0.273571	-1.360057
33	6	0	3.583605	0.164306	0.901711
34	6	0	3.784504	-0.821565	-0.104473
35	6	0	3.049713	1.336440	0.271203
36	6	0	2.930147	1.067330	-1.127360
37	1	0	3.423851	-0.782673	-2.313623
38	1	0	3.785656	0.041747	1.957439
39	1	0	4.121021	-1.835598	0.062414
40	1	0	2.814254	2.267058	0.770115
41	1	0	2.583308	1.755898	-1.886632

7a

SCF Done: E(RB+HF-LYP) = -2102.97759515 A.U. after 18 cycles

Center Number	Atomic Number	Atomic Type	Coordinates (Angstroms) X	Y	Z
1	44	0	-0.874863	0.989590	0.005224
2	44	0	1.556686	-0.426852	-0.003187
3	17	0	0.763857	-2.731783	0.025609
4	16	0	0.237512	0.071772	1.889012
5	16	0	0.209330	0.039395	-1.882658
6	6	0	-0.622377	-1.336656	2.681667
7	6	0	-0.665453	-1.380219	-2.639673
8	6	0	-2.128927	-0.480644	0.020864
9	6	0	-3.046468	-1.341500	0.030659
10	6	0	-3.610835	-2.691122	-0.012937
11	8	0	-5.082235	-2.239174	-0.107753
12	1	0	-1.549967	-0.955585	3.115974
13	1	0	-0.806666	-2.137083	1.968832
14	1	0	0.034901	-1.691103	3.480012
15	1	0	-1.623919	-1.017455	-3.019375
16	1	0	-0.793451	-2.188396	-1.922411
17	1	0	-0.045169	-1.714979	-3.475512
18	1	0	-3.483304	-3.299227	0.885368
19	1	0	-3.418981	-3.274538	-0.914124
20	1	0	-5.597071	-2.498322	0.685322
21	6	0	-1.065580	2.998673	-1.179864
22	6	0	-0.924225	3.053634	1.111533
23	6	0	-2.327114	2.573608	-0.663058
24	6	0	-2.238955	2.601759	0.771199
25	6	0	-0.201508	3.298335	-0.087141
26	1	0	-0.807198	3.064465	-2.228555
27	1	0	-0.541337	3.166541	2.117479
28	1	0	-3.202356	2.322747	-1.246515
29	1	0	-3.037742	2.384391	1.467029
30	1	0	0.817859	3.650872	-0.158513
31	6	0	3.505923	-0.408975	-1.168573
32	6	0	3.522394	-0.369462	1.138825
33	6	0	3.709674	-1.199885	-0.001993
34	6	0	3.214473	0.958884	0.676058
35	6	0	3.204767	0.934607	-0.746701
36	1	0	3.576094	-0.757312	-2.190167
37	1	0	3.605351	-0.683421	2.170575
38	1	0	3.898769	-2.264698	0.014792
39	1	0	3.040078	1.821977	1.304372
40	1	0	3.020852	1.775633	-1.401645
41	1	0	-4.518868	-1.156177	-0.002699

8a

SCF Done: E(RB+HF-LYP) = -2026.60436132 A.U. after 11 cycles

Center Number	Atomic Number	Atomic Type	Coordinates (Angstroms) X	Y	Z
1	44	0	0.000000	1.387496	0.000000
2	44	0	0.446094	-1.415763	0.000000
3	17	0	-1.724472	-2.497110	0.000000
4	16	0	-0.174038	-0.118232	1.850718
5	16	0	-0.174038	-0.118232	-1.850718
6	6	0	1.621308	2.631280	-1.149984
7	6	0	1.621308	2.631280	1.149984
8	6	0	0.546509	3.468790	-0.716690
9	6	0	0.546509	3.468790	0.716690
10	6	0	2.289474	2.121834	0.000000
11	1	0	1.876824	2.421090	-2.180486
12	1	0	1.876824	2.421090	2.180486
13	1	0	-0.120260	4.031839	-1.355576
14	1	0	-0.120260	4.031839	1.355576
15	1	0	3.161110	1.482127	0.000000
16	6	0	1.805767	-2.836886	-1.155660
17	6	0	1.805767	-2.836886	1.155660
18	6	0	1.335153	-3.524094	0.000000
19	6	0	2.578598	-1.710201	0.713950
20	6	0	2.578598	-1.710201	-0.713950
21	1	0	1.609364	-3.116519	-2.182013
22	1	0	1.609364	-3.116519	2.182013
23	1	0	0.676119	-4.381577	0.000000
24	1	0	3.090356	-1.006341	1.356555
25	1	0	3.090356	-1.006341	-1.356555
26	6	0	-1.893471	-0.330948	2.442782
27	6	0	-1.893471	-0.330948	-2.442782
28	6	0	-1.864244	1.717584	0.000000
29	6	0	-3.090064	2.050262	0.000000
30	6	0	-4.382119	2.358435	0.000000
31	1	0	-4.726814	3.392382	0.000000
32	1	0	-5.154007	1.588533	0.000000
33	1	0	-2.159362	0.572252	-2.998452
34	1	0	-2.159362	0.572252	2.998452
35	1	0	-2.579326	-0.521004	-1.621433
36	1	0	-2.579326	-0.521004	1.621433
37	1	0	-1.884107	-1.187290	-3.121806
38	1	0	-1.884107	-1.187290	3.121806

9a

SCF Done: E(RB+HF-LYP) = -2218.76282850 A.U. after 2 cycles

Center Number	Atomic Number	Atomic Type	Coordinates (Angstroms) X	Y	Z
1	44	0	1.607185	-0.652774	-0.128240
2	44	0	-0.483977	1.264297	0.218488
3	16	0	-0.087777	-0.163328	-1.676162
4	16	0	0.488544	-0.201490	1.875389
5	6	0	-1.307905	-1.519061	-1.856756
6	6	0	-0.588395	-1.565274	2.456519
7	17	0	0.872186	-2.956067	-0.019269
8	1	0	-0.769527	-2.359064	-2.300424
9	1	0	-1.741493	-1.825776	-0.906036
10	1	0	-2.084369	-1.176571	-2.544650
11	1	0	0.076600	-2.381329	2.746782
12	1	0	-1.281876	-1.914615	1.692907
13	1	0	-1.117024	-1.198435	3.341864
14	6	0	3.650199	0.081515	0.640347
15	6	0	3.355256	-0.231386	-1.631989
16	6	0	3.665871	-1.322035	0.388067
17	6	0	3.478296	-1.511212	-1.028486
18	6	0	3.445647	0.752956	-0.604158
19	1	0	3.769788	0.549933	1.608791
20	1	0	3.185802	-0.039968	-2.683577
21	1	0	3.806455	-2.108806	1.116227
22	1	0	3.425517	-2.465686	-1.533223
23	1	0	3.410882	1.823102	-0.755266
24	6	0	-0.062922	3.154512	1.508614
25	6	0	-0.830021	3.360920	-0.667788
26	6	0	-1.209437	3.402339	0.717678
27	6	0	0.565411	3.087652	-0.724339
28	6	0	1.036676	2.933451	0.616766
29	1	0	-0.025328	3.116800	2.588946
30	1	0	-1.475096	3.555441	-1.513953
31	1	0	-2.209529	3.573123	1.093154
32	1	0	1.155916	3.005575	-1.626934
33	1	0	2.054987	2.741367	0.920661
34	6	0	-2.419731	0.476157	0.989847
35	6	0	-2.690161	0.816847	-0.173652
36	6	0	-3.532371	0.961302	-1.381728
37	8	0	-4.368946	-0.192600	-1.448617
38	1	0	-2.613477	0.051135	1.954214
39	1	0	-4.130267	1.880045	-1.285804
40	1	0	-2.913605	1.060627	-2.282441
41	1	0	-5.117439	-0.003742	-2.037439
42	6	0	-4.182839	-3.520535	0.722901
43	8	0	-3.543577	-2.248395	0.636690
44	1	0	-3.645098	-4.097887	1.478538
45	1	0	-4.139543	-4.070498	-0.227141
46	1	0	-5.232547	-3.431969	1.035165
47	1	0	-3.991549	-1.720507	-0.046974

12a

SCF Done: E(RB+HF-LYP) = -2218.74826656 A.U. after 10 cycles

Center Number	Atomic Number	Atomic Type	Coordinates (Angstroms) X	Y	Z
1	44	0	0.523202	1.118116	0.051463
2	44	0	-1.847760	-0.430578	-0.044706
3	17	0	-0.877833	-2.649306	0.389288
4	16	0	-0.335144	-0.056991	-1.818904
5	16	0	-0.823115	0.450924	1.886153
6	6	0	0.623968	-1.507038	-2.399794
7	6	0	-0.075320	-0.761555	3.039224
8	6	0	1.778433	-0.437213	0.412139
9	6	0	2.183424	-1.613647	0.556602
10	6	0	2.880222	-2.887419	0.549545
11	8	0	3.627603	-2.995891	-0.663395
12	1	0	1.656821	-1.197276	-2.572505
13	1	0	0.573069	-2.322032	-1.680660
14	1	0	0.171175	-1.807898	-3.348248
15	1	0	0.822460	-0.309569	3.468493
16	1	0	0.147983	-1.700092	2.537332
17	1	0	-0.811463	-0.924374	3.830889
18	1	0	2.927124	-0.195743	0.435798
19	1	0	3.526310	-2.980394	1.435109
20	1	0	2.090485	-3.651270	0.630792
21	1	0	4.003065	-3.890931	-0.713072
22	6	0	0.434716	3.292219	0.845772
23	6	0	0.957245	2.905537	-1.357976
24	6	0	1.784465	2.817641	0.797251
25	6	0	2.110369	2.581606	-0.582879
26	6	0	-0.079400	3.345171	-0.479336
27	1	0	-0.107730	3.549419	1.746230
28	1	0	0.877959	2.816796	-2.433460
29	1	0	2.454258	2.713849	1.640214
30	1	0	3.060897	2.232470	-0.964417
31	1	0	-1.064555	3.681159	-0.771919
32	6	0	-3.924838	-0.607065	0.787263
33	6	0	-3.617327	-0.523150	-1.499123
34	6	0	-3.880540	-1.391697	-0.405994
35	6	0	-3.504657	0.818772	-0.992105
36	6	0	-3.705132	0.766810	0.414445
37	1	0	-4.118037	-0.979970	1.783722
38	1	0	-3.508337	-0.823034	-2.532729
39	1	0	-3.965491	-2.468749	-0.457860
40	1	0	-3.323819	1.706339	-1.582704
41	1	0	-3.690767	1.609895	1.092333
42	6	0	6.017979	-0.030338	0.081980
43	8	0	4.671377	-0.277066	-0.335346
44	1	0	6.032664	0.956820	0.548546
45	1	0	6.704986	-0.023382	-0.772593
46	1	0	6.362332	-0.771502	0.815217
47	1	0	4.621000	-1.165084	-0.737840

13a

SCF Done: E(RB+HF-LYP) = -2218.77884081 A.U. after 39 cycles

Center Number	Atomic Number	Atomic Type	Coordinates (Angstroms) X	Y	Z
1	44	0	0.023768	1.407733	-0.115273
2	44	0	-1.511153	-0.971091	0.054970
3	17	0	0.001950	-2.825265	0.431481
4	16	0	-0.238133	-0.290766	-1.786954
5	16	0	-0.560649	0.179542	1.858631
6	6	0	1.286376	-1.249404	-2.120626
7	6	0	0.862563	-0.649414	2.659566
8	6	0	1.837937	1.010792	0.095056
9	6	0	3.120359	0.802524	0.183190
10	6	0	3.962818	0.852681	1.438219
11	8	0	4.341970	-0.494795	1.731553
12	1	0	1.891448	-0.657119	-2.812373
13	1	0	1.843823	-1.497429	-1.221796
14	1	0	0.962874	-2.168323	-2.616254
15	1	0	1.307090	0.078912	3.343829
16	1	0	1.587577	-1.021189	1.940564
17	1	0	0.453549	-1.485696	3.231321
18	1	0	3.624643	0.401502	-0.707081
19	1	0	3.400522	1.295587	2.269632
20	1	0	4.846045	1.476907	1.246614
21	1	0	5.005966	-0.482018	2.440518
22	6	0	-1.051032	3.333724	0.692058
23	6	0	-0.894882	3.003408	-1.579175
24	6	0	0.294186	3.620604	0.302412
25	6	0	0.392676	3.412057	-1.112931
26	6	0	-1.786393	2.962262	-0.469523
27	1	0	-1.439142	3.390921	1.700765
28	1	0	-1.142390	2.760081	-2.604434
29	1	0	1.083081	3.975178	0.951734
30	1	0	1.270019	3.575643	-1.723861
31	1	0	-2.837965	2.714665	-0.504798
32	6	0	-3.424718	-1.607438	1.113346
33	6	0	-3.243464	-1.814722	-1.182087
34	6	0	-3.188730	-2.526901	0.049454
35	6	0	-3.510801	-0.437115	-0.883319
36	6	0	-3.625512	-0.309274	0.534958
37	1	0	-3.447290	-1.850646	2.167085
38	1	0	-3.098653	-2.239885	-2.166225
39	1	0	-2.943969	-3.574080	0.163329
40	1	0	-3.632719	0.352870	-1.612269
41	1	0	-3.850047	0.596950	1.081887
42	6	0	5.634993	-2.174838	-1.563407
43	8	0	4.523521	-1.487969	-0.995057
44	1	0	5.512419	-2.142419	-2.648735
45	1	0	5.668370	-3.227095	-1.250299
46	1	0	6.592737	-1.698874	-1.308569
47	1	0	4.612138	-1.489191	-0.024374

14a

SCF Done: E(RB+HF-LYP) = -2218.75710627 A.U. after 40 cycles

Center Number	Atomic Number	Atomic Type	Coordinates (Angstroms) X	Y	Z
1	44	0	0.451622	1.050873	0.217455
2	44	0	-1.868631	-0.514886	-0.141434
3	17	0	-1.288046	-2.872126	0.034875
4	16	0	-0.156718	-0.176476	-1.724301
5	16	0	-0.792774	-0.062758	1.903887
6	6	0	0.859534	-1.660258	-2.065282
7	6	0	0.070967	-1.483869	2.668453
8	6	0	1.981720	-0.148286	0.571024
9	6	0	3.001056	-0.835013	0.767653
10	6	0	3.914940	-1.768819	1.453040
11	8	0	5.117829	-1.957344	0.646582
12	1	0	1.758713	-1.331500	-2.593706
13	1	0	1.103220	-2.197595	-1.152816
14	1	0	0.268757	-2.304788	-2.720143
15	1	0	0.829902	-1.078697	3.343351
16	1	0	0.503476	-2.138019	1.915434
17	1	0	-0.675586	-2.033934	3.246538

18	1	0	3.425510	-2.740003	1.600091
19	1	0	4.215314	-1.374651	2.431152
20	1	0	5.600794	-2.735728	0.966803
21	1	0	3.549080	-0.644900	-0.706729
22	6	0	5.111720	0.313572	-1.836124
23	8	0	4.318742	-0.866567	-1.483565
24	1	0	4.447714	0.981941	-2.381883
25	1	0	5.920919	-0.023062	-2.483372
26	1	0	5.500080	0.787273	-0.932048
27	1	0	4.866359	-1.490623	-0.898030
28	6	0	0.065434	3.091541	1.280595
29	6	0	0.501043	3.060368	-0.978324
30	6	0	1.461906	2.848740	1.116693
31	6	0	1.733036	2.828615	-0.294899
32	6	0	-0.526863	3.227057	-0.007984
33	1	0	-0.455741	3.147761	2.227386
34	1	0	0.370999	3.091914	-2.052339
35	1	0	2.188980	2.743206	1.909976
36	1	0	2.705793	2.722676	-0.754406
37	1	0	-1.568030	3.433722	-0.212478
38	6	0	-4.006268	-0.391139	0.646952
39	6	0	-3.598439	-0.456160	-1.627787
40	6	0	-4.017933	-1.226553	-0.506276
41	6	0	-3.324841	0.876187	-1.167796
42	6	0	-3.577837	0.916592	0.237554
43	1	0	-4.271324	-0.692865	1.651198
44	1	0	-3.500080	-0.815881	-2.643035
45	1	0	-4.235269	-2.285900	-0.514886
46	1	0	-3.008549	1.704405	-1.787747
47	1	0	-3.491608	1.781528	0.881453

15a

SCF Done: E(RB+HF-LYP) = -2218.75748087 A.U. after 1 cycles

Center Number	Atomic Number	Atomic Type	Coordinates (Angstroms) X	Y	Z
1	44	0	0.488859	1.006884	0.228444
2	44	0	-1.880501	-0.477886	-0.142045
3	17	0	-1.390018	-2.853001	0.071427
4	16	0	-0.131273	-0.236530	-1.702871
5	16	0	-0.818024	-0.037226	1.911379
6	6	0	0.820654	-1.774138	-1.998248
7	6	0	-0.032214	-1.483173	2.711190
8	6	0	1.977597	-0.261053	0.636297
9	6	0	2.941792	-0.976584	0.923031
10	6	0	3.968110	-1.888087	1.421577
11	8	0	5.077881	-1.961397	0.448021
12	1	0	1.601745	-1.533940	-2.726554
13	1	0	1.240972	-2.171220	-1.077509
14	1	0	0.133275	-2.504694	-2.428531
15	1	0	0.719804	-1.101383	3.406716
16	1	0	0.401797	-2.157511	1.977752
17	1	0	-0.818463	-1.999840	3.266992
18	1	0	3.576516	-2.903957	1.544243
19	1	0	4.376893	-1.547092	2.380663
20	1	0	5.869300	-2.323460	0.880645
21	6	0	0.162213	3.067302	1.262805
22	6	0	0.629577	2.996811	-0.988760
23	6	0	1.551129	2.773856	1.122767
24	6	0	1.843210	2.730220	-0.284800
25	6	0	-0.405644	3.210286	-0.036027
26	1	0	-0.370792	3.150686	2.200879
27	1	0	0.515552	3.022934	-2.064743
28	1	0	2.261571	2.651891	1.928704
29	1	0	2.820960	2.597027	-0.727600
30	1	0	-1.435537	3.452021	-0.258090
31	6	0	-4.022032	-0.282136	0.609171
32	6	0	-3.585870	-0.358118	-1.659905
33	6	0	-4.046586	-1.115035	-0.546274
34	6	0	-3.272203	0.963012	-1.194233
35	6	0	-3.543814	1.010758	0.207532
36	1	0	-4.312849	-0.575370	1.608723
37	1	0	-3.484085	-0.719801	-2.674131
38	1	0	-4.299829	-2.166262	-0.559900
39	1	0	-2.919797	1.780199	-1.809062
40	1	0	-3.436801	1.871462	0.853981
41	6	0	4.559613	-0.289387	-2.374515
42	8	0	4.655329	0.039646	-0.943577
43	1	0	3.952995	0.486860	-2.837318
44	1	0	4.110155	-1.275970	-2.496432
45	1	0	5.575704	-0.262750	-2.764517
46	1	0	3.736383	0.013886	-0.474058
47	1	0	5.096949	-0.751745	-0.407979

16a

SCF Done: E(RB+HF-LYP) = -2218.75322640 A.U. after 40 cycles

Center Number	Atomic Number	Atomic Type	Coordinates (Angstroms) X	Y	Z
1	44	0	0.525748	0.931431	0.383742
2	44	0	-1.874019	-0.416806	-0.239539
3	17	0	-1.625241	-2.801991	0.161637
4	16	0	0.086911	-0.402370	-1.543074
5	16	0	-1.063009	0.054955	1.917453
6	6	0	0.986369	-1.999608	-1.574154
7	6	0	-0.474828	-1.391004	2.871619
8	6	0	1.872814	-0.341450	0.999069
9	6	0	2.808890	-1.062509	1.388999
10	6	0	3.875406	-1.842921	1.758513
11	1	0	2.012632	-1.797383	-1.896615
12	1	0	0.965328	-2.490231	-0.604689
13	1	0	0.489724	-2.629377	-2.315703
14	1	0	0.185524	-1.013783	3.657006
15	1	0	0.029434	-2.114379	2.236822
16	1	0	-1.358695	-1.849127	3.322005
17	1	0	3.734725	-2.909225	1.933940
18	1	0	4.699532	-1.405301	2.318198
19	6	0	0.201944	3.077389	1.245193
20	6	0	0.977548	2.829314	-0.906484
21	6	0	1.574343	2.692184	1.324315
22	6	0	2.059686	2.540200	-0.018941
23	6	0	-0.165632	3.167537	-0.128396
24	1	0	-0.448791	3.259321	2.090647
25	1	0	1.019728	2.794310	-1.987493
26	1	0	2.153809	2.576141	2.229755
27	1	0	3.074707	2.293911	-0.301110
28	1	0	-1.133440	3.458452	-0.511916
29	6	0	-4.064630	0.036154	0.230297
30	6	0	-3.377082	-0.314879	-1.949528
31	6	0	-4.032875	-0.909722	-0.833172
32	6	0	-2.998505	1.018159	-1.575874
33	6	0	-3.422069	1.234563	-0.227962
34	1	0	-4.492379	-0.125781	1.210483
35	1	0	-3.198421	-0.787882	-2.905629
36	1	0	-4.382820	-1.931441	-0.778707
37	1	0	-2.507089	1.737068	-2.217673
38	1	0	-3.310195	2.146585	0.342575
39	8	0	5.040627	-2.129346	0.229236
40	1	0	4.736024	-2.930579	-0.232944
41	1	0	4.829432	-1.364311	-0.387992
42	6	0	4.674140	0.100338	-2.733788
43	8	0	4.306166	-0.106454	-1.357872
44	1	0	4.460600	1.129114	-3.041291
45	1	0	4.157760	-0.599235	-3.401287
46	1	0	5.749826	-0.069365	-2.795593
47	1	0	3.356189	0.055424	-1.234764

17a

SCF Done: E(RB+HF-LYP) = -2218.75661502 A.U. after 1 cycles

Center Number	Atomic Number	Atomic Type	Coordinates (Angstroms) X	Y	Z
1	44	0	-0.535860	-0.673569	0.297389
2	44	0	2.097958	0.209552	-0.200550
3	17	0	2.152424	2.625855	0.033663
4	16	0	0.278631	0.363807	-1.685727
5	16	0	1.085454	0.001430	1.907495
6	6	0	-0.363458	2.054370	-1.962293
7	6	0	0.645070	1.570534	2.742708
8	6	0	-1.660970	0.836025	0.641468
9	6	0	-2.520078	1.732622	0.851848
10	6	0	-3.464945	2.658744	1.055663
11	1	0	-1.388105	1.956541	-2.331153
12	1	0	-0.319538	2.652994	-1.056724
13	1	0	0.264748	2.504489	-2.734804
14	1	0	-0.158731	1.347166	3.448984
15	1	0	0.354456	2.334680	2.026162
16	1	0	1.533553	1.896660	3.289114
17	1	0	-3.381034	3.663364	0.646571
18	1	0	-4.302239	2.487802	1.726225
19	6	0	-0.666297	-2.780969	1.320169
20	6	0	-1.254320	-2.548458	-0.890503
21	6	0	-1.944394	-2.144462	1.279195
22	6	0	-2.315350	-2.002467	-0.100941
23	6	0	-0.242335	-3.036456	-0.015123
24	1	0	-0.109949	-3.014137	2.218877
25	1	0	-1.225433	-2.576460	-1.972019
26	1	0	-2.541453	-1.856637	2.133649
27	1	0	-3.240549	-1.579103	-0.474316
28	1	0	0.675807	-3.523878	-0.311182
29	6	0	4.178541	-0.450724	0.441101
30	6	0	3.650276	-0.295930	-1.803926
31	6	0	4.323164	0.350152	-0.729007
32	6	0	3.081540	-1.514050	-1.299812
33	6	0	3.408946	-1.610466	0.086830
34	1	0	4.579838	-0.221520	1.419001
35	1	0	3.577339	0.072288	-2.818368
36	1	0	4.802270	1.318635	-0.774465
37	1	0	2.527334	-2.239474	-1.880503
38	1	0	3.148953	-2.422591	0.752613
39	8	0	-5.323131	2.307665	-0.497661
40	1	0	-5.300408	2.848485	-1.302287
41	1	0	-5.238607	1.377637	-0.805587
42	6	0	-6.530020	-0.893782	-0.483321

43	8	0	-5.354052	-0.433895	-1.177621
44	1	0	-6.662192	-1.974338	-0.606200
45	1	0	-7.428890	-0.370100	-0.827380
46	1	0	-6.373145	-0.669911	0.572869
47	1	0	-5.477647	-0.617454	-2.122623

18a

SCF Done: E(RB+HF-LYP) = -2334.50096213 A.U. after 2 cycles

Center Number	Atomic Number	Atomic Type	Coordinates (Angstroms) X	Y	Z
1	44	0	0.033211	1.342268	-0.035784
2	44	0	-1.849851	-0.807787	-0.042603
3	17	0	-0.882135	-3.022003	0.185992
4	16	0	-0.327556	-0.314318	-1.752198
5	16	0	-0.612805	-0.062053	1.809862
6	6	0	0.998675	-1.559975	-1.942479
7	6	0	0.684542	-1.251721	2.326278
8	1	0	1.763090	-1.147625	-2.604810
9	1	0	1.434853	-1.850332	-0.989227
10	1	0	0.528409	-2.430168	-2.406371
11	1	0	1.200770	-0.827437	3.190123
12	1	0	1.390413	-1.473382	1.527666
13	1	0	0.167388	-2.167759	2.617248
14	6	0	2.197815	0.853144	-0.363877
15	6	0	2.128518	1.170782	0.836571
16	6	0	2.671444	1.395803	2.194086
17	8	0	3.617609	0.354486	2.454408
18	1	0	2.700248	0.511022	-1.264932
19	1	0	3.161304	2.380643	2.217582
20	1	0	1.873459	1.402965	2.946182
21	1	0	4.161625	0.610745	3.216778
22	6	0	-1.055850	3.215733	0.798872
23	6	0	-0.715506	2.991825	-1.482215
24	6	0	0.297607	3.544640	0.519559
25	6	0	0.508902	3.401638	-0.897906
26	6	0	-1.681001	2.855536	-0.434911
27	1	0	-1.525717	3.229078	1.773609
28	1	0	-0.880908	2.790062	-2.532351
29	1	0	1.029081	3.887457	1.238446
30	1	0	1.435093	3.587704	-1.424514
31	1	0	-2.721860	2.605979	-0.567449
32	6	0	-3.904949	-1.025988	0.996020
33	6	0	-3.681684	-1.351345	-1.287336
34	6	0	-3.809419	-2.009948	-0.026638
35	6	0	-3.687538	0.056179	-1.041795
36	6	0	-3.819572	0.257151	0.374249
37	1	0	-3.999697	-1.219312	2.056087
38	1	0	-3.593280	-1.836604	-2.249804
39	1	0	-3.776483	-3.079128	0.128742
40	1	0	-3.639315	0.823798	-1.802526
41	1	0	-3.891344	1.205737	0.888886
42	6	0	4.479633	-2.961240	0.916405
43	8	0	3.891561	-1.755845	0.419300
44	1	0	4.370170	-3.715922	0.135037
45	1	0	3.964615	-3.314730	1.818107
46	1	0	5.547494	-2.834149	1.137595
47	1	0	3.943048	-1.067757	1.109459
48	6	0	5.338554	-0.312327	-2.655209
49	8	0	4.047613	-0.600444	-2.128357
50	1	0	5.882573	-1.229557	-2.917385
51	1	0	5.952536	0.273392	-1.955782
52	1	0	5.196322	0.274327	-3.566235
53	1	0	4.145105	-1.115103	-1.296509

20a

SCF Done: E(RB+HF-LYP) = -2334.49783931 A.U. after 1 cycles

Center Number	Atomic Number	Atomic Type	Coordinates (Angstroms) X	Y	Z
1	44	0	-0.295492	-1.075360	0.176084
2	44	0	2.107674	0.369737	-0.193240
3	17	0	1.662843	2.644106	0.578244
4	16	0	0.233635	0.391680	-1.623275
5	16	0	1.327728	-0.570097	1.835953
6	6	0	-0.743470	1.934684	-1.733036
7	6	0	0.826995	0.597001	3.158840
8	1	0	-1.804382	1.678914	-1.680141
9	1	0	-0.462541	2.627926	-0.943831
10	1	0	-0.515605	2.369314	-2.710283
11	1	0	-0.163861	0.317285	3.521788
12	1	0	0.846105	1.621782	2.789457
13	1	0	1.555960	0.479182	3.964598
14	6	0	-2.108671	-0.062719	1.115764
15	6	0	-1.857885	1.120326	1.362285
16	6	0	-1.719088	2.550841	1.581609
17	8	0	-2.592366	3.224579	0.666327
18	1	0	-2.940269	-0.762442	1.104367
19	1	0	-1.996653	2.773893	2.623852
20	1	0	-0.670248	2.845505	1.436286
21	1	0	-2.426729	4.179132	0.730969
22	6	0	0.136140	-3.273888	0.566633
23	6	0	-0.861454	-2.656175	-1.425897
24	6	0	-1.240838	-3.020992	0.824770
25	6	0	-1.861170	-2.642898	-0.423949
26	6	0	0.385826	-3.015046	-0.817218
27	1	0	0.873203	-3.576529	1.298457
28	1	0	-1.004935	-2.393887	-2.465526
29	1	0	-1.743145	-3.141018	1.775261
30	1	0	-2.903319	-2.370397	-0.557355
31	1	0	1.331024	-3.135020	-1.327365
32	6	0	4.302362	-0.128038	0.266114
33	6	0	3.666396	0.703759	-1.793359
34	6	0	4.266366	1.039644	-0.542276
35	6	0	3.341270	-0.696274	-1.759553
36	6	0	3.725656	-1.208048	-0.486258
37	1	0	4.686668	-0.188333	1.275483
38	1	0	3.506051	1.380314	-2.621655
39	1	0	4.574512	2.030581	-0.237255
40	1	0	2.893251	-1.257131	-2.569254
41	1	0	3.633633	-2.231834	-0.149138
42	6	0	-5.175843	2.171473	-1.849682
43	8	0	-4.228569	1.477880	-1.031795
44	1	0	-5.582005	1.444952	-2.556702
45	1	0	-4.697850	2.980347	-2.415780
46	1	0	-6.000548	2.586587	-1.256169
47	1	0	-3.820757	2.114006	-0.413147
48	6	0	-5.957923	-1.354496	0.391978
49	8	0	-4.605257	-1.108663	0.013008
50	1	0	-6.625924	-1.369544	-0.479342
51	1	0	-6.325741	-0.606496	1.107585
52	1	0	-5.992045	-2.337422	0.868258
53	1	0	-4.548484	-0.212679	-0.392473

21a

SCF Done: E(RB+HF-LYP) = -2334.49117437 A.U. after 1 cycles

Center Number	Atomic Number	Atomic Type	Coordinates (Angstroms) X	Y	Z
1	44	0	0.119570	1.237801	0.068358
2	44	0	-2.023432	-0.598927	-0.135684
3	17	0	-1.026645	-2.697051	0.650133
4	16	0	-0.285211	-0.280771	-1.703230
5	16	0	-1.327102	0.535904	1.810806
6	6	0	0.904788	-1.658517	-1.904946
7	6	0	-0.595043	-0.485185	3.143329
8	6	0	1.573423	-0.036323	0.782998
9	6	0	2.032141	-1.103927	1.218510
10	6	0	2.644302	-2.360177	1.611152
11	8	0	3.331535	-2.940436	0.489178
12	1	0	1.896751	-1.234664	-2.079679
13	1	0	0.906776	-2.313580	-1.037275
14	1	0	0.580261	-2.207597	-2.793240
15	1	0	0.237432	0.069708	3.581989
16	1	0	-0.275139	-1.452886	2.762599
17	1	0	-1.380238	-0.617105	3.892492
18	1	0	3.331008	-2.226758	2.460042
19	1	0	1.820219	-3.010840	1.940582
20	1	0	3.553557	-3.861295	0.702649
21	6	0	-0.317167	3.425939	0.691492
22	6	0	0.197397	2.943477	-1.496428
23	6	0	1.088303	3.193239	0.621031
24	6	0	1.412348	2.889459	-0.746732
25	6	0	-0.871460	3.269725	-0.613682
26	1	0	-0.872578	3.660770	1.589970
27	1	0	0.104366	2.745184	-2.556141
28	1	0	1.786414	3.275392	1.442785
29	1	0	2.400829	2.690407	-1.134800
30	1	0	-1.910341	3.395169	-0.884827
31	6	0	-4.206970	-0.733637	0.445312
32	6	0	-3.564895	-1.097918	-1.742316
33	6	0	-3.964755	-1.737748	-0.536732
34	6	0	-3.569152	0.323200	-1.514592
35	6	0	-3.968414	0.547329	-0.167015
36	1	0	-4.525650	-0.907441	1.463996
37	1	0	-3.300604	-1.595790	-2.665385
38	1	0	-4.003234	-2.805710	-0.370326
39	1	0	-3.326957	1.081602	-2.246784
40	1	0	-4.084161	1.508569	0.315666
41	6	0	5.641442	-1.452587	-2.016285
42	8	0	4.480751	-1.076278	-1.263780
43	1	0	5.934672	-0.585937	-2.611600
44	1	0	5.410343	-2.282681	-2.692399
45	1	0	6.474472	-1.736669	-1.361387
46	1	0	4.162642	-1.835851	-0.728367
47	6	0	4.879161	1.223643	1.198458
48	8	0	3.920671	1.057670	0.133850
49	1	0	5.838297	1.529783	0.773581
50	1	0	5.006564	0.295895	1.767885
51	1	0	4.507817	2.010915	1.855712
52	1	0	4.236084	0.315440	-0.478571
53	1	0	2.753965	0.525651	0.564428

22a

SCF Done: E(RB+HF-LYP) = -2334.50623438 A.U. after 2 cycles

Center Number	Atomic Number	Atomic Type	Coordinates (Angstroms) X	Y	Z
1	44	0	0.103942	1.085387	0.137713
2	44	0	-2.192437	-0.525585	-0.144418
3	17	0	-1.609567	-2.828719	0.405061
4	16	0	-0.374324	-0.406506	-1.641836
5	16	0	-1.263811	0.240692	1.881866
6	6	0	0.656222	-1.916281	-1.714262
7	6	0	-0.493326	-1.047758	2.927652
8	6	0	1.581373	-0.109841	0.773134
9	6	0	2.479651	-0.844807	1.187525
10	6	0	3.335688	-1.856954	1.784164
11	8	0	4.002661	-2.645824	0.732568
12	1	0	1.534206	-1.670741	-2.320302
13	1	0	0.940945	-2.258091	-0.723737
14	1	0	0.066742	-2.685633	-2.217303
15	1	0	0.241556	-0.553192	3.568003
16	1	0	-0.039545	-1.829090	2.323475
17	1	0	-1.292011	-1.471118	3.541900
18	1	0	4.109079	-1.427060	2.435179
19	1	0	2.739795	-2.558306	2.380387
20	1	0	4.464330	-3.392626	1.152368
21	6	0	-0.263895	3.268138	0.871395
22	6	0	0.208621	2.879694	-1.345452
23	6	0	1.129887	2.979147	0.772685
24	6	0	1.427495	2.735030	-0.614048
25	6	0	-0.831367	3.214134	-0.434084
26	1	0	-0.799111	3.476559	1.788607
27	1	0	0.097134	2.742507	-2.413165
28	1	0	1.834049	2.984289	1.593454
29	1	0	2.399269	2.521984	-1.037199
30	1	0	-1.865498	3.402546	-0.687176
31	6	0	-4.374198	-0.307100	0.477120
32	6	0	-3.820732	-0.682396	-1.735847
33	6	0	-4.316399	-1.292659	-0.549194
34	6	0	-3.569329	0.701658	-1.446444
35	6	0	-3.911399	0.933523	-0.079274
36	1	0	-4.704987	-0.468967	1.493950
37	1	0	-3.657987	-1.177527	-2.683465
38	1	0	-4.538467	-2.343881	-0.426503
39	1	0	-3.208439	1.438727	-2.151350
40	1	0	-3.857887	1.878228	0.444960
41	6	0	5.128905	-1.622895	-2.308969
42	8	0	5.324555	-1.229921	-0.916420
43	1	0	5.638197	-0.881314	-2.923240
44	1	0	4.063713	-1.662814	-2.547082
45	1	0	5.593197	-2.599999	-2.439345
46	1	0	4.824265	-1.865996	-0.262393
47	1	0	4.947716	-0.236206	-0.709339
48	6	0	5.138486	1.838327	0.490082
49	8	0	4.339844	0.961339	-0.336052
50	1	0	6.033310	2.088150	-0.081021
51	1	0	5.422191	1.352425	1.429541
52	1	0	4.578984	2.753317	0.699432
53	1	0	3.531253	0.655306	0.162000

23a

SCF Done: E(RB+HF-LYP) = -2334.49369901 A.U. after 17 cycles

Center Number	Atomic Number	Atomic Type	Coordinates (Angstroms) X	Y	Z
1	44	0	0.107550	1.092861	0.180467
2	44	0	-2.185107	-0.531810	-0.174582
3	17	0	-1.677307	-2.715640	0.765670
4	16	0	-0.228778	-0.593621	-1.472602
5	16	0	-1.520585	0.514814	1.821623
6	6	0	0.827443	-2.071985	-1.258960
7	6	0	-0.895199	-0.592495	3.137585
8	6	0	1.433026	0.018696	1.065940
9	6	0	2.327489	-0.633933	1.666599
10	6	0	3.199390	-1.423259	2.327267
11	1	0	1.854433	-1.789175	-1.508067
12	1	0	0.745296	-2.467870	-0.249635
13	1	0	0.461688	-2.813118	-1.974975
14	1	0	-0.250685	0.004605	3.788100
15	1	0	-0.371381	-1.449541	2.722318
16	1	0	-1.769037	-0.930683	3.700189
17	1	0	2.891439	-2.397279	2.701206
18	1	0	4.144064	-1.051347	2.710670
19	6	0	-0.392098	3.355556	0.495938
20	6	0	0.529392	2.668872	-1.495659
21	6	0	0.996509	3.099575	0.723778
22	6	0	1.573038	2.677803	-0.520997
23	6	0	-0.680367	3.095188	-0.872718
24	1	0	-1.101938	3.680356	1.245576
25	1	0	0.641829	2.378675	-2.532171
26	1	0	1.523894	3.246512	1.656649
27	1	0	2.613412	2.433309	-0.694991
28	1	0	-1.639162	3.215228	-1.357368
29	6	0	-4.422636	-0.195526	0.161112
30	6	0	-3.636039	-0.992735	-1.860400
31	6	0	-4.266081	-1.363509	-0.636418
32	6	0	-3.403907	0.424485	-1.822684
33	6	0	-3.887022	0.916632	-0.573008
34	1	0	-4.859962	-0.157962	1.149764
35	1	0	-3.385339	-1.662126	-2.672131
36	1	0	-4.516740	-2.371708	-0.336132
37	1	0	-2.962420	1.011198	-2.617238
38	1	0	-3.881607	1.946541	-0.242433
39	8	0	4.603285	-2.505083	0.913552
40	1	0	4.364664	-3.445635	0.874012
41	1	0	4.446936	-2.157764	-0.008029
42	6	0	5.727977	1.254616	0.332923
43	8	0	4.428034	1.046314	-0.245072
44	1	0	6.381014	1.587856	-0.475336
45	1	0	6.128754	0.327154	0.760212
46	1	0	5.697593	2.032678	1.104057
47	1	0	3.810781	0.775097	0.459368
48	6	0	5.098197	-1.686290	-2.596820
49	8	0	4.203712	-1.382087	-1.519818
50	1	0	6.147750	-1.562007	-2.301646
51	1	0	4.891173	-1.055075	-3.468662
52	1	0	4.930920	-2.729529	-2.872788
53	1	0	4.324273	-0.441131	-1.250360

1b

SCF Done: E(RB+HF-LYP) = -973.531325993 A.U. after 16 cycles

Center Number	Atomic Number	Atomic Type	Coordinates (Angstroms) X	Y	Z
1	44	0	0.043535	-0.000099	-0.239741
2	15	0	1.591357	-1.771884	0.067345
3	15	0	1.590472	1.772472	0.067308
4	6	0	-1.878282	-1.166294	-0.139899
5	6	0	-2.101165	-0.000956	-0.934538
6	6	0	-1.475154	-0.719946	1.160500
7	6	0	-1.878772	1.165386	-0.141326
8	6	0	-1.475426	0.720822	1.159600
9	1	0	2.176958	-2.325681	-1.094988
10	1	0	2.176496	2.326744	-1.094578
11	1	0	1.099782	-2.956821	0.652920
12	1	0	1.098129	2.957171	0.652689
13	1	0	2.766386	-1.618198	0.835073
14	1	0	2.765106	1.619256	0.835730
15	1	0	-2.011498	-2.190951	-0.458931
16	1	0	-2.362315	-0.001685	-1.986341
17	1	0	-1.243294	-1.345935	2.012260
18	1	0	-2.012059	2.189620	-0.461689
19	1	0	-1.243874	1.347930	2.010626

2b

SCF Done: E(RB+HF-LYP) = -1165.42565379 A.U. after 14 cycles

Center Number	Atomic Number	Atomic Type	Coordinates (Angstroms) X	Y	Z
1	44	0	0.379837	0.027171	-0.024586
2	15	0	1.015282	2.073839	-0.945260
3	15	0	-0.405763	1.172697	1.850005
4	6	0	-1.225069	0.285558	-1.569485
5	6	0	-1.813649	-0.140470	-0.554360
6	6	0	-2.987788	-0.624899	0.207492
7	6	0	1.215265	-1.838881	-1.093066
8	6	0	0.560852	-2.268863	0.107089
9	6	0	2.302978	-1.000932	-0.722236
10	6	0	1.243512	-1.689868	1.212351
11	6	0	2.315688	-0.879484	0.707260
12	1	0	1.393048	2.087610	-2.305084
13	1	0	-1.039560	0.434379	2.873036
14	1	0	2.123133	2.763314	-0.403587
15	1	0	0.516156	1.884771	2.649298
16	1	0	0.083495	3.134169	-0.969751
17	1	0	-1.376684	2.186414	1.686277
18	8	0	-4.126198	-0.452475	-0.609607
19	1	0	-1.160324	0.595124	-2.596790
20	1	0	-2.820276	-1.681047	0.477637
21	1	0	-3.073490	-0.068106	1.156277
22	1	0	-4.888099	-0.853983	-0.161486
23	1	0	0.939297	-2.117608	-2.101196
24	1	0	-0.290111	-2.934525	0.160802
25	1	0	3.010834	-0.545627	-1.403602
26	1	0	1.008165	-1.851808	2.256661
27	1	0	3.057677	-0.359823	1.298712

3b

SCF Done: E(RB+HF-LYP) = -1165.40490543 A.U. after 10 cycles

Center Number	Atomic Number	Atomic Type	Coordinates (Angstroms) X	Y	Z

1	44	0	0.607153	0.026467	-0.069144
2	15	0	0.663532	2.298340	-0.672077
3	15	0	-0.787578	0.496376	1.765382
4	1	0	0.373286	2.682354	-2.002288
5	1	0	1.904753	2.955684	-0.535074
6	1	0	-0.149814	3.251695	-0.017222
7	1	0	-1.714224	-0.487976	2.166509
8	1	0	-0.172352	0.741698	3.013002
9	1	0	-1.659298	1.605830	1.727759
10	6	0	2.084819	-1.294004	-1.195669
11	6	0	1.427620	-2.102241	-0.195268
12	6	0	2.795541	-0.266270	-0.522977
13	6	0	1.741870	-1.571795	1.077866
14	6	0	2.558223	-0.397812	0.889659
15	1	0	2.071986	-1.468891	-2.263408
16	1	0	0.809866	-2.969419	-0.388084
17	1	0	3.411836	0.489627	-0.992556
18	1	0	1.418143	-1.973041	2.029761
19	1	0	3.011690	0.197057	1.670948
20	6	0	-1.405532	-0.399273	-1.158468
21	6	0	-2.585265	-0.661996	-0.981918
22	6	0	-3.978073	-0.936504	-0.642117
23	8	0	-4.428027	0.093246	0.227160
24	1	0	-0.587678	-0.124544	-1.834707
25	1	0	-4.552764	-0.975787	-1.582637
26	1	0	-4.054005	-1.933224	-0.178165
27	1	0	-5.376458	-0.042922	0.384977

4b

SCF Done: E(RB+HF-LYP) = -1165.40489093 A.U. after 14 cycles

Center Number	Atomic Number	Atomic Type	Coordinates (Angstroms) X	Y	Z
1	44	0	0.612257	0.024933	-0.068359
2	15	0	0.687341	2.268546	-0.767588
3	15	0	-0.658663	0.603800	1.820228
4	1	0	0.348133	2.600459	-2.099650
5	1	0	1.947406	2.901019	-0.710699
6	1	0	-0.077044	3.265632	-0.119710
7	1	0	0.021452	0.975919	3.001133
8	1	0	-1.577790	1.671804	1.746351
9	1	0	-1.512392	-0.382393	2.355383
10	6	0	-1.443419	-0.416805	-0.919298
11	6	0	-2.631645	-0.685973	-0.808140
12	6	0	-4.043549	-0.974644	-0.580952
13	8	0	-4.626050	0.133837	0.086647
14	1	0	-0.651579	-0.135078	-1.645350
15	1	0	-4.508693	-1.167878	-1.562674
16	1	0	-4.134883	-1.906240	0.001911
17	1	0	-5.580237	-0.030382	0.159534
18	6	0	1.982136	-1.403789	-1.206869
19	6	0	1.386313	-2.127233	-0.109452
20	6	0	2.760672	-0.349888	-0.660296
21	6	0	1.807133	-1.519883	1.097874
22	6	0	2.629742	-0.382774	0.771367
23	1	0	1.882870	-1.646374	-2.256712
24	1	0	0.740866	-2.991174	-0.195793
25	1	0	3.354105	0.357123	-1.225683
26	1	0	1.549509	-1.849670	2.096356
27	1	0	3.152903	0.250221	1.475211

5b

SCF Done: E(RB+HF-LYP) = -1165.39305260 A.U. after 12 cycles

Center Number	Atomic Number	Atomic Type	Coordinates (Angstroms) X	Y	Z
1	44	0	-0.574478	0.023883	0.005735
2	15	0	0.018489	1.478645	1.728670
3	15	0	-0.282273	1.659669	-1.622090
4	6	0	1.404278	-0.490713	-0.183851
5	6	0	2.635833	-0.621224	-0.412503
6	6	0	4.069877	-0.803049	-0.576646
7	6	0	-1.536164	-1.844245	0.915022
8	6	0	-1.429075	-2.047455	-0.502785
9	6	0	-2.421620	-0.739950	1.120916
10	6	0	-2.219918	-1.066144	-1.154998
11	6	0	-2.838155	-0.242891	-0.146615
12	1	0	0.719837	0.970126	2.845371
13	1	0	0.610759	1.430992	-2.695323
14	1	0	-1.007857	2.157450	2.422339
15	1	0	-1.417068	2.024916	-2.378621
16	1	0	0.853015	2.587903	1.458803
17	1	0	0.160804	2.962261	-1.287566
18	8	0	4.748651	-0.375124	0.583984
19	1	0	1.615539	-1.481320	0.385371
20	1	0	4.268110	-1.857875	-0.830321
21	1	0	4.337045	-0.218106	-1.477031
22	1	0	5.700549	-0.514922	0.449417
23	1	0	-1.094474	-2.459021	1.687730
24	1	0	-0.850288	-2.818392	-0.994645
25	1	0	-2.732498	-0.352706	2.083063
26	1	0	-2.362820	-0.977918	-2.224151
27	1	0	-3.546404	0.556081	-0.318582

6b

SCF Done: E(RB+HF-LYP) = -1165.43722803 A.U. after 12 cycles

Center Number	Atomic Number	Atomic Type	Coordinates (Angstroms) X	Y	Z
1	44	0	-0.480168	-0.032381	-0.009319
2	15	0	-1.293818	-1.760153	-1.364717
3	15	0	-0.331500	-1.475139	1.823324
4	6	0	1.281653	-0.423326	-0.505699
5	6	0	2.533558	-0.551257	-0.859991
6	6	0	3.695311	-0.303580	0.087120
7	8	0	4.159234	1.013955	-0.162220
8	1	0	-1.413775	-1.497201	-2.744871
9	1	0	-2.585034	-2.277396	-1.122043
10	1	0	-0.573989	-2.971284	-1.426689
11	1	0	0.259214	-0.971226	3.000664
12	1	0	-1.508367	-2.018003	2.384320
13	1	0	0.418291	-2.662376	1.687247
14	1	0	2.767321	-0.722010	-1.912224
15	1	0	4.471397	-1.055822	-0.110841
16	1	0	3.363401	-0.427546	1.128265
17	1	0	5.060191	1.093757	0.190752
18	6	0	-0.104096	2.223271	-0.153561
19	6	0	-0.690328	1.945007	1.117314
20	6	0	-1.052063	1.876062	-1.159722
21	6	0	-2.043062	1.492269	0.895822
22	6	0	-2.259053	1.447900	-0.496505
23	1	0	0.900062	2.589423	-0.322758
24	1	0	-0.232357	2.130695	2.080128
25	1	0	-0.920544	1.994122	-2.227046
26	1	0	-2.766311	1.247341	1.662838
27	1	0	-3.177710	1.151963	-0.987737

7b

SCF Done: E(RB+HF-LYP) = -1165.36306027 A.U. after 30 cycles

Center Number	Atomic Number	Atomic Type	Coordinates (Angstroms) X	Y	Z
1	44	0	0.565096	0.045773	0.001908
2	15	0	0.499681	1.831412	-1.485150
3	15	0	0.183106	1.436541	1.822111
4	6	0	-1.355047	-0.135877	-0.196396
5	6	0	-2.605893	-0.306981	-0.223194
6	6	0	-3.930078	-0.448022	-0.826801
7	8	0	-4.694890	-0.630573	0.507162
8	1	0	0.196034	1.570626	-2.840035
9	1	0	1.657207	2.617481	-1.684751
10	1	0	-0.424617	2.878636	-1.268306
11	1	0	-0.529141	0.914816	2.925153
12	1	0	1.280151	1.982563	2.525402
13	1	0	-0.563544	2.624440	1.648847
14	1	0	-3.558965	-0.557338	0.917046
15	1	0	-4.097295	-1.335557	-1.442852
16	1	0	-4.365178	0.439981	-1.287452
17	1	0	-5.080460	-1.528511	0.588122
18	6	0	0.936861	-2.216408	-0.130712
19	6	0	1.523883	-1.738111	1.075623
20	6	0	1.598317	-1.592429	-1.228645
21	6	0	2.605090	-0.851644	0.717236
22	6	0	2.648833	-0.764650	-0.689723
23	1	0	0.108578	-2.908381	-0.200724
24	1	0	1.263402	-2.050844	2.078093
25	1	0	1.405530	-1.774259	-2.277335
26	1	0	3.273769	-0.353786	1.407194
27	1	0	3.355852	-0.183875	-1.268418

8b

SCF Done: E(RB+HF-LYP) = -1088.99352210 A.U. after 40 cycles

Center Number	Atomic Number	Atomic Type	Coordinates (Angstroms) X	Y	Z
1	44	0	0.205324	0.039296	-0.001880
2	15	0	-0.296907	1.615742	-1.643532
3	15	0	-0.323249	1.558230	1.686911
4	6	0	-1.608314	-0.546601	-0.014452
5	6	0	-2.795721	-1.003311	-0.019436
6	6	0	-4.026966	-1.500364	-0.024215
7	1	0	-0.732047	1.135102	-2.896031
8	1	0	0.717709	2.494287	-2.080227
9	1	0	-1.321221	2.556339	-1.401209
10	1	0	-0.629948	1.033883	2.959703
11	1	0	0.634245	2.523854	2.065700
12	1	0	-1.441575	2.401240	1.514783
13	1	0	-4.210785	-2.574561	-0.022348
14	1	0	-4.906974	-0.857672	-0.030081
15	6	0	1.126852	-2.001550	-0.548427

16	6	0	1.278234	-1.817781	0.858150
17	6	0	1.874060	-0.978442	-1.207214
18	6	0	2.146065	-0.693294	1.058763
19	6	0	2.522038	-0.174222	-0.208576
20	1	0	0.544885	-2.774488	-1.031856
21	1	0	0.852589	-2.439648	1.634089
22	1	0	1.983233	-0.869737	-2.278928
23	1	0	2.476949	-0.319801	2.020035
24	1	0	3.203531	0.645994	-0.389174

9b

SCF Done: E(RB+HF-LYP) = -1281.16463614 A.U. after 1 cycles

Center Number	Atomic Number	Atomic Type	Coordinates (Angstroms) X	Y	Z
1	44	0	-0.828967	-0.089244	-0.057329
2	15	0	0.321904	-2.050479	-0.609466
3	15	0	0.620700	0.137924	1.779752
4	1	0	-0.104209	-2.742456	-1.763969
5	1	0	0.322720	-3.128499	0.302823
6	1	0	1.704125	-1.921348	-0.857966
7	1	0	0.800944	1.412519	2.351969
8	1	0	0.186387	-0.556624	2.931044
9	1	0	1.952844	-0.310304	1.694800
10	6	0	0.064468	0.568340	-1.959555
11	6	0	0.574434	1.340539	-1.116723
12	6	0	1.440167	2.473180	-0.728782
13	8	0	2.473466	1.989368	0.142055
14	1	0	-0.095907	0.194889	-2.955903
15	1	0	1.873006	2.911400	-1.639073
16	1	0	0.848344	3.247786	-0.222379
17	1	0	3.023318	2.745008	0.407984
18	6	0	-2.894822	0.269109	-1.018083
19	6	0	-2.683400	1.299141	-0.043411
20	6	0	-2.916345	-0.984735	-0.344641
21	6	0	-2.564038	0.674484	1.226044
22	6	0	-2.683779	-0.748515	1.047822
23	1	0	-3.041665	0.422440	-2.078953
24	1	0	-2.638788	2.361772	-0.240213
25	1	0	-3.090256	-1.948615	-0.805731
26	1	0	-2.428250	1.185485	2.171010
27	1	0	-2.698159	-1.492363	1.833303
28	6	0	4.862175	-1.013692	0.035575
29	8	0	3.463508	-0.730369	0.013214
30	1	0	4.970563	-2.086301	0.212140
31	1	0	5.377949	-0.476303	0.843283
32	1	0	5.346080	-0.768762	-0.919484
33	1	0	3.337510	0.226241	-0.128149

10b

SCF Done: E(RB+HF-LYP) = -1281.13849934 A.U. after 35 cycles

Center Number	Atomic Number	Atomic Type	Coordinates (Angstroms) X	Y	Z
1	44	0	-1.080616	0.002511	-0.051616
2	15	0	0.053058	-1.678182	-1.250311
3	15	0	0.344429	-0.321385	1.789879
4	6	0	-3.022288	0.626503	-1.071539
5	6	0	-2.870638	1.421133	0.125278
6	6	0	-3.106614	-0.735111	-0.672759
7	6	0	-2.862786	0.554529	1.241467
8	6	0	-2.967408	-0.801909	0.755885
9	1	0	-0.155013	-1.757492	-2.646510
10	1	0	-0.241836	-3.021444	-0.927152
11	1	0	1.464036	-1.724536	-1.201711
12	1	0	0.563084	0.775669	2.655815
13	1	0	-0.043511	-1.267510	2.764539
14	1	0	1.683483	-0.723651	1.576103
15	1	0	-3.121062	1.004301	-2.080739
16	1	0	-2.781570	2.499420	0.161144
17	1	0	-3.253075	-1.581585	-1.331481
18	1	0	-2.788182	0.854976	2.278412
19	1	0	-3.048732	-1.693645	1.362743
20	6	0	0.493533	1.601509	-0.885488
21	6	0	1.586923	2.031551	-0.549129
22	6	0	2.880291	2.501193	-0.074761
23	8	0	3.897149	1.572123	-0.450555
24	1	0	-0.318855	1.511078	-1.597298
25	1	0	3.061888	3.491985	-0.519116
26	1	0	2.841155	2.640835	1.017283
27	1	0	4.760117	1.962602	-0.235384
28	6	0	4.458248	-2.021117	0.274834
29	8	0	3.298979	-1.207185	0.102584
30	1	0	4.114924	-3.020541	0.552664
31	1	0	5.109979	-1.644950	1.075793
32	1	0	5.044400	-2.100893	-0.650542
33	1	0	3.588979	-0.310794	-0.155941

11b

SCF Done: E(RB+HF-LYP) = -1281.13983497 A.U. after 32 cycles

Center Number	Atomic Number	Atomic Type	Coordinates (Angstroms) X	Y	Z
1	44	0	-1.046605	0.007707	-0.070949
2	15	0	-0.040411	-1.881041	-1.056931
3	15	0	0.285834	-0.312277	1.840913
4	6	0	-2.889369	0.829436	-1.151550
5	6	0	-2.700541	1.587751	0.061465
6	6	0	-3.128325	-0.521687	-0.785050
7	6	0	-2.829738	0.703307	1.158580
8	6	0	-3.057136	-0.625269	0.645360
9	1	0	0.947842	-1.699859	-2.045366
10	1	0	-0.918268	-2.734697	-1.758975
11	1	0	0.618288	-2.846529	-0.269355
12	1	0	-0.134842	-1.246754	2.813507
13	1	0	1.618381	-0.722932	1.619654
14	1	0	0.481690	0.805511	2.679580
15	1	0	-2.892375	1.228319	-2.157406
16	1	0	-2.504993	2.650252	0.121297
17	1	0	-3.324824	-1.337456	-1.468691
18	1	0	-2.763087	0.977016	2.203740
19	1	0	-3.258906	-1.511409	1.231607
20	6	0	0.661505	1.334434	-0.610950
21	6	0	1.715187	1.947821	-0.505625
22	6	0	3.014458	2.577587	-0.319376
23	8	0	4.012096	1.553132	-0.306502
24	1	0	-0.044557	0.965624	-1.411371
25	1	0	3.185435	3.292663	-1.139043
26	1	0	3.018956	3.153013	0.619524
27	1	0	4.884437	1.971153	-0.223535
28	6	0	4.182078	-2.115294	0.184763
29	8	0	3.088832	-1.208832	0.049900
30	1	0	3.763796	-3.101444	0.402621
31	1	0	4.851279	-1.834579	1.009849
32	1	0	4.771155	-2.186853	-0.739563
33	1	0	3.453729	-0.323273	-0.138929

12b

SCF Done: E(RB+HF-LYP) = -1281.12952548 A.U. after 31 cycles

Center Number	Atomic Number	Atomic Type	Coordinates (Angstroms) X	Y	Z
1	44	0	-0.964536	0.029934	0.028786
2	15	0	-0.153231	-0.947797	1.997865
3	15	0	-1.257977	2.103440	1.038797
4	6	0	0.945510	0.636386	-0.533390
5	6	0	1.976695	1.257467	-0.870560
6	6	0	3.305376	1.791150	-1.111580
7	8	0	4.150801	1.401225	-0.027175
8	1	0	1.239474	-1.094866	2.177127
9	1	0	-0.546499	-2.279927	2.254072
10	1	0	-0.480029	-0.401184	3.261754
11	1	0	-0.248783	3.090328	0.949221
12	1	0	-2.346888	2.881856	0.587236
13	1	0	-1.507633	2.209429	2.428778
14	1	0	1.449927	-0.391089	-0.545084
15	1	0	3.689039	1.428918	-2.077646
16	1	0	3.214534	2.887719	-1.193281
17	1	0	5.040056	1.759809	-0.187518
18	6	0	-1.613041	-1.809188	-1.166593
19	6	0	-1.481631	-0.715886	-2.076080
20	6	0	-2.658186	-1.470902	-0.238447
21	6	0	-2.409563	0.300947	-1.711323
22	6	0	-3.145879	-0.177496	-0.567231
23	1	0	-1.073700	-2.745490	-1.209638
24	1	0	-0.774584	-0.656954	-2.893514
25	1	0	-3.027724	-2.100973	0.560012
26	1	0	-2.571500	1.234027	-2.233459
27	1	0	-3.959202	0.336793	-0.072551
28	6	0	3.812830	-2.511564	-0.062000
29	8	0	3.034520	-1.343464	0.211055
30	1	0	3.112721	-3.339929	-0.190448
31	1	0	4.486233	-2.749631	0.770610
32	1	0	4.402946	-2.405777	-0.981992
33	1	0	3.634082	-0.582379	0.331989

13b

SCF Done: E(RB+HF-LYP) = -1281.16683417 A.U. after 12 cycles

Center Number	Atomic Number	Atomic Type	Coordinates (Angstroms) X	Y	Z
1	44	0	-1.127900	-0.054529	0.042006
2	15	0	-1.112769	1.776677	1.495422
3	1	0	-1.288790	3.058599	0.933864
4	1	0	-2.078685	1.854307	2.522879
5	1	0	0.047617	2.022268	2.258616
6	15	0	-0.517527	-1.490886	1.783068
7	1	0	-0.192258	-2.819473	1.439901
8	1	0	-1.430151	-1.749403	2.829590
9	1	0	0.622011	-1.168899	2.548943

10	6	0	0.693997	0.204899	-0.332002
11	6	0	1.955674	0.329144	-0.637200
12	6	0	2.663209	1.624149	-0.970951
13	8	0	3.670806	1.827137	0.025961
14	1	0	2.601091	-0.560620	-0.632956
15	1	0	1.955787	2.463405	-0.992953
16	1	0	3.115848	1.524392	-1.966627
17	1	0	4.223316	2.575582	-0.254965
18	6	0	-1.691858	-0.353229	-2.157837
19	6	0	-2.471236	0.725555	-1.646090
20	6	0	-2.051005	-1.534108	-1.444597
21	6	0	-3.375749	0.186821	-0.658938
22	6	0	-3.119055	-1.192457	-0.535845
23	1	0	-0.935037	-0.282144	-2.927366
24	1	0	-2.454641	1.747506	-2.001272
25	1	0	-1.658131	-2.527012	-1.619216
26	1	0	-4.126949	0.746180	-0.115932
27	1	0	-3.638506	-1.880862	0.118646
28	6	0	5.697030	-1.606316	0.083727
29	8	0	4.695482	-0.797019	-0.521262
30	1	0	5.670406	-2.577649	-0.416469
31	1	0	5.518302	-1.762966	1.157878
32	1	0	6.701984	-1.181191	-0.045665
33	1	0	4.692455	0.082712	-0.101706

14b

SCF Done: E(RB+HF-LYP) = -1281.13918961 A.U. after 10 cycles

Center Number	Atomic Number	Atomic Type	Coordinates (Angstroms) X	Y	Z
1	6	0	-0.892818	-1.393775	-1.760107
2	6	0	-1.883083	-0.407829	-2.032313
3	6	0	-1.294615	-2.134428	-0.609814
4	6	0	-2.936657	-0.572805	-1.060992
5	6	0	-2.579402	-1.629524	-0.193505
6	1	0	0.024240	-1.535110	-2.316205
7	1	0	-1.881132	0.286875	-2.861187
8	1	0	-0.775684	-2.981636	-0.182164
9	1	0	-3.853114	0.001274	-1.016084
10	1	0	-3.175005	-2.006603	0.627463
11	44	0	-0.987454	0.042328	0.026751
12	15	0	-0.657009	-0.206028	2.301013
13	15	0	-1.583969	2.275862	0.240298
14	6	0	0.901603	0.629535	-0.209724
15	6	0	2.091481	0.939426	-0.405659
16	6	0	3.290871	1.696863	-0.797362
17	8	0	4.482558	0.878131	-0.564926
18	1	0	0.629664	-0.020666	2.863686
19	1	0	-0.941592	-1.468291	2.872063
20	1	0	-1.376585	0.581060	3.234692
21	1	0	-0.624753	3.296394	0.047391
22	1	0	-2.574622	2.760154	-0.643126
23	1	0	-2.144800	2.768987	1.444634
24	1	0	2.535241	-0.607473	-0.277013
25	1	0	3.387760	2.614094	-0.204504
26	1	0	3.250173	1.969061	-1.860018
27	1	0	5.240507	1.280318	-1.018979
28	6	0	3.587077	-1.959274	1.004815
29	8	0	3.346323	-1.357386	-0.309077
30	1	0	2.723037	-2.584324	1.223542
31	1	0	3.712665	-1.176668	1.755916
32	1	0	4.483748	-2.572075	0.919410
33	1	0	4.085115	-0.690421	-0.526231

15b

SCF Done: E(RB+HF-LYP) = -1281.13955445 A.U. after 1 cycles

Center Number	Atomic Number	Atomic Type	Coordinates (Angstroms) X	Y	Z
1	44	0	-0.959989	0.051525	0.024647
2	15	0	-0.620363	-0.076854	2.305169
3	15	0	-1.593283	2.278192	0.123318
4	6	0	0.929480	0.697188	-0.244748
5	6	0	2.074390	1.109943	-0.463966
6	6	0	3.363578	1.695272	-0.815575
7	8	0	4.446621	0.749375	-0.465483
8	1	0	0.675258	0.083526	2.857331
9	1	0	-0.957024	-1.287918	2.954479
10	1	0	-1.295644	0.795764	3.195505
11	1	0	-0.651847	3.297120	-0.149502
12	1	0	-2.609629	2.695066	-0.765758
13	1	0	-2.139163	2.832767	1.307990
14	1	0	3.552816	2.620925	-0.260853
15	1	0	3.431232	1.908254	-1.889867
16	1	0	5.258583	0.997433	-0.938952
17	1	0	2.358910	-0.737664	-0.309657
18	6	0	-0.853283	-1.444254	-1.718054
19	6	0	-1.875093	-0.494062	-1.999469
20	6	0	-1.210144	-2.159697	-0.537642
21	6	0	-2.902667	-0.654052	-0.999773
22	6	0	-2.496365	-1.671726	-0.106548
23	1	0	0.052902	-1.580506	-2.293256
24	1	0	-1.907645	0.174001	-2.849295
25	1	0	-0.664492	-2.984334	-0.098983
26	1	0	-3.834767	-0.106112	-0.953991
27	1	0	-3.063101	-2.037043	0.739833
28	6	0	3.338895	-2.030214	1.001000
29	8	0	3.175855	-1.377992	-0.305198
30	1	0	2.483612	-2.690871	1.130520
31	1	0	3.385669	-1.274570	1.787252
32	1	0	4.260774	-2.607135	0.948709
33	1	0	3.915204	-0.647332	-0.449189

16b

SCF Done: E(RB+HF-LYP) = -1281.13705942 A.U. after 30 cycles

Center Number	Atomic Number	Atomic Type	Coordinates (Angstroms) X	Y	Z
1	44	0	1.032016	-0.010897	0.029947
2	15	0	0.690442	-0.517685	2.260893
3	15	0	1.914471	-2.109939	-0.406483
4	6	0	-0.735003	-0.790052	-0.383846
5	6	0	-1.824423	-1.297285	-0.713065
6	6	0	-3.026391	-1.840842	-1.138911
7	8	0	-4.386338	-1.350673	-0.034262
8	6	0	-4.144685	2.341020	0.508644
9	8	0	-3.709671	1.137898	-0.146460
10	1	0	-0.329671	0.155130	2.974819
11	1	0	1.733149	-0.324280	3.196480
12	1	0	0.337462	-1.838147	2.626319
13	1	0	1.633193	-2.705639	-1.656392
14	1	0	3.316403	-2.288073	-0.403771
15	1	0	1.568070	-3.208209	0.414818
16	1	0	-3.191448	-2.912721	-1.033320
17	1	0	-3.509606	-1.423770	-2.021676
18	1	0	-4.160495	-1.697586	0.849101
19	1	0	-4.254037	-0.340887	0.015544
20	1	0	-3.782864	3.221740	-0.031196
21	1	0	-3.808090	2.378511	1.551468
22	1	0	-5.235004	2.333494	0.481615
23	1	0	-2.738314	1.088627	-0.178615
24	6	0	0.828302	1.709078	-1.486186
25	6	0	2.087389	1.080159	-1.688983
26	6	0	0.814813	2.269763	-0.172456
27	6	0	2.885976	1.288122	-0.505875
28	6	0	2.101849	2.016361	0.417681
29	1	0	0.015466	1.734835	-2.199539
30	1	0	2.411818	0.591605	-2.598476
31	1	0	0.022262	2.860633	0.266424
32	1	0	3.910526	0.971271	-0.363963
33	1	0	2.419877	2.341527	1.400278

17b

SCF Done: E(RB+HF-LYP) = -1281.14188895 A.U. after 1 cycles

Center Number	Atomic Number	Atomic Type	Coordinates (Angstroms) X	Y	Z
1	44	0	-1.192596	-0.039865	0.017965
2	6	0	0.335611	0.993468	-0.505029
3	6	0	1.353159	1.634337	-0.897525
4	6	0	2.435763	2.282817	-1.330945
5	1	0	2.758446	3.221093	-0.886342
6	1	0	3.014581	1.933641	-2.181017
7	15	0	-0.574505	0.260948	2.241328
8	1	0	0.567167	-0.428868	2.702728
9	1	0	-1.468338	-0.092634	3.277041
10	1	0	-0.232697	1.556753	2.686603
11	15	0	-2.450778	1.920766	0.032130
12	1	0	-2.795302	2.484340	-1.214952
13	1	0	-3.729596	1.934998	0.632920
14	1	0	-1.911095	3.071847	0.645966
15	8	0	4.684482	1.433933	-0.420803
16	1	0	5.277663	2.018273	0.074889
17	1	0	4.607001	0.623107	0.129317
18	6	0	5.345082	-1.871852	-0.091384
19	8	0	4.643279	-1.052899	0.855974
20	1	0	5.278940	-2.932871	0.176847
21	1	0	6.399500	-1.583204	-0.180209
22	1	0	4.858026	-1.716874	-1.055584
23	1	0	5.083168	-1.146552	1.715151
24	6	0	-0.746257	-1.711680	-1.484320
25	6	0	-2.009316	-1.144084	-1.821904
26	6	0	-0.853860	-2.293813	-0.187848
27	6	0	-2.922612	-1.436924	-0.744859
28	6	0	-2.219224	-2.140279	0.254025
29	1	0	0.148922	-1.673239	-2.089961
30	1	0	-2.259350	-0.652500	-2.752525
31	1	0	-0.072425	-2.828573	0.335760
32	1	0	-3.971120	-1.168752	-0.714422
33	1	0	-2.632186	-2.511855	1.182831

18b

SCF Done: E(RB+HF-LYP) = -1396.89910960 A.U. after 28 cycles

Center Number	Atomic Number	Atomic Type	Coordinates (Angstroms) X	Y	Z
1	44	0	1.137840	0.112787	0.043219
2	15	0	0.092750	2.087014	0.764694
3	15	0	0.022348	-1.007841	1.767989
4	1	0	-0.239878	3.072526	-0.181644
5	1	0	0.897785	2.856341	1.634891
6	1	0	-1.099430	2.064570	1.511362
7	1	0	0.204941	-2.398676	1.911031
8	1	0	0.341257	-0.617103	3.088209
9	1	0	-1.384937	-0.931238	1.818202
10	6	0	-0.425596	0.195382	-1.536540
11	6	0	-0.286275	-1.024745	-1.307402
12	6	0	-0.634744	-2.451013	-1.457359
13	8	0	-1.593841	-2.784329	-0.438021
14	6	0	-4.685544	-1.081827	0.775198
15	8	0	-3.350874	-0.679172	0.451723
16	6	0	-3.829021	2.665676	-0.901867
17	8	0	-2.701599	1.818838	-0.701969
18	1	0	-0.927221	1.050168	-1.957565
19	1	0	-1.063547	-2.598387	-2.458991
20	1	0	0.249895	-3.093055	-1.366150
21	1	0	-1.825936	-3.723160	-0.534269
22	1	0	-5.148908	-0.254699	1.317066
23	1	0	-4.690609	-1.968364	1.421782
24	1	0	-5.278981	-1.290053	-0.124446
25	1	0	-2.899552	-1.417328	-0.003328
26	1	0	-3.018749	0.953798	-0.362419
27	1	0	-4.386081	2.840773	0.029627
28	1	0	-4.521163	2.260053	-1.653125
29	1	0	-3.457892	3.628039	-1.264377
30	6	0	2.876677	0.410900	-1.452853
31	6	0	2.910479	-0.943802	-0.986015
32	6	0	3.082586	1.261651	-0.334391
33	6	0	3.140831	-0.922724	0.418344
34	6	0	3.225194	0.445138	0.839302
35	1	0	2.728711	0.727906	-2.476398
36	1	0	2.808769	-1.827845	-1.601051
37	1	0	3.140181	2.342449	-0.366217
38	1	0	3.249412	-1.790871	1.055820
39	1	0	3.453518	0.793407	1.837754

19b

SCF Done: E(RB+HF-LYP) = -1396.87498621 A.U. after 36 cycles

Center Number	Atomic Number	Atomic Type	Coordinates (Angstroms) X	Y	Z
1	44	0	1.316482	-0.009565	0.099396
2	15	0	0.509988	1.645821	1.568758
3	15	0	0.968806	-1.698729	1.677711
4	1	0	0.433118	2.980756	1.122022
5	1	0	1.278901	1.859854	2.736563
6	1	0	-0.759401	1.546508	2.176207
7	1	0	-0.045021	-2.668442	1.491024
8	1	0	2.051109	-2.580286	1.897518
9	1	0	0.687849	-1.414141	3.036694
10	6	0	-0.707440	-0.373570	-0.820037
11	6	0	-1.356299	-1.377735	-1.123199
12	6	0	-2.188212	-2.545315	-1.339091
13	8	0	-3.186199	-2.582241	-0.312180
14	1	0	-0.932041	0.718731	-0.825313
15	1	0	-2.640879	-2.488344	-2.341099
16	1	0	-1.558797	-3.450066	-1.321720
17	1	0	-3.809026	-3.300573	-0.514557
18	6	0	-5.133492	0.391517	1.021449
19	8	0	-4.019493	0.232744	0.141575
20	6	0	-2.514007	3.012309	-1.324647
21	8	0	-2.030310	2.083530	-0.352413
22	1	0	-5.337273	1.462094	1.093465
23	1	0	-4.920913	0.006023	2.027406
24	1	0	-6.028565	-0.106402	0.627783
25	1	0	-3.814545	-0.718140	0.055954
26	1	0	-3.296710	3.654510	-0.902181
27	1	0	-2.912877	2.503836	-2.211977
28	1	0	-1.673501	3.642562	-1.625175
29	1	0	-2.771994	1.475550	-0.111086
30	6	0	2.422085	1.148099	-1.511598
31	6	0	2.305293	-0.210707	-1.954186
32	6	0	3.196736	1.134644	-0.307365
33	6	0	2.988142	-1.056202	-1.042547
34	6	0	3.532993	-0.221265	0.000213
35	1	0	2.043374	2.021980	-2.023235
36	1	0	1.758501	-0.540013	-2.828238
37	1	0	3.500119	2.002851	0.263954
38	1	0	3.103201	-2.128202	-1.129396
39	1	0	4.151478	-0.549096	0.825119

20b

SCF Done: E(RB+HF-LYP) = -1396.87607984 A.U. after 1 cycles

Center Number	Atomic Number	Atomic Type	Coordinates (Angstroms) X	Y	Z
1	44	0	1.315360	-0.045833	0.089090
2	15	0	0.584215	1.600054	1.605305
3	15	0	1.110532	-1.710191	1.716418
4	6	0	-0.645247	-0.766280	-0.566291
5	6	0	-1.512743	-1.580669	-0.871404
6	6	0	-2.578601	-2.514965	-1.196675
7	8	0	-3.654379	-2.322426	-0.266375
8	1	0	0.436737	2.921795	1.145064
9	1	0	1.440734	1.846185	2.703716
10	1	0	-0.629373	1.459330	2.307898
11	1	0	0.835565	-3.025839	1.283497
12	1	0	2.220310	-1.988285	2.546249
13	1	0	0.121010	-1.623393	2.722201
14	1	0	-0.642397	0.374737	-0.557419
15	1	0	-2.913789	-2.345780	-2.231214
16	1	0	-2.195354	-3.545970	-1.142461
17	1	0	-4.386867	-2.905475	-0.527416
18	6	0	-5.125707	0.856821	0.919926
19	8	0	-4.095324	0.513189	-0.006564
20	1	0	-5.186812	1.947108	0.946613
21	1	0	-4.909754	0.491171	1.932898
22	1	0	-6.098152	0.463492	0.597882
23	1	0	-4.012698	-0.461139	-0.044719
24	6	0	-2.019464	2.877407	-1.314813
25	8	0	-1.767820	1.910034	-0.297942
26	1	0	-2.734400	3.638312	-0.976049
27	1	0	-2.406551	2.415394	-2.232516
28	1	0	-1.072238	3.374133	-1.543998
29	1	0	-2.614316	1.424588	-0.125854
30	6	0	2.221184	0.980732	-1.737268
31	6	0	2.245691	-0.438993	-1.967280
32	6	0	3.041743	1.241753	-0.600760
33	6	0	3.063112	-1.043700	-0.982146
34	6	0	3.540142	-0.003482	-0.102014
35	1	0	1.715100	1.717230	-2.346071
36	1	0	1.714077	-0.958763	-2.753390
37	1	0	3.255677	2.218078	-0.184267
38	1	0	3.295520	-2.098001	-0.908421
39	1	0	4.230475	-0.128328	0.721356

21b

SCF Done: E(RB+HF-LYP) = -1396.87350899 A.U. after 30 cycles

Center Number	Atomic Number	Atomic Type	Coordinates (Angstroms) X	Y	Z
1	44	0	-1.323175	0.037541	0.118305
2	15	0	-0.609173	-1.532674	1.689283
3	15	0	-1.165727	1.769948	1.661613
4	1	0	-0.377886	-2.864433	1.280422
5	1	0	-1.472414	-1.812076	2.775121
6	1	0	0.578314	-1.342148	2.433233
7	1	0	-0.765159	3.044257	1.198411
8	1	0	-2.323698	2.167880	2.369163
9	1	0	-0.283312	1.690327	2.765525
10	6	0	0.603446	0.639788	-0.493454
11	6	0	1.489657	1.417561	-0.875502
12	6	0	2.599900	2.246914	-1.314523
13	8	0	3.660283	2.177927	-0.342030
14	6	0	5.094961	-0.863302	1.130513
15	8	0	4.177662	-0.549126	0.076006
16	6	0	1.967286	-2.444395	-1.553332
17	8	0	1.860503	-1.687927	-0.332129
18	1	0	1.105452	-0.544322	-0.471396
19	1	0	2.958321	1.920116	-2.302364
20	1	0	2.246414	3.283758	-1.423867
21	1	0	4.378111	2.764242	-0.635753
22	1	0	5.112423	-1.950257	1.232271
23	1	0	4.785742	-0.419532	2.084929
24	1	0	6.104661	-0.518941	0.880143
25	1	0	4.103190	0.426928	-0.018853
26	1	0	2.622983	-3.303523	-1.389396
27	1	0	2.363238	-1.828823	-2.368046
28	1	0	0.966350	-2.796233	-1.807791
29	1	0	2.773236	-1.310901	-0.102620
30	6	0	-2.183473	-1.092435	-1.673120
31	6	0	-2.168111	0.305390	-1.995621
32	6	0	-3.066592	-1.261084	-0.558795
33	6	0	-3.015777	0.988578	-1.086657
34	6	0	-3.570904	0.015824	-0.178314
35	1	0	-1.684294	-1.880481	-2.219632
36	1	0	-1.593320	0.764989	-2.788494
37	1	0	-3.322307	-2.204074	-0.091877
38	1	0	-3.229643	2.049307	-1.093230
39	1	0	-4.293129	0.209000	0.603316

22b

SCF Done: E(RB+HF-LYP) = -1396.88761473 A.U. after 1 cycles

Center Number	Atomic Number	Atomic Type	Coordinates (Angstroms) X	Y	Z
1	44	0	1.386927	-0.083941	0.080731
2	15	0	0.820373	-1.030370	2.102233
3	15	0	2.172665	-2.089213	-0.756857
4	6	0	-0.424622	-0.701587	-0.588681
5	6	0	-1.506210	-1.129767	-1.003469
6	6	0	-2.673491	-1.748258	-1.604593
7	8	0	-3.793396	-1.786177	-0.643653
8	1	0	-0.334365	-0.575619	2.786843
9	1	0	1.716459	-0.959181	3.195481
10	1	0	0.534714	-2.415409	2.176972
11	1	0	1.856579	-2.437858	-2.090898
12	1	0	3.566665	-2.321747	-0.817893
13	1	0	1.797114	-3.314390	-0.153579
14	1	0	-3.011269	-1.214552	-2.503838
15	1	0	-2.464006	-2.787087	-1.886880
16	1	0	-4.537110	-2.256661	-1.059422
17	6	0	-4.498500	0.320604	1.891222
18	8	0	-4.309504	0.459079	0.451695
19	1	0	-4.590434	1.326701	2.298804
20	1	0	-3.651505	-0.205107	2.338101
21	1	0	-5.424405	-0.232197	2.049043
22	1	0	-4.160289	-0.463943	0.004266
23	6	0	-2.445517	2.646790	-1.258672
24	8	0	-2.290305	1.718333	-0.161823
25	1	0	-3.217445	3.359965	-0.967185
26	1	0	-2.744161	2.131153	-2.177325
27	1	0	-1.505590	3.179548	-1.419475
28	1	0	-1.669454	0.981527	-0.416920
29	1	0	-3.432637	1.068918	0.202401
30	6	0	1.202927	2.192054	0.211109
31	6	0	1.486665	1.849585	-1.151585
32	6	0	2.340266	1.803451	0.992963
33	6	0	2.767086	1.235391	-1.197023
34	6	0	3.305963	1.212118	0.137003
35	1	0	0.325513	2.706394	0.578182
36	1	0	0.843184	2.018083	-2.004607
37	1	0	2.448739	1.949517	2.060431
38	1	0	3.267877	0.885325	-2.090448
39	1	0	4.283725	0.851622	0.425730

23b

SCF Done: E(RB+HF-LYP) = -1396.87828630 A.U. after 36 cycles

Center Number	Atomic Number	Atomic Type	Coordinates (Angstroms) X	Y	Z
1	44	0	1.411340	-0.005932	0.066181
2	15	0	1.401512	-1.653882	1.697772
3	15	0	2.642294	-1.326878	-1.395290
4	6	0	-0.205298	-0.810041	-0.670686
5	6	0	-1.249049	-1.333724	-1.135662
6	6	0	-2.386007	-1.930770	-1.587359
7	1	0	0.224510	-1.842479	2.456371
8	1	0	2.321569	-1.561490	2.765679
9	1	0	1.627659	-3.006064	1.349260
10	1	0	2.585137	-1.031553	-2.775211
11	1	0	4.047012	-1.397040	-1.256308
12	1	0	2.367962	-2.711119	-1.466901
13	1	0	-2.400607	-2.993696	-1.816346
14	1	0	-3.163986	-1.355821	-2.082912
15	8	0	-3.745849	-2.271726	-0.071194
16	1	0	-3.295794	-2.854891	0.563652
17	1	0	-3.822694	-1.382066	0.405102
18	6	0	-5.008605	0.560990	1.733142
19	8	0	-3.799559	0.061548	1.150181
20	1	0	-5.784445	0.740993	0.977916
21	1	0	-4.818251	1.488973	2.284126
22	1	0	-5.368236	-0.195108	2.434146
23	1	0	-3.444125	0.724296	0.512656
24	6	0	1.473846	2.146753	-0.746924
25	6	0	2.773381	1.863445	-0.204162
26	6	0	0.536113	2.109485	0.330850
27	6	0	2.641138	1.623761	1.184628
28	6	0	1.244824	1.760820	1.516130
29	1	0	1.261439	2.412981	-1.773614
30	1	0	3.700344	1.846009	-0.763975
31	1	0	-0.529587	2.284099	0.251768
32	1	0	3.444773	1.410810	1.876644
33	1	0	0.817078	1.681145	2.507267
34	6	0	-3.145424	2.242021	-1.894801
35	8	0	-2.545743	1.601143	-0.760697
36	1	0	-3.807657	3.017500	-1.506172
37	1	0	-3.736195	1.539411	-2.496325
38	1	0	-2.387358	2.713182	-2.530985
39	1	0	-1.914913	0.920160	-1.062295